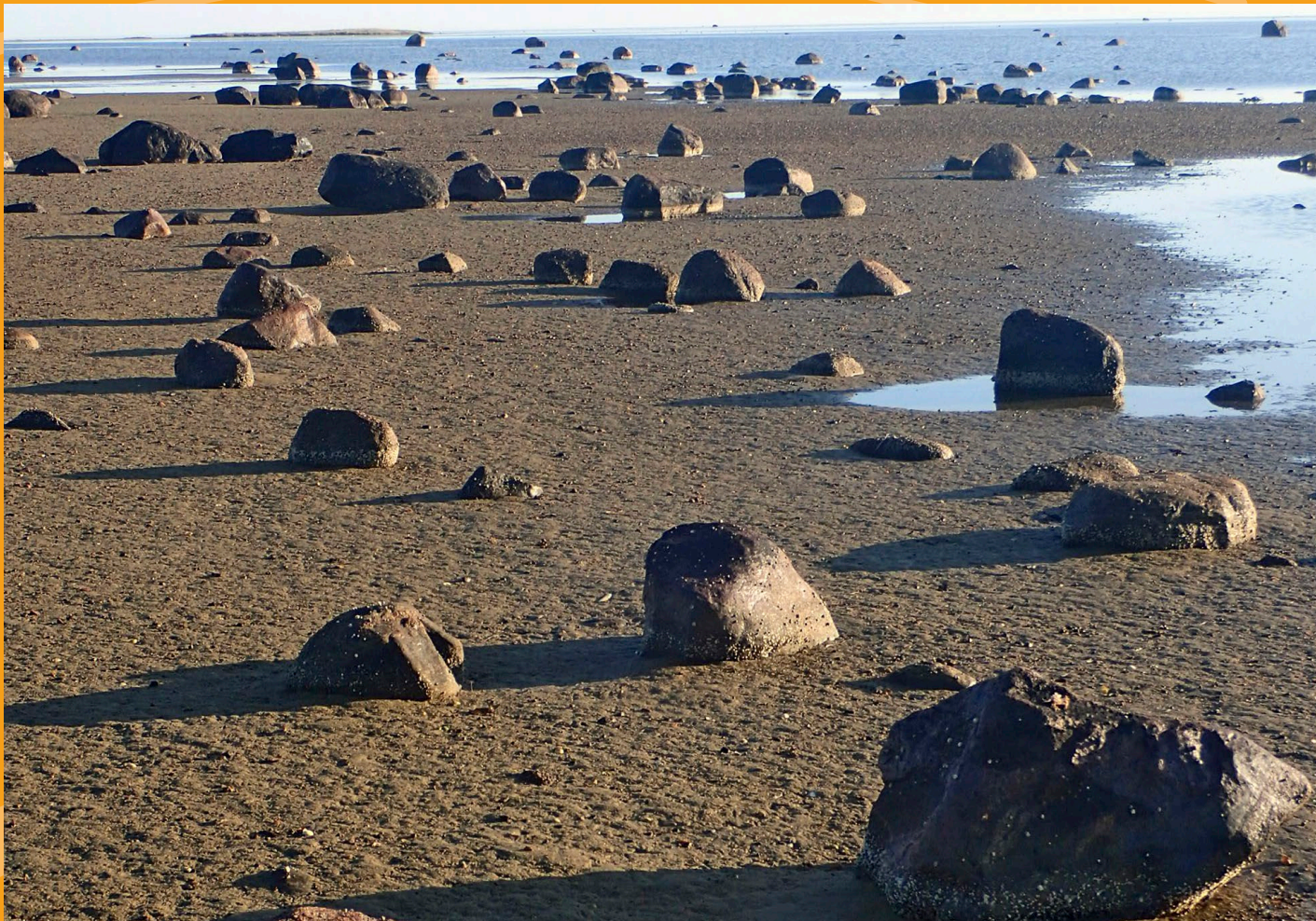


# Bulletin of the Geological Society of Denmark



VOLUME 64 | 2016 | COPENHAGEN





# Bulletin of the Geological Society of Denmark

is published by the Geological Society of Denmark  
(DGF, Dansk Geologisk Forening), founded in 1893

## Chief editor

*Lotte Melchior Larsen*, Geological Survey of Denmark and Greenland (GEUS), Øster Voldgade 10, DK-1350 Copenhagen K, Denmark.  
Tel: +45 91333889; E-mail: lml@geus.dk

*Erik Thomsen*, Department of Geoscience, University of Aarhus, Høegh-Guldbergs Gade 2, DK-8000 Aarhus C, Denmark. Tel: +45 87156443; E-mail: erik.thomsen@geo.au.dk; (palaeontology and stratigraphy).

## Scientific editors

*Lars B. Clemmensen*, Department of Geosciences and Natural Resource Management, University of Copenhagen, Øster Voldgade 10, DK-1350 Copenhagen K, Denmark.  
Tel: +45 35322449; E-mail: larsc@ign.ku.dk; (clastic sedimentology, sedimentary basins and palaeoclimatology).

*Henrik Tirsgaard*, Mærsk olie og Gas AS, Esplanaden 50, DK-1263 Copenhagen K, Denmark. Tel: +45 61209140; E-mail: Henrik.tirsgaard@maerskoil.com; (carbonate sedimentology, petroleum geology and sedimentary basins).

*Ole Graversen*, Department of Geosciences and Natural Resource Management, University of Copenhagen, Øster Voldgade 10, DK-1350 Copenhagen K, Denmark.  
Tel: +45 35322537; E-mail: oleg@ign.ku.dk; (structural geology and tectonics).

*J. Richard Wilson*, Department of Geoscience, University of Aarhus, Høegh-Guldbergs Gade 2, DK-8000 Aarhus C, Denmark. Tel: +45 25321169; E-mail: jrw@geo.au.dk; (igneous petrology and geochemistry).

*Michael Houmark-Nielsen*, Natural History Museum of Denmark, University of Copenhagen, Øster Voldgade 5–7, DK-1350 Copenhagen K, Denmark.  
Tel: +45 35324344; E-mail: michaelhn@snm.ku.dk; (Quaternary geology).

The *Bulletin* publishes contributions of international interest in all fields of geological sciences, with a natural emphasis on results of new work on material from Denmark, the Faroes and Greenland. Contributions based on foreign material may also be submitted to the *Bulletin* if the subject is relevant for the geology of the area of primary interest. The rate of publishing is one volume per year. All articles are published as pdf-files immediately after acceptance and technical production.

*Jesper Milàn*, Geomuseum Faxe, Østsjællandss Museum, Østervej 2, DK-4640 Faxe, Denmark.  
Tel: +45 23319488; E-mail: jesperm@oesm.dk; (palaeontology).

Scientific editing and reviewing are done on an unpaid collegial basis; technical production expenses are covered by the membership fees.

*Lars Nielsen*, Department of Geosciences and Natural Resource Management, University of Copenhagen, Øster Voldgade 10, DK-1350 Copenhagen K, Denmark.  
Tel: +45 35322454; E-mail: ln@ign.ku.dk; (geophysics).

The bulletin is freely accessible on the web page of the Geological Society of Denmark:  
<http://2dggf.dk/publikationer/bulletin/index.html>

*Stig Schack Pedersen*, Geological Survey of Denmark and Greenland (GEUS), Øster Voldgade 10, DK-1350 Copenhagen K, Denmark.  
Tel: +45 21252733; E-mail: sasp@geus.dk (structural geology, tectonics).

## Instructions to authors:

See inside the back cover and also <http://2dggf.dk/publikationer/bulletin/vejledning.html>

*Jan Audun Rasmussen*, Museum Mors, Fossil- og Molermuseet, Skarrehagevej 8, DK-7900 Nykøbing Mors, Denmark.  
Tel: +45 42149792; E-mail: jan.rasmussen@museummors.dk; (palaeontology).

---

*Cover:* Coastal flat at the south coast of Læsø, Kattegat. The flat is an abrasion plain of glacio-marine clays with a residual deposit of boulders. The boulders were originally deposited in the clay as dropstones from icebergs both before and after the last glaciation. Such boulder-strewn abrasion plains are marked landscape elements on southern Læsø and coastal flats south of the island. See this volume pp 1–55: Hansen, J.M. *et al.*: Continuous record of Holocene sea-level changes and coastal development of the Kattegat island Læsø (4900 years BP to present).  
Photo: © Conny Andersen, photo book 'Mit Læsø'.

# Continuous record of Holocene sea-level changes and coastal development of the Kattegat island Læsø (4900 years BP to present)

JENS MORTEN HANSEN, TROELS AAGAARD, JENS STOCKMARR, INGELISE MØLLER, LARS NIELSEN, MERETE BINDERUP, JAN HAMMER LARSEN & BIRGER LARSEN



Hansen, J.M., Aagaard, T., Stockmarr, J., Møller, I., Nielsen, L., Binderup, M., Larsen, J.H. & Larsen, B., 2016. Continuous record of Holocene sea-level changes and coastal development of the Kattegat island Læsø (4900 years BP to present). © 2016 by Bulletin of the Geological Society of Denmark, Vol. 64, pp. 1–55. ISSN 2245-7070. ([www.2dgf.dk/publikationer/bulletin](http://www.2dgf.dk/publikationer/bulletin)).

Received 30 June 2014  
Accepted in revised form  
9 May 2015  
Published online  
28 January 2016

Læsø is the largest island of the Kattegat–Skagerrak region and exposes a vast array of relative sea-level (RSL) indicators, mainly raised beach ridges, swales, lagoons and saltmarshes. The physical environment of continuous glacial rebound, excessive supply of sediment, shallow surrounding waters, low amplitudes of near-shore waves, and micro-tidal conditions produced numerous sea-level proxies of both barrier coasts and saltmarshes. About 1200 RSL/age index points reflect not only short-term sea-level highstands as in most other parts of Europe, but also short-term sea-level lowstands, which in less regressive environments have normally been removed by coastal erosion or obscured by berms from subsequent highstands. Based on a high-precision lidar digital terrain model, the beach ridges have been mapped, typified, levelled and correlated relative to their order of appearance. Transformation of this relative chronology to a robust absolute age model of the RSL changes has been made on the basis of 119 optically stimulated luminescence (OSL) datings,  $^{14}\text{C}$  datings, and tree-ring datings. By ground penetrating radar (GPR) and terrain analyses, the height of the swash zone (run-up) has been determined in order to transform the ridge elevations to a detailed curve of the RSL/age relation. The curve reveals eight centennial sea-level oscillations of 0.5–1.1 m superimposed on the general trend of the RSL curve, including a Little Ice Age lowstand of 0.6 m at 1300 AD. The island grew from now eroded landscapes of Weichselian glacio-marine deposits, including the oldest known post-Weichselian forested area in Scandinavia. During the last 4900 years new coastal landscapes have formed continuously, resulting in around 4000 km of still visible, raised palaeo-shorelines in mostly uncultivated landscapes. After formation of the oldest preserved beach-ridge complex, numerous sea-level proxies formed in a strongly regressive environment caused by glacial rebound supplemented with local uplift due to extensive erosion during Boreal and Atlantic time of the 1700 km<sup>2</sup> glacio-marine platform upon which the island is still being built. The combined uplift produced a relative sea-level fall of 10.3 m, corresponding to a mean vertical regression rate of 2.1 mm/year and a mean horizontal regression rate of 2 m/year, and formed eight distinct types of raised coastal landscapes where well separated beach ridges and saltmarshes developed continuously.

The oldest preserved part of Læsø appeared 4900 years BP as the eastern tip of a 10 km long barrier-spit system growing from a raised glacio-marine landscape, now represented only by boulder reefs west and north-west of the present island. Around 4000 years BP another barrier-spit system appeared to the south, growing northwards from another raised glacio-marine landscape at the raised boulder reefs in the town of Byrum and the abrasion landscapes of Rønnerne. Around 3000 years BP these two initial barrier-spit systems united and formed one major barrier between the present towns Vesterø and Byrum. To the north-east, a third glacio-marine landscape provided materials for the development of the eastern end of the island. Thus, around 2500 BP the island had become one triangular, completely detached island ('the old triangle') between Vesterø, Byrum and Bansten Bakke. From this detached stage, nine subsequent barrier-spit systems grew to the east and formed the present Østerby peninsula, while a series of nine barrier-island complexes developed south-west of 'the old triangle'. To the south and south-east, low-energy coasts developed and formed low beach ridges and saltmarsh landscapes.

*Keywords:* Læsø, Holocene, beach ridge, relative sea-level curve, isostatic rebound, Lidar DTM, optically stimulated luminescence (OSL) dating.

Jens Morten Hansen [jmh@geus.dk], Jens Stockmarr [sto@geus.dk], Ingelise Møller, Merete Binderup, Birger Larsen, Geological Survey of Denmark and Greenland (GEUS), Øster Voldgade 10, DK-1350 Copenhagen K, Denmark. Troels Aagaard [taa@ign.ku.dk], Lars Nielsen [ln@ign.ku.dk], Department of Geosciences and Natural Resource Management, Copenhagen University, Øster Voldgade 10, DK-1350 Copenhagen K, Denmark. Jan Hammer Larsen [jhl@kystmuseet.dk], Coastal Museum of Northern Jutland, Bangsbo Division, Dronning Margrethesvej 6, 9900 Frederikshavn, Denmark.

The island of Læsø covers an area of 118 km<sup>2</sup> and is situated in northern Kattegat in the transition zone between the Baltic Sea and the North Sea. The main island and about 50 islets in its vicinity are situated on a platform with water depths less than 10 m, covering around 1700 km<sup>2</sup>. The area inside the 3 m isobath covers around 400 km<sup>2</sup>. An area of about 208 km<sup>2</sup> is covered by less than 0.3 m of water and comprises the present islands and a 90 km<sup>2</sup> temporarily dry sand platform south of the main island (Fig. 1, Fig. 2).

In contrast to all other major marine forelands of the Skagerrak, Kattegat, Danish Straits and the south-

ern Baltic Sea, Læsø has no central or marginal core of an older and more elevated landscape of different origin than the marine foreland itself (cf. the general hypothesis on the formation of marine forelands by Schou 1945, 1969a–g). Except for several residual boulder reefs, no such *xenomorphic landscapes* of different origin and sediment composition have been preserved within the present coastline of the island.

The present vegetation and animal wildlife on Læsø possess many characteristics of remote islands (cf. EU's *Natura 2000* plan for Læsø at [www.laesoe.dk](http://www.laesoe.dk) and the proposal by Olesen (2005) of Læsø as Marine

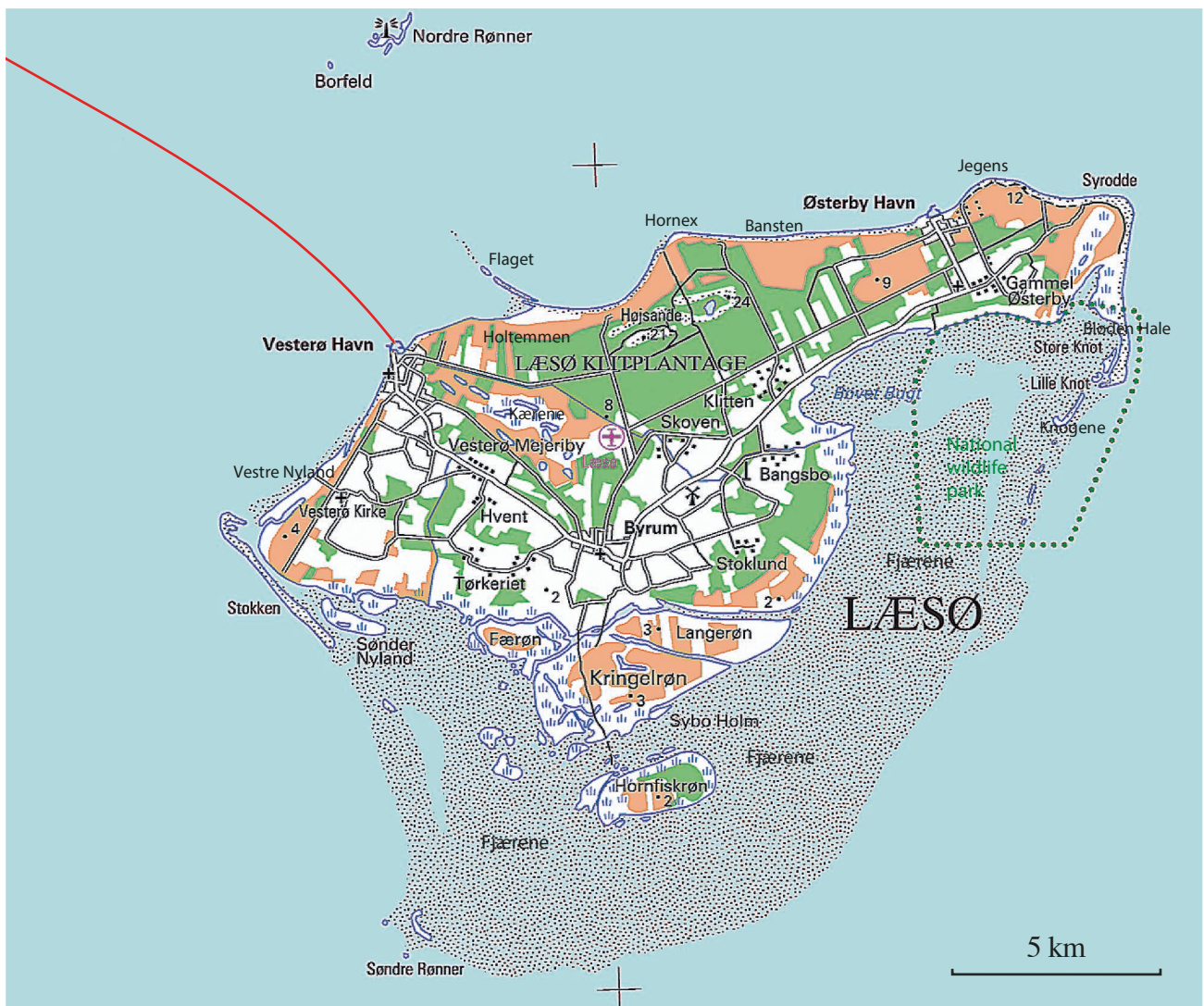


**Fig. 1.** Topographic map of Læsø. Map copyright Geodatastyrelsen 2006, with some place names added. Size of figure is 30×30 km. Geographical position: 11°00' E, 57°10' N (lower cross); 11°00' E, 57°20' N (upper cross).

National Park). However, some geological, archaeological and biological studies indicate that the island was once attached to older, now completely eroded landscapes and has a considerably longer history than indicated from its present wildlife, outline, position and shoreline ages (Hansen 1995, 2015; Bradshaw *et al.* 1999).

Thus, a robust description of the coastal history of Læsø should provide explanations for how detachment of the island from older and more elevated (xenomorphic) landscapes eventually took place, how initial stages of the outline and position of the island have been altered by erosion and redeposition, and how younger, detached stages of the island developed.

Based on such reconstructions it is our intention to present a relative sea-level curve for the past 4900 years, which greatly extends the findings of Hansen *et al.* (2012) for the past *c.* 900 years.

## Pre-history of Læsø until the development of late Holocene coastal landscapes

This chapter gives a brief review of the late Quaternary history of the central northern Kattegat region. It touches on some issues which have been clarified by the present study and are presented later in the text, but which are needed in the context here.

### The early, middle and late Weichselian glaciomarine environment of the Kattegat region

Compared to other major parts of Danish waters the Quaternary geology of southern Skagerrak and northern Kattegat has been considerably less studied. Consequently, specific knowledge about the Quaternary structure is sparse around Læsø and to some

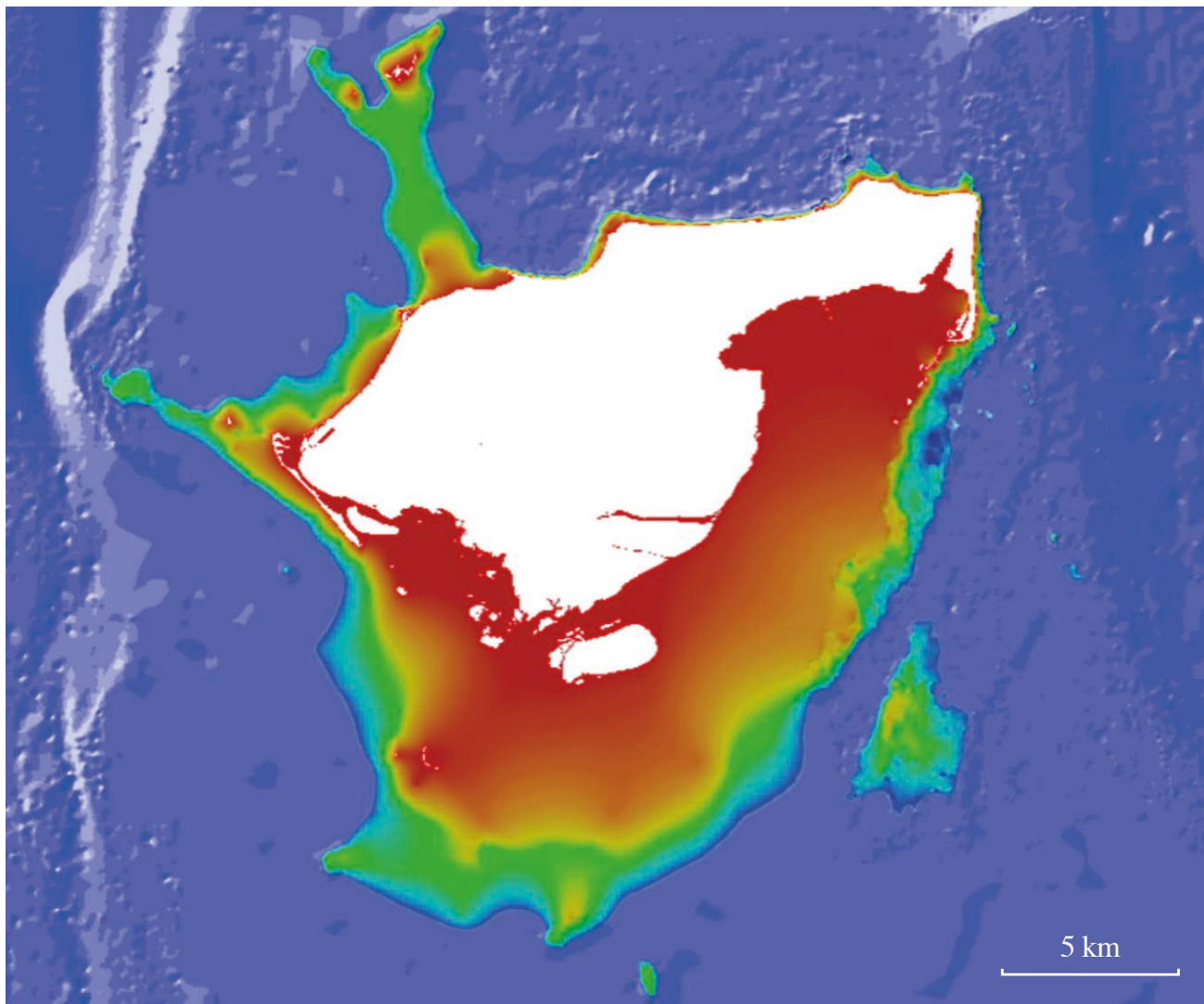


**Fig. 2.** Topography of the seabed around Læsø. Blue: water depths of 10 to 3 m. Other colours: water depths of 3 to 0 m. White: land. Size of figure is 35×35 km. Compiled by the Geological Survey of Denmark and Greenland.

extent rests with general conceptions derived from neighbouring regions. Until the Litorina transgression peaked in the Læsø region *c.* 6300 years BP (Christensen 1995), the landscape of northern Kattegat was probably characterized by landforms that had mainly been formed by glacial load and some glacio-tectonic deformation (Larsen *et al.* 1986; Bahnson *et al.* 1986; Vangkilde-Pedersen *et al.* 1993) of the >180 m thick deposits of early to middle Weichselian glacio-marine clays and silts (Bahnson 1986) which in this work are OSL (optically stimulated luminescence) dated to the period 37000–19000 years BP. As seen from correlations of five scientific boreholes (Bahnson *et al.* 1986) and from beach exposures along northern Læsø, these partly fossiliferous glacio-marine clays and silts have been glacio-tectonically deformed by the Scandinavian ice cap when it covered the Kattegat area during the early to middle Weichselian.

On top of the compacted glacio-marine formation, much less compacted late Weichselian glacio-marine clays and silts form a 0–15 m blanket of partly eroded deposits (on Læsø dated to the period 13800–12900 years BP, Table 1) which is mainly preserved in depressions in the glacially compacted and deformed landscape of early to middle Weichselian glacio-marine deposits. This second series of glacio-marine clays and silts was deposited when the Scandinavian ice cap had melted back to a line east of Læsø near the Swedish west coast.

As in most other parts of the central northern Kattegat area, no strictly glacial deposits in the form of diamictic tills and moraines have been found on Læsø, neither in the five scientific boreholes of Bahnson *et al.* (1986) nor in the approximately 200 geotechnical wells (for water supply and after natural gas) that have been made on Læsø (Fredericia 1985; for updates see the well database Jupiter at [www.geus.dk](http://www.geus.dk)). A similar situation exists in large parts of the northern Kattegat sea where Weichselian tills and moraines are extremely sparse (Lykke-Andersen 1992a, b; Lykke-Andersen *et al.* 1993a, b).

Thus, the common conception of a Weichselian ice cover of Kattegat including the Læsø region is mostly founded in necessity from robust models of the Weichselian glaciation of more south-western parts of Denmark (e.g. Houmark-Nielsen 2003, 2004; Houmark-Nielsen & Kjær 2003). The most robust empirical indications of a Weichselian ice cover of the Læsø area are ‘extradomainal’ glacial deformations (Bahnson *et al.* 1986) and, as seen from several geotechnical reports from constructional works on Læsø, an evident glacial load compaction of the early to middle Weichselian glacio-marine deposits. Such extradomainal glacial deformations, without preserved tills and moraines from the glaciers which have caused the deformations, are frequent in most parts of Denmark, and the

concept of extradomainal deformation constitutes an important basis for the glacial kineto-stratigraphy (Berthelsen 1978) and the general glacial stratigraphy of Denmark (Houmark-Nielsen 2004).

The early, middle and late Weichselian glacio-marine substrate of Læsø has been cut by a near-surface fault with up to 4 m vertical throw that passes through the southern part of the island (Hansen 1986); cf. Japsen & Britze (1991), Vejbæk & Britze (1994) and discussion in Gregersen & Voss (2014). The fault is related to the Fennoscandian Border Zone (or Sorgenfrei–Tornquist Zone) and probably developed during the relatively fast glacial isostatic adjustment (GIA) in the early Holocene, similar to major faulting effects of the GIA in south-western Sweden (see discussions on GIA-related neotectonics and seismicity in Mörner 1978, 1995, 2014 and Bungum *et al.* 2010).

### **The Boreal regression**

During Boreal time the Læsø region formed the northern part of a large emerged landscape stretching from Sjælland to 10 km north of Læsø, surrounded to the west and east by rivers streaming northwards from the Baltic Sea through Lillebælt, Storebælt, Øresund and from fjords in eastern Jutland. Evidence for the existence of this landscape is also mainly built on necessity from robust models of the Boreal period in Denmark and Sweden (Iversen 1967; Noe-Nygaard *et al.* 2006). On Læsø, additional evidence comes from two <sup>14</sup>C datings: One is of a Pinus trunk found in situ in 2010 by one of us (JHL) about 1 km south-west of Læsø at a water depth of 2 m, and in this work <sup>14</sup>C-dated to 10274 years BP (calibrated). Another <sup>14</sup>C dating is of a reworked lump of fresh-water gyttja in the sea cliff north of Vesterø Havn, dated by Mörner (1969) to 7750 years BP. Applying Mörner’s (1969, 1980) and Pässe & Anderson’s (2005) isostatic baselines for the south-westwards tilting of south-western Scandinavia after late glacial time, the –2 m level of the Læsø pine trunk fits well with Krog’s (1965, 1968) finding of slightly younger pine trunks below –23 m in Storebælt.

### **The Atlantic Litorina transgression and erosion**

The Boreal landscape that formed on top of the >180 m thick deposits of glacio-marine clays, silts and coarser ice-rafted materials was drowned during the so-called Litorina transgression. As the Litorina sea successively inundated the landscapes of the Kattegat region, substantial erosion took place and the upper parts of the clayey and silty pre-existing formations were eroded to leave a widespread residual conglomerate composed of coarse materials that were originally contained in the clays and silts of the glacio-marine formations (Hansen 1995, 2015; Hansen *et al.* 2012).

While the erosion by the Litorina transgression

mostly formed prominent sea cliffs in the glacial landscapes along the margins of Kattegat (Schou 1945, 1969d), the Litorina sea erosion of the Læsø region is represented by a large number of boulder reefs (Fig. 3) at distances of up to 12 km from the present island. In other parts of central Kattegat only one small 'knoll' was not completely transgressed and eroded to the levels of the Litorina transgression (Jessen 1897, 1936; Lykke-Andersen 1990); this knoll constitutes the western side of the island of Anholt 70 km SSE of Læsø, where a 5 km<sup>2</sup> glacial landscape is surrounded, mainly to the east, by 17 km<sup>2</sup> of Holocene beach deposits to a maximum level of 13 m above present mean sea level (MSL) (Bjørnsen *et al.* 2008; Clemmensen *et al.* 2012b).

The many boulder reefs of the northern Kattegat area – as well as a 0.5–2 m thick continuous abrasion conglomerate on top of the glacio-marine deposits and below the Holocene marine deposits on Læsø – have been derived by erosion of the two glacio-marine deposits in which boulders and other types of coarse material were dropped from melting icebergs during both the early and late Weichselian marine periods (Jessen 1897, 1922; Hansen 1977, 1995, 2015; Bahnson *et al.* 1986). Four nearly identical <sup>14</sup>C datings of *Balanus* and *Mytilus* adhering to large boulders that were dug out of the residual conglomerate at both the north and the south coast of Læsø indicate that the erosion of the glacio-marine and Boreal landscape had ceased around 3200 years BP (Table 1), and the landscape had become covered by younger marine sand within the outline of the present island.

During this work, we obtained OSL age determinations of marine sand deposits at the highest possible position in

the oldest part of present Læsø. The results indicate that the area became sea-covered no later than 6300 years BP and remained so until the present island emerged c. 4900 years BP (Table 1, plot in Fig. 15). Thus, the Holocene archipelago of Læsø has been deposited on top of a diachronous abrasion platform formed from the onset of the Litorina transgression of the region prior to 6300 years BP until c. 3200 years BP. Beneath and around Læsø this abrasion platform is found in an area of about 400 km<sup>2</sup> with a top level of –4 to +2 m above MSL (Hansen 1977, 1995, 2015; Hansen *et al.* 2012; cf. Larsen *et al.* 1986).

### Glacial isostatic adjustment (GIA) and local relaxation uplift

Compared to analogies in northern Jutland (Denmark) and Halland (Sweden), the raised beach deposits of Læsø are found at 1–3 m higher levels than should be expected (Hansen 1977, 1980, 1995; Bahnson *et al.* 1986). Hansen *et al.* (2012) described how this level difference may be caused by a supplementary, isostatic relaxation uplift that occurs in northern Kattegat in response to the above described Holocene erosion of pre-existing landscapes. By granulometric comparison of the eroded glacio-marine deposits with the re-deposited coarser material which has formed the Holocene beach, dune and marine deposits at Læsø, it was calculated that c. 10 m of glacio-marine clay and silt had been removed from the platform, and that this unloading would have accelerated the GIA, provided that the eroded material was transported a sufficient distance away from Læsø. Moreover, during the late Weichselian glacio-marine transgression, relative sea level rose to c. 70 m above MSL (Jessen 1922, Mertz 1924).



**Fig. 3.** Nordre Rønner (viewed from north-east), a raised boulder reef with a lighthouse, 8 km north of Vesterø Havn (Fig. 1). (Photo: Eigil Holm).

Thereafter, unloading of a substantially larger water column in northern Kattegat than in the higher terrains of northern Jutland and western Sweden may have further accelerated the isostatic uplift of the central part of the region. By comparison of uplift rates of the youngest saltmarsh shorelines at Læsø with uplift rates of the tide gauges at the same GIA isolines in Jutland and western Sweden, Hansen *et al.* (2012) found that the supplementary relaxation uplift would presently be 0.82 mm/yr added to the regional glacial rebound of the tide gauges (GIA presently 1.50 mm/year) yielding a total present isostatic uplift of Læsø by 2.32 mm/year.

## Methods and data

The reconstruction of the coastal development and relative sea levels of Læsø is mainly based on three new sets of data. These are, firstly, a detailed digital terrain model (part of governmental 'Denmark's Elevation Model', see description below); secondly, 119 absolute age determinations, mainly OSL datings (see age model below and Table 1); and thirdly, 15 km of ground penetrating radar (GPR) profiles measured in 2009, supplementing Andreasen's 50 km of GPR measured in 1986 (report from Læsø Kommune 1989), some

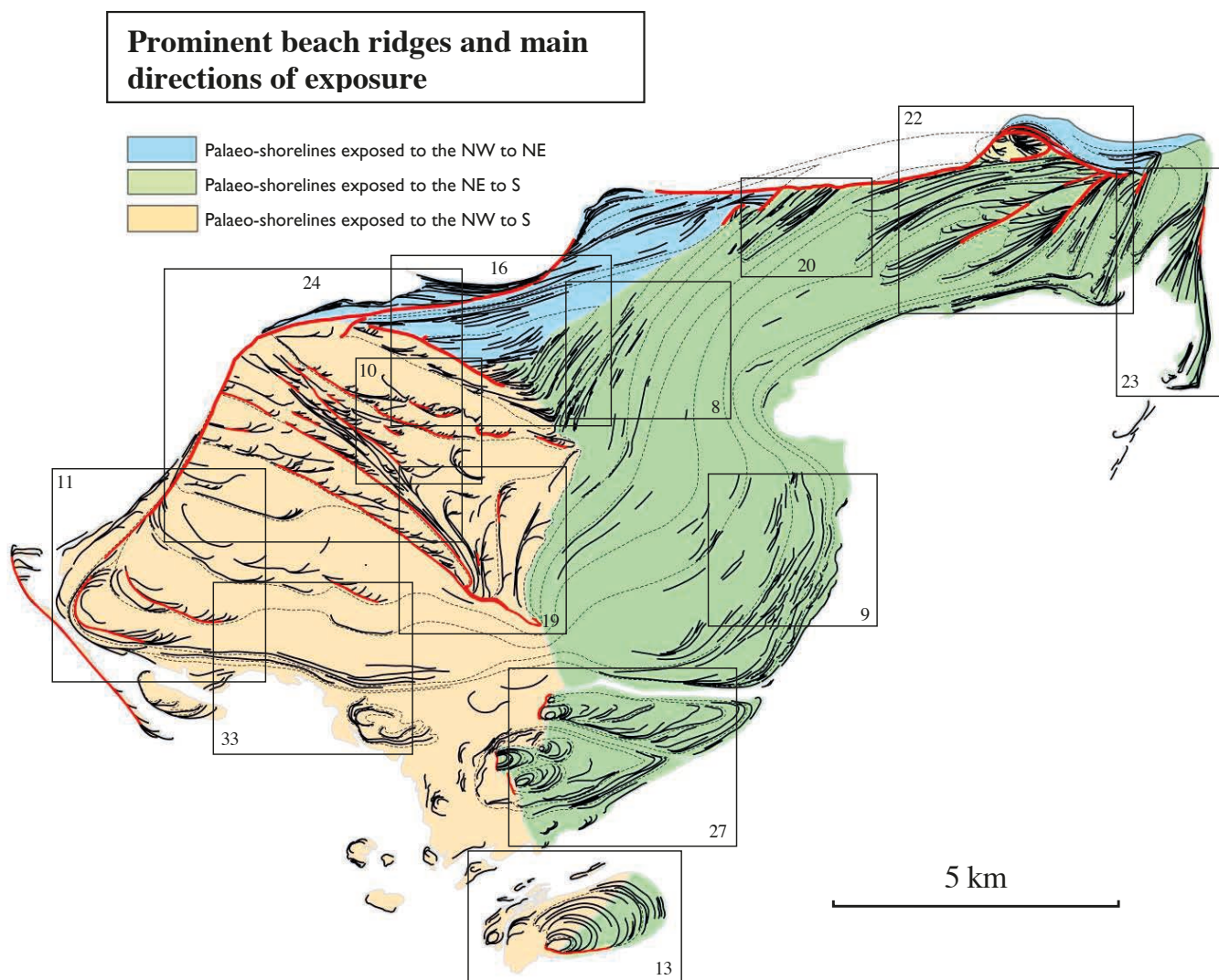


**Fig. 4.** Overview map of the most prominent beach ridges of Læsø, where around 4000 line-kilometres of such palaeo-shorelines are still visible. Three regions show where beach ridges have been exposed to the north (blue), to the south-east (green), and to the south-west (brown). Red lines indicate erosional structures such as brinks and cliffs. Dotted curves: Timelines (isochrons of the age model in Fig. 36). Black frames indicate locations of text figures of maps of the digital terrain model. Frame numbers refer to figure numbers.

of which have previously been published (Hansen 1995). The applied methods are described below.

## Beach-ridge mapping, chronology and levelling

Mapping, chronological order and present levels of beach ridges have been determined from a digital terrain model (DTM) produced in 2006 from an advanced airborne laser-scanning survey. The real grid cell size of this DTM is c. 3 m<sup>2</sup> and the global, vertical precision is generally claimed by the lidar company to be better than 6 cm. Our independent Differential GPS level control on Læsø shows that the global (absolute), vertical precision is better than 4 cm in two separate test areas (Stoklund and Bansten Bakke). Moreover, we found that the local (relative) vertical precision of the present shoreface of the large sand flat south of Læsø, which was partly dry the day the DTM was measured, is c. 1 cm within distances of 1 km or more.

### Determination of beach-ridge levels

From the DTM, levels of 1200 transects with a length of 100–500 m have been measured in three main areas (Fig. 4) where the ridges have been exposed to the north, south-west and south-east, respectively, and where the relative chronology of ridges is easily established (see below). The transects were oriented along the beach-ridge crests in order to determine the mean *base level of ridge crests* (BLRC) of each transect. By applying the base level of the crest transects, small aeolian dunes on top of the ridge crests as well as obvious erosional structures and ditches can be excluded. For each of the beach-ridge transects, the mean z coordinate (elevation) of the BLRC was calculated both manually and by a general mathematical algorithm, excluding outliers such as minor peaks (mainly small dunes) and narrow lows (mainly deflation carvings and ditches). The method is illustrated in Hansen *et al.* (2012, figs 2, 3).

The significance of applying base levels of beach-ridge crests (reduced for height of swash) for RSL reconstruction – instead of swale levels and other types of RSL proxies – is discussed later.

### Absolute age determinations

All absolute age determinations known to us (November 2014) of materials from Læsø are listed in Table 1. Of these, 20 <sup>14</sup>C, tree-ring and thermo-luminescence datings have previously been published in various contexts. For this work, we have acquired 99 new absolute age determinations. <sup>14</sup>C datings have been performed at the AMS-laboratory at Aarhus University. OSL datings have been performed at the Nordic Laboratory for Luminescence Dating, Risø,

Denmark, and the Labor OSL laboratory, Waterville, USA. Tree-ring datings of a large, buried medieval vessel were performed at Moesgaard Museum, Aarhus.

### Age modelling of coastal progradation

After identification of the oldest preserved beach ridge (see later section “4900–4000 years BP”), the age model presented here of the coastal progradation builds on four independent sets of chronology data:

- 1) observed, relative chronology of, and distances between, the numerous beach ridges.
- 2) absolute age determination of a number of selected beach ridges (Table 1), supplemented with
- 3) absolute age determinations of marine and terrestrial deposits that respectively pre-date and post-date beach deposits (Table 1, plot in Fig. 15).
- 4) cultural evidence such as ages and positions of archaeological finds, ages and positions of medieval churches, the settlements and agricultural phases of the island, ages and positions of ancient harbour and vessel finds, the positions of c. 1700 known ruins after medieval and renaissance salt production huts built on the contemporaneous shores on southern Læsø, and the position of shorelines on old reliable maps.

Of these four datasets, 1) and 2) are most important for building the age model, while 3) and 4) must not contradict the age model.

By applying the classical Stenonian principles of superposition and intersection, the exact chronological order of all observable beach ridges can be established within each of the three main areas.

Until recently, correlation of beach ridges between the three main areas of Læsø has been a major problem because the beach ridges of the three areas (Fig. 4) are only sporadically interconnected and traceable between the areas. Thus, until development of the detailed DTM, a complete history of the entire island has been dependent on relatively imprecise level correlations and a few absolute <sup>14</sup>C age determinations (carbonate shell material is generally not preserved in the uppermost sediments, i.e. in the beach deposits). However, after refinement of the OSL dating technique, the greatly increased number of reliable absolute age determinations since 2006 (Table 1) has provided the basis for a robust, coherent, absolute age model of the coastal history of the island (result in Fig. 36).

The procedure for the construction of the age model for the island is outlined in Table 2.

Table 1. Compilation of absolute age determinations of materials from Læsø known to us (November 2014)

No.	Coordinates Degr. E	Coordinates Degr. N	Terrain m	Depth m	Level m	Type	Ag years BP	Cal. year AD	+/- years BP	Collec- ted AD	Collector (sample ID)	Environment (interpretation)	Published (reference)
1	10.8754	57.2546	1.99	0.3	1.69	OSL	740	1267	60	2007	A. Nielsen	Beach ridge	this work
2	10.8756	57.2537	2.39	0.3	2.09	OSL	113	1896	15	2009	T.Aagaard (0B)	Aeolian	this work
3	10.8855	57.2684	2.03	0.3	1.73	OSL	189	1820	14	2009	T.Aagaard (0A)	Aeolian	this work
4	10.8861	57.2535	3.08	0.45	2.63	OSL	850	1159	90	2009	T.Aagaard (1)	Beach ridge	this work
5	10.8903	57.2626	3.39	0.35	3.04	OSL	1400	609	90	2009	T.Aagaard (2)	Beach ridge	this work
6	10.8999	57.271	4.24	1.5	2.74	OSL	1590	418	90	2008	A. Murray	Beach ridge	this work
7	10.9128	57.2824	5.42	1	4.42	OSL	2230	-222	140	2008	A. Murray	Beach ridge	this work
8	10.9298	57.2886	6.84	0.45	6.39	OSL	3000	-991	180	2009	T.Aagaard (9)	Beach ridge	this work
9	10.9351	57.2912	7.39	0.4	6.99	OSL	3200	-1191	220	2009	T.Aagaard (10)	Beach ridge	this work
10	10.939	57.2927	8.05	0.5	7.55	OSL	3240	-1231	240	2009	T.Aagaard (11)	Beach ridge	this work
11	10.9401	57.277	6.07	0.55	5.52	OSL	2910	-901	180	2009	T.Aagaard (6)	Beach ridge	this work
12	10.9574	57.2945	7.4	0.54	6.86	<sup>14</sup> C	2680	-730	100	1970	J.Stockmarr	Terr. (charcoal)	this work
13	10.9622	57.2975	9.1	0.2	8.9	<sup>14</sup> C	1610	340	100	1970	J.Stockmarr	Terr. (Quercus)	this work
14	10.9622	57.2975	9.1	0.85	8.25	<sup>14</sup> C	3355	-1405	80	1970	J.Stockmarr	Terrestrial (peat)	this work
15	10.9655	57.2711	5.58	0.45	5.13	OSL	2430	-421	150	2009	T.Aagaard (7)	Beach ridge	this work
16	10.9675	57.2737	7.94	0.3	7.64	OSL	1190	819	130	2009	T.Aagaard (5)	Aeolian	this work
17	10.9725	57.2868	8.94	0.6	8.34	OSL	3750	-1741	230	2009	T.Aagaard (12)	Beach ridge	this work
18	10.9919	57.2911	11.05	0.5	10.55	OSL	4900	-2890	300	2010	J.M.Hansen (03)	Litoral	this work
19	10.9989	57.3018	8.52	0.4	8.12	OSL	3340	-1330	180	2010	J.M.Hansen (01)	Beach ridge	this work
20	10.9989	57.3018	8.52	6.5	2.02	OSL	6300	-4292	500	2008	B.Larsen (B2)	Marine	this work
21	10.9989	57.3018	8.52	7.5	1.02	OSL	5700	-3692	400	2008	B.Larsen (B2)	Marine	this work
22	10.9989	57.3018	8.52	8.5	0.02	OSL	19700	-17692	1700	2008	B.Larsen (B2)	Glaciomarine ?	this work
23	11.0007	57.2934	10.77	0.5	10.27	OSL	4000	-1990	200	2010	J.M.Hansen (02)	Litoral	this work
24	11.0007	57.2934	10.77	2.5	8.27	OSL	4300	-2292	200	2008	B.Larsen (B1)	Marine	this work
25	11.0007	57.2934	10.77	3.5	7.27	OSL	4800	-2792	300	2008	B.Larsen (B1)	Marine	this work
26	11.0007	57.2934	10.77	4.5	6.27	OSL	4300	-2292	200	2008	B.Larsen (B1)	Marine	this work
27	11.0007	57.2934	10.77	5.5	5.27	OSL	4600	-2592	300	2008	B.Larsen (B1)	Marine	this work
28	11.0007	57.2934	10.77	6.5	4.27	OSL	4400	-2392	200	2008	B.Larsen (B1)	Marine	this work
29	11.0096	57.2833	9.16	0.15	9.01	OSL	3500	-1490	200	2010	J.M.Hansen (04)	Beach-litoral	this work
30	11.0096	57.2833	9.16	0.5	8.66	OSL	4800	-2790	300	2010	J.M.Hansen (05)	Marine	this work
31	11.0096	57.2833	9.16	8.5	0.66	OSL	4800	-2792	400	2008	B. Larsen (B3)	Marine	this work
32	11.0096	57.2833	9.16	10.5	-1.34	OSL	37000	-34992	4000	2008	B. Larsen (B3)	Glaciomarine	this work
33	11.0127	57.2923	10.75	13.5	-2.75	<sup>14</sup> C	12987	-11037	180	1967	O.Michelsen	Glaciomarine (shell)	Michelsen 1967
34	11.0052	57.2882	10.05	0.8	9.25	<sup>14</sup> C	3375	-1425	100	1970	J.Stockmarr	Terrestrial (peat)	this work
35	10.9334	57.2484	1.26	0.52	0.74	OSL	1369	642	112	2011	J.M.Hansen (M)	Marine	this work
36	10.9334	57.2484	1.26	0.36	0.9	OSL	241	1770	23	2011	J.M.Hansen (M)	Marsh ridge	this work
37	10.9337	57.2498	1.69	0.7	0.99	OSL	1951	60	154	2011	J.M.Hansen (N)	Marine	this work
38	10.9337	57.2498	1.69	0.38	1.31	OSL	1471	540	144	2011	J.M.Hansen (N)	Marine	this work
39	10.9337	57.2498	1.69	0.17	1.52	OSL	611	1400	64	2011	J.M.Hansen (N)	Marsh ridge	this work
40	10.9345	57.2522	2.01	0.38	1.63	OSL	1950	61	166	2011	J.M.Hansen (L)	Marine	this work
41	10.9346	57.253	2.31	0.43	1.88	OSL	1569	442	137	2011	J.M.Hansen (K)	Marine	this work
42	10.9354	57.2558	2.26	0.46	1.8	OSL	2015	-4	162	2011	J.M.Hansen (J)	Marine	this work
43	10.947	57.2446	0.99	0.49	0.5	OSL	1680	331	210	2011	J.M.Hansen (A)	Marine	this work
44	10.9465	57.2453	1.19	0.48	0.71	OSL	233	1778	50	2011	J.M.Hansen (B)	Marsh ridge	this work

Table 1 continued. Compilation of absolute age determinations of materials from Læsø known to us (November 2014)

No.	Coordinates Degr. E	Coordinates Degr. N	Terrain m	Depth m	Level m	Type	Ag years BP	Cal. year AD	+/- years BP	Collec- ted AD	Collector (sample ID)	Environment (interpretation)	Published (reference)
45	10.9465	57.2453	1.19	0.27	0.92	OSL	190	1821	43	2011	J.M.Hansen (B)	Marsh ridge	this work
46	10.9499	57.2595	3.71	0.84	2.87	OSL	1872	139	153	2011	J.M.Hansen (H)	Marine	this work
47	10.9499	57.2595	3.71	0.48	3.23	OSL	1688	323	138	2011	J.M.Hansen (H)	Litoral	this work
48	10.9501	57.2602	3.64	0.43	3.21	OSL	1716	295	140	2011	J.M.Hansen (G)	Litoral	this work
49	10.9509	57.2617	3.6	0.39	3.21	OSL	2011	0	170	2011	J.M.Hansen (F)	Marine	this work
50	10.9509	57.2617	3.6	0.19	3.41	OSL	1759	252	133	2011	J.M.Hansen (F)	Litoral	this work
51	10.9589	57.2442	1.25	0.5	0.75	OSL	1253	758	109	2011	J.M.Hansen (O)	Marine	this work
52	10.9589	57.2442	1.25	0.39	0.86	OSL	300	1711	36	2011	J.M.Hansen (O)	Litoral	this work
53	10.9589	57.2442	1.25	0.18	1.07	OSL	274	1737	28	2011	J.M.Hansen (O)	Marsh ridge	this work
54	10.9600	57.2453	1.98	0.71	1.27	OSL	667	1344	97	2011	J.M.Hansen (E)	Litoral	this work
55	10.9600	57.2453	1.98	0.29	1.69	OSL	594	1417	47	2011	J.M.Hansen (E)	Marsh ridge	this work
56	10.9631	57.2468	2.66	0.62	2.04	OSL	1728	283	141	2011	J.M.Hansen (I)	Marine	this work
56a	10.9623	57.2555	1.83	0.32	1.51	OSL	1794	217	310	2011	J.M.Hansen (D)	Marine	this work
57	10.9667	57.2500	1.99	1.5	0.49	<sup>14</sup> C	12933	-10983	210	1973	Tauber & Krogh	Glaciom. (Saxicava)	Krog 1968
57a	10.9646	57.2483	2.12	0.38	1.74	OSL	1819	192	285	2011	J.M.Hansen (C)	Marine	this work
58	10.9667	57.2500	2.06	1.5	0.56	<sup>14</sup> C	13793	-11843	180	1973	Tauber & Krogh	Glaciom. (Saxicava)	Krog 1968
59	10.9965	57.2669	7.75	0.8	6.95	OSL	4100	-2090	200	2010	J.M.Hansen (08)	Marine	this work
60	11.0041	57.266	7.0	0.6	6.4	OSL	3990	-1980	200	2010	J.M.Hansen (07)	Marine	this work
61	11.0041	57.266	7.0	0.35	6.65	OSL	580	1430	40	2010	J.M.Hansen (06)	Aeolian	this work
62	11.0052	57.2616	5.11	1	4.11	<sup>14</sup> C	3182	-1232	200	1977	Jensen (1872)	Marine (whale)	Hansen 1977
63	11.0434	57.2394	1.66	0.2	1.46	Dendro	543	1466	0	2009	J.Vellev	Marsh ridge (pole/Pinus)	this work
64	10.8627	57.2319	-2	0	-2	<sup>14</sup> C	10274	-8324	41	2009	J.H.Larsen (A.Fischer)	Terr. (trunk/Pinus)	this work
65	11.0102	57.2029	2.34	0.65	1.69	OSL	420	1589	30	2009	J.M.Hansen (1)	Marsh ridge	Hansen et al. 2012
66	11.0102	57.2029	2.34	0.4	1.94	OSL	340	1669	30	2009	J.M.Hansen (2)	Aeolian	Hansen et al. 2012
67	11.0131	57.2035	2.08	0.75	1.33	OSL	380	1629	30	2009	J.M.Hansen (3)	Litoral	Hansen et al. 2012
68	11.0131	57.2035	2.08	0.35	1.73	OSL	280	1729	30	2009	J.M.Hansen (5)	Aeolian	Hansen et al. 2012
69	11.0123	57.2069	1.91	0.55	1.36	OSL	330	1679	20	2009	J.M.Hansen (7)	Marsh ridge	Hansen et al. 2012
70	11.012	57.2079	1.78	0.3	1.48	OSL	320	1689	20	2009	J.M.Hansen (9)	Marsh ridge	Hansen et al. 2012
71	11.0078	57.2083	1.57	0	1.57	Map	220	1786	0	2006	R. Sci. Acad.	Shoreline	Hansen et al. 2012
72	11.0394	57.2108	0.22	1.8	-1.58	<sup>14</sup> C	3297	-1347	23	2010	J.M.Hansen	Marine (Balanus)	this work
73	11.0375	57.212	0.2	1.8	-1.6	<sup>14</sup> C	3347	-1397	29	2010	J.M.Hansen	Marine (Balanus)	this work
74	11.0535	57.2658	2.6	0.33	2.27	OSL	1800	209	140	2009	J.M.Hansen (07)	Marine	Hansen et al. 2012
75	11.0578	57.2614	2.05	0.15	1.9	OSL	700	1309	70	2009	J.M.Hansen (05)	Marsh ridge	Hansen et al. 2012
76	11.0578	57.2614	2.05	0.35	1.7	OSL	1660	349	110	2009	J.M.Hansen (06)	Marine	Hansen et al. 2012
77	11.0623	57.2599	2.16	0.35	1.81	OSL	870	1139	60	2009	J.M.Hansen (08)	Marsh ridge	Hansen et al. 2012
78	11.0647	57.2597	1.98	0.45	1.53	OSL	780	1229	50	2009	J.M.Hansen (12)	Marsh ridge	Hansen et al. 2012
79	11.0698	57.2605	1.82	0.35	1.47	OSL	820	1189	80	2009	J.M.Hansen (15)	Marsh ridge	Hansen et al. 2012
80	11.0719	57.2601	1.77	0.35	1.42	OSL	660	1349	40	2009	J.M.Hansen (16)	Marsh ridge	Hansen et al. 2012
81	11.0759	57.259	1.43	0.3	1.13	OSL	530	1479	40	2009	J.M.Hansen (17)	Marsh ridge	Hansen et al. 2012
82	11.0776	57.2585	1.61	0.25	1.36	OSL	420	1589	30	2009	J.M.Hansen (03)	Marsh ridge	Hansen et al. 2012
83	11.0817	57.2572	0.97	0.2	0.77	OSL	260	1749	40	2009	J.M.Hansen (01)	Marsh ridge	Hansen et al. 2012
84	11.0797	57.2693	1.48	0.2	1.28	Dendro	530	1463	1	1993	J.Vellev	Marsh ridge (pole)	Vellev 1993
85	11.0787	57.2709	1.45	0	1.45	TL	523	1470	50	1993	J.Vellev (Mejdahl)	Marsh ridge	Vellev 1993
86	11.0441	57.2884	5.12	1	4.12	<sup>14</sup> C	3245	-1295	100	1993	J.M.Hansen	Marine (whale)	Hansen 1995

Table 1 continued. Compilation of absolute age determinations of materials from Læsø known to us (November 2014)

No.	Coordinates Degr. E	Coordinates Degr. N	Terrain m	Depth m	Level m	Type	Ag years BP	Cal. year AD	+/- years BP	Collec- ted AD	Collector (sample ID)	Environment (interpretation)	Published (reference)
87	11.0757	57.294	0.59	2	-1.41	Dendro	628	1381	0	2009	J.M.Hansen	Mar. (ship/Quercus)	this work
88	11.025	57.3154	4.05	0.3	3.75	OSL	290	1717	20	2007	A.Nielsen	Aeolian	this work
89	11.0305	57.3113	8.55	0.3	8.25	OSL	2900	-893	160	2007	A.Nielsen	Aeolian	this work
90	11.0636	57.3073	9.01	0.3	8.71	OSL	1460	549	130	2009	M.Binderup (07)	Aeolian	this work
91	11.0636	57.3073	9.01	0.6	8.41	OSL	2000	9	140	2009	M.Binderup (07A)	Aeolian	this work
92	11.1183	57.3069	4.83	0.5	4.33	OSL	310	1699	30	2009	M.Binderup (01)	Aeolian	this work
93	11.0871	57.3179	2.68	2	0.68	OSL	2610	-602	140	2008	A.Murray	Marine	this work
94	11.0893	57.318	3.95	3.9	0.05	<sup>14</sup> C	3380	-1430	50	1976	J.M.Hansen	Marine (Mytilus)	Hansen 1977
95	11.0893	57.318	3.95	3.9	0.05	<sup>14</sup> C	3340	-1390	50	1976	J.M.Hansen	Marine (Balanus)	Hansen 1977
96	11.0925	57.3179	7.94	3.5	4.44	OSL	2580	-572	150	2008	A.Murray	Marine	this work
97	11.0951	57.3179	6.09	5	1.09	OSL	2380	-372	140	2008	A.Murray	Marine	this work
98	11.1212	57.3152	5.41	0.3	5.11	OSL	830	1178	60	2008	M.Binderup (09)	Aeolian	this work
99	11.1212	57.3152	5.41	0.6	4.81	OSL	1570	438	220	2008	M.Binderup (08)	Beach ridge	this work
100	11.1314	57.3097	2.88	0	2.88	Dendro	1365	640	0	2005	P.Lysdahl	Litoral (pole/Taxus)	Hansen 1995
101	11.1402	57.3043	2.52	0.3	2.22	OSL	400	1608	50	2008	M.Binderup (10)	Aeolian	this work
102	11.1477	57.3152	4.98	0.3	4.68	OSL	2280	-272	160	2008	M.Binderup (03)	Beach ridge	this work
103	11.1439	57.3236	6.33	0.3	6.03	OSL	1860	148	180	2008	M.Binderup (04)	Aeolian	this work
104	11.1519	57.3257	3.28	0.3	2.98	OSL	1650	358	140	2008	M.Binderup (5A)	Beach ridge	this work
105	11.1783	57.3146	2.28	0.3	1.98	OSL	1050	958	110	2008	M.Binderup (06)	Beach ridge	this work
106	11.192	57.3146	1.28	0.3	0.98	OSL	260	1747	10	2007	A.Nielsen	Beach ridge	this work
107	10.9315	57.298	1	0	1	<sup>14</sup> C	7750	-5800	120	1969	N.A.Möner	Terr. (reworked gytja)	Möner 1969
108	10.9971	57.2716	8.11	0.63	7.48	OSL	3740	-1727	270	2013	J.M.Hansen (5)	Beach ridge	this work
109	10.9864	57.293	10.84	0.46	10.38	OSL	5550	-3537	440	2013	J.M.Hansen (7)	Marine?	this work
110	10.9864	57.293	10.84	0.62	10.22	OSL	5210	-3197	430	2013	J.M.Hansen (8)	Marine?	this work
111	10.9901	57.2919	10.67	0.56	10.11	OSL	4840	-2827	350	2013	J.M.Hansen (10)	Beach ridge	this work
112	10.9911	57.2915	10.87	0.35	10.52	OSL	3890	-1877	350	2013	J.M.Hansen (11)	Beach ridge	this work
113	10.9911	57.2915	10.87	0.6	10.27	OSL	6100	-4087	380	2013	J.M.Hansen (12)	Marine	this work
114	10.9959	57.2869	9.63	0.37	9.26	OSL	5550	-3537	400	2013	J.M.Hansen (13)	Marine	this work
115	10.9851	57.2962	10.52	0.53	9.99	OSL	4470	-2457	280	2013	J.M.Hansen (14)	Beach ridge	this work
116	10.9777	57.2999	9.33	0.45	8.88	OSL	4890	-2877	330	2013	J.M.Hansen (17)	Marine?	this work
117	10.9774	57.3011	7.84	0.35	7.49	OSL	5200	-3187	310	2013	J.M.Hansen (18)	Marine	this work

This compilation comprises all age determinations known to us by November 2014. Coordinates are in decimal degrees.

Ages: BP (before present) relates to the year of collection (<sup>14</sup>C-samples to 1950 according to international convention). Dating methods: OSL: Optically Stimulated Luminescence.

<sup>14</sup>C: Radiometric dating. Dendro: Tree-ring counting. TL: Thermo-luminescence. Coring technique: due to water saturation of fine-grained sand deposits some boreholes may have caved during coring (only samples collected by B. Larsen).

## Compensation for vertical displacement of sea-level proxies (RSL displacement)

Terrain levels of beach-ridge landscapes combine several types of active and previously active agents. Thus, in the case of Læsø (Hansen *et al.* 2012) the levels of the 1200 measured mean base levels of ridge crests (BLRC) can be described as:

$$\text{BLRC} = \text{RSL} + \text{S} + \text{D} - \text{E}$$

where

$$\text{RSL} = \text{ASL} + (\text{U}_L + \text{U}_R + \text{U}_I) - \text{C}$$

and RSL is the relative shore-level displacement, S is the height of swash (run-up), D is the thickness of possible aeolian dunes on top of the crests, E is the depth of possible, local erosion (deflation, ditches, streams), ASL is the absolute ('eustatic') sea level of the region,

Table 2. Procedure for construction of the age model of the island

1: Identification and chronological numbering of continuous series of subsequent beach-ridges within each of the three main areas, supplemented with a similar chronological numbering of continuous beach-ridges of the originally separate saltmarsh islets of Langerøn, Kringelrøn and Hornfiskrøn south of the main island.

2: Measurement of mean base levels of ridge crests (BLRC) of identified beach-ridges (calculation method, see Hansen *et al.* (2012) and next section) and relation of these levels to the chronological order of the ridges.

3: Level correlation of the chronologically ordered beach-ridges of the three main areas and saltmarsh islets.

4: Transformation of the exact chronology of beach-ridges to an absolute age model of the coastal progradation by application of the collated absolute age determinations. By linear interpolation, based on the distances

between the beach-ridges, an absolute interpolate age is assigned to each of the beach-ridges.

5: By comparison of the age/level curves of each of the three main areas, prominent peaks and lows are adjusted by at most 100 years to the age of that part of the curves with most absolute age determinations.

6: Correlation of all curves of step 5 such that interpolated age differences of more than 10 years will not occur. Then every single one of the 1200 measured beach-ridge levels from the three main areas is assigned with a measured (when existing) or interpolated absolute age.

7: Construction of one single, integrated RSL curve of the island is done on the basis of step 6 by calculating age and level means of every 10 year interval of the 1200 measured beach-ridges.

$U_L$  is local tectonic uplift,  $U_R$  is regional relaxation uplift,  $U_I$  is glacio-isostatic adjustment (GIA), and  $C$  is (negligible) compaction of underlying, unconsolidated sediments. Because RSL constitutes the sum of absolute sea level (ASL) and vertical terrain changes ( $U$  and  $C$ ), the present RSL reconstruction is only dependent on how base levels of beach-ridge crests (BLRC) were measured in order to avoid effects of small dunes ( $D$ ) and erosional features ( $E$ ) and how BLRC measurements were compensated for height of swash ( $S$ ).

On Læsø, the geological parameters of  $U$  and  $C$  were thoroughly examined by Hansen *et al.* (2012) in two test areas where these geological agents could be parameterized for the last *c.* 900 years. However, in other areas and regions the problem of geological background noise is still a global, often unrecognized and mostly unsolved problem in sea-level reconstructions and tide-gauge measurements (see discussion below on 'Identification of geological background noise in a low seismicity region'). Therefore, in the present context of RSL reconstruction we abstain from absolute sea-level (ASL) calculations.

### Estimation of swash heights (run-up) by ground penetrating radar (GPR)

In GPR cross-sections of beach ridges (examples in Fig. 18 and Fig. 25), the relative sea level (RSL) of the actual beach ridge can be identified as the points where relatively steep reflectors of beach faces downlap on less steep reflectors of the upper shore face (Tamura *et al.* 2008; Nielsen & Clemmensen 2009; Clemmensen & Nielsen 2010; Clemmensen *et al.* 2012a; Hede *et al.* 2013). On the basis of cross-shore GPR and levelling profiles on Feddet (Sjælland), Hede *et al.* (2013) showed that the inclinations of beach-face reflectors (mean around 5°) and upper shoreface reflectors (mean around 1°) are clearly separated into two distinct populations. Moreover, Hede *et al.* (2013) showed that the inclina-

tions found by cross-shore levelling clearly correspond to inclinations found by cross-shore GPR profiling of beach ridges at the same locations, when levels of the shorelines of the actual beach ridges are identified by downlap of steep reflectors on less steep reflectors.

At Læsø we used the method of GPR identification of downlaps in the depth interval of 0.3–2.5 m below the surface levels of the beach-ridge terrains. About 15 km of reflection GPR profiles were measured in 2009 in the south-western and northern parts of Læsø. The GPR data was acquired using a pulseEKKO PRO system manufactured by Sensors & Software™, equipped with 250 MHz shielded transmitter and receiver antennae providing the required resolution for the purpose (Nielsen & Clemmensen 2009). The antenna separation was 0.38 m and the spatial and temporal sampling was 0.05 m and 0.4 ns, respectively. Topography along the GPR sections was measured with a Trimble GPS system with an accuracy of *c.* 0.02 m in open areas while the topographical information in forests was depicted from the DTM. A standard processing sequence was applied to the data (e.g. Nielsen & Clemmensen 2009; Hede *et al.* 2015), including dewowing to suppress the low-frequency inductive part of the GPR signal, low-pass filtering to reduce high-frequency noise and increase signal-to-noise ratio, migration to move dipping reflections into their proper subsurface position and collapse diffraction hyperbolas, and a robust automatic gain control function with an operator length of either four or eight pulses to account for loss of amplitude due to geometrical spreading and attenuation. GPR velocity information was obtained from sparsely observed diffraction hyperbolas revealing velocities about 0.1–0.12 m/ns in the most shallow and dry sediment, decreasing to about 0.06 m/ns in the deeper and completely water saturated sediments. The migration, the time-to-depth conversion and the topographical correction

were performed using a constant velocity field with an average of 0.08 m/ns as the velocity information from the diffraction hyperbolas was too sparse to set up 1D or 2D velocity fields. The uncertainty on the determination of the velocities was transferred to the time-to-depth conversion, resulting in an underestimation of the depth of up to 0.5–1.0 m within the upper 3 m of the subsurface where the velocities can be higher than 0.08 m/ns.

This data set has allowed determination of swash heights for the two main areas faced to the north and to the south-west (Fig. 4). Thus, by subtracting depths of the downlap points from the actual BLRC level the swash heights can be determined.

About 50 km of GPR profiles measured with an early version of the GPR technique (Andreassen 1986) from other parts of Læsø have also been available, but due to the use of an antenna with a lower frequency the data resolution mostly does not allow identification of the downlap levels.

#### Estimation of swash heights (run-up) by terrain level analyses

In the main area faced to the east and south-east (Fig. 4), determination of swash heights is mainly based

on the lidar digital terrain model terrain level. This can be done in two ways that supplement each other:

1) By comparison of the BLRC of the individual beach ridges with the levels of neighbouring swales, when both mean levels of ridges and swales are measured parallel to the beach-ridge direction.

2) By profiling perpendicular to the length direction of the beach ridges and applying a mathematical transform (corresponding to the BLRC-transform) in order to find the actual base level of the swales.

We found that method 1 is applicable in terrains where beach ridges are well separated, whereas it is not applicable in terrains of condensed high- and low-ridge plains. Method 2 is generally applicable when repeated in several parallel profiles. In areas where modern GPR data are available, there is good agreement between the GPR downlap method and both lidar model methods, although thus determined swash heights are about 0.1–0.2 m lower than when determined by GPR profiling. This small, but general difference probably shows that the downlap point may be situated up to 0.2 m below mean water level, depending on the coastal exposure. Alternatively, small errors in the GPR velocity estimate may lead to a small bias in depth estimation of the downlap points.

Table 3. Contents of the RSL series database for Læsø. See Fig. 4 and Fig. 5 for the various areas and Fig. 1 for place names. The coastal types are described in the Results chapter

---

**Læsø south-west:** Beach-ridges from the oldest parts of present Læsø (the ‘top’ of the island) to Stokken at the south-western corner.

Coastal types and ages of ridges:

- Condensed high-ridge plain of the ‘top’ of the island (4900–4000 years BP)
- Barrier spit and lagoon systems of Kærene and more south-westwards (4000–2500 years BP)
- Barrier island and lagoon systems of south-western Læsø (2500 years BP to present)

**Læsø north:** Beach-ridges from the oldest parts of present Læsø (the ‘top’ of the island) to the north coast at Hornex and Holtemmen.

Coastal types and ages of ridges:

- Condensed high-ridge plain from the top of the island to Hornex (4900 years BP to present)
- Condensed high-ridge plain from the top of the island to the high cliff at Holtemmen (4900–3000 years BP)
- Condensed high-ridge plain from the high cliff to present shoreline at Holtemmen (c. 1000 years BP to present)

**Læsø east:** Beach-ridges from Bansten along the northern and central part of the Østerby peninsula to Bløden Hale.

Coastal types and ages of ridges:

- A series of nine attached barrier spit and lagoon systems (3500 years BP to present)

**Læsø south-east:** Beach-ridges and saltmarsh ridges formed from the ‘top’ of the island to the present coastline at Stoklund and Bangsbo.

Coastal types and ages of ridges:

- Condensed high-ridge plain from the ‘top’ to south-east of Højsande (4900–3500 years BP)
- Condensed low-ridge plain (raised saltmarsh) from south-east of Højsande to the present coast of Stoklund and Bangsbo (3500 years BP to present)

**Læsø south:** Raised saltmarsh ridges of Tørkeriet. Coastal type and ages of ridges:

- Attached, condensed low-ridge plain and present saltmarsh (1700 years BP to present)

**Læsø, Rønnerne:** Saltmarsh ridges originally formed around raised boulder reefs on the shallow abrasion platform of southern Læsø.

Coastal types and ages of ridges:

- Detached, concentric low-ridge plain of Langerøn (c. 1000 years BP to present)
  - Detached, concentric low-ridge plain of Kringelrøn (c. 1000 years BP to present)
  - Detached, concentric low-ridge plain of Hornfiskrøn (900 years BP to present)
-

## Database for measured and modelled RSL/age index points

By combination of the procedures described above, a database presently containing more than 1200 entries has been created for the RSL/age relation, including also distances between subsequent ridges, data on age and level uncertainties, and modelled isostatic uplift. The database also comprises already published results by Hansen *et al.* (2012) from the saltmarshes and low heathers of Hornfiskrøn, Stoklund and Bangsbo.

The following periods are covered by RSL/age index points from a number of geographically separated areas:

4900–4000 years BP: Three areas exposed to the north, south-west, and south-east.

4000–3500 years BP: Three (four) areas exposed the north (two), south-west, and south-east.

3500 years BP to present: Four areas exposed to the south-west, north, east, and south-east.

1700–900 years BP to present: Nine areas exposed to the north (two), south-west (one), south (four), south-east (one), and east (one).

Thus, the entire period 4900 years BP to present is represented by index points from at least three geographically separate areas which are exposed towards different main directions (N, SW, and SE to E), while young sections also include exposures towards the south. The contents of the database are detailed in Table 3.

## Pollen analyses

Pollen analyses of peat samples from swales in the oldest preserved part of the island have been performed in order to illustrate the vegetation of this small beach-ridge landscape, and if the maturity of this coastal vegetation would suggest connection to larger, more fertile and now completely eroded glacio-marine landscapes.

In the pollen diagrams (Figs 29–31) tree pollen counts have been reduced by 4 (*Betula*, *Pinus*, *Alnus*, *Corylus* and *Quercus*) or by 2 (*Ulmus*) or multiplied by 2 (*Tilia* and *Fraxinus*) in order to compensate for differences in pollen productivity between species (Andersen 1970), before calculating their percentages of the total number of tree pollen.

## Results

### Types of raised coastal landscapes

The typification of raised coastal landforms used here is based on detailed beach-ridge mapping of all parts

of Læsø as they can be traced from the DTM, supplemented by field studies of the coastal development, vegetation history (Hansen 1994, 1995), medieval settlement and salt industry (Hansen 2010). Thus, the land- and seascapes of the present island can be classified into a number of distinct morphological types based on the origin of the landscapes and the original coastal setting and processes (Fig. 5). Each type of coastal landscape is here given a short morphological definition, a general explanation and examples of locations.

### Raised boulder reefs

Piles of boulders jutting out of the sea bottom, sea surface or landscape (Fig. 3, Fig. 6).

The boulder reefs comprise the coarse residual after erosion of the glacio-marine substrate of the region upon which the boulders rest (Fig. 7). The boulders may subsequently have been pushed together and piled up in boulder reefs by ice packing in periods when they were situated close to the sea level of the time. Ice packing processes are still active on the shallow platform south of Læsø when the shallow water freezes to the bottom, forming a widespread ice sheet. During strong winds and high water levels the ice sheet is lifted free of the bottom, and the wind is able to drag frozen-in boulders around, often leaving more than 100 m long plough marks behind them. In areas with high concentrations of large boulders the ice packing process may be able to pile boulders, thus forming new boulder reefs.

The islands of Nordre Rønner and Borfeld 8 km north of Vesterø Havn, as well as Søndre Rønner 5 km south-west of Hornfiskrøn (Fig. 1), are emerged boulder reefs. The large submerged boulder reef of Læsø Trindel 12 km north of Østerby Havn has been nearly removed by stone fishing, but since 2009 it has been reconstructed by dumping of large quantities of imported Norwegian granite blocks. Inside the present outline of Læsø, raised boulder reefs are found in the town Byrum (Bakken and Tingstedet), at the south-western side of Hornfiskrøn ('Engelskmandens Grav', Fig. 6), in the landscape of Tørkeriet (most boulders are removed), and in the 'umbos', i.e. the incipient nuclei of Langerøn, Kringelrøn and Færøn.

### Raised abrasion plains ('sand-paper plains')

Plains characterized by widespread, often monolithic boulders resting directly upon the eroded glacio-marine platform, which here and there may also exhibit a residual cover of gravel and stones (Fig. 7).

In most places the abrasion residual of gravel and stones is covered by a thin layer of sand, whereas

## Coastal progradation types of Læsø

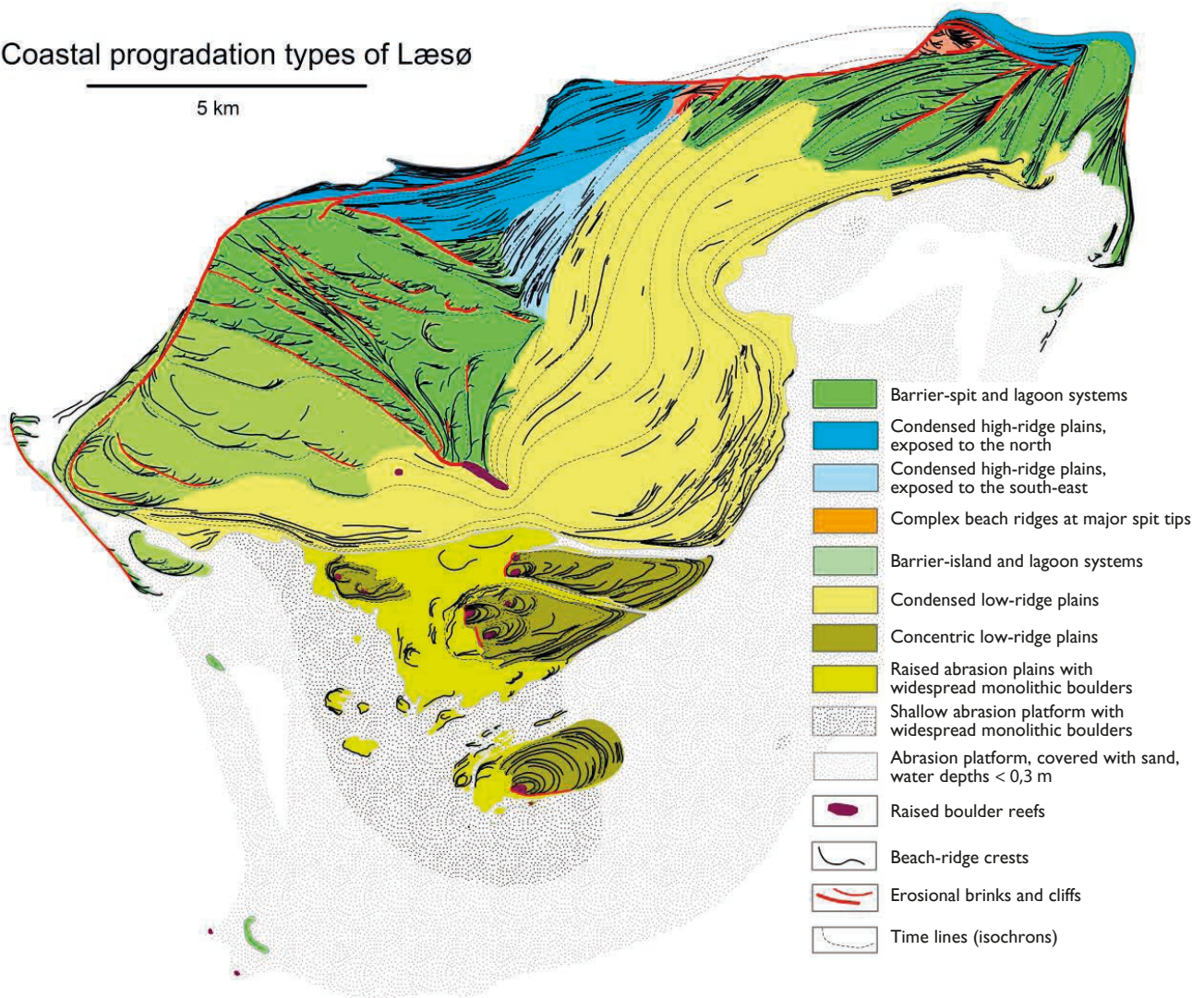


Fig. 5. Coastal progradation types of Læsø, each representing a specific type of coastal origin, morphology and landscape.



Fig. 6. Raised boulder reef around which the saltmarsh island of Hornfiskrøn has been formed, in this case 'Engelskmandens Grav' viewed from south-east.  
(Photo: Lasse Gudmundsson).

boulders jut out of the sand. This kind of landscape is one of the most characteristic Læsø landscapes, e.g. in low saltmarshes forming the western parts of Rønnerne and the western part of Hornfiskrøn. The thin cover of sand on the abrasion plain forms a surface where the elevation above MSL controls the extent of frequent surges. Thereby the saltmarsh vegetation from 0 to 100 cm above MSL becomes clearly divided into a series of level-defined vegetation zones (see Hansen 1995 for classification, levels and vegetation map of Rønnerne).

#### **Condensed high-ridge plains (‘high-rippled washboard plains’)**

Laterally stacked beach ridges forming plains of basically parallel ridges and swales where the widths of swales are of the same order as the widths of ridges (Fig. 8).

Swash heights have been relatively large, enabling formation of gravelly and stony sand berms, mostly up to 0.2–0.9 m above swale level but not exceeding 1.5 m above mean sea level of the time. As deduced from occurrences at e.g. the high part of Holtemmen and the area south of Højsande, such plains developed at quasi-linear beaches where the shoreface was relatively steep. At present, formation of stacked high-ridge plains can be observed at the northern coast of the low part of Holtemmen.

#### **Condensed low-ridge plains (‘low-rippled washboard plains’)**

Vertically accreted sand ridges forming wide plains of basically parallel ridges and swales at coasts protected by shallow water to large distances from the shore (Fig. 9).

Relative to the swales, the height of such beach ridges is generally less than 0.25 m and mostly 0.10–0.15

m. Swash heights were low, typically less than 0.2 m, even during storms, and the beach ridges were mainly formed during storm surges when fine-grained sand was caught in the halophile vegetation growing close to the shoreline (Hansen *et al.* 2012). At present, such beach ridges are generally formed behind a 3–5 km broad sandy coastal plain with water depths less than 0.3 m, where beach ridges accrete to a height of mostly 0.35 m and at maximum 0.6 m before isostatic uplift and invasion of halophile vegetation creates a new low beach ridge on the extremely shallow sand flat some 50–200 m seaward of the preceding beach ridge. Most parts of the agricultural landscapes of southern and south-eastern Læsø, as well as present-time saltmarshes of Bangsbo, Stoklund and Tørkeriet, have formed as such low-ridge plains.

#### **Barrier-spit and lagoon plains (‘tail-fan plains’)**

Spits growing alongshore from a nucleus of pre-existing land from where eroded material has been re-deposited in classic spit complexes (Fig. 10).

The spits are generally straight or slightly convex towards the sea and recurve distally towards the hindlying lagoon. Proximally, most spits are eroded and truncate older recurved spits of the same barrier system. This erosion and truncation may continue to where the youngest part of the barrier recurves towards the lagoon. Overwash fans may occur inside the eroded parts of the spits. Landscapes formed by such spit-and-lagoon systems characterize the raised wetland of Kærene, most of the area immediately south-west of Kærene, and most parts of the Østerby peninsula. At present, the formation of a spit complex can be studied by the growth of Bløden Hale at the easternmost part of Læsø.



**Fig. 7.** Raised abrasion plain (‘sandpaper plain’) with numerous boulders resting on top of the eroded glacio-marine clayey platform. Western part of Kringelrøn. (Photo: Lasse Gudmundsson).

### Barrier-island and lagoon plains ('staircase plains')

In contrast to barrier-spit complexes which are dominated by alongshore transport of sediment, barrier islands appearing seaward of the coastline of the main island were formed by cross-shore sediment transport at a time when sediment sources for alongshore transport disappeared (Fig. 11, Fig. 12).

Originally, such barrier islands have been convex and growing laterally to both sides, forming series of recurved spits at both ends, while the central parts of the islands were gradually straightened during storms by beach erosion and redeposition as overwash fans on the leeward side of the barrier. Through such processes, the hindlying lagoon narrowed and in some

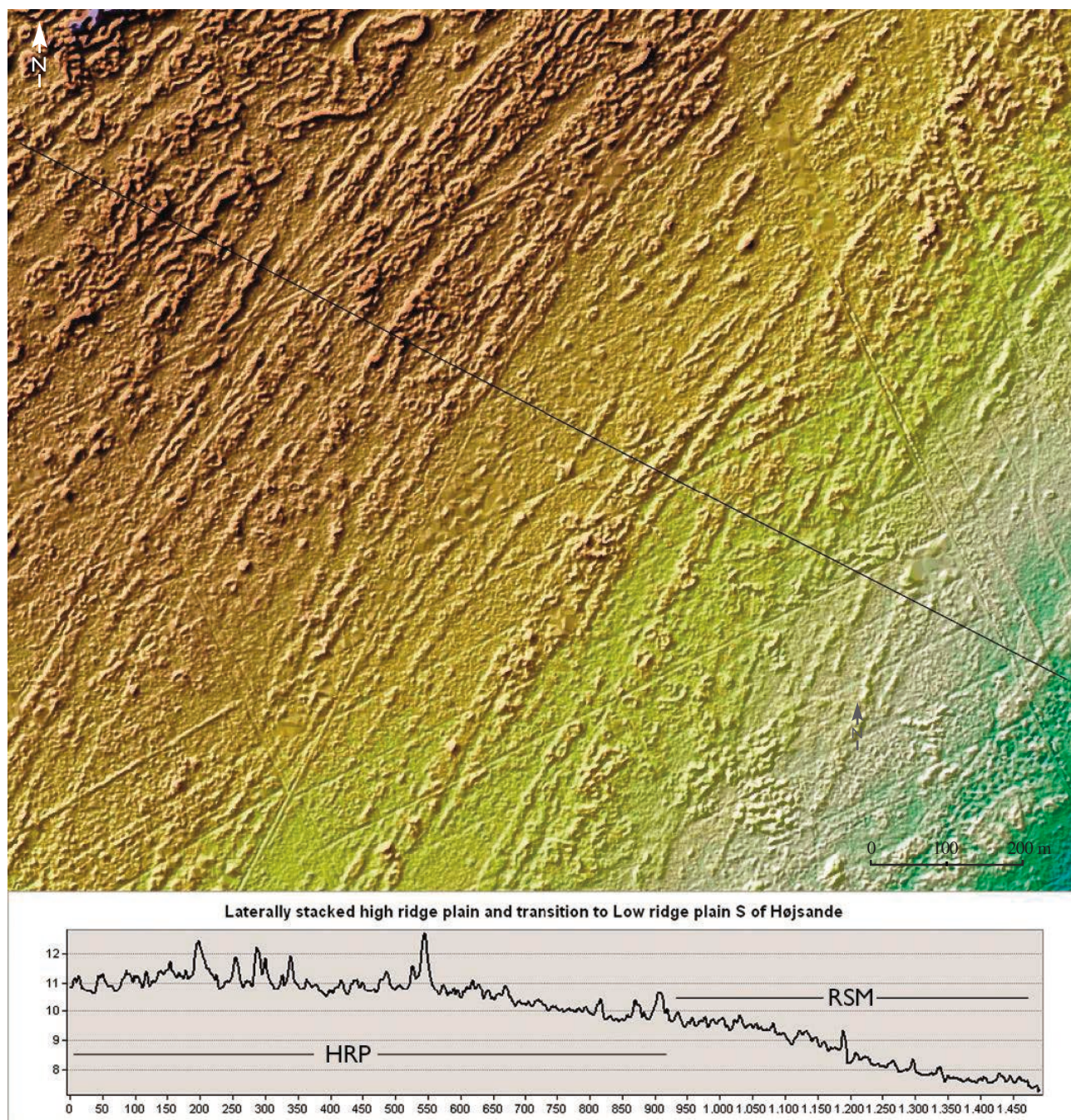


**Fig. 8.** Digital terrain model (DTM) of an area south of Højsande exposing a condensed high-ridge plain (HRP, 'high-rippled wash-board plain') that originally was formed as laterally stacked, linear beach ridges, and a condensed low-ridge plain ('low-rippled wash-board plain') that originally was mostly formed as raised saltmarshes (RSM). In the north-western part of the area there is an incoherent cover of aeolian sand, often in the form of 'dune-ruin' rings consisting of the vegetated foot of larger dunes of which the barren higher (central) parts have been completely eroded by the wind. The profile shows levels (m above MSL) and distance (m) along the black line.

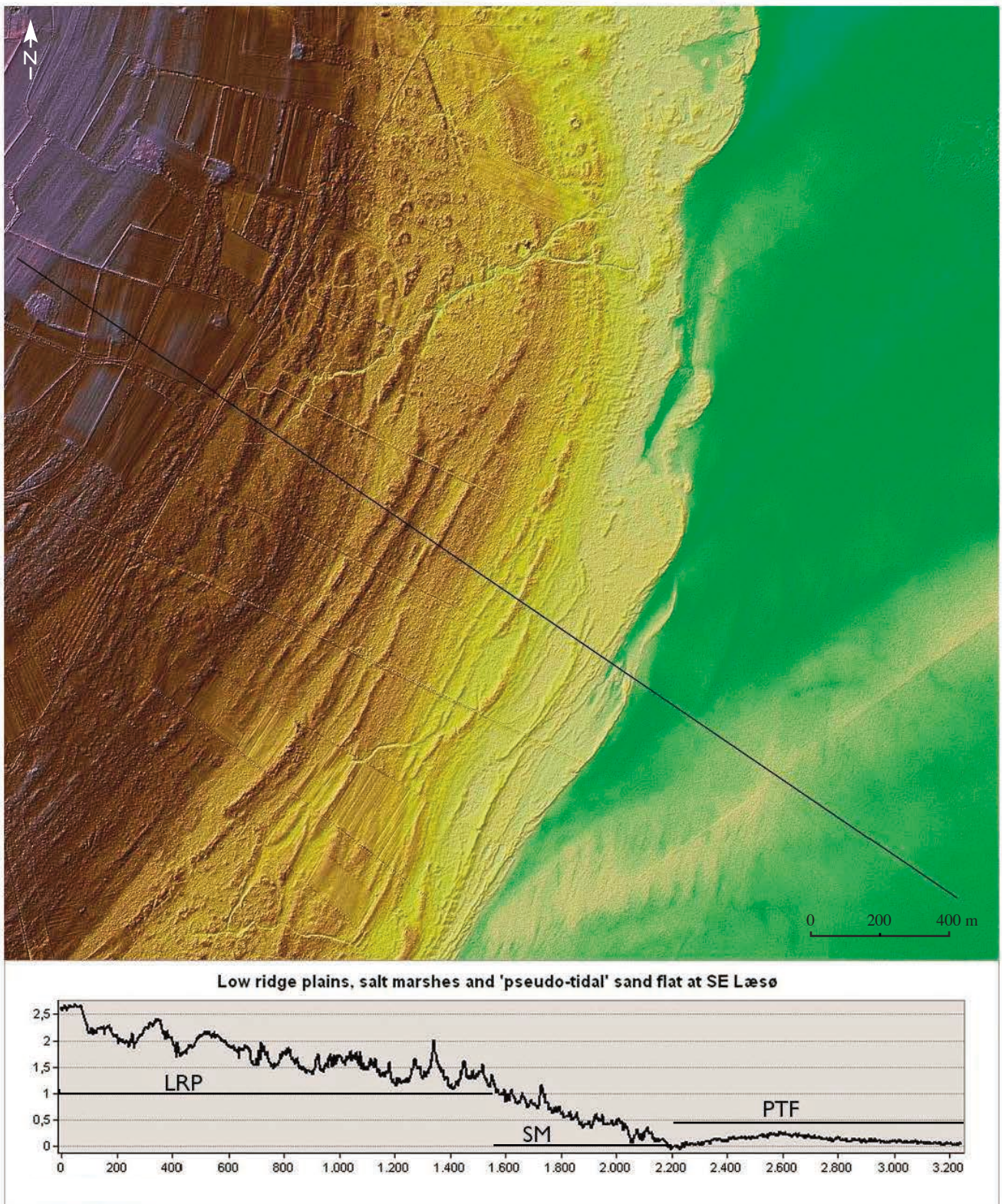


**Fig. 9.** Digital terrain model (DTM) of the Bangsbo and Stoklund areas of south-eastern Læsø showing a condensed low-ridge plain (LRP, 'low-rippled wash-board plain') that originally was formed as saltmarsh, the present saltmarsh (SM), and the partly dry pseudo-tidal sand flat (PTF). The many circular structures in the upper part of the figure are 20–50 cm high ruins of salt-production huts. The profile shows levels (m above MSL) and distance (m) along the black line.

cases completely disappeared when the central part of the barrier connected with pre-existing land. Mostly one, and more rarely both, of the distal ends of the barriers have been preserved. Agricultural landscapes originally formed as barrier islands and lagoons can be found over most of south-western Læsø. Consecutive series of barrier islands may form a 'stair-case landscape' due to a combination of land uplift and

shoreline straightening of the barrier islands. Such terraced landscapes dominate south-western Læsø, where the surface of each terrace is situated within a narrow elevation range and separated from the subsequent terrace by a relatively steep slope or an erosional cliff. At present, the 5 km long barrier island Stokken at the south-western corner of Læsø represents this kind of depositional process, while smaller barrier islands

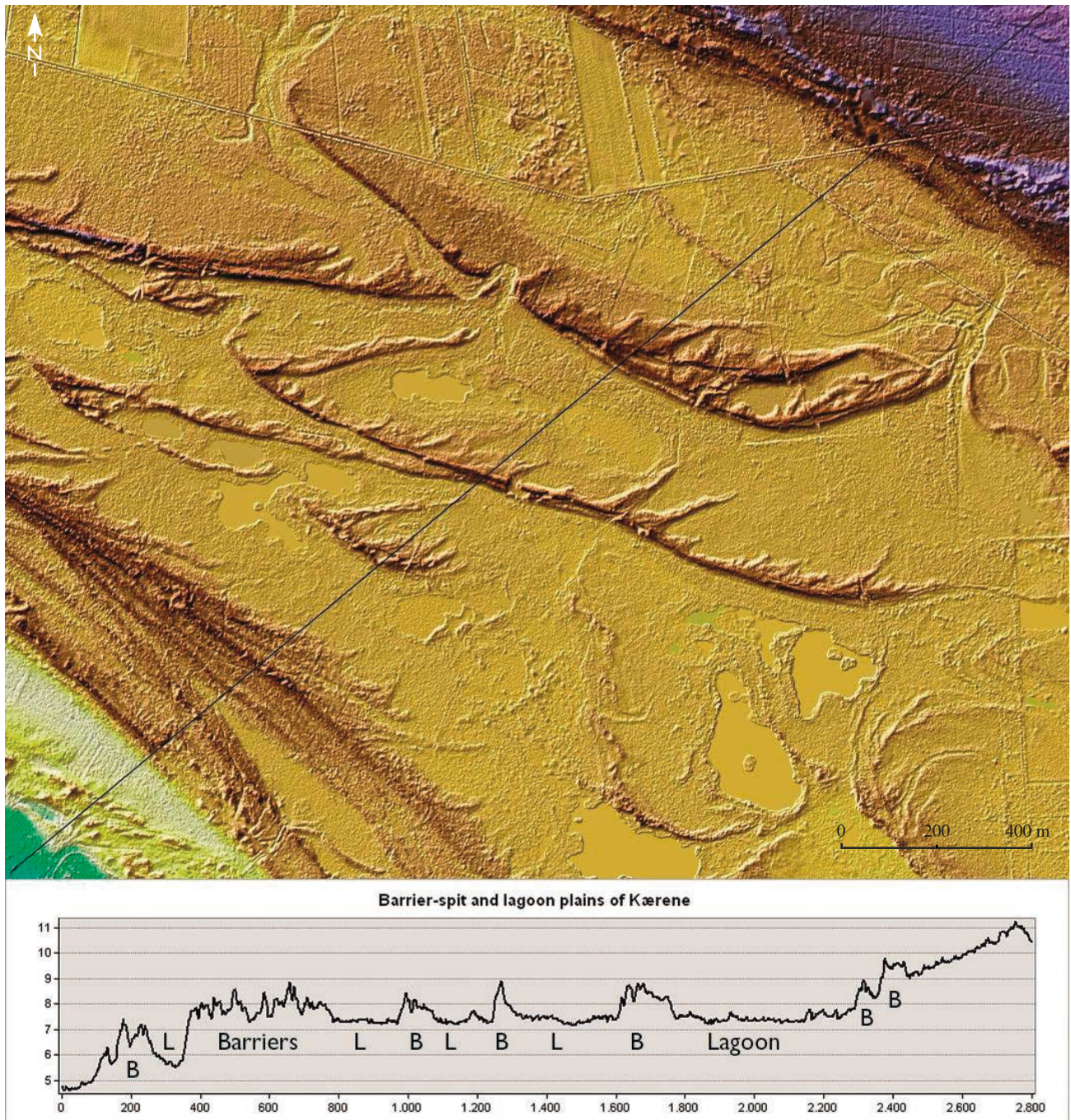


**Fig. 10.** Digital terrain model (DTM) of the raised barrier-spit and lagoon plain (raised 'tail-fan plain') of Kærene between the towns of Vesterø Havn and Byrum. The profile shows levels (m above MSL) and distance (m) along the black line. B: raised barriers. L: raised lagoons.

(Knogene) are emerging south of the Østerby peninsula. At a distance of 5 km south-west of Hornfiskrøn, another 1 km long barrier island began emerging c. 1990 about 700 m inside the boulder reefs of Søndre Rønner.

**Concentric low-ridge plains ('mussel-shell plains')**  
Vertically accreted sand ridges, originally forming isolated islets around raised boulder reefs, surrounded

by extensive shallow water areas (Fig. 13).

Basically, this kind of landscape is comparable with low-ridge plains that are attached to a pre-existing landscape. The main difference is that unattached low-ridge islets and plains comprise successive, concentric, low beach ridges formed around the raised boulder reef. Seen from the air, such islets are usually shaped like mussel-shells with clearly visible

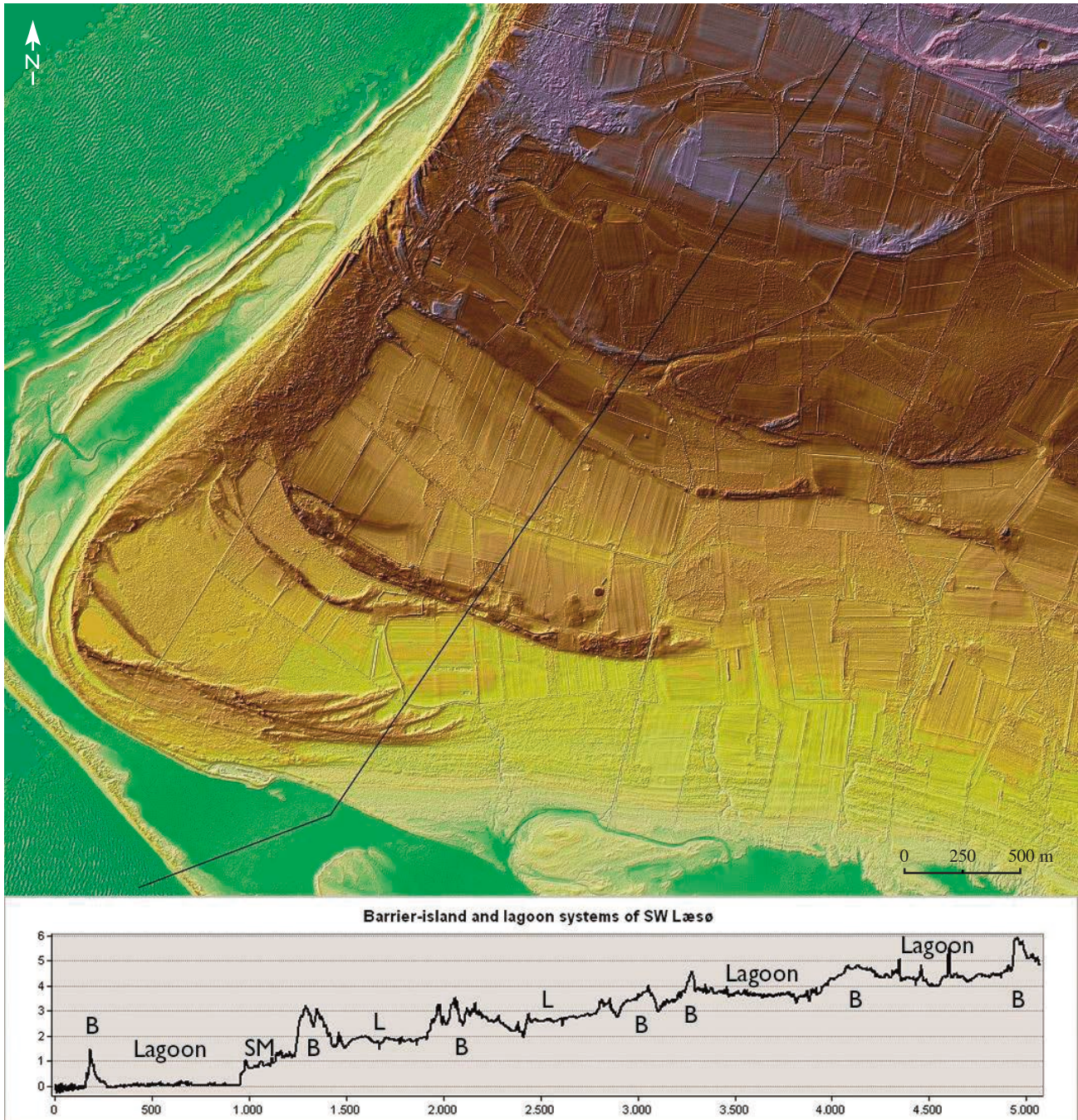


**Fig. 11.** Digital terrain model (DTM) of barrier-island and lagoon plains (raised 'stair-case plains') of south-western Læsø. To the lower left is seen a part of the present barrier island, Stokken. The profile shows levels (m above MSL) and distance (m) along the black line. B: raised barriers. L: raised lagoons.

concentric growth lines. The growth and position of the islets may be governed by local updoming of the substrate as documented in the case of Hornfiskrøn by Hansen *et al.* (2012). Beach ridges exposed to the main wind direction may be eroded, and coastal progradation is largest in the opposite direction. This kind of landscape is represented by the saltmarshes and low heathers of Rønnerne (Langerøn, Kringelrøn, Færøn and Hornfiskrøn) and by a number of islets still emerging south-west of Læsø.

### Shallow, temporarily dry sand plains ('pseudo-tidal flats')

Widespread (about 90 km<sup>2</sup>), coherent flats or plains with water depths less than 0.3 m that have formed south of Læsø by deposition of a thin (mostly 1–2 m) layer of fine-grained sand on top of the eroded glaciomarine platform (Fig. 14, Fig. 28).

In several places the sand cover is less than 1 m thick or absent, and in such areas the residual conglomerate on top of the clayey platform may be directly exposed, while single, or groups of, large monolithic boulders jut out of the sand. This is seen in large parts of the sand plain, particularly in the areas south, north and west of Hornfiskrøn, west of Kringelrøn, south-west of Færøn and south of Tørkeriet (Fig. 14). The cover of fine-grained sand has most likely been transported and deposited by storms at the margins of the sand flat where also low barrier islands may occur, e.g. the low barrier 0.5 km north-east of Søndre Rønner, the islet SSE of Søndre Nyland, and the low barrier islands of Knotterne and Knogene south-east of Læsø. From such marginal positions exposed to weak wave action,

fine-grained sand may be transported onshore during rising water and storm surges.

In periods of up to one month, mainly during the spring and summer months, large parts of the sand flat are dry. During such periods a millimetre-thin crust of temporarily salt-cemented sand normally develops on top of the plains. Such events usually take place 1–4 times every year, and during such periods some aeolian transport occurs, for example when a rain shower has dissolved the salt crust, followed by formation of thin windblown sandsheets and dunes before the next inundation. (photos in Hansen 1977, 1994).

In contrast to normal tidal flats, e.g. the Wadden Sea, this land- and seascape is 'pseudo-tidal' and biologically extremely barren due to the strongly changing environmental conditions over a year (Hansen 1995). The slow alternation between submerged and emerged, and between salt and fresh conditions ensures that the sand flats are nearly barren of macroscopic stationary inhabitants except for the millimetre-long crustacean *Corophium volutator* and a few other species with a very short reproductive cycle. Moreover, due to evaporation during dry periods the salt concentrations in the pore water are mostly between 4 and 16 % (the salt concentration in Kattegat is about 2.4 %). Therefore, also deeply burrowing species like lugworms (*Arenicola maritima*) occur only in places where the pore water salt concentrations are low enough (< 4 %). Some environmentally robust blue-green algae may here and there form thin, loosely coherent algal mats during longer periods of sea coverage. At the innermost part of the sand flat, where it is mainly dry, halophytes like *Statice (Limonium)* and *Salicornia* often form incoherent vegetation.



**Fig. 12.** View from the west of the northern end of the barrier island Stokken with series of recurved spits pointing to the east. Overwash fans are seen to fill in the lagoon by erosion of the west coast of the barrier island. Active as well as abandoned channels of the lagoon are visible. Length of the shown part of Stokken is 800 m. (Photo: Eigil Holm).

### Carbonate cementation of beach, saltmarsh and seabed deposits

Besides these widespread land- and seascapes it should be mentioned that seepage of methane from the glacio-marine clays and silts may locally and occasionally lead to formation of strongly cemented parts of present seabeds, beach faces and saltmarshes, or internally in the marine deposits. Gas occurrences in the glacio-marine deposits are well known from northern Jutland, Kattegat and Læsø (Fredericia & Grambo-Rasmussen 1985; Laier 1992; Laier *et al.* 1992). Gas seepage from younger sediments is also known from sedimentary structures at Læsø (described from the cliff at Bansten by Hansen 1977) and most likely

also from the northern tip of Jutland (Skagen Odde) (Nielsen & Johannessen 2009). Bacterial activity at places where gas seeps to the surface may give rise to cementation by formation of calcite, aragonite or gypsum (Jørgensen 1980) in the matrix of the sediment (Pedersen *et al.* 1989; Jensen *et al.* 1992; Jørgensen 1992). Cemented parts of the seabed around Læsø, of beach faces along the north coast of Læsø, and of the residual conglomerate exposed on Rønnerne, may take form as decimetre-sized to more than 50 m long, hard plates looking much like concrete. In other places cementation is formed around vertical gas pipes deeper in the seabed. Such vertical pipe-like cementations may later be eroded free of the sea bottom to form up to 10

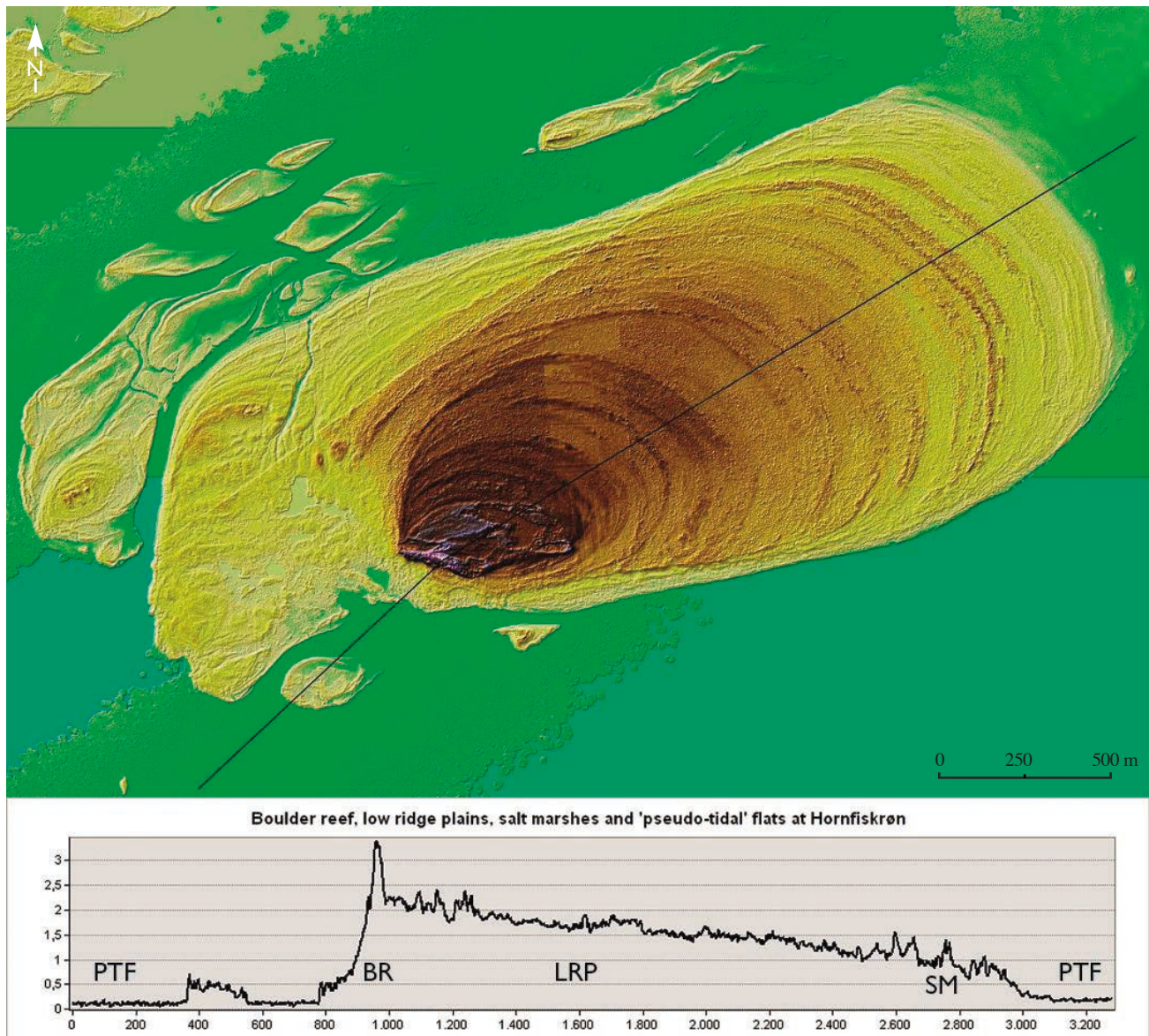


**Fig. 13.** Digital terrain model (DTM) of the concentric low-ridge plain (raised 'mussel-shell plain') of Hornfiskrøn. The profile shows levels (m above MSL) and distance (m) along the black line. BR: the raised boulder reef ('Engelskmandens Grav', photo in Fig. 6). LRP: raised low-ridge plain. SM: present saltmarsh. PTF: pseudo-tidal sand flat.

m high and 2 m wide vertical structures of cemented sand, gravel and fossils (locally named 'corals') that act as substrate for a highly specialized epifauna and algal vegetation. These hard structures are characteristic of the seabed around Læsø and were first described by Nordmann (1903), who already then revealed a precise understanding of this unusual phenomenon.

### Reconstruction of the emergence, growth and coastal development of Læsø

The overall relation of ages, levels and depositional environments of the emerging island and its pre-history can be deduced by plotting the ages of dated samples versus the level of the individual samples. Then, by drawing shore level lines above marine samples and below terrestrial samples and by detailing such lines where the samples represent beach deposits, the level/age relation of relative sea levels (RSL) and terrain levels (RSL plus estimated heights of wave run-up) can be compared with more detailed analyses of beach-ridge levels and their relative chronology of appearance (Fig. 15).

Applying the DTM, a total of about 4000 km of beach ridges have been identified and mapped throughout Læsø. Thus, even low beach ridges are mostly traceable over 1–3 km and frequently up to 7 km in 110 km<sup>2</sup> of the surface of the island. Only in the inland dune fields of Højsande and in the coastal dune fields of eastern Læsø, i.e. in a total area of about 8 km<sup>2</sup>, the beach ridges are mostly obscured. This provides a unique situation where the geometry and relative chronology of the numerous beach ridges can be unambiguously observed and numbered. The island comprises three main areas in which

the beach-ridge formation has progressed towards north, south-east and south-west, respectively (Fig. 4). In order to present basic results of how these sea-level proxies of the present island have been formed, the coastal types and stages are illustrated in Fig. 5, while the results of the emergence history (the age model) and relative sea-level (RSL) displacement are presented later in Fig. 36 and Fig. 38.

The numerous and well separated beach ridges make it possible to establish a formation chronology of the coastal progradation in each of the three main areas. To define a starting point for this chronological numbering of the seaward progradation of the beach-ridge systems it is necessary to know exactly which of the beach ridges is the oldest one in the most elevated candidate area. This problem has been solved by GPR profiling whereby it can be shown which of the ridges has been formed first, and which have been formed subsequently by lateral accretion to the oldest preserved spit. This position was already indicated by Hansen's (1977) studies of aerial photographs, and more robustly by Andreassen's (1986) pioneer GPR profiling. Andreassen's GPR profiling indicated the 'initial spot' to be situated within a 1 km<sup>2</sup> area where northern beach deposits are inclined to the north, while southern beach deposits are inclined to the south. This small area was classified by Hansen (1994, 1995) as the oldest preserved part of the island.

The growth history of Læsø presented below (and in Fig. 4, Fig. 5, Fig. 36) is mainly based on the high-resolution DTM of the island, which forms the basis for a more precise palaeo-shoreline mapping than previously published at scale 1:50,000, as well as a vegetation/level map at scale 1:15,000 of the saltmarshes



**Fig. 14.** Abrasion plain ('sand-paper plain') and sand flat (pseudo-tidal flat) with many boulders resting on the eroded glacio-marine clay platform and jutting out of a thin Holocene sand cover. The largest boulder in front of the photo juts 90 cm out of the sand. South coast of Tørkeriet. (Photo: Conny Andersen).

of Rønnerne (Hansen 1995). The growth history is a result of many years of field work on the past and present coastal development which has previously been published (Jessen 1897; Michelsen 1967; Mörner 1969; Hansen 1977, 1980, 1994, 1995, 2010, 2015; Bahnson *et al.* 1986; Olesen 2005; Hansen *et al.* 2012).

The absolute ages presented in the headings of each sub-section are derived from Table 1, the result of the age model presented in Fig. 36, and the above described 1200 RSL/age index points of the database.

### Formation of a sandy shoal where the present island emerged

Trunks of a *Pinus* forest from the Boreal continental period found 1 km south-west of Stokken show that the Holocene transgression stood more than 2 m below MSL around 10274 years BP (calibrated), while <sup>14</sup>C and OSL datings of the oldest late Holocene marine deposits on Læsø (Table 1, Fig. 15) show that the Litorina transgression at Læsø reached above the highest levels of the preserved beach ridges, i.e. at least 11–12 m above MSL around 6300–5700 years

BP, and that the present island emerged some 800 to 1400 years later (c. 4900 years BP) at a relative sea level of 10.3 m above MSL (Fig. 17).

The ages of the marine deposits between the abrasion platform and the older beach ridges show that the present island emerged after relatively fast deposition of 6–12 m of marine sand in a >30 km<sup>2</sup> area (Michelsen 1967; Hansen 1977, 1995). This amount of marine sand (> 0.3 km<sup>3</sup>) was deposited/redeposited during at least 2500 years (OSL ages of c. 6300 to 4000 years BP). Thus, the erosion of the pre-existing late glacial landscape and redeposition on its surface is clearly related to the transgression by the Litorina sea. The transgression probably began submerging and eroding the Læsø platform c. 8500 years BP and raised the RSL of the region with >13 m from below -2 m (Fig. 15).

Mainly due to the relatively rapid crustal uplift of the area, the RSL transgression soon turned into a RSL regression, which in this region began around 6300 years BP (Fig. 15 and Christensen 1995). As the regression continued, the erosion also continued at

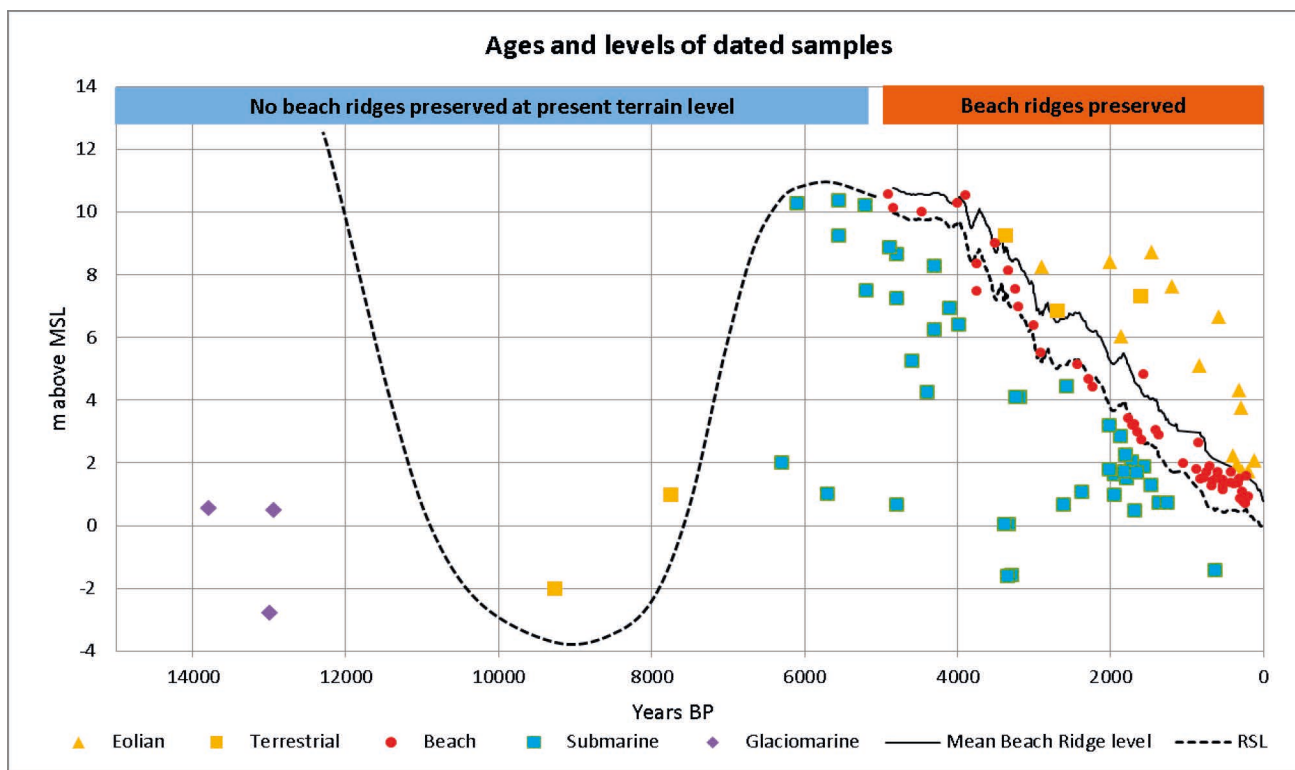


**Fig. 15.** Level vs age diagram of absolute age datings in Table 1 (except for two samples with older ages). Results are shown according to the interpretation of the sedimentary environment of the samples. Yellow triangles: Aeolian sand (i.e. fine-grained sand above beach deposits). Yellow squares: Peat, freshwater gyttja and tree trunks. Red circles: Beach deposits (i.e. mostly relatively medium- to coarse-grained sand with pebbles and stones). Blue squares: Marine deposits (i.e. fossil shells, teeth of two individuals of sperm whale, or fine-grained sand without pebbles). Purple diamonds: Glacio-marine deposits (i.e. fossil shells of *Saxicava arctica*). Solid black curve: Crest level of the island's beach ridges (see text for reconstruction method). Dashed curve below solid curve: Reconstructed RSL (see text for transformation of crest levels to RSLs). Dashed curve for ages older than 4900 years BP: Proposed RSL of the late glacial sea, the Boreal regression and the Litorina transgression until Læsø emerged at 4900 years BP.

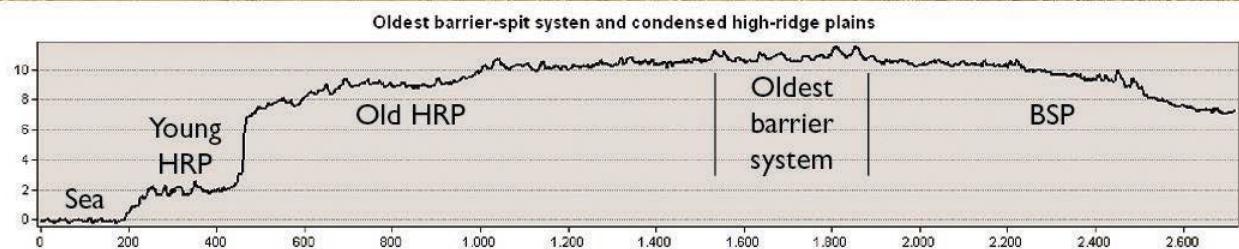
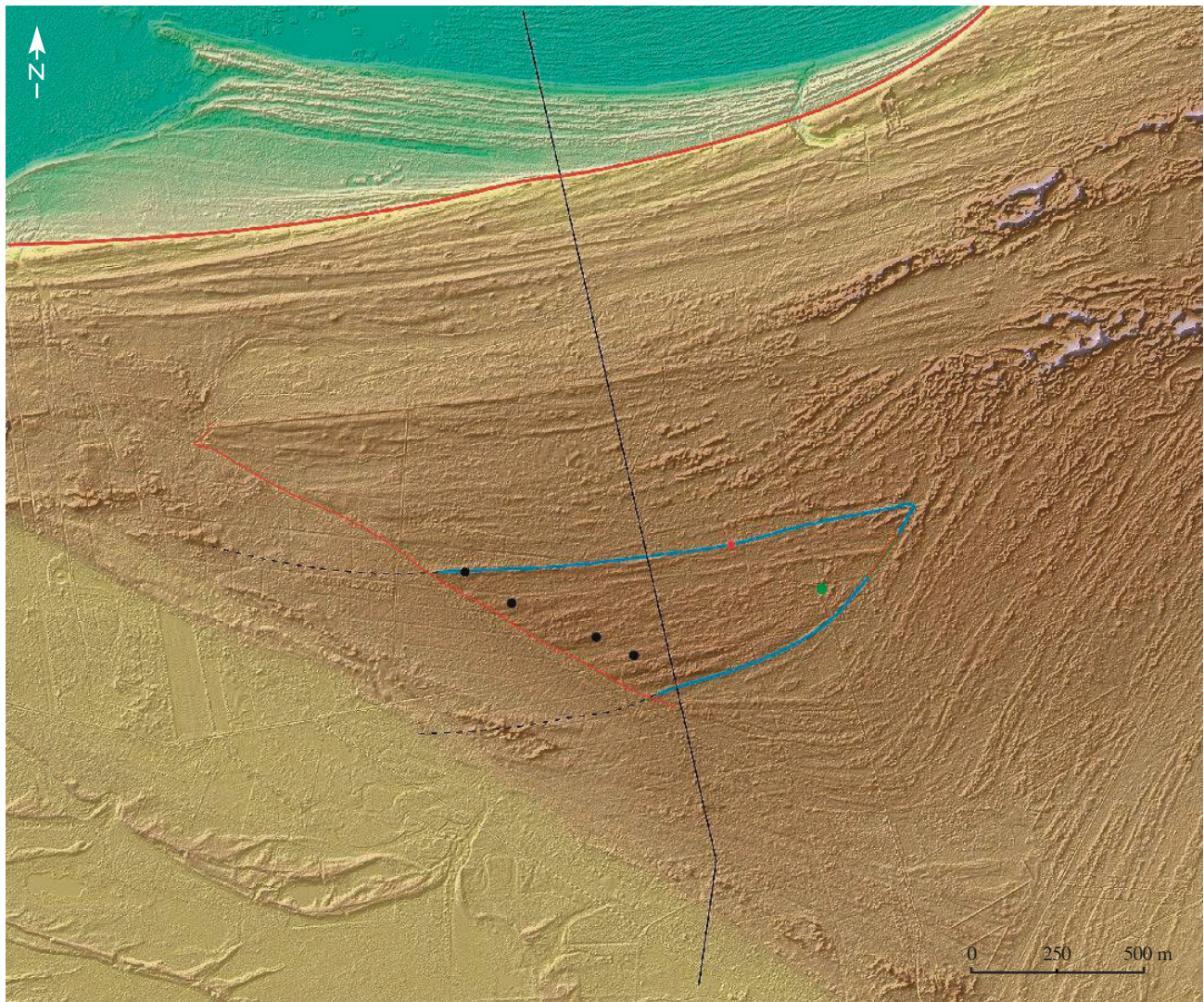


**Fig. 16.** Digital terrain model (DTM) of the oldest preserved part of Læsø, which formed as the easternmost part of a barrier-spit system that subsequently prograded to the north, south, south-east and north-east and was later eroded to the south-west (red line). Blue line indicates the position of Læsø's oldest preserved beach-ridge system, which both to the north and to the south is fringed by younger beach ridges. Black dots: Position of Læsø's oldest OSL dated samples of beach sand found at the present terrain surface (max. 4900 years BP, cf. Fig. 17). Red dot: Position of core boring with five OSL datings ranging from 4300 to 4800 years BP (2.5–6.5 m below terrain). The red dot also shows the position of Læsø's so-called 'birth-stone'. Green dot: Position of pollen samples (Fig. 30) from a thin peat layer (14C-dating: 3375 years BP) deposited in a swale of the initial barrier-spit system, showing that the oldest known forest of post-Boreal stages was dominated by *Taxus* (yew). North of the initial barrier-spit system are seen two generations of condensed high-ridge plains (Old HRP and Young HRP) at Holtemmen along Læsø's north-coast. The two plains are separated by an up to 6 m high cliff (long red line) that was formed after 3000 years BP until c. 1500 years BP. To the south-west are seen parts of the barrier-spit and lagoon plains of Kærene, where the shown double barrier was formed c. 3750 years BP. The profile shows levels (m above MSL) and distance (m) along the black line. BSP: Barrier spits.

more marginal parts of the platform until c. 3200 years BP, which is indicated by four <sup>14</sup>C datings of *Balanus* and *Mytilus* attached to boulders both north and south of Læsø, lying on top of the glacio-marine platform and covered with younger marine sand.

### Emergence of the present island

On top of this sandy shoal the oldest preserved beach ridges of the emerging island were formed c. 4900 to 4000 years BP (see below), i.e. c. 1400–2300 years after the Holocene transgression had culminated in the region. In the berms of the oldest beach ridges, reworked flint tools and pottery are frequently found; these are from a fisher and seal-hunter culture (the Pit-Ceramic culture) that in the south-western Scandinavian coastal regions had adapted to the high sea level of the Litorina transgression and consequent loss of land. The culture existed only in the period c. 5200 to c. 4800 years BP and the Læsø finds probably originate from settlements along the coasts of western Sweden or northern Jutland. The artefacts (Lysdahl 1985, 1987) were probably brought to the emerging coasts of the shoal during seal hunting trips (Hansen 1995).

### The period 4900 – 4000 years BP: The first barrier system attached to older landscapes

The oldest parts of the present island are represented by the eastern part of a 0.7 km broad and 1.5 km long recurved spit system in the highest part of Læsø's beach sediments (between blue lines in Fig. 16) at terrain levels of maximum 11.3 m (corresponding to a RSL of 10.3 m).

OSL datings of this oldest preserved spit system (Fig. 17) show that it was formed between c. 4900 and c. 4000 years BP. The oldest beach ridge has been identified in several GPR sections showing that the ridge at a terrain level of up to 10.8 m is bordered on both sides by slightly younger beach ridges facing to the north and to the south, respectively (Fig. 18). From this and neighbouring ridges, and from the substrate of the ridges, a total of 20 OSL datings have been obtained. Within an OSL age uncertainty range of mostly 200–350 years it is concluded that the oldest beach ridge appeared c. 4900 years BP.

The shape of the preserved part of the spit system shows that the spits migrated from a position north-west to west of Vesterø Havn and recurved towards

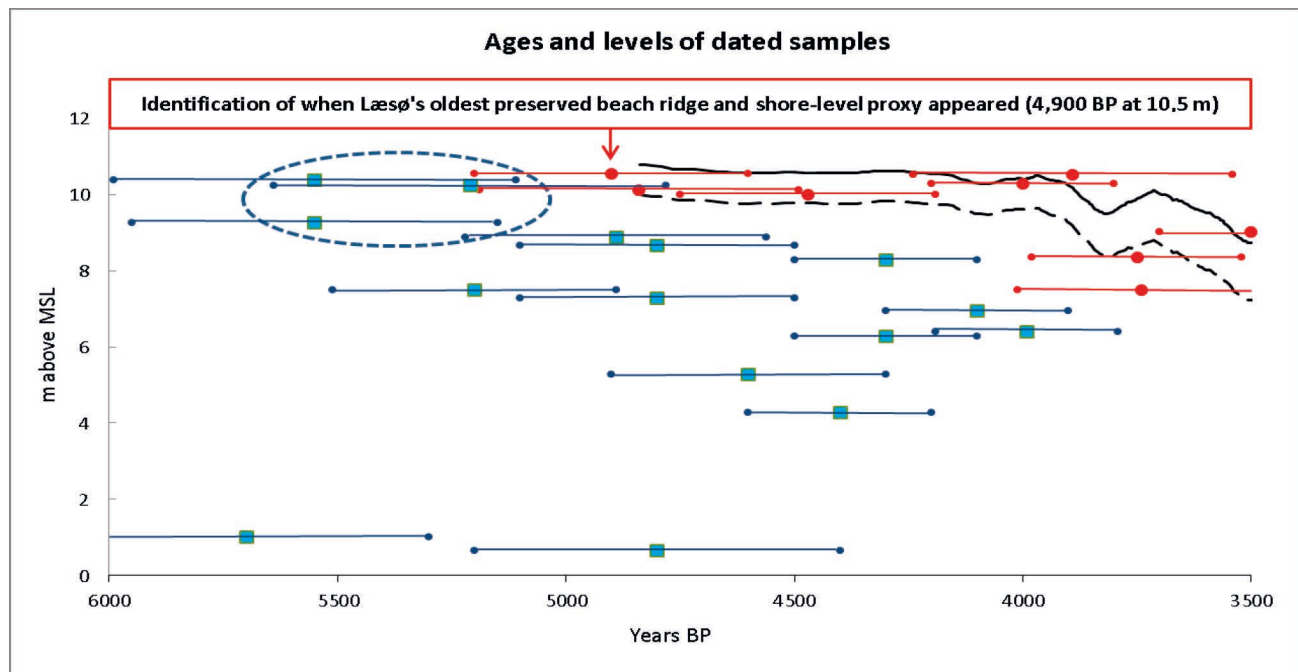


**Fig. 17.** Expanded right part of Fig. 15, addressing when exactly the oldest preserved parts of Læsø emerged. Because the raised shorelines at Læsø are situated up to 3 m higher than contemporaneous shorelines at comparable isostatic isolines in northern Jutland and western Sweden, it has often been discussed if the 'top' of Læsø could be older than suggested by Hansen (1977, 1980, 1994, 1995). The 22 OSL dated samples from the oldest beach-ridge complex, its substrate and nearby beach ridges show that the oldest preserved part of Læsø emerged c. 4900 years BP at a present terrain level of 11 m (sample level 10.5 m; RSL=10.3 m), i.e. 1000–2000 years 'too late' compared to the general isostatic position. It should be mentioned that the three encircled samples have been collected from layers below the OSL dated beach deposit samples at the same locations, thus ruling out that the 'top' of Læsø at a terrain level of 11 m is significantly older than c. 4900 years.

the north-east at its eastern tip. A GPR section crossing the spit system (Fig. 18) displays that while the spit grew eastward it also prograded both to the north and to the south. While the underlying 6–12 m of marine sand is almost devoid of coarse material, the stone and gravel of the superposed spit system most likely was supplied from an emerged land area composed of glacio-marine deposits with a significant content of coarse material. According to the palaeo-shoreline erosional geometry, e.g. the orthogonal relation between the present coastline and raised beach ridges at Vesterø Havn (Fig. 4, Fig. 5, Fig. 36), the source area must have been situated west and north-west of the preserved parts of the spits, i.e. most probably outside

the present north-western coastline, or 6 km or more west or north-west of the preserved part of the system. Judging from the occurrence of large boulders and boulder reefs in the sea north-west of Læsø, as well as the geometry of the spit systems that formed during the ensuing 1500 years, the most probable source area is situated up to 8 km west to north-west of the present island. This area is now completely eroded down to the emerged boulder reefs of Nordre Rønner and Borfeld, to the 8 km long, shallow, sand covered reef, Flaget, between Nordre Rønner and Læsø, and to the many small submerged boulder reefs west to north-west of Vesterø Havn at app. 2–4 m below MSL. Most of these small, submerged boulder reefs have now been

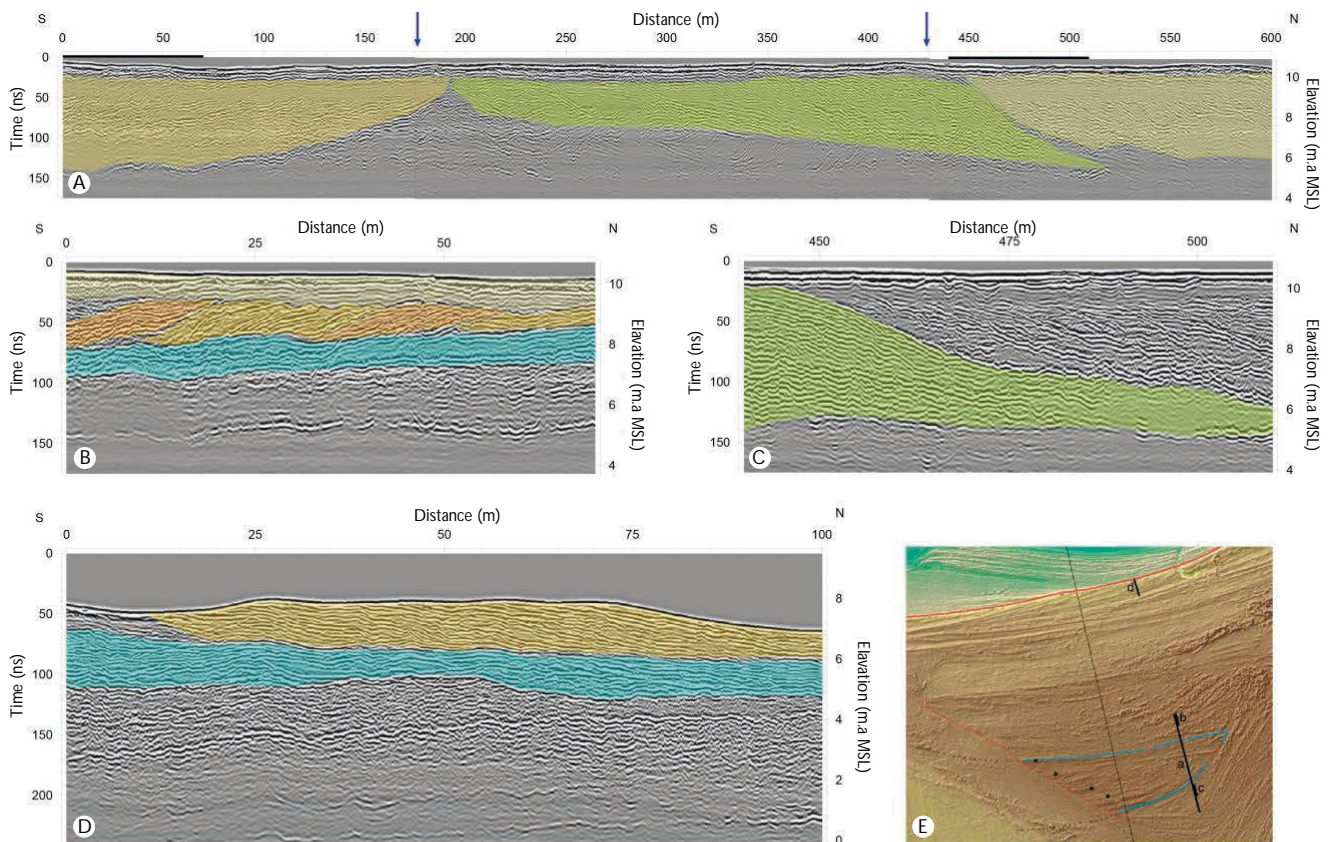


**Fig. 18.** GPR sections of the oldest preserved spit complex of Læsø (A) and subsequent beach ridges formed on the northern side (B) and southern side (C) of the oldest spit. A, a 600 m long GPR profile displays how the oldest part of the island prograded (between the blue arrows). Beach-ridge plains evolved both to the south (0–180 m) and to the north (430–600 m) of the oldest part. Enlargements of the profile sections at 0–70 m and 440–510 m are shown in (B) and (C), respectively. B, section showing that the more steeply dipping beach-ridge and beach deposits (orange) downlap on the more gently sloping shoreface deposits (light blue). The beach ridge is overlain by aeolian sand deposits (light yellow). C, section showing that the oldest northward-dipping spit deposits are overlain by steeply dipping beach and shoreface deposits, illustrating that the island at this stage was more exposed to the south-south-east than to the north, i.e. probably protected by a pre-existing, later completely eroded land area between Nordre Rønner and Læsø. D, section displaying the northernmost and youngest part of the oldest generation of the condensed high-ridge plain. The ridge crests are slightly truncated upwards by wind deflation and cut east of the section by the 6 m high cliff between the old and the subsequent much younger condensed high-ridge plain. Below the coloured parts of the sections are seen major sedimentary structures of the sandy shoal upon which the island's beach deposits were formed. E, subarea of Fig. 16 showing the positions of the GPR sections in A to D.

removed and applied for harbour building at many places in Denmark. Only the most heavy boulders (> 20 tonnes) have not been removed.

### **The period 4000 – 2500 years BP: Linear beach-ridge plains, barrier-spit and lagoon systems, and formation of a twin island**

Shortly after the formation of the oldest preserved system of recurved spits, linear beach-ridge plains began evolving on the south-western, south-eastern and northern side of the initial spit system (Fig. 16). OSL datings indicate that the development of linear beach-ridge plains continued on the south-western side of the initial spit system until c. 3900 years BP, and on the south-eastern and northern sides until c. 3000 years BP.

Around 3900 years BP a new barrier-spit and lagoon system began migrating south-eastwards from Vesterø Havn (Fig. 10, Fig. 24) sourced from the above mentioned area situated west and north-west of Læsø. Simultaneously, another source area began developing to the south near the present centre of Læsø (Fig. 19), where the town of Byrum was initially built on a 1.5 km long and 0.3 km broad boulder reef now protruding from the superimposed younger beach deposits. Here, the Byrum spit and lagoon system began developing around 4000 years BP from a raised, but gradually completely eroded glacio-marine landscape which is now only represented by the raised boulder reef in Byrum and by hundreds of widespread large boulders resting on top of the eroded glacio-marine platform south of Byrum. Due to erosion of this landscape, a large coarse-grained barrier spit (previously exploited in several gravel pits) began migrating to the north. Soon after appearance of the first barrier spit, several new barrier spits and lagoons developed from the Byrum source area at still more westerly positions, while a system of low beach ridges and saltmarsh plains began developing on the eastern leeward side of the initial Byrum barrier (Fig. 19).

Before the Byrum barrier-spit system connected with the Vesterø barrier-spit system, there was a 1 km broad strait between the two 'twin-islands' of the Byrum system and the oldest part of the island that emerged 6 km north of Byrum some 500–1000 years earlier (Fig. 5, Fig. 36). East of the strait a narrower gap developed between the Byrum system and an east-growing recurved spit system from the northern island. This recurved spit system protruded into the sea east of the two initial islands, forming an eastward bulge in the later shoreline pattern when the two islands had coalesced c. 3000 years BP.

Gradually, the Vesterø and Byrum systems inter-fingered with each other and ultimately (c. 3000 years BP) they formed one large 7 km long barrier from Vesterø Havn to Byrum (Fig. 19 and Fig. 24) (on top of

which the road 'På Remmerne' between Byrum and Vesterø Havn has been built in the 1980s). Moreover, the two systems formed the presently 7 km long and up to 3 km broad wetland of Kærene, where present moors and lakes represent former lagoons, while heather ridges between them represent former barriers (Fig. 10).

After c. 3000 years BP and during the following c. 500 years, the Vesterø barrier-spit and lagoon system continued developing and several long spits migrated 5–7 km from a position seaward of the present west coast to Byrum, while further development of the Byrum spit/lagoon system had ceased (as seen in Fig. 19 and Fig. 24).

### **The period 3200 – 2500 years BP: Initial development of the Østerby peninsula**

Simultaneously with the development of barrier spits and lagoons on the south-western side of the island, the north-eastern tip of the island developed with a series of coarse-grained beach ridges. At Bansten (Fig. 20) the beach ridges of this north-eastern tip of the initial Østerby peninsula are cut by an up to 8 m high sea cliff, providing an excellent exposure across the internal structures of the tip (detailed description in Hansen 1977). In the eastern and middle part of the sea cliff, strata with abundant and well preserved trace fossils of the heart urchin *Echinocardium cordatum* are interbedded with strata burrowed by the lugworm *Arenicola marina* (Fig. 21). This interbedding of strata with species living at distinctly different water depths indicate that RSL oscillated significantly in the period 3200–2800 years BP according to absolute age datings of the exposed strata of the cliff. In the eastern part of the cliff, a 300 m long section exposes very coarse-grained beach deposits of the south-east coast of the triangular stage, while in the western part of the cliff more fine-grained beach deposits represent the north coast of the triangular stage.

In the period c. 3200 to 2500 years BP, the north-eastern tip of the island grew 5 km to the east and formed a long complex spit of which the easternmost tip is preserved at Jegens (Fig. 22), where the internal construction of the tip of the spit can be seen in the 7 m high sea cliff east of Østerby Havn. The geometry of the very coarse-grained beach ridges in the preserved parts of the spit indicates that this system was initially derived from glacial or glacio-marine raised landscapes or shoals north of the present island where now a number of boulder reefs represent eroded shoals or completely eroded landscapes that supplied coarse materials for the growth of the long spit.

Moreover, the geometry of the very coarse-grained beach ridges on the preserved part of the easternmost tip of the large spit at Jegens show that the tip was

initially formed as a separate island supplied with materials from the north, and with beach ridges exposed to the west (Fig. 22). However, soon after the formation of this small coarse-grained island it connected with the large spit system growing eastwards from Bansten. Today, the middle part of the 6 km long spit has been eroded, and it might be questioned if it ever existed in one piece. However, several GPR sections from the north coast and southwards

(Andreasen 1986) clearly show that all beach ridges along the north coast of Læsø between Bansten and Østerby Havn were exposed towards the south and south-east, as also seen from the southward inclination of the raised beach deposits in the sea cliffs east of Bansten. Thus, the northernmost beach ridges at the present north coast are parts of later stages of the long spit, and the south- and south-east-facing geometry of the beach ridges at the present north coast shows

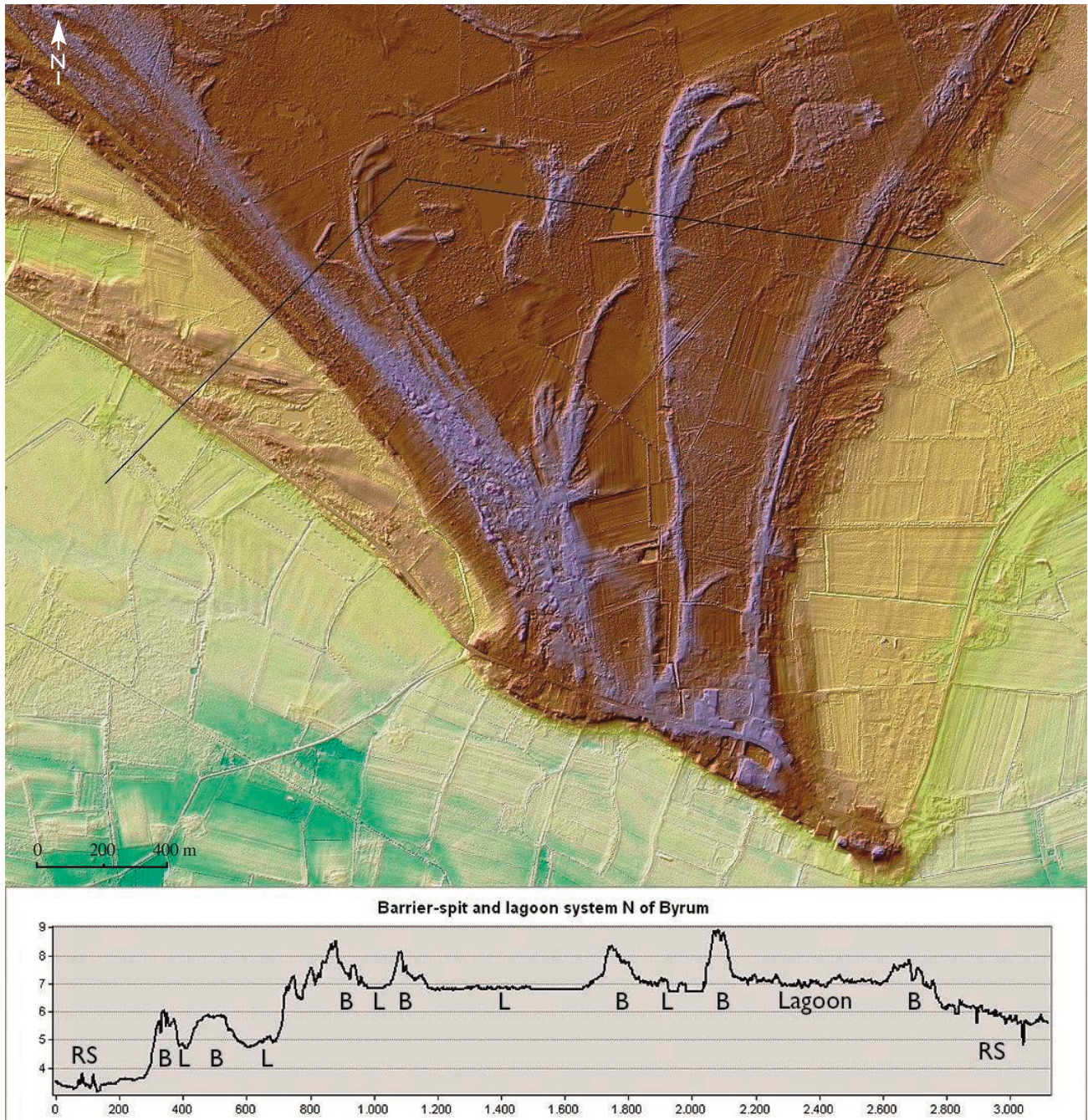


Fig. 19. Digital terrain model (DTM) of the barrier-spit and lagoon plains (raised 'tail-fan plains') north of the town Byrum, which is situated on a raised boulder reef forming the 4 m high cliff in the lower part of the figure. The profile shows levels (m above MSL) and distance (m) along the black line. B: raised barriers. L: raised lagoons. RS: raised saltmarshes (condensed low-ridge plains).

that substantial later erosion has taken place from the north, whereby 3 km of the middle part of the spit were removed so that only its root at Bansten and its easternmost tip at Jegens have been preserved.

**The period 2500 years BP – present: Barrier-spit and lagoon systems of the Østerby peninsula**  
 After development of the 6 km long complex spit of the triangular stage, the development of the Østerby

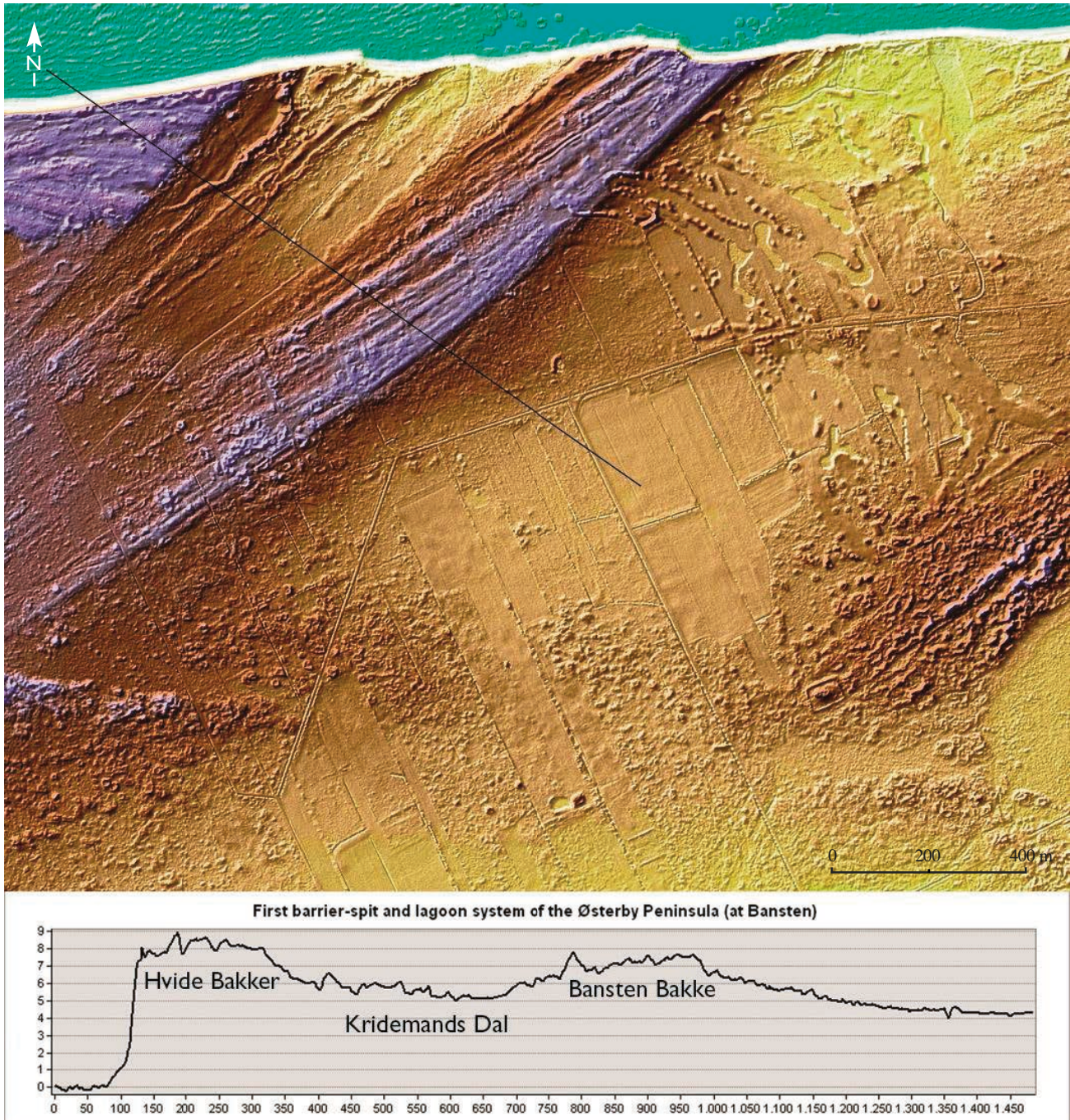


Fig. 20. Digital terrain model (DTM) of the raised barrier-spit and lagoon system at Bansten, i.e. the first of nine barrier-spit systems forming the Østerby peninsula at the south-eastern side of the older triangular island. The raised spit (Bansten Bakke) and raised lagoon (Kridemands Dal) are both cut by the 8 m high present sea cliff. The barrier-spit system in the upper left part of the figure (Hvide Bakker) was formed on the north coast of the older triangular island. The odd terrain morphology seen in the upper right part is caused by terrain regulations of a gulf club. The rectangular structure seen in the lower right part of the figure is the ruin and cemetery of the medieval Hals Church.

peninsula was continued with the formation of a 3.5 km long and very coarse-grained barrier complex (the Hals complex) that grew in west-south-westerly direction from the acute eastern tip of the peninsula. Barrier growth ceased around 1500 years BP and at that time it formed an attached, complex barrier with a shallow lagoon behind. On this barrier the medieval church of Hals (Fig. 20) was built c. 1250 AD, some 750 years after the barrier had been formed, while new settlers in the village of Hals cultivated the raised former lagoons on both sides of the barrier and probably also more westerly in more raised landscapes. Today, the position of westerly fields of the parish of Hals may be indicated by the straight northwards extension of a dune field (lower left of Fig. 20), probably showing that the settlers built a 2 km long shelter belt here. In the 18<sup>th</sup> century the village, its fields and church were destroyed by migrating dune fields most of which continued into the bay of Bovet during the late 18<sup>th</sup> and early 19<sup>th</sup> century. Presently, the barrier system is intensively exploited by gravel digging (Fig. 22).

After development of the initial Bansten and successive Hals barriers, a series of seven further barrier and lagoon complexes formed at the south and east coast of the gradually enlarged Østerby peninsula (Figs 20, 22, 23). The oldest of these is the Gammel Østerby complex which developed until c. 1000 years BP. On the northern side of its lagoon a small Iron Age harbour has been found. The poles were made of yew (*Taxus baccata*), a species that also dominated the forests of the island 3000 years earlier. Tree-ring

dating has shown that the trees were felled in 640 AD (Lysdahl 1985).

Gradually, the growth directions of the barrier complexes swung from west-south-west to south (Fig. 5, Fig. 36). On average the individual barrier and lagoon complexes were formed within periods of 200–250 years. The presently developing barrier complex (Bløden Hale, Fig. 23) grows rapidly towards the south. In 1950 the barrier began passing its lagoon (Bløden) and grew rapidly in front of two small barrier islands (Store Knot and Lille Knot) that had appeared in the first half of the 20<sup>th</sup> century on the eastern edge of the very shallow sand platform south of the Østerby peninsula. During the last 60 years the Bløden Hale barrier has grown 1.5 km towards the south.

#### The period 2500–2000 years BP: Detachment of the island from older eroded landscapes

Around 2500 years BP the barrier and beach-ridge systems formed a triangular area with a present size of app. 45 km<sup>2</sup> (Figs 4, 5, 36). As seen from the geometry of the palaeo-shorelines to the south, west and north-west, this triangular area appears to have become detached from previous source areas, i.e. glacio-marine landscapes or shoals that had finally been completely eroded to below sea level of the time.

Such pre-existing, xenomorphic landscapes most likely included parts of the large arc-shaped area between Læsø and Nordre Rønner, where the eastern side of the present sand-reef of Flaget now forms an 8 km long shallow arc. To the south-east the arc is being

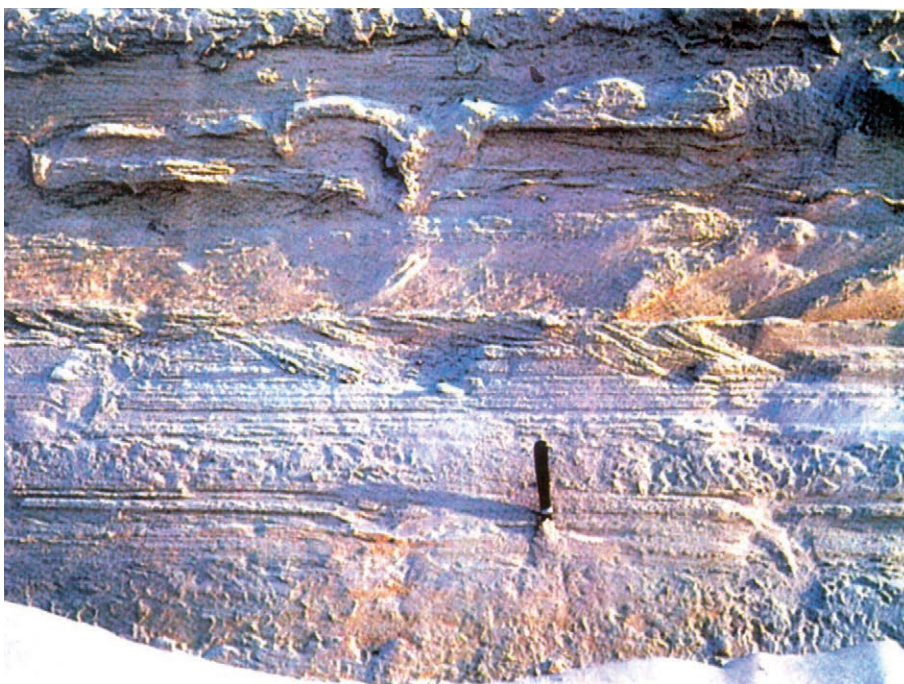


**Fig. 21.** Trace fossils after the heart urchin *Echinocardium cordatum* (in layers behind and below the knife and in the uppermost part of the picture) and trace fossils after the lugworm *Arenicola marina* (funnel-shaped structures in upper part of the picture) exposed in the sea cliff at Bansten. The sea cliff exposes a cross section of the marine substrate (deposited c. 3200 to 2800 years BP) of a large, complex spit system ending 4 km east of the section at Jegens east of Østerby Havn. At present the two species live at distinctly different water depths. The sequence of trace fossils indicates a temporary sea-level fall by 1 m or more, corresponding to the >0.7 m lowstand at c. 2900 years BP found from beach-ridge levels elsewhere on Læsø (Table 4).

re-shaped by the presently north-west growing sand barrier, and to the north the arc is generally submerged under less than 1 m of water. However, as seen from the

east-west trending beach-ridge pattern of the older part of the Holtemmen area, such a probable xenomorphic arc landscape had been completely detached from Læsø

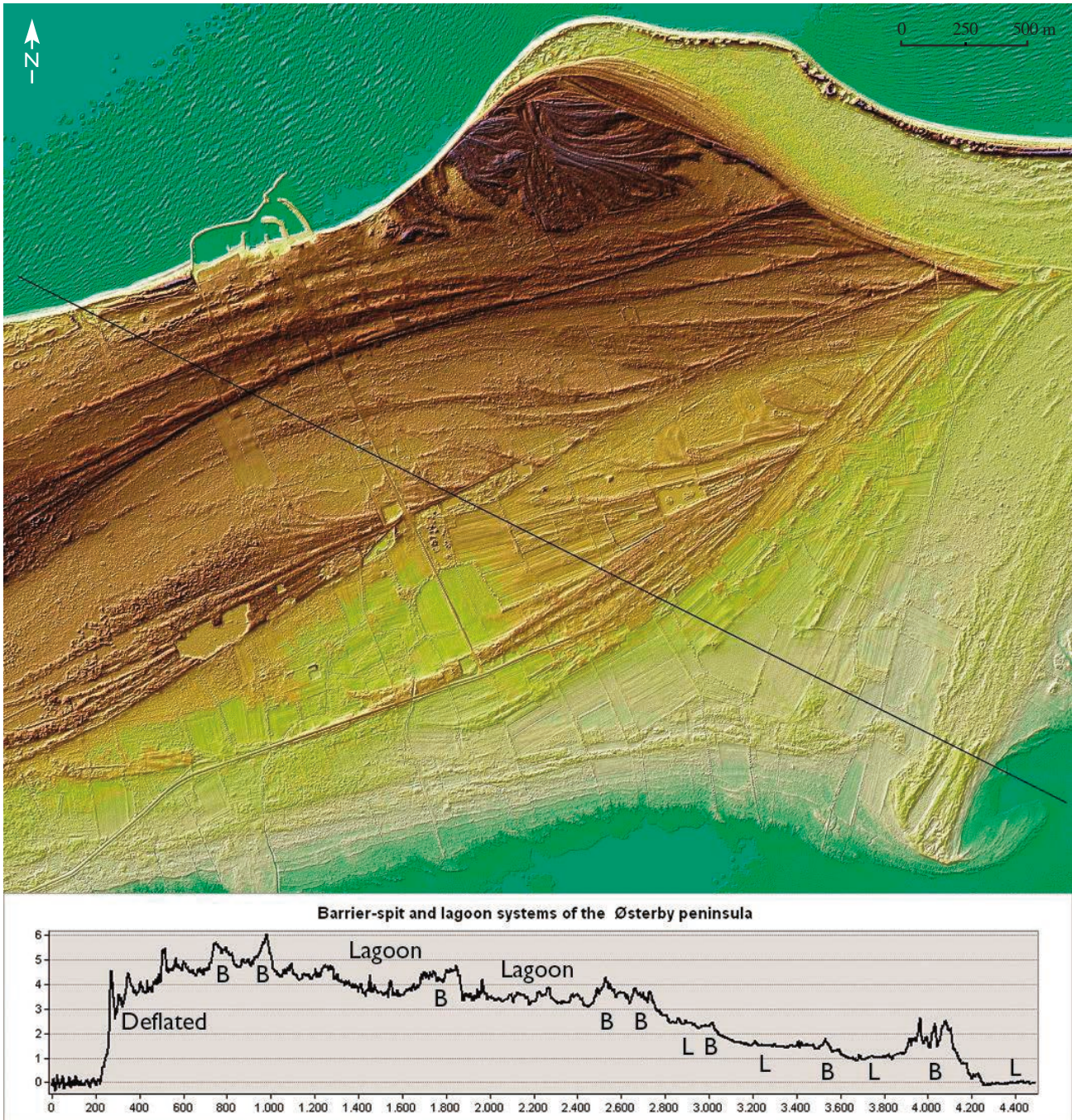
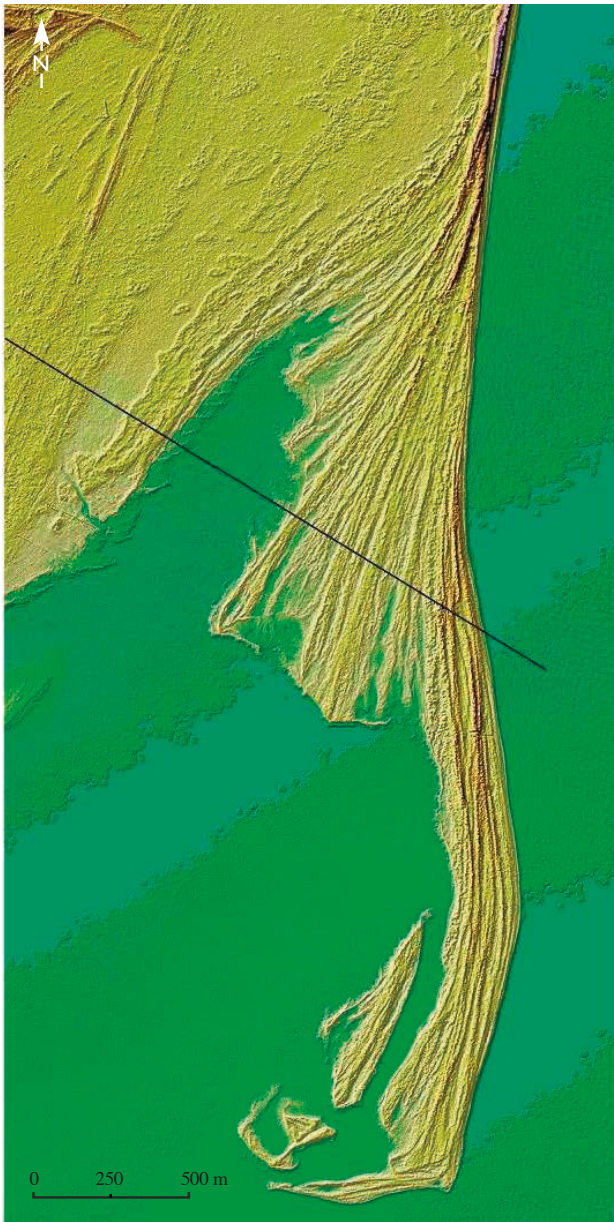
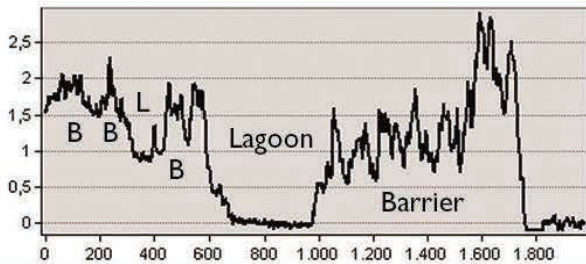


Fig. 22. Digital terrain model (DTM) of raised barrier-spit and lagoon plains of the Østerby peninsula. East of Østerby Havn (harbour) is seen the preserved acute tip of the (now partly eroded) complex spit system stretching from Bansten 4 km west of the harbour (Fig. 4, 5 and 36). The complex spit geometry of the oldest acute eastern tip of the island (800–1500 m east of the harbour) indicate that the tip was initially formed by sediment supply from a landscape north of the harbour before it united with the spit system growing from Bansten. The figure shows parts of five subsequent barrier-spit and lagoon systems (and some gravel pits). All barrier spits are faced to the south-east to east, and barriers close to the coast west of Østerby harbour (at 250–500 m on the profile) have been eroded (lowered) by wind deflation. To the south is seen a young saltmarsh landscape facing the bay of Bovet. The profile shows levels (m above MSL) and distance (m) along the black line. B: raised barrier spits. L: raised lagoons.



**Barrier-spit and lagoon systems at Bløden Hale**



**Fig. 23.** Digital terrain model (DTM) of the barrier-spit and lagoon system of Bløden Hale (barrier) and Bløden (lagoon). Most of the 2 km long 'tail' in front of the two islets has been formed after 1950. The >2.5 m high tops at the east side of Bløden Hale are beach ridges topped with aeolian dunes. The profile shows levels (m above MSL) and distance (m) along the black line. B: raised barriers. L; raised lagoon.

at the latest around 3500 years BP. This interpretation does not exclude that a xenomorphic arc still extended from Nordre Rønner and some kilometres to the south and south-east, but the part nearest to the older high-ridge plain at Holtemmen had definitely disappeared when these ridges were formed. More westerly, i.e. immediately north of Vesterø Havn, where many boulders are found at the shore on the west side of Flaget, there may still have been a xenomorphic connection between Nordre Rønner and Læsø until the 6–8 m high erosional cliff between the older and the younger high-ridge plains of Holtemmen had been formed.

It is not possible exactly to date when the high cliff at Holtemmen began developing. The eroded parts have ages around 4000–3500 years BP, and the formation of a younger high-ridge landscape at the seaside of the cliff began around 1500 years BP or even later. Aeolian drapings on the low beach ridges in front of the cliff were formed during the 17–18<sup>th</sup> century (Table 1). The east–west trend of the older, long and nearly straight ridges shows that pre-existing land immediately north of them had disappeared no later than 3500 years BP and that the present easterly extension of the large arc of Flaget must be a younger feature, although initiated by a pre-existing, more westerly landscape. Consequently, the eastern side of the arc of Flaget is considered to have been built from sand derived by erosion of the western side of the arc, so that the arc by this process of erosion and re-deposition gradually shifted to a more easterly position. This interpretation may also explain the position of many boulders west of Flaget, in particular Læsø's probably largest monolithic boulder, Friises Sten, which is situated 1 km west of the middle part of Flaget, whereas boulders, stone and gravel are not observed on the eastern side of Flaget.

As seen from the palaeo-shoreline pattern at Vesterø Havn up to 2 km south of the harbour, raised beach ridges that developed in the time interval 3500–2500 years BP are perpendicular to the present coast (Fig. 24). These beach ridges were formed by alongshore transport as barrier spits attached to a landscape containing coarse materials, probably a xenomorphic, glacio-marine or glacial landscape west of Vesterø Havn, where now a number of submerged boulder reefs are found at water depths down to 4 m. In the town Byrum at the southern corner of the old triangular area, a steep palaeo-cliff with a height of up to 4 m separates the triangular area from the younger saltmarsh landscape that formed south, east and west of Byrum during the last 2000 years (Fig. 19).

After 2500–2000 years BP, the island had no emerged major contact with glacio-marine land masses to the south, west and north-west (Fig. 11, Fig. 19), and this probably led to a depletion of sources that caused the development of the erosional cliff along the north coast

of Læsø. Instead, the continued coastal progradation of the south-western, eastern, south-eastern and southern parts of the island appears to have been supplied by erosion of the detached western and northern sides of the island, and by erosion of the constantly rising sea-

bed. Likewise, the geometry of the palaeo-shorelines in the eastern part of the present island indicates that coastal progradation continued, mainly supplied by coarse materials derived from the seabed and from erosion of the north coast.

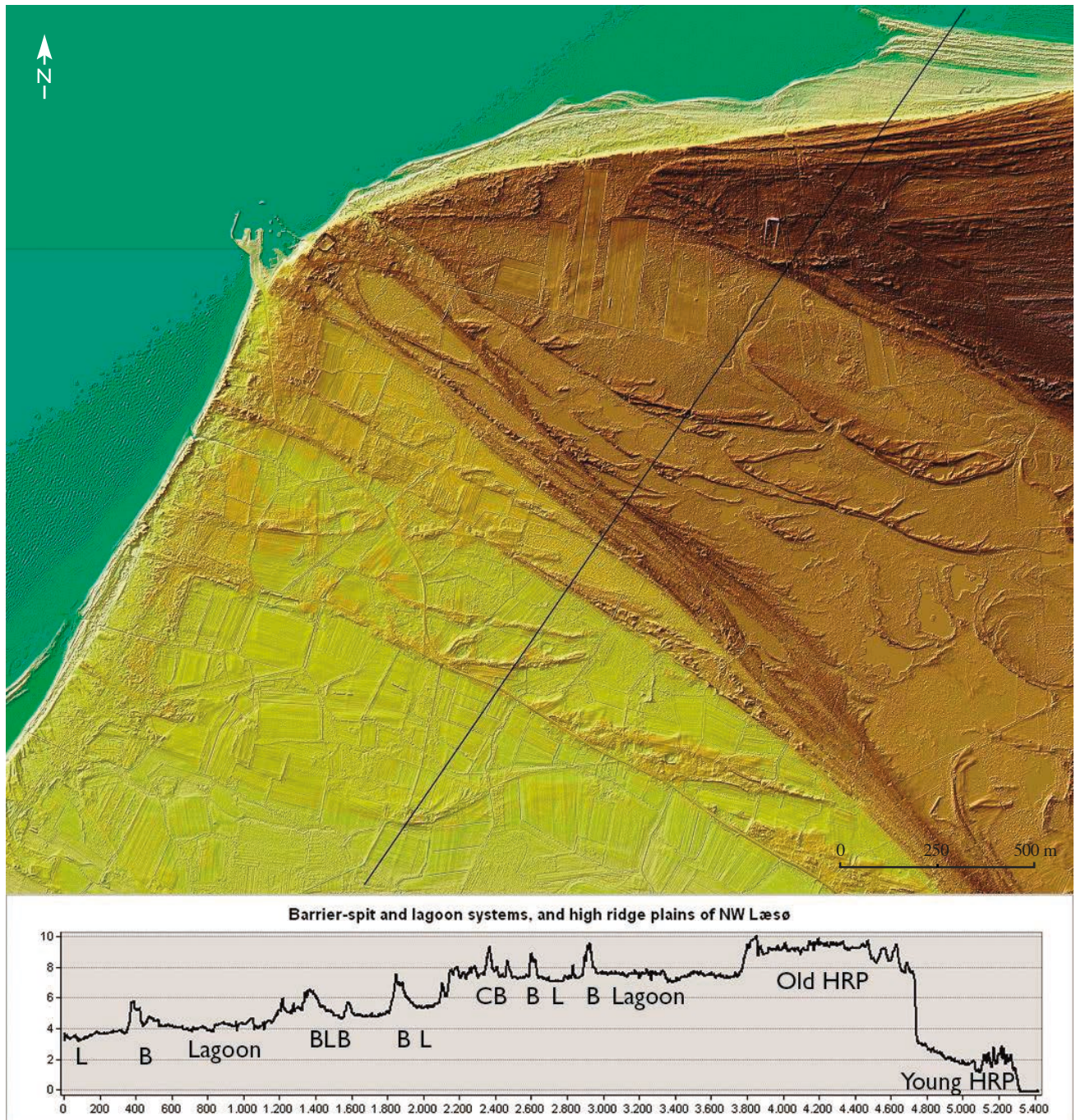


**Fig. 24.** Digital terrain model (DTM) of north-west Læsø showing raised high-ridge plains (Old HRP, 8–10 m above MSL), raised barrier-spit and lagoon plains (B and L, 5–9 m above MSL) and raised barrier-island and lagoon systems (B and L, 3–6 m above MSL). In the raised barrier-spit and lagoon systems, a 7 km long complex barrier is found (CB, 7–8 m above MSL), stretching from the harbour to the town Byrum (Fig. 19). The barriers are almost perpendicular to the present coastline, indicating strong erosion in the past. To the north is seen the raised cliff (8 m above MSL) between the old and young condensed high-ridge plains of Holtemmen. The profile shows levels (m above MSL) and distance (m) along the black line.

For obvious reasons, it is unknown how much material the erosion and formation of ancient sea cliffs supplied to the continued growth of the detached south-western, southern and south-eastern coasts. However, if it is assumed that the slopes and elevations of the removed parts of the island are comparable to the slopes and elevations of the preserved parts, it can be roughly estimated that the removed volume comprises about 30% of the volume that was deposited during the formation of younger parts of Læsø. Consequently, the main part of the sediment contributing to the formation of the younger parts of Læsø was supplied by erosion of the seabed. This is in good agreement with the fact that most of the top of the eroded glacio-marine platform after 2500 years BC was situated at water depths less than 4 m, and that the water depth continuously decreased due to isostatic uplift. At south-western and south-eastern Læsø, most beach ridges formed after 2500 years BP consist of sand, indicating material supply by erosion at some water depth, while many ridges of the older (attached) stages have a considerable content of gravel and stone that most likely were derived by erosion of emerged xenomorphic landscapes or seabed close to sea level.

#### **The period 2500 years BP – present: Barrier-island and lagoon systems of the south-west coast**

After detachment of the island from older and completely eroded xenomorphic landscapes, the coastal progradation of the south-western part of the island was supplied mainly by erosional products from the seabed and by erosional retreat of the north-western and northern coasts (Figs 4, 5). This supply of mainly sand and much less gravel together with isostatic uplift resulted in a series of nine unattached barrier islands, each separated by a time span of 200–300 years (Fig. 11). A GPR section of some of the youngest raised barrier-island and lagoon systems (Fig. 25) displays the internal structure of such systems, including seaward inclined shoreface deposits of barriers, sub-horizontal stratification of lagoon deposits, and erosional structures of draining channels of the lagoons.

The present barrier island of Stokken at the south-west corner of Læsø (Figs 4, 5, 11, 12, 26) developed during the last 100 years. Studies of air photograph (1945–2015) show that the barrier island formed initially at least some 500–700 m from the coast and subsequently migrated 300–500 m closer to the coast (Paradeisis-Stathis 2015). Over time, alongshore sediment transport extended the barrier in both directions. To the north-west, a series of presently five recurved spits developed successively. At the same time, many barrier breaches and washover fans (Fig. 26) transported beach and dune sand from the

seaward side to the lagoon. The position of concrete pylons (for navigation marks) erected in 1965 indicate that since then the barrier has grown to a length of 4 km and has migrated about 300 m landward.

Bird (2008, p. 237) applied Stokken (then named “Knotten”) as a school example of barrier islands in isostatically regressive environments.

In 1991 a new barrier island emerged rapidly 1.5 km west of the north tip of Stokken. During less than one year the island grew to a length of 300 m. The island formed on the inner part of a 10 km long reef stretching northwestwards from Stokken and was built mainly of gravel, stones and about 10% of large reworked, fossil (stone age) shells of *Ostrea* and *Cypripina*. After three years the island disappeared again.

The ongoing and future development of Stokken may be illustrated by the way the two barriers of Vestre Nyland and Sønder Nyland (Fig. 1, Fig. 11) developed from a single barrier island that formed off Læsø at the beginning of the 19<sup>th</sup> century (not on the 1786 map, but on the 1888 map). As now observed at Stokken, this barrier island extended alongshore and migrated landwards. By the end of the 19<sup>th</sup> century, the north-western end of the barrier reached land (Vestre Nyland) and the northern part of the lagoon turned into a brackish lagoon and presently a nearly fresh lake that is drained into the sea through a narrow channel. The south-eastern end of the barrier (Sønder Nyland) never reached land before it was protected from the sea by the emergence of the next barrier island (Stokken) and became a non-migrating island in the lagoon behind Stokken.

Some of the older barriers and lagoons that emerged in south-western Læsø during the last c. 2500 years follow a similar development, while other palaeo-barriers are separated from the preceding barrier with a much broader palaeo-lagoon than seen at Vestre Nyland (Fig. 11). Most of the former barriers are composed of mainly sand, but among them are also two prominent barrier systems of mainly gravel and coarser material, namely the large barrier behind Sønder Nyland (formed c. 800 years BP) and the barrier, formed c. 1500 years BP, on which the medieval church of Vesterø was built. Such occurrences of coarse-grained barriers interspersed among sand barriers may indicate that the isostatic uplift and erosion of the seabed have occasionally exposed glacial, glacio-marine or even younger formations at shallow water depths such that coarse material could be eroded and transported onshore by wave action.

#### **The period 2500 years BP – present: Low-ridge plains and saltmarshes of south-eastern Læsø**

After 2500 years BP, while the formation of the barrier and lagoon coasts of the Østerby peninsula took

place, a completely different kind of coastal landscape began developing on the eastern side of the oldest and easternmost barrier of the Byrum barrier and lagoon system (Figs 8, 9).

The eastward prograding coasts that formed here are characterized by much lower beach ridges than in other contemporaneous parts of Læsø. While the swash height of the barrier systems of northern Læsø are mostly between 0.8 and 1.5 m, the height differences of the ridges and swales in the south-eastern beach-ridge plain are generally less than 0.3 m, often less than 0.2 m (cf. Figs 8, 9), indicating a low-energy environment with small wave heights, resembling the present south and south-east coasts where the 3–5 km broad and very shallow sand platform limits the wave height at the coastline to no more than 0.2 m, even during strong winds (Hansen *et al.* 2012). Where elevated more than 2 m above MSL, most parts of this type of landscape have been cultivated since medieval times, and it is consequently difficult to determine from the lidar maps if all of the landscape emerged as a broad saltmarsh plain similar to the present southern and south-eastern coastal zone.

Separate finds of two large sperm whale skeletons

(*Phyceter catodon*) with  $^{14}\text{C}$  ages of c. 3200 years BP (Hansen 1977, 1995) in the marine sand below the beach ridges in this landscape, app. 0.5 km and 1 km outside the south-eastern coast of the 'old triangle', suggest that the water depths before 2500 years BP were considerably larger than at the present south-eastern coasts. Consequently, the low height of the older beach ridges may be a leeward effect, indicating that south-east storms had no significant effects on the south-eastern coasts in the period 3500 to 2500 years BP.

However, there is a strong contrast between the prominent coarse-grained beach ridges that formed at the eastern end of the Østerby peninsula simultaneously with the constantly prograding, low-relief coasts of south-eastern Læsø (Fig. 9) and north of the bay of Bovet (Fig. 22). This may indicate that strong east to south-east storms during the period 2500 to 1000 years BP were more prominent, and that the bay of Bovet initially was considerably deeper and unprotected from the open sea to the east, while the shallow platform south-east of Læsø had already developed around 2500 years BP, but clearly separated from the deeper waters of the bay to the north. As indicated

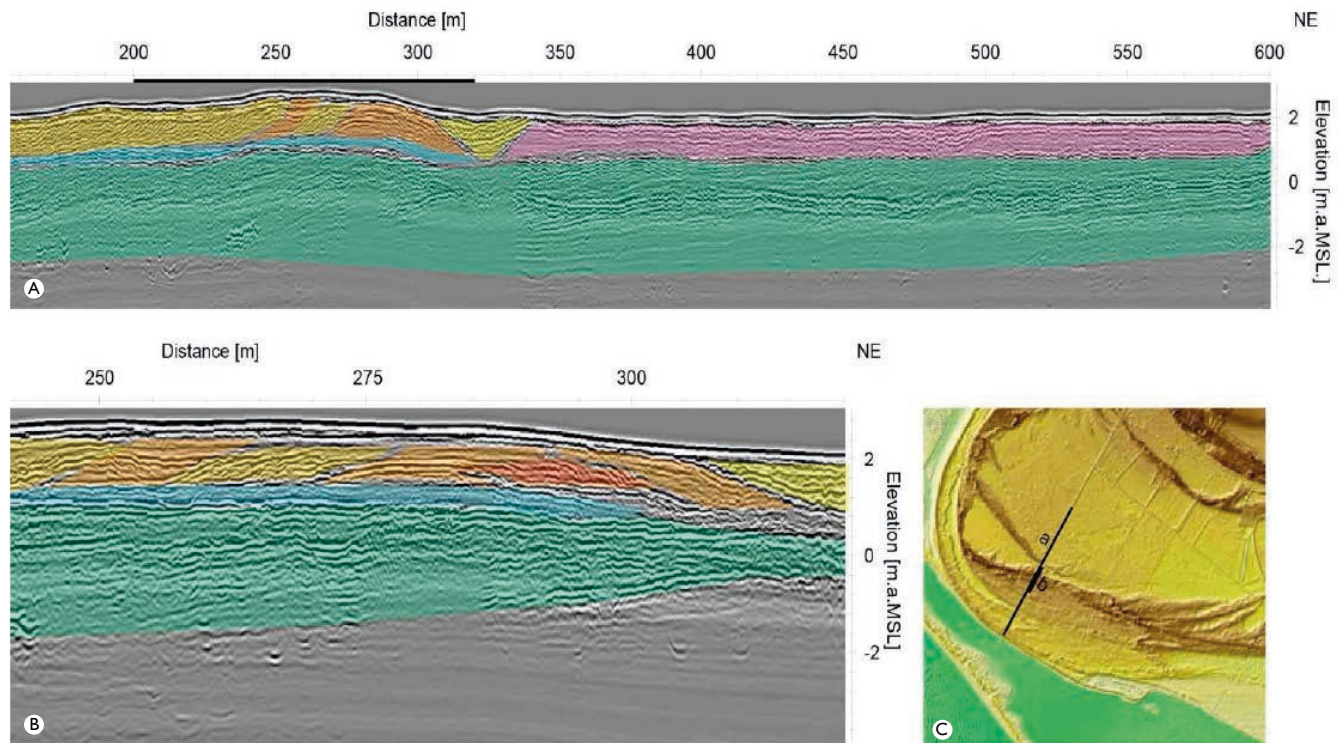


**Fig. 25.** A, GPR section from the south-west coast of Læsø traversing a raised barrier-island and lagoon system. About three sets of seaward (south-westwards) dipping reflections indicate that more than one generation of barriers have prograded seawards (light orange) separated by areas with doming or horizontal reflections (orange). A channel structure (yellow), probably a draining channel of the raised lagoon, separates the barrier from the flat lagoon deposits (pink) with subhorizontal reflections. Subhorizontal shoreface sediments (blue) and older marine deposits are overlain by the barrier. B, enlargement of the north-eastern and oldest part of the barrier. C, subarea of Fig. 11 showing the position of the GPR sections in A and B.

by the level of the top of the constantly rising glacio-marine platform south, south-west and east of Byrum (now around MSL), the water depths at c. 1000 years BP most probably had been reduced to less than 2 m to distances of several kilometres from the south and south-east coasts of that time.

#### **The period 2500 years BP – present: Development of the bay of Bovet**

It is well documented by archaeological finds and historical sources that the water depths in the bay of Bovet, south of the Østerby peninsula and north of the very shallow waters off south-eastern Læsø, were larger than today until the 17<sup>th</sup> and 18<sup>th</sup> century, when the bay was partly filled with aeolian sand from dune fields that migrated across the island from the west and north-west and covered the medieval church of Hals, its village and fields and migrated further to the east and south-east where much of the dune sand ended in the bay of Bovet (Hansen 1995). Before these events the bay was used as a natural harbour for even large vessels (e.g. Stoklund 1973).

In 2010 we found a large medieval vessel 700 m inside the present coastline of the bay, buried under 1.5 m of sand. Tree-ring studies of the planks show that the material is oak, felled in 1383–86 AD in the southern Baltic region. Also recently, a boulder reef including a very large boulder of about 260 tonnes was located 0.5 m below terrain close to the medieval vessel, indicating that the vessel may have been wrecked on this boulder reef and that also the innermost part of Bovet at that time was accessible to large ships.

Today the bay of Bovet is protected to the east by the young barrier of Bløden Hale and a row of young barrier islands (Knotterne and Knogene) that began developing at the mouth of the bay during the 19<sup>th</sup> and 20<sup>th</sup> century. Presently, large parts of the sandy

bottom are often dry and the water depth of the centre of the bay is at maximum 1 m, while the water depth of its draining channel between Bløden Hale and Knogene is 4–6 m.

#### **The period 1000 years BP – present: Saltmarshes of southern Læsø (Rønnerne)**

Shortly after the peak of the medieval sea-level highstand c. 1000 years BP, a number of small and one large boulder reef emerged south of the island (Figs 6, 7, 13, 27) as a result of the long ongoing regional glacial isostatic adjustment as well as the local relaxation uplift (Hansen *et al.* 2012). Thus, a part of the abrasion platform formed a 30–40 km<sup>2</sup> and steadily growing area with extremely shallow water depths, where numerous monolithic boulders on top of the eroded glacio-marine surface jut out of a thin layer of sand (Figs 7, 14). By ice packing, some of the boulders have been piled together to form boulder reefs of various sizes, while others are too large to be moved by such action.

Around such boulder reefs, sand accumulated near sea level and slightly above, forming areas where halophytes like *Salicornia* and *Statice* could invade the new land. Thus, the islands of Langerøn, Kringelrøn, Færøn and Hornfiskrøn began developing as saltmarshes at the shallowest parts of the abrasion platform. Continued accretion takes place in the outer vegetated zone, mostly during storm surges, when sand is caught in the halophile vegetation on top of low beach ridges fringing the raising islands. The islands grew and grow forming shoreline patterns resembling growth rings of mussel shells (Figs 13, 27, 33). As the growth of land continued, some of the initially five small islands of Kringelrøn and Langerøn joined and formed two larger islands, which subsequently merged with each other and Færøn and now form the southern part of the main island. The island of Hornfiskrøn is still separated from the main island by a 1 km broad and extremely shallow sound,



**Fig. 26.** The barrier island Stokken viewed from the north. The picture shows the straightening process of barriers and recurved spits by erosion and formation of overwash fans during storm surges, resulting in a steadily narrower lagoon. (Photo: Eigil Holm).

while new saltmarsh islands continuously emerge and grow at the platform south-west of Læsø.

### **The large sand flat south of Læsø and formation of hypersaline groundwater**

As the upper part of the large sand flat south of Læsø (overview in Figs 1, 2, 5) came still closer to sea level it also remained dry for weeks and months, mainly during spring periods (April to May) dominated by southerly winds, when the sea level of Kattegat is generally around 25 cm lower than during autumn and winter periods of mainly westerly to northerly winds. This periodic drying and the ensuing evaporation of the salty pore water leads to crystallisation of salt on top of the sand. During the next incursion of the sea, this salt dissolves to form a nearly saturated brine (Fig. 28) which, due to its high density, percolates downwards into the sand and accumulates on top of the glacio-marine clay and silt platform, normally less than 2 m below the surface of the sand flat (Hansen 2010).

At the beginning of the 12<sup>th</sup> century, widespread accumulations of such nearly salt-saturated brines were discovered by monks from Jutland who founded a salt industry on the island c. 1150 AD. The salt brine was extracted from shallow wells at the south-eastern shores of Kringelrøn and Langerøn and on the south-eastern coast of the main island (Bangsbo and Stoklund). The brine was evaporated by heating in large iron pans in huts built over or close to the wells (Velle 1991, 1993, 2001). During the following four centuries the number of salt production huts steadily grew and culminated c. 1585 AD, when around 135 simultaneously active salt production huts were situated on a 7 km long row from Bangsbo to Kringelrøn along the south-eastern shores of the saltmarshes (Hansen 2010). The salt production was important for the salt supply of Denmark–Norway and culminated with a total annual export of around 2000 tonnes of salt. A total of 1700 ruins of salt production huts have been discovered on the ancient, raised beaches (Velle 1993, Hansen 2010) (Fig. 27); this large number reflects that the production wells, pans and huts had to be moved seawards as the shores moved due to the isostatic uplift as well as sedimentary progradation of the shores. On average the wells, pans and huts were moved every 19 years (Hansen 2010), corresponding to the Lunar nodal oscillation period, which in combination with the isostatic uplift caused sea-level drops of 7 cm at intervals of 18.6 years and, consequently, displacements by 100–200 m of the shoreline along the extremely flat shoreface of the south-eastern coasts (Hansen 2011).

### **Terrain level effects of forestation, deforestation, agriculture and salt industry**

The preservation of relative terrain levels of sea-level proxies, and thereby sea-level reconstruction, is dependent on the subsequent vegetation development and land-use practices, because continuous existence of natural vegetation may preserve relative terrain levels, whereas long-time agricultural practices such as ploughing, draining, extraction of peat and digging of turf reduce terrain levels. Likewise, precise measurements of sea-level proxies to some extent are dependent on correct understanding of the local environmental and climatic changes. In the case of the decimetre-scale precision at which we attempt to reconstruct the RSL development of Læsø, the initial vegetation and forestation is important in order to understand how sea-level proxies have been preserved, while knowledge about subsequent practices of land-use are important in order to understand where and how levels of sea-level proxies may have been altered. This section intends to provide a summary of terrestrial developments of relevance for the RSL reconstruction at the attempted decimetre-scale precision.

#### **Initial forestation of the island**

As described below, there is circumstantial evidence that the region contained a forested Boreal landscape prior to the Litorina transgression c. 6300 years BP. However, after the flooding and until preserved parts of the island emerged c. 4900 years BP there is no direct evidence of the forestation of the region.

During the period 4900 to 2500 years BP, the oldest preserved parts of Læsø were still attached to a raised glacio-marine landscape north-west of the present island. Trunks of pine, stems of oak, and pollen analyses (see below) from peat on the small preserved part of Læsø's initial beach-ridge landscape indicate that the early coastal landscape, despite its small preserved size (2 km<sup>2</sup>), was vegetated by meadows and a relatively mature forest which would hardly develop in such environments unless it was attached to a more fertile and considerably larger land area. This would also explain how the island later, when it was much larger and completely detached, could become a refuge for the formerly widespread Boreal pine that still covers poor soils in southern Norway and western Sweden, but which is extinct in Denmark with the exception of Læsø where a few large trees and many seedlings have survived until present time and today may be considered endemic – the so-called 'Læsø pine'. A find of red deer (*Cervus elaphus*) in peat on the Østerby peninsula supports this theory, as does king Valdemar Sejr's *Liber Census Daniae* from 1231 which mentions royal hunting of red deer on Læsø, indicating that this large animal

maintained the initial light-open forest and meadow landscape and survived more than 1000 years on the completely detached, but by then much larger island.

#### Evidence from pollen analyses

Due to the widespread practice of 'concentration agriculture' during the 17<sup>th</sup> to early 20<sup>th</sup> centuries, Læsø's

original moors and bogs are now nearly devoid of peat because this has been intensively exploited for fuel and soil improvement (Stoklund 1980, 1986, 1990, 1999; Hansen 1995). Nevertheless, in the 1970s one of us (JS) found and analysed two small peat profiles for pollen, and the results illustrate the initial forestation and vegetation of the older parts of the island.

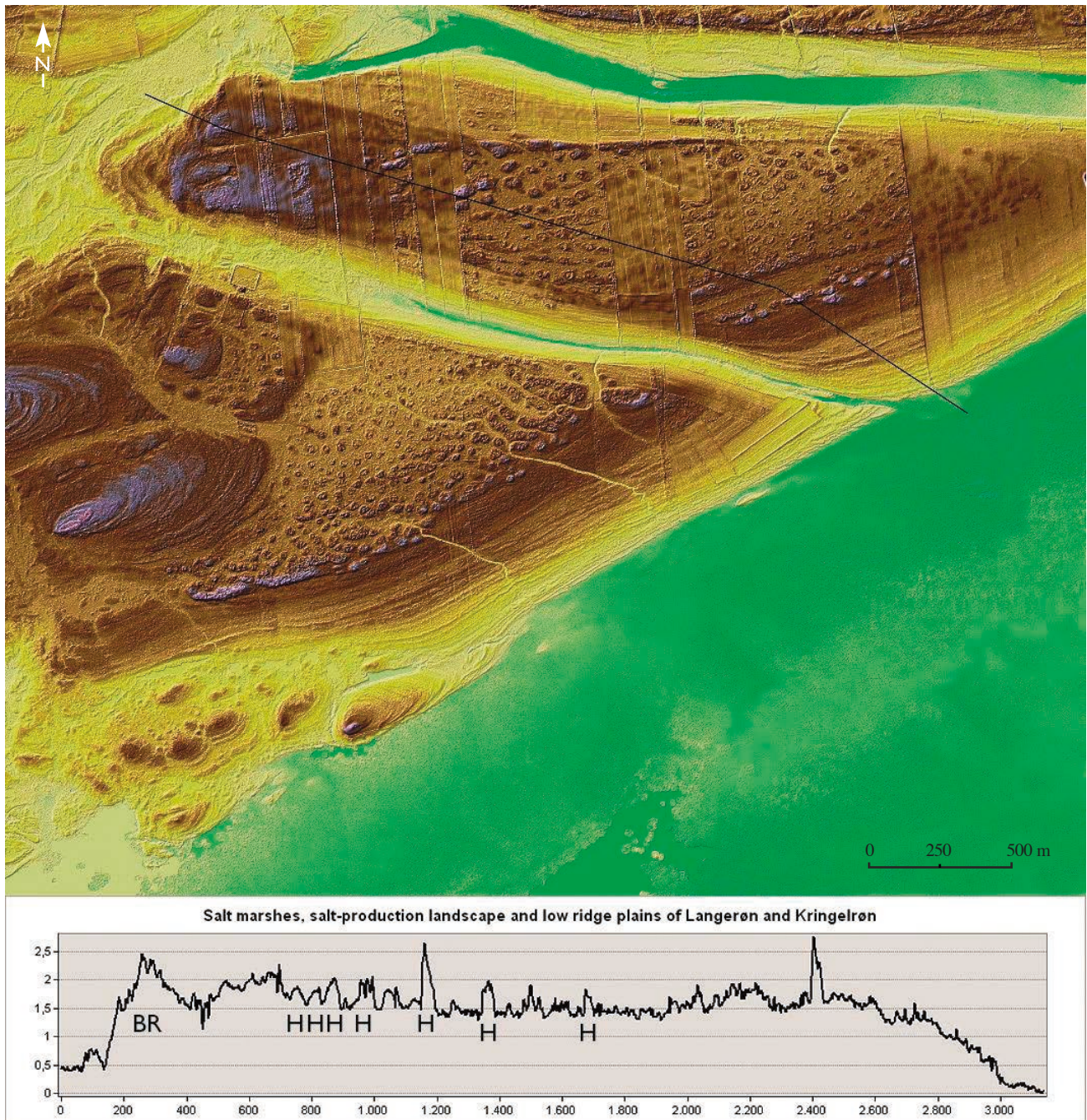


**Fig. 27.** Digital terrain model (DTM) of the raised concentric low-ridge plain of Langerøn (upper part) and Kringelrøn (lower part). The highest parts of the landscape in the centres of concentric beach ridges are small raised boulder reefs. The many 'dots' of the two former islets are ruins after salt production huts built at the shore of any time in the period 1150–1652 AD. In all 899 ruins have been identified on the two islets. The profile shows levels (m above MSL) and distance (m) along the black line. BR: raised boulder reef. H: ruins of salt production huts.

The initial forest on the higher and older part of the island consisted of a light-open forest of trees with light seeds like birch (*Betula*), pine (*Pinus*), willow (*Salix*) alder (*Alnus*) and to a minor degree poplar (*Populus*). Also climax forest trees with heavier seeds like oak (*Quercus*), hazel (*Corylus*), lime (*Tilia*), elm (*Ulmus*), ash (*Fraxinus*), and yew (*Taxus*) were present. It is clear from all pollen analyses that grasses (*Gramineae*) played a dominant role, corresponding well with the origin of the name of the island (in the old Anglo-Saxon language 'Læsø' (læsoy) means 'grass island').

Pollen analyses (Fig. 29) of peat from a swale of Læsø's oldest beach-ridge system that formed 4900–4000 years BP (<sup>14</sup>C dated to 3375 years BP) show that the forest of that period (at least at that very location) was dominated by yew (*Taxus baccata*) and grasses (*Gramineae*) with minor amounts of light-open forest trees as well as climax forest trees such as ash (*Fraxinus*). Also note the occurrence of *Plantago lanceolata*, *Plantago* cf. *media*, *Artemisia* and *Chenopodium*, indicating the nearby coast and maybe also some human influence.

The diagram from peat at Træbakke (Fig. 30, <sup>14</sup>C dated to 3355 years BP), which according to our age model is slightly younger than the above-mentioned vegetation, represents the lower part of a thin peat profile very close to the western tip of the preserved part of Læsø at that time. The pollen diagram indicates a light-open forest dominated by birch (*Betula*), pine (*Pinus*), hazel (*Corylus*), ash (*Fraxinus*) and oak (*Quercus*) with alder (*Alnus*) and willow (*Salix*) indicating moist soils, and with only minor amounts of other climax forest trees. The amount of grasses is high and weeds like *Plantago lanceolata*, *Artemisia* and *Chenopodium* are again present. The high amount of coastal indicators

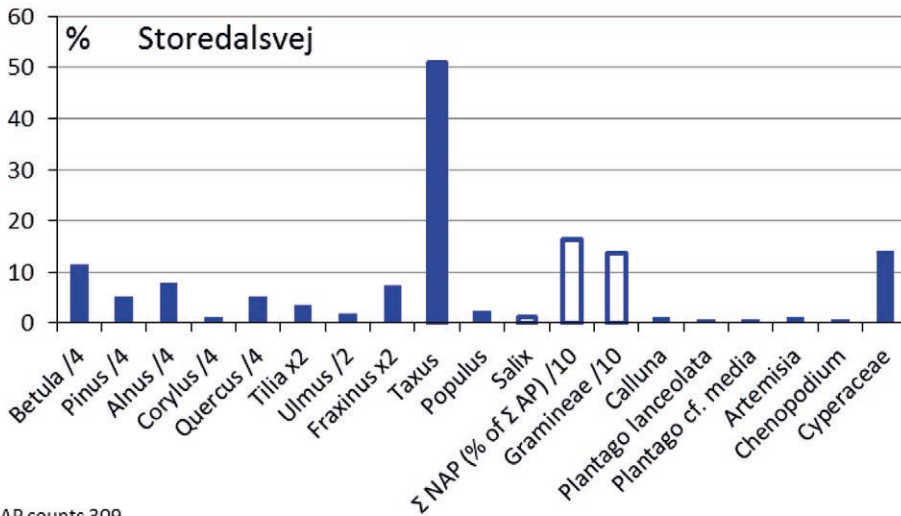
(*Plantago lanceolata*, *Plantago maritima*, *Artemisia* and *Chenopodium*) indicate that the site was close to the coast. However, the tree distribution also indicates a nearby rather mature forest cover. Yew is common in similar poor, light-open forests of southern Sweden.

Figure 31 shows pollen analyses of four samples from a peat found in a younger part of the 'old triangle'. Sample 71/984 is taken from a layer with charcoal that is <sup>14</sup>C dated to 2680 years BP. After the charcoal formation (burning), an increase in yew (*Taxus*), willow (*Salix*), elm (*Ulmus*) and poplar (*Populus*) and a decrease in pine (*Pinus*), lime (*Tilia*), ash (*Fraxinus*), grass cover (*Gramineae*), heather (*Calluna*) and weeds (*Plantago lanceolata* and *Chenopodium*) is significant.

Yew (*Taxus*) is very rare in other parts of Denmark (only finds of single pollen grains), but it is obvious that it was abundant on Læsø until more recent time. However, until the early medieval age *Taxus* was a dominant pioneer tree of many southern Scandinavian coastal zones (Sarmaja-Koronen *et al.* 1991), but because all parts of *Taxus* are highly poisonous to humans, cattle and horses, the species has been sought extinguished from inhabited areas. South of Østerby Havn a harbour for small vessels was built of poles of *Taxus* felled in 640 AD, and from the medieval settlement of the island around 1100–1300 AD some location names may indicate which kind of forest the settlers met and cleared for agriculture (Stoklund 1980, 2007; Hansen 1995). Thus, the medieval Danish name of *Taxus* appears in two local names (Irumgård and Irum Have) on south-east Læsø, while Hornex and Jegens Odde on the north part of the island refer to *Quercus*. The name 'Lunden' of a forest on the central part of the island means a mixed, mainly deciduous forest.



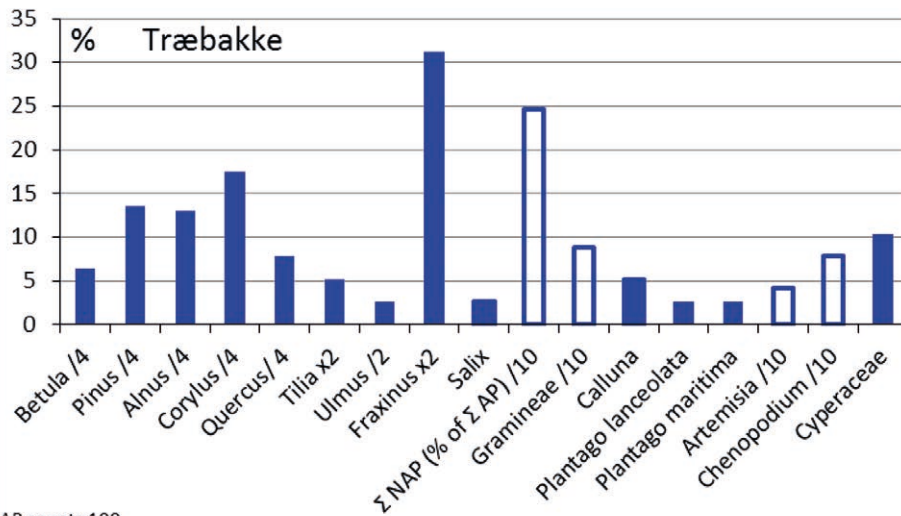
**Fig. 28.** After days or weeks of drying, evaporation and salinization of the sand surface, the sea returns to the sand flat south of Læsø as a widespread thin film of sea water with an initial salt content of 2–2.5%. By dissolving salt that crystallized during the preceding period and by mixing with hypersaline pore water, the film of incoming sea water becomes nearly salt saturated. Consequently, the water film becomes a heavy salt brine with a salt content of 10–16% that percolates downwards until it hits the low-permeable glacio-marine clay platform 1–3 m beneath the surface or already accumulated, equally heavy salt brine. (Photo: Lasse Gudmundsson).



AP counts 309

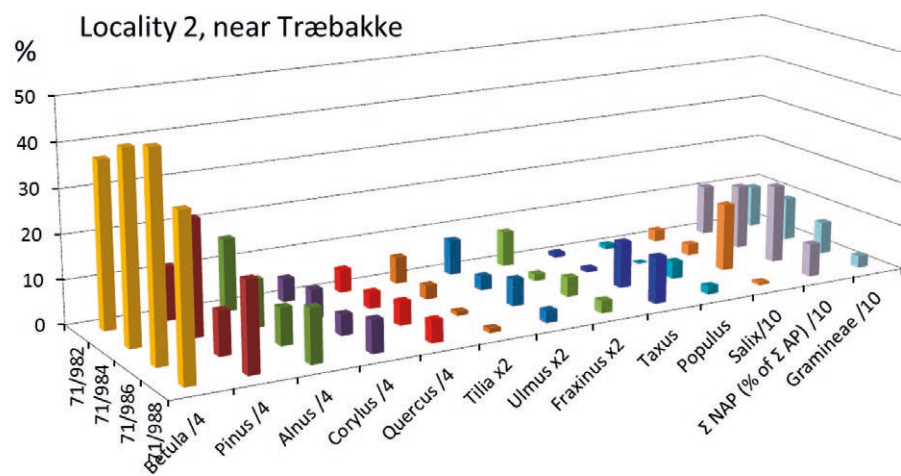
len ( $\Sigma$ AP) is given in the lower left corner of the diagram. The extremely high concentration of yew (*Taxus*) pollen could make it plausible that the yew pollen derive from a local stand of trees. Non-arbores pollen grains are almost entirely grasses (*Gramineae*).

**Fig. 29.** Pollen counts from a thin peat profile (No. 34 in Table 1, green dot in Fig. 16) from the oldest preserved part of Læsø that formed in a spit system 4900–4000 years BP (peat  $^{14}$ C dated to 3375 years BP). The y axis represents percentages relative to total Arboreal (tree) Pollen ( $\Sigma$ AP). The counts are reduced as indicated to give a more proper forest tree distribution compared to herbs (see Methods chapter). Some pollen counts of herbs, especially grasses, or bushes (Non-Arbores Pollen, NAP) are reduced by 10 for better overview only (white columns). The total counted tree pollen ( $\Sigma$ AP) is given in the lower left corner of the diagram. The extremely high concentration of yew (*Taxus*) pollen could make it plausible that the yew pollen derive from a local stand of trees. Non-arbores pollen grains are almost entirely grasses (*Gramineae*).



AP counts 100

**Fig. 30.** Pollen counts from the bottom of an almost 1 m thick peat profile at Træbakke (No. 14 in Table 1). Explanation as in Fig. 29. This part of the island was formed as a condensed high-ridge plain 4000–3500 years BP. The peat is  $^{14}$ C dated to 3355 years BP. The age may be underestimated as the peat contained many younger alder roots of which all visible parts were removed before dating. No yew (*Taxus*) were found (only 100 pollen grains were counted) and ash (*Fraxinus*) is dominating, together with grasses (*Gramineae*), *Artemisia* and *Chenopodium*.



AP counts 352,506,1087,771

**Fig. 31.** Pollen diagram from a ditch side peat profile, 16 cm thick. Explanation as in Fig. 29. This landscape was formed as a barrier-spit and lagoon plain 3500–3000 years BP. Sample 71/984 was  $^{14}$ C dated to 2680 years BP (No. 12 in Table 1). There are 2 cm between the samples and sample 71/982 is the bottom. The counts are reduced by the indicated factors for pollen productivity in order to give a more realistic forest tree distribution. *Salix*, NAP (non-arbores pollen) and *Gramineae* are reduced by a factor 10 in order not to dominate the diagram.

### Post-detachment period and development of endemic wildlife characteristics

The present fauna on Læsø has many endemic traits and is rich in migratory flying animals but poor in non-migratory wildlife, in particular mammals. There is an absence of many species that are widespread elsewhere in Denmark, such as small mammals, reptiles and amphibians. These traits are most probably caused by the complete detachment of Læsø c. 2500–2000 years BP from larger and more fertile landscapes, and reinforced by the nearly complete manmade deforestation of the island during the 17<sup>th</sup> to first part of the 20<sup>th</sup> century.

The vegetational diversity of Læsø is generally larger than in most other sandy parts of Denmark (cf. EU's Natura 2000 and habitat protection plans), and this situation is first and foremost caused by the highly intensive agricultural practices in other parts of Denmark. On Læsø around 75% of the land remained

undrained and unploughed until the 1920s when a forest plantation program was initiated (and partly obstructed by the locals). After 1950, increasing parts of the island came under nature conservation, thus preserving about 40 % of the area from agriculture, plantation and urbanization. Thus, Læsø's presently relatively diverse vegetation is mainly an effect of less deteriorated conditions than elsewhere in Denmark.

### Settlement, salt industry, deforestation and crises of the Little Ice Age

The initial settlement of the island is mostly referred to the 12<sup>th</sup> century. The discovery at that time of hyper-saline groundwater under the beaches of south-east Læsø, and the resulting salt industry, was contemporaneous with a sea-level drop of 0.8 m that commenced c. 1200 AD and culminated c. 1300 AD (see section below and Hansen 2010, Hansen *et al.* 2012). These saline groundwater deposits were continuously formed until

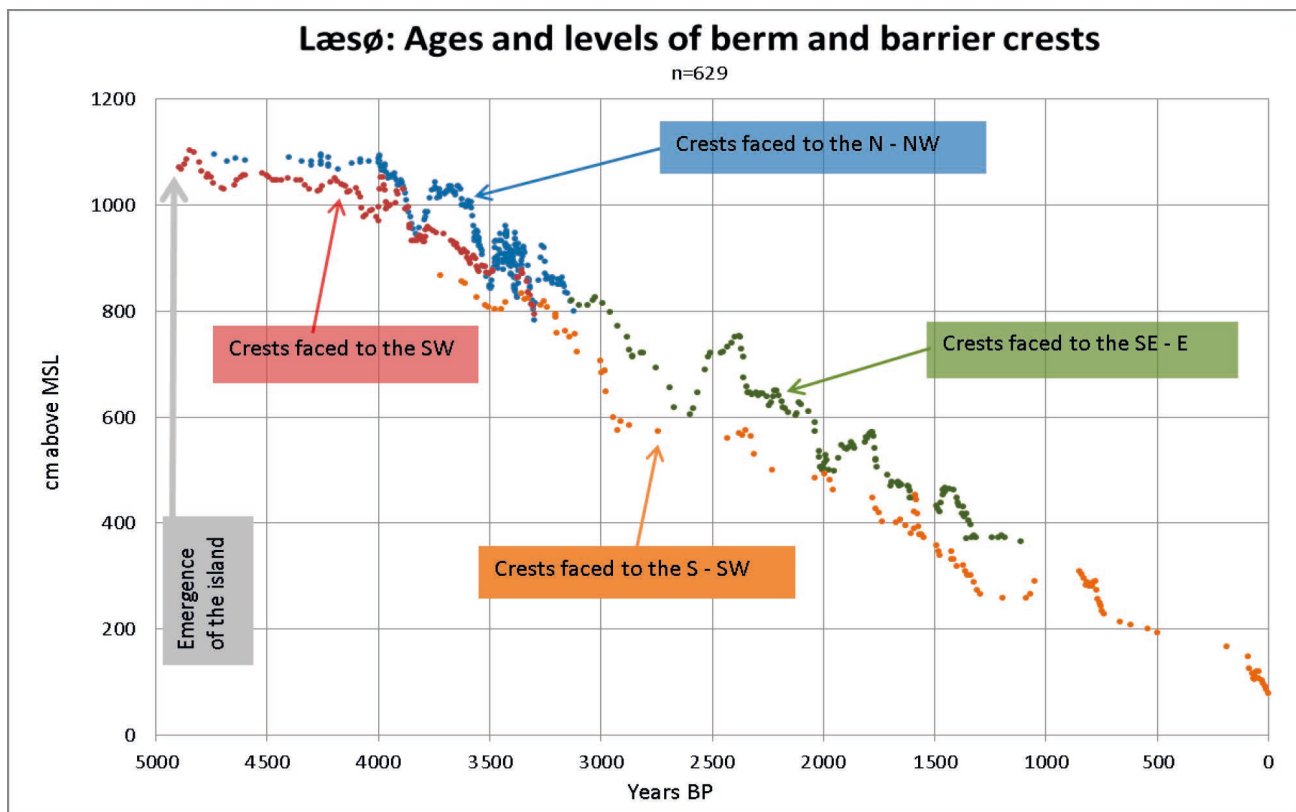


**Fig. 32.** Levels of raised berms, barrier-spit and barrier-island beach-ridge crests on Læsø measured by the BLRC method and plotted against ages of the ridges as inferred by the age model of the island. The diagram shows applied measurements from areas without inland or coastal dune fields (i.e. measurements from Højsande and Bløden Hale are excluded). Levels of raised, cultivated saltmarshes of south-eastern Læsø are also excluded due to lowering of the terrain by 600 years of agricultural practices (including widespread digging of turf). Colours indicate coastal exposure directions corresponding to the regions shown in Fig 4. Note differences in levels of ridges exposed to the north, east and south-east compared to ridges exposed to the south-west, west and south. To some extent these level difference are caused by the general isostatic SW-tilting of the region and differences in height of the swash (maximum 0.7 m). The remaining level differences are probably caused by local geological 'background noise' such as differences in local relaxation uplift and compaction (see Discussion).

the number of salt production huts peaked c. 1585 AD.

Soon after establishment of the initial salt industry many settlers arrived to the island, and less than 100 years after the discovery of hypersaline brines three churches (1219–1250) had been built. Simultaneously, the most fertile parts of Læsø south of the sandy 'old triangle' and north of the saltmarshes had been cleared of forests and cultivated around the medieval churches of Byrum, Vesterø and Hals. Together, the growing number of farms and expansion of the salt industry reduced the nearly complete forest coverage before settlement began to a few hectares in 1750 AD. A consequence of this development was that wood for fences and fuel was substituted by turf (Vellev 1993; Hansen 1995), a practice that lowered the terrain of the farmlands and ultimately laid much of the cultivated land open for wind deflation.

Because of declining formation of hypersaline ground water, the salt industry declined severely from 1600 AD and ceased completely in 1652 AD (Vellev 1993, Hansen 2010), contemporaneously with man-made deforestation and climatic changes related to the last and coldest phase of the Little Ice Age (Hansen 2010). Thus, the timing of changes in salt industry and agricultural practices (Stoklund 1999) relates Læsø's ecological and economic crises to climatic changes, consequent overpopulation and the Little Ice Age sea-level fall, which on Læsø reached two local minima, i.e. around 1300 AD and 1700 AD (Hansen *et al.* 2012).

### Relative sea-level reconstruction (4900 years BP to present)

Relative sea-level changes (RSL) constitute the sum of absolute sea level (ASL) and vertical terrain changes (U and C, see section on Methods and Data). Consequently, the present RSL reconstruction is independent of data on ASL and isostatic terrain level changes. The present RSL reconstruction is mainly dependent on how base levels of beach-ridge crests (BLRC) have been measured in order to avoid effects of small dunes (D) and erosional features (E). Another main issue is how BLRC measurements have been compensated for height of swash (S). Thus, a robust reconstruction of relative sea levels on Læsø during the last 4900 years can be built on the basis of the methods described above, i.e. respecting the following:

Measurements of base levels of beach-ridge crests (BLRC).

Compensations for height of swash (run-up) according to GPR profiling, supplemented with terrain analyses and types of coastal landscape.

Observable chronology of raised beach ridges, swales, lagoons, saltmarshes, forestation and cultural history marks of the island.

Absolute age determinations of samples of sediment and fossils in beach deposits (dating emergence), in marine deposits (pre-dating emergence), and in terrestrial deposits (post-dating emergence).

No use or cautious application of level data from areas that have been ploughed and drained since the medieval settlement or exploited for intensive salt production.

Due to the different nature of barrier ridges and saltmarsh ridges the RSL reconstruction has been made in two forms: One for exposed barrier coasts (4900 years BP to present) and one for saltmarsh coasts (1500 years BP to present).

### Sea-level reconstruction based on beach ridges of exposed coasts

Figure 32 shows 629 BLRC points representing exposed coasts, i.e. condensed beach-ridge, barrier-spit and barrier-island landscapes showing the RSL changes of the three main areas of the island which have continuously been exposed towards the main directions south-west, north and south-east (Fig. 4) throughout the period after 4900 years BP. RSL/age index points respect the exact formation chronologies and levels as established from the DTM. The absolute ages are modelled from the 119 absolute age determinations as described in Table 2.

The successions of the BLRC points from the three main directions of coastal growth follow the same long-term and short-term trends quite well, whereas level differences of 0.5–1.5 m between south-westerly exposed coasts (lowest) and northerly as well as south-easterly exposed barrier coasts are obvious. Of this level difference, 0.1–0.2 m is caused by isostatic south-westward tilting, whereas the remaining 0.4–1.3 m is mainly explained by differences in exposure. Thus, the fetch distances to the north are by far the largest, and fetch distances to the south-east are intermediate between those to the south-west and the north. This may explain the fact that the north, east and south-east coasts of the oldest and eastern parts of Læsø are mainly built of condensed, often coarse-grained beach-ridge plains (north) and coarse-grained barrier-spit plains (south-east and east), whereas the south-west coasts are mainly built of sandy barrier-spit and barrier-island plains.

The older part of the large plains of fine-grained condensed, low-ridge landscapes of south-eastern Læsø have not been included in the reconstruction because this part of the island has been ploughed, drained and partially used for cutting of turf through more than 600 years, which obviously has lowered and smoothed the original terrain.

### Sea-level reconstruction based on saltmarsh beach ridges

Because absolute ('eustatic') sea-level oscillations during the last 1000–2000 years are generally considered to be at the scale of decimetres (see Discussion section), it is crucial to develop methods which are capable of quantifying small post-sedimentation terrain level changes at the same small scale.

In a previous study of raised saltmarshes, Hansen *et al.* (2012) have shown that the saltmarsh landscapes of southern Læsø allow extraordinarily precise determination of past sea levels due to excellent possibilities for compensation for local post-sedimentation terrain level changes, i.e. compensation for 'background noise' such as normally undetectable neo-tectonic effects, local effects of draining and ploughing and other types

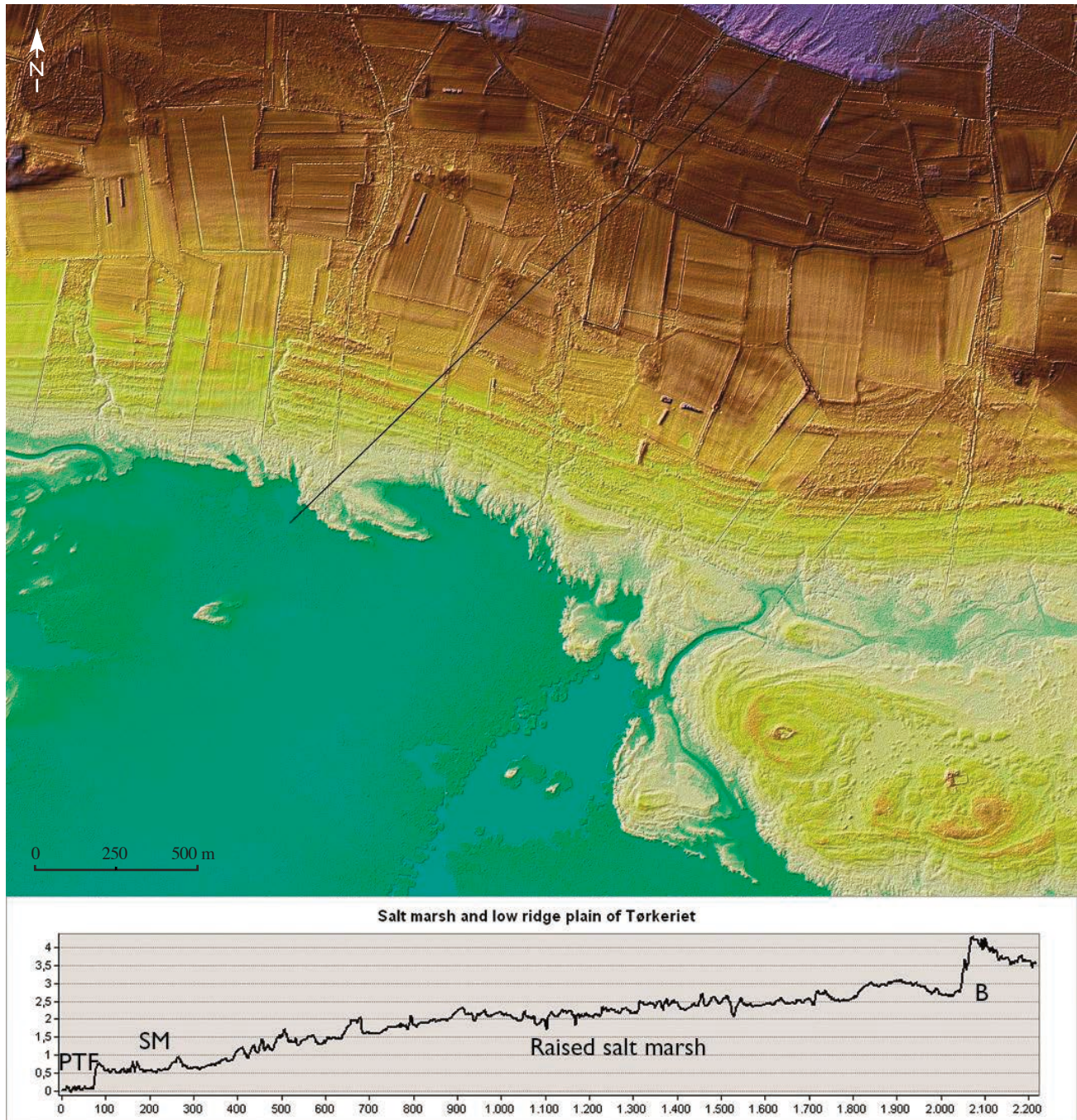


Fig. 33. Digital terrain model (DTM) of the Tørkeriet area in south-western Læsø (and Færøen, lower right) showing raised low-ridge plains (raised saltmarshes) between an older barrier (B) and the present saltmarsh (SM) fringing the pseudo-tidal flat (PTF). Levels of 35 beach ridges all 2–5 km long have been measured precisely along 381 transects each of 200 m length (Fig. 34).

of compaction. This has been done by ‘back-stripping’ of saltmarsh ridges to their original horizontal position in the reverse order of formation chronology (method in Hansen 2009; Hansen *et al.* 2012).

The area of Tørkeriet is shown in Fig. 33 and new BLRC data from this area are shown in Fig. 34. Although up to 20 cm of the observed differences in level may be explained by draining and ploughing of some parts of the area, the identified level differences (20–65 cm) of coherent ridges underline the importance of compensation for ‘geological background noise’ in studies of sea levels of the latest Holocene.

Figure 35 shows the RSL curve resulting from ‘back-stripping’ the BLRC levels (Fig. 34) as well as the result of detailed, previously published (Hansen *et al.* 2012) level studies of two other saltmarsh areas on Læsø (Hornfiskrøn and Stoklund). In each of these saltmarsh areas, many 3–5 km long, coherent saltmarsh ridges formed during the last 1000–2000 years. Compared to neighbouring swales, the ridges are very low (mostly less than 20 cm). After back-stripping, the individual ridges have vertical level differences of maximum 32 cm. The mean curve of back-stripped saltmarsh ridges from these areas is applied for the period after 1250 years BP in the reconstruction of an integral RSL curve for Læsø.

Table 4. Centennial lowstands and highstands on Læsø in the period 4000 years BP to present (Fig. 38).

High/low	Period		RSL, m	Amplitude
Highstand	4000 BP	2000 BC	9.7	
<b>Lowstand</b>	<b>3800 BP</b>	<b>1800 BC</b>	<b>8.5</b>	<b>-0.8 m</b>
Highstand	3700 BP	1700 BC	8.8	
<b>Lowstand</b>	<b>3500 BP</b>	<b>1500 BC</b>	<b>7.2</b>	<b>-1.1 m</b>
Highstand	3400 BP	1400 BC	7.7	
	to 3000 BP	1000 BC	6.3	
<b>Lowstand</b>	<b>2900 BP</b>	<b>900 BC</b>	<b>5.3</b>	<b>&gt;0.7 m</b>
Highstand	2800 BP	800 BC	5.6	
<b>Lowstand</b>	<b>2700 BP</b>	<b>700 BC</b>	<b>5.0</b>	<b>-0.5 m</b>
Highstand	2400 BP	400 BC	5.3	
	to 2100 BP	100 BC	4.6	
<b>Lowstand</b>	<b>2000 BP</b>	<b>0 AD</b>	<b>3.7</b>	<b>&gt;0.6 m</b>
Highstand	1800 BP	200 AD	4.0	
<b>Lowstand</b>	<b>1600 BP</b>	<b>400 AD</b>	<b>2.6</b>	<b>-0.7 m</b>
Highstand	1400 BP	600 AD	2.6	
<b>Lowstand</b>	<b>1300 BP</b>	<b>700 AD</b>	<b>1.6</b>	<b>-0.5 m</b>
Highstand	1100 BP	900 AD	1.7	
<b>Lowstand</b>	<b>700 BP</b>	<b>1300 AD</b>	<b>0.5</b>	<b>-0.6 m</b>
Highstand	450 BP	1550 AD	0.5	
	to 220 BP	1780 AD	0.5	

Amplitude of the eight lowstands are calculated as the mean difference between lowstand levels and levels of the two neighbouring highstands:

### Integral age model and RSL curve for Læsø

An age model for the emergence of all parts of Læsø is presented in Fig. 36, corresponding to the growth history of the island as described above in the chapter on *Reconstruction of the emergence, growth and coastal development of Læsø* and according to the principles described in the section on *Age modelling of coastal progradation* (Table 2).

In Fig. 37 all of the 1200 RSL/age index points of exposed coasts (Fig. 32) and saltmarshes (Fig. 34) are merged into one common RSL/age curve, cf. steps 6 and 7 in Table 2. The solid line represents BLRC measurements of exposed coasts (4900 years BP to present).

The dashed blue curve in Fig. 37 represents all BLRC measurements of exposed beach ridges after reduction for height of swash (run-up) as described in the section on *Estimation of swash heights (run-up) by ground penetrating radar (GPR)*, and the dashed red line represents back-stripped BLRC measurements of the saltmarshes of southern Læsø (1250 years BP to present). The actual identification of RSL by GPR of barrier landscapes is indicated by black dots. The resulting, integral RSL curve of exposed coasts (dashed blue) is calculated on the basis of these GPR identifications in such a way that the general shape and oscillations of the BLRC curve are maintained, but lowered to a best fit with the RSL points of the GPR surveys. At stretches of the RSL curve where GPR data are not available, the inferred swash heights have been checked with terrain analyses as described in the section on *Estimation of swash heights (run-up) by terrain level analyses*.

The resulting RSL curve for Læsø is presented in Fig. 38, where also peaks of short-term highstands and lowstands have been connected above and below the RSL curve (blue band). Through this procedure, short-term (centennial) oscillations can be identified, i.e. oscillations that are normally not identified in regions of less regression and coastal growth (see Discussion). The present study suggests that short-term lowstands of 50 cm or more occurred eight times during the period 4000 years BP to present, as set out in Table 4.

Comparable observations of sea-level highstands have been published from the Swedish west coast as numbered Postglacial Transgression Maxima (PTM) (Mörner 1969, 1980). Thus, PTM 6–PTM 10 of the Swedish west coast correspond well to contemporaneous highstands identified on Læsø, whereas lowstands are more clearly developed on Læsø. This difference may be explained by the sparse sediment sources of the granitic and metamorphic bedrock terrain of western Sweden.

The RSL curve for Læsø also shows many similarities to the RSL curve of the Kattegat island of Samsø (Sander *et al.* 2015), including a relatively stable development 5000–4000 years BP, thereafter a relatively fast fall until around 3000 years BP, as well

as highstands in the period 3000–2000 years BP. As at the Swedish west coast, the lowstands at Samsø are less pronounced compared to Læsø. The difference is most probably caused by the smaller preservation potential of lowstands in less GIA-raised regions (Samsø mean 0.5 mm/year, Læsø mean 2.1 mm/year). General implications of the present identification of centennial lowstands are discussed below.

## Discussion

The use of raised beach ridges as indicators of relative sea levels (sea-level proxies) of the past has a long record in modern scientific literature of Scandinavia, going back to the beginning of the 20<sup>th</sup> century. On the basis of Wilhelm Ramsay's initial ideas, Mertz (1924) and von Post (1933) began understanding how eustatic sea-level changes in combination with isostatic uplift of the Scandinavian peninsula and the Baltic region had dramatically changed sea levels of the Baltic sea and Kattegat after flooding and unloading of the region by melting of Weichselian ice caps.

A major break-through also took place when Mörner (1969), on the basis of detailed RSL/age studies of beach ridges and marine deposits of western Swedish river valleys, was able to calculate regional inclinations of raised beach ridges and thus before others became able to distinguish between the two major components of relative sea-level displacement, i.e. absolute (eustatic) sea-level changes and isostatic rebound (GIA). In later reviews, Mörner (e.g. 1980) pointed out that the beach deposits of the Kattegat region are excellent 'sea-level laboratory' objects in search for understanding the interplay between eustatic sea-level changes and post-glacial isostatic rebound.

With respect to isostatic models of the Holocene (late glacial to present) uplift, Pässe & Andersson's (2005) study of the Scandinavian peninsula is an important supplement to the observations by Mörner and other authors, resulting in many empirically documented series of the different patterns in RSL change at various positions around the centre and margins of the Weichselian glaciation of Scandinavia and the Baltic. Thus, north-east of Mörner's (1969) find of an isostatic bend perpendicular to the general Scandinavian uplift

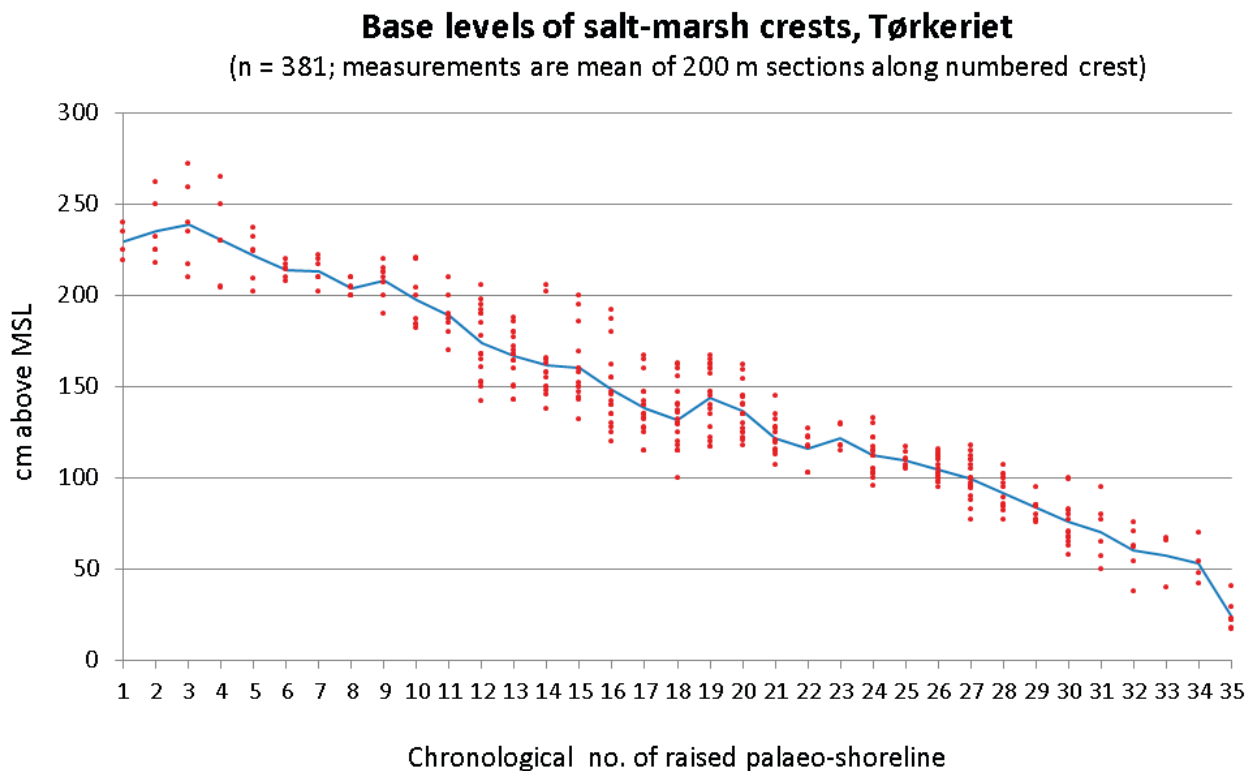


**Fig. 34.** Levels of 35 coherent and up to 5 km long saltmarsh crests of Tørkeriet, south-western Læsø (back-stripped curve of the measurements shown in Fig. 35). Each red dot represents the base level of ridge crests of 200 m long transects along the crest (BLRC method). The crests are arranged in chronological order according to the time of appearance (1: oldest; 35 youngest). Blue line represents the mean level of the 35 crests. The scatter of the individual crest levels varies between 20 and 65 cm and reflects local geological 'background noise', variations in the sedimentary heights of the crests (which relative to hindlying swales are about 10 cm), and a relative levelling precision between 1 and maximum 6 cm.

between the islands of Læsø and Anholt (70 km south of Læsø), Pässe and Andersson's (2005) empirical model also fits well with our RSL curve of Læsø, when our Læsø RSL/age index points are detrended for the local relaxation/uplift caused by post-Boreal erosion of the Læsø platform (Hansen *et al.* 2012).

### Beach ridges as relative sea-level indicators

Raised beach ridges are generally proxies of the sea level at the time of deposition, such that the crest level of a certain beach ridge minus the swash height represents sea level when the ridge was formed. In northern Denmark where the GIA has been larger than the RSL rise during the late Holocene, formation of ridge-and-swale landscapes is a general characteristic of such regressive sedimentary regimes, regardless of whether the ridges were formed as berms, barrier spits or barrier islands and the depressions between them have been formed as swales between laterally stacked berms or by growth of barrier systems.

Because the swash height may be difficult to determine without GPR or lidar, the base levels of hindlying as well as subsequent swales have often been applied in regressive sedimentary environments of the Kattegat–Skagerrak seas, e.g. in the reconstruction of the large spit Skagen Odde, the northern tip of Jutland (Nielsen *et al.* 2006; Nielsen 2008; Nielsen & Johannessen 2009, 2010; Clemmensen & Murray 2010, Clemmensen *et al.* 2012a) and the Kattegat island of Anholt (Mörner 1969; Bjørnson *et al.* 2008; Clemmensen *et al.* 2012b). Moreover, Bendixen *et al.* (2014) have shown that in a non-regressive sedimentary environment of south-east Denmark (Feddet), beach ridges represent superimposed berms of several storm surge events.

On Læsø we found that the differences between ridge and swale levels in several types of beach-ridge landscapes are smaller than indicated from GPR profiling and identification of downlap structures representing MSL of the time. This problem first and foremost relates to laterally stacked beach ridges

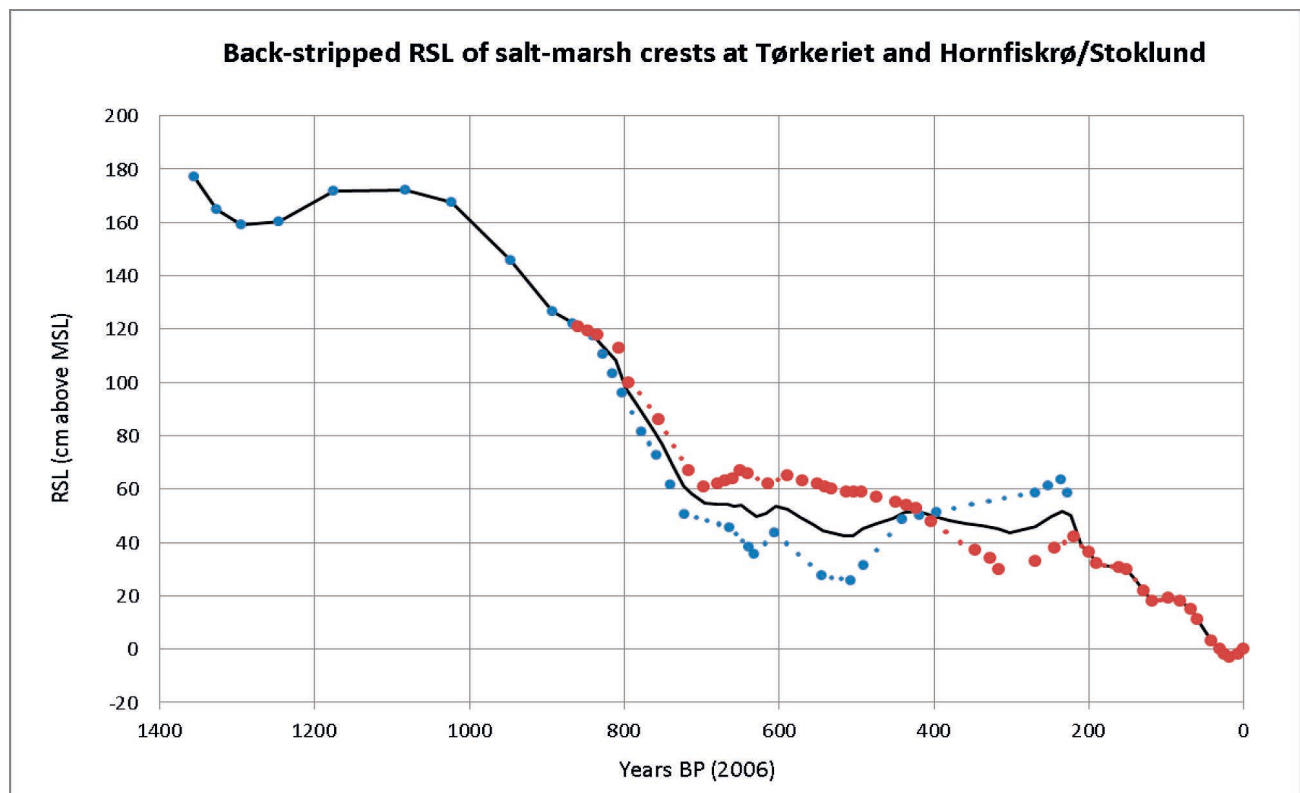


**Fig. 35.** RSL/age index points of raised saltmarsh crests. Brown dots: Index points of Hornfiskrøn and the Stoklund–Bangsbo area (data from Hansen *et al.* 2012). Blue dots: Result of back-stripping of 381 new BLRC measurements of raised saltmarsh ridges at Tørkeriet (Fig. 34) in comparison with the raised saltmarshes at Hornfiskrøn and Stoklund–Bangsbo, for identification of local geological ‘background noise’. The index points of all areas have been back-stripped by the method described by Hansen *et al.* (2012). The large blue dots show the resulting RSL index points of 32 crests that can be traced over 3–5 km. Small blue and brown dots are linear interpolations in order to construct the mean RSL curve (solid black line) of the two data sets that have been back-stripped for local, geological ‘background noise’ (and height of swash). The remaining RSL differences between the two data sets (mean 18 cm; max. 32 cm) are probably close to the limits of what can be compensated for in a low seismicity region with excellent representation of long, coherent and well separated saltmarsh crests.

(berms), where only incipient swales have been formed or have been partially eroded. This type of ridge-and-swale landscape forms large parts of Danish marine forelands in areas with slower coastal progradation than in the present case. On Læsø we have classified such landscapes, where swale levels may be imprecise RSL proxies, as *condensed high-ridge plains* (high-rippled washboard plains). Here, RSL identification should consequently be based on GPR profiling (cf. Hede *et al.* 2013). Also in raised saltmarsh landscapes, here classified as *condensed low-ridge plains* (low-rippled washboard plains), swale levels are generally slightly higher than the mean sea level of the time because the beach ridges are formed by vertical accretion during high water, so that the sedimentary process may

also affect the nearest hindlying swale during storm surges. In consequence we suggest that RSL/age index points obtained by lidar profiling exhibit a level difference not exceeding +0.2 m, mostly less than +0.1 m, as compared to RSL levels obtained by GPR profiling.

#### Exact chronology of beach ridges and uncertainty of assigned ages

The constant growth of Læsø provides two independent sources of geochronology, firstly and most importantly the exact observable order of appearance of beach ridges in each of the three main areas (Fig. 4), and secondly the laboratory age determinations listed in Table 1. The main purpose of these is to assign absolute ages to the observed chronology of

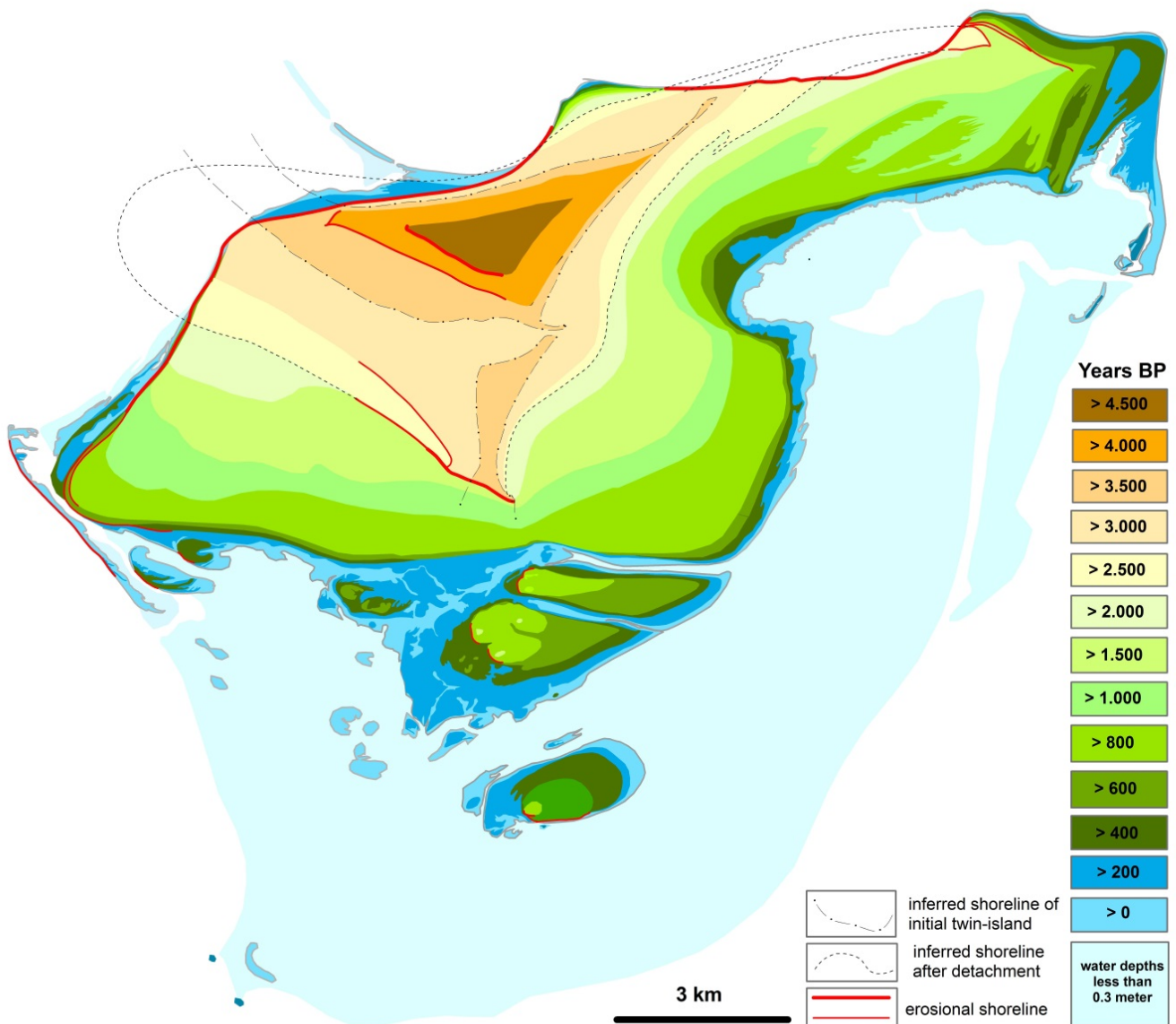


Fig. 36. Age model of the older, still preserved shorelines on Læsø. See text for description of the construction method.

palaeo-shorelines (cf. the section on *Age modelling of coastal progradation*). If two laboratory age determinations oppose the observed chronological order, then the observed chronology ranks above laboratory measurements and, consequently, analytical uncertainties of the relevant samples must be considered. The 1200 RSL/age index points respect this elementary principle of stratigraphical ranking and are further supported by the procedure of age modelling in which the assigned age of each index point is proportional to the distances between beach ridges.

The analytical uncertainties of all absolute age determinations are listed in Table 1, and the mean uncertainty of laboratory datings is 7.2 % of the assigned ages. However, the absolute age modelling is based on 12–37 samples within each time interval of 1000 years. Consequently, the uncertainties of ages assigned to the RSL curve (Fig. 38) are considered to be much lower than those of the individual samples. Moreover, the chronological order of index points is exact (certain). We consider the uncertainty of assigned ages to be <100 years for the period 5000–2000 BP, <50 years for the period 2000–1000 BP, and <25 years for the period 1000 BP to present.

### Identification of geological ‘background noise’ in a low seismicity region

In sea-level reconstructions, the conclusion of Moucha *et al.* (2008) on long-term sea-level modelling has often been cited: “There is no such thing as a stable continental platform”. As any large long-term change is composed of smaller short-term changes, Moucha *et al.*'s (2008) conclusion also applies to late Holocene sea-level reconstructions.

Hansen *et al.* (2012) showed that geological ‘background noise’ is a crucial parameter for reconstruction of the last 900 years of absolute sea-level changes, because amplitudes of late Holocene sea-level changes (Woodworth *et al.* 2009; Cronin 2012 ) are comparable to amplitudes of normal geological background noise in regions of low seismicity such as Denmark (Andersen *et al.* 1974; Lykke-Andersen & Borre 2000; Khan *et al.* 2006), other parts of Scandinavia (Bungum *et al.* 2010; Hill *et al.* 2010), Central Europe (Scheck-Wenderoth & Lamarche 2004), and the east coast of north America (Engelhart *et al.* 2009). The present study correlates well with these and our previous findings of geological background noise and demonstrates how causes and magnitudes of relatively

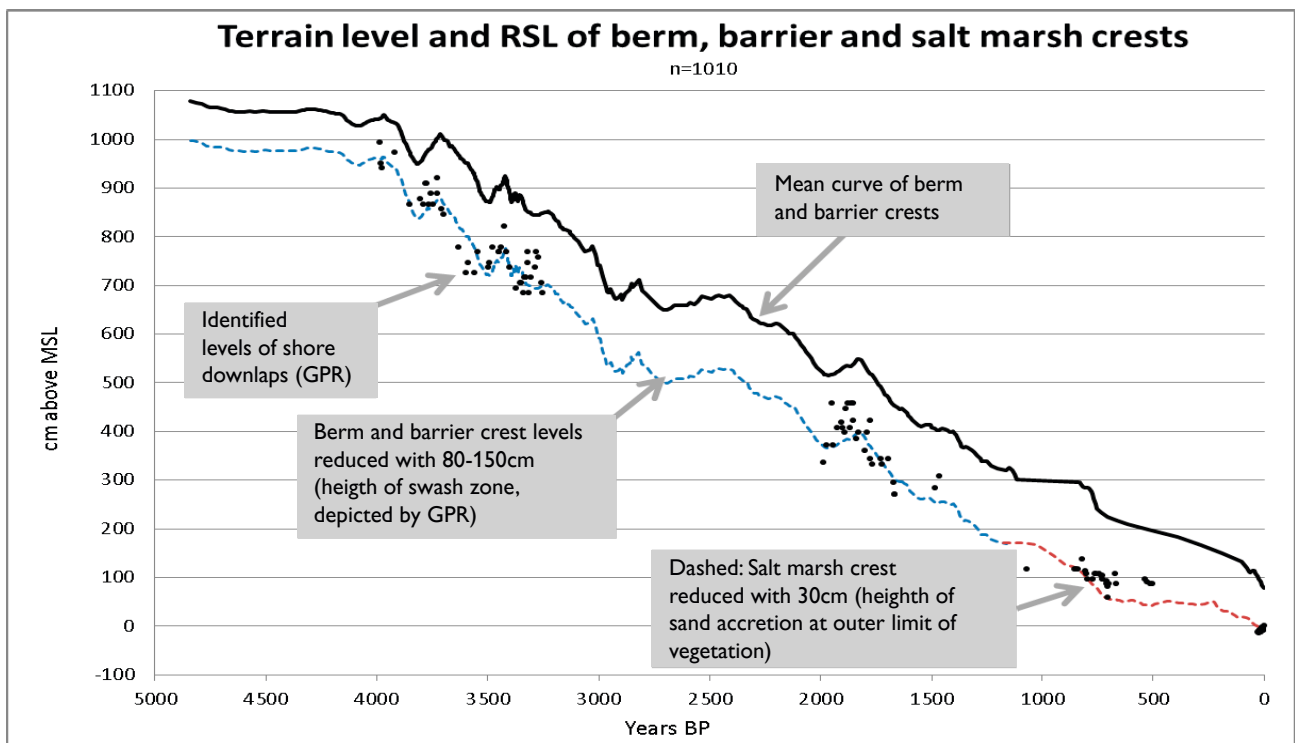


**Fig. 37.** Solid black curve: Mean level of raised berm and barrier ridges on Læsø (Fig. 32). Black dots: RSL levels of downlap structures determined by GPR profiling. Dashed blue curve: RSL of these sea-level proxies detrended for height of swash as found by GPR profiling. Dashed red curve: RSL of saltmarshes on Læsø (Fig. 35). The RSL curve of raised barriers is detrended for height of swash in such a way that the shape of the curve is maintained, but the curve is lowered to best fit with the RSL points as identified by GPR profiling.

short-term land-level changes of the Kattegat region may provide a better understanding of small relative sea-level changes.

Consequently, even along passive continental margins problems may arise for reconstruction of reliable late Holocene sea-level curves from areas where possibilities for multi-site, precise and coherent levelling of sea-level proxies are not at hand. Thus, except for a few cases of detrending for sediment compaction (e.g., Horton & Shennon 2002; Edwards 2006), published sea-level curves for low seismicity regions are not detrended at all for geological background noise. Compensations for tectonic background noise have mainly been done in regions of higher seismicity, e.g. Lambeck *et al.* (2004) in a study of Italy and in many studies of the north American west coast. Proportional differences between sea-level index points and sea-level curves from different locations may therefore be large compared to the general conception of small sea-level changes during the last 2000 years.

Obviously, this lack of detrending is a problem when hypotheses on a rapidly rising present sea level, as seen from tide gauge records, are based on the untenable concept of a relatively stable sea level during the last 1000–2000 years. Detailed and robust measurements

of the magnitude of sea-level oscillations prior to any substantial present sea-level rise are therefore required.

#### Unique representation of short-term lowstands

Another general problem of sea-level reconstructions is that it is a matter of discussion whether transgressive, stable and slightly regressive environments are capable to produce or preserve visible or separate sea-level proxies of short-term (multidecadal to centennial) lowstands. Even in micro-tidal environments, sea-level oscillations merely produce and preserve relatively high, complex berms which have mainly been formed over decades or centuries by storm surges (Bendixen *et al.* 2014). Consequently, sea-level curves based on such relatively stable isostatic environments may only illustrate sea-level highstands or storm surge levels, whereas short-term lowstands are missing or blurred. Unawareness of this situation may lead to unrealistic conceptions of short-term sea-level stability of the past (cf. Table 4).

Due to strong isostatic uplift, micro-tidal conditions, excessive supply of sediment and shallow surroundings, the horizontal coastal growth of Læsø (mean 2 m/year) has been enhanced by a

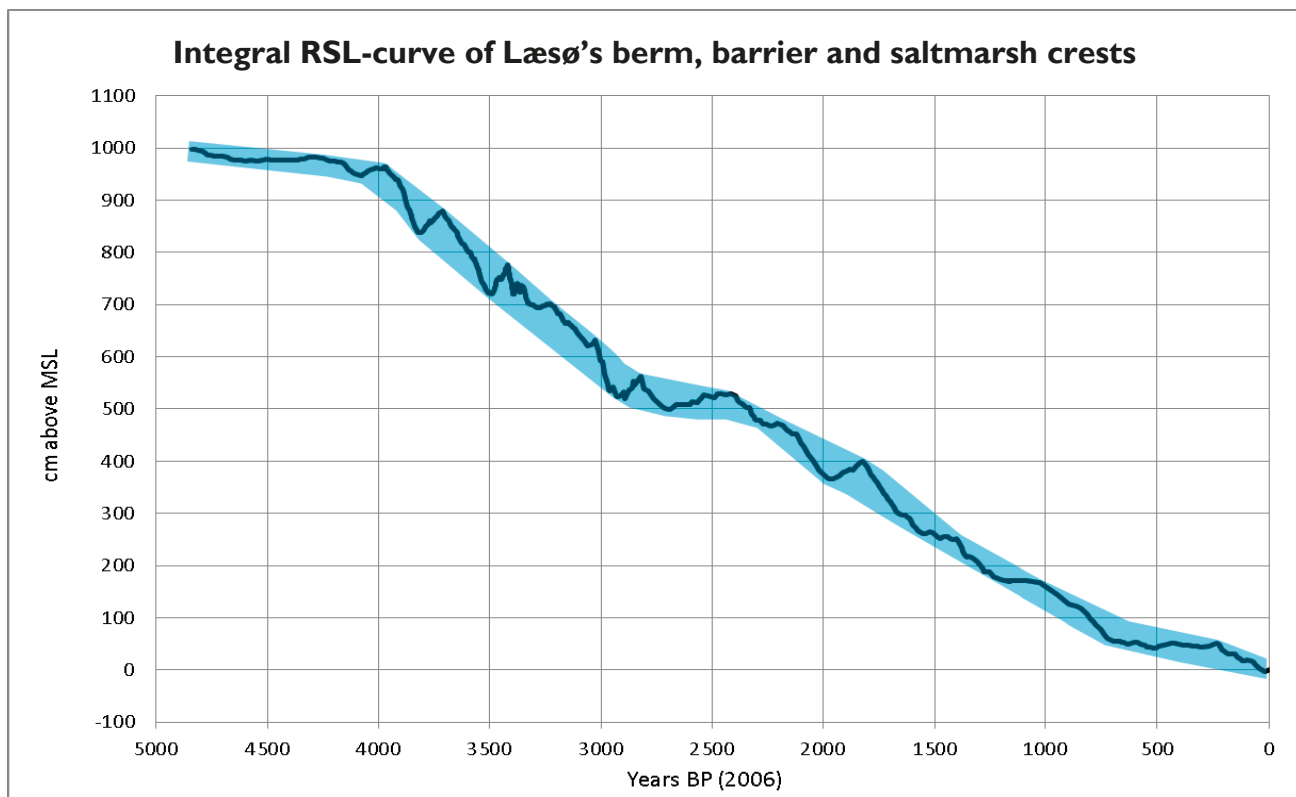


**Fig. 38.** Integral RSL curve of berm, barrier and saltmarsh crests on Læsø. The curve is detrended for height of swash and geological 'background noise' (Figs 32 and 35). Blue band: Limits of short-term sea-level oscillations. The vertical widths of the blue band indicate that the sea level oscillated many times within limits of 0.5–1.1 m of the general trend of the RSL curve, e.g. 0.6 m during the Little Ice Age lowstand between 850 to 200 years BP (1250–1800 AD).

continuously regressive environment where oscillations between short-term lowstands and subsequent highstands generally have not caused widespread erosion or produced large complex berms obscuring the directly observable beach-ridge chronology. Consequently, we consider the beach-ridge systems of Læsø to represent a unique micro-tidal and strongly regressive environment where proxies of both short-term sea-level highstands and lowstands have been preserved, and where short-term (multidecadal to centennial) sea-level oscillations and variability can be reconstructed for the last 4900 years in beach-ridge landscapes and most precisely for the last 2000 years in saltmarsh landscapes (Fig. 38 and Table 4).

## Conclusions

Due to strong isostatic uplift, surplus of sediment, micro-tidal amplitudes and shallow water depths, the island of Læsø provides an excellent environment for reconstruction of continuous records of sea-level changes during the late Holocene. We show that this mid-Kattegat setting has created at least three simultaneously developing systems of beach ridges during the last 4900 years. Increasingly large parts of the island have been formed as raised saltmarshes during the last 3000 years. Thus, all periods of the last 4900 years are covered by at least three and up to eight separate, coherent and continuous sea-level records,

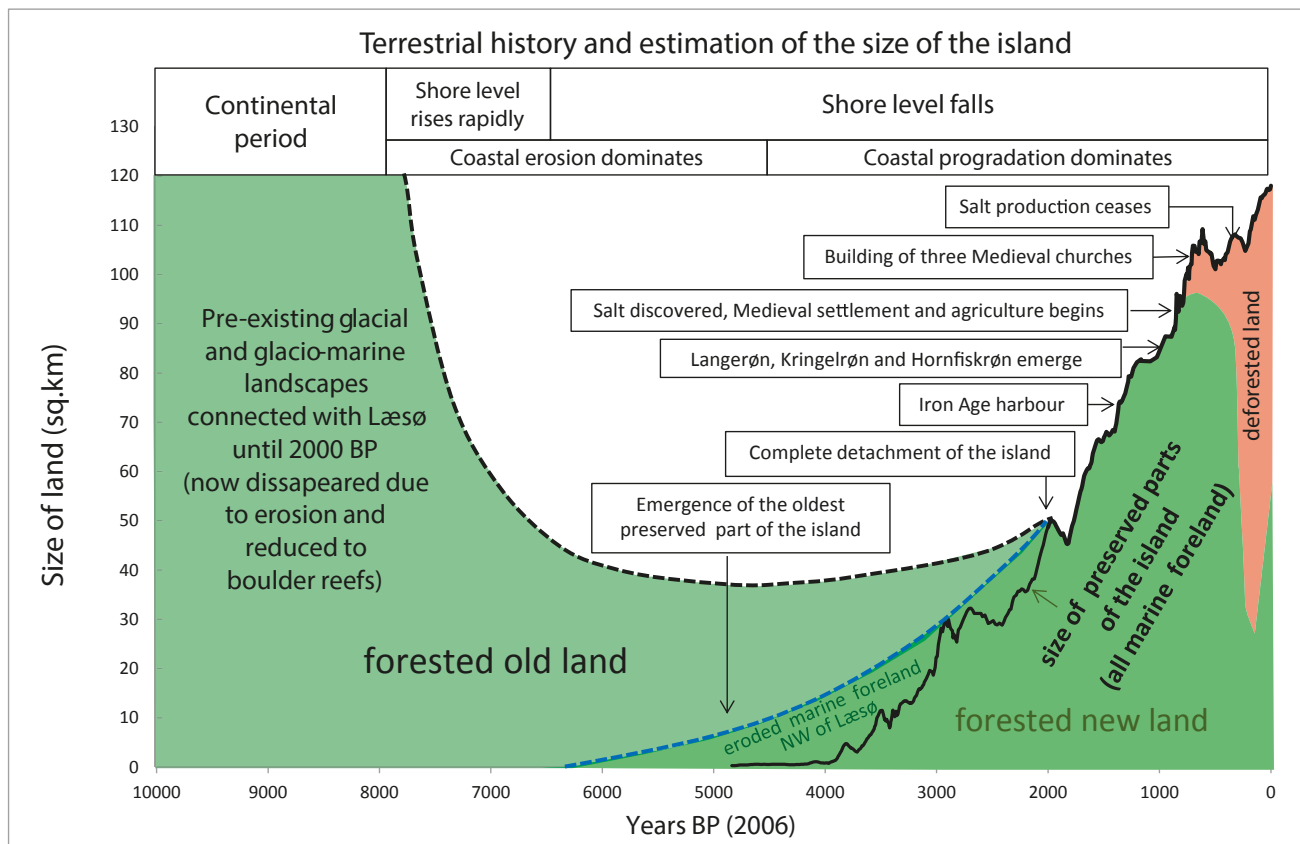


**Fig. 39.** Diagrammatic illustration of the coastal history and size of Læsø with indications of significant natural and cultural events. During the Boreal continental period, the Læsø-region was separated from Jutland and Sweden by large rivers to the west and east, whereas the region was attached to large landmasses between the rivers. During the maximum of the Litorina transgression (at Læsø c. 6300 years BP), all parts of present middle and northern Kattegat were flooded by the sea except for areas around the islands of Læsø and Anholt. Coloured areas: Estimated size of Læsø (before 2000 years BP, including now eroded glacio-marine landscapes and marine forelands mainly northwest of the preserved parts of the island). Solid curve: Size of preserved parts of the island; the curve is constructed by reversing the RSL curve in Fig. 38 and fitting it to the size of land areas in Fig. 36. The diagram indicates that the size of Læsø (including attached glacio-marine landscapes) was smallest in the period 6000 to 3000 years BP (around 40 km<sup>2</sup> or 30% of the present size), but large enough for survival of a stock of large herbivores (e.g. red deer) until after medieval settlements, and large enough for survival of mature, light-open forests including the Læsø pine (*Pinus silvestris* var. *laesoensis*), which became extinct elsewhere in the Baltic region. The attached glacio-marine landscapes were completely eroded to sea level or lower after 2500–2000 years BP and are now only represented by numerous boulder reefs both inside and outside of the present shoreline of Læsø.

i.e. continuous records of beach-ridge coasts exposed to the north, south-east to east, and south-west (4900 years BP to present) and saltmarsh coasts exposed to the south-east (3000 years BP to present) and south (2000 years BP to present).

Not only proxies of sea-level highstands are represented – as in less regressive environments – but also proxies of sea-level lowstands have often been preserved. This situation is mainly caused by strong uplift and the unique hydrographic setting of the island. Thus, the identified general RSL fall of 10.3 m (Fig. 38) reveals a mean vertical regression rate of 2.1 mm/year and a mean horizontal regression rate of 2 m/year, and eight short-term sea-level oscillations in the range of 0.5–1.1 m during the last 4900 years (Table 4), corresponding to short-term (centennial) absolute ('eustatic') sea-level changes.

### **Origin, coastal progradation and detachment from pre-existing landscapes**

The present study explains how the island of Læsø emerged from a pre-existing, now eroded glacio-marine landscape and how the coastal development during the last 4900 years is related to a strongly regressive sedimentary environment, sea-level oscillations and changes in exposure, water depths and sedimentary sources. A summarizing figure of the above described pre-history, emergence, coastal growth, forestation, settlement, salt industry, deforestation and land-use is shown in Fig. 39 where the main events of the coastal history are highlighted.

### **Identification of geological 'background noise'**

The coastal landscapes of Læsø make it possible to reconstruct several independent sea-level curves from closely spaced, but separate areas of the same low seismicity region. Because normal tectonic level changes, as well as terrain level changes due to land-use practices, by definition are local, this situation provides a rare opportunity for identification of small-scale terrain-level changes, which are likely to appear in all cultivated landscapes and most low seismicity areas such as Scandinavia, other parts of north-western Europe and eastern north America. From such assumed stable geological environments, similar small local changes usually cannot be detected.

### **Continuous record of sea-level changes during the last 4900 years**

Many studies of beach ridges and other sea-level proxies of the Kattegat Sea have given both coherent and detailed knowledge about early Holocene (late glacial) and mid Holocene relative sea-level changes, while understanding of the late Holocene, in particular the last 2000 years, has been at a less

coherent and precise level. The island of Læsø has been formed after 4900 years BP by continuous coastal progradation, forming more than 4000 km of well separated, still visible barrier and saltmarsh beach ridges. Thus, a coherent and detailed record of Late Holocene RSL changes can be constructed on the basis of 1200 RSL/age index points, including the last 2000 years about which knowledge on European and American sea-level changes is generally incomplete because of lack of studies on lowstand proxies. For the last 1000 years the sea-level curve of Hansen *et al.* (2012) is supplied with many new RSL/age index points displaying a 80 cm RSL fall (1200–1300 AD) at the onset of the Little Ice Age.

### **Centennial sea-level oscillations of 0.5–1.1 m**

The strongly regressive regime, shallow surrounding waters and continuous surplus of sediment in combination with a micro-tidal amplitude of only 0.2 m has created a unique sedimentary environment, where proxies of short-term sea-level oscillations of the last 4900 years have continuously been preserved in the form of both highstand and lowstand proxies, while lowstand sea-level proxies in less regressive environments appear to have been eroded or obscured by subsequent highstands in most other parts of north-western Europe and north-eastern America. By comparing the detailed RSL curve with its general trends (Fig. 38), eight short-term (centennial) sea-level oscillations can be identified, showing that RSL oscillated 0.5–1.1 m around the generally falling RSL (Table 4).

## **Acknowledgements**

We are indebted to Geocenter Denmark for grants to the Refleks project and for discussions with its other participants including Morten Pejrup, Lars Clemmensen, Mikkel Hede, Nanna Noe-Nygaard, Andrew Murray, Lars Henrik Nielsen and Peter Johannessen, who worked at other coastal sites. We are also indebted to Eigil Holm for providing excellent aerial photographs, Lasse Gudmundsson for both photographs and inspiring assistance with OSL sampling, Frank Andreasen for his large pioneer work on Læsø with GPR profiling, Peter Roll Jacobsen for assisting with supplementary GPR profiling (2010), to Benny Scharck for preparing illustrations, to two anonymous reviewers, and to the editor (Lotte Melchior Larsen) for careful reading and clarification, constructive suggestions on the structure and focus of the article. The Carlsberg Foundation and the Danish Council for Independent Research supplied grants for OSL dating. GEUS is thanked for general support and technical assistance.

## References

- Andersen, O. B., Kejlso, E. & Remmer, O. 1974: Secular movements within Jutland as determined from repeated precise levellings 1885–94 and 1943–53. *Geodætisk Instituts Skrifter* 3, 1–70.
- Andersen, S.T. 1970: The relative pollen productivity and pollen representation of north European trees, and correction factors for tree pollen spectra. *Danmarks Geologiske Undersøgelse Række 2 No. 96*, 99 pp.
- Andreasen, F. 1986: Rapport over prospektering efter sten og grusforekomster på Læsø. *Fredningsstyrelsen*. (Unpublished data report with app. 50 km of GPR profiles).
- Bahnsen, H. 1986: Lithologisk undersøgelse af materiale fra seks boringer på Læsø. *Danmarks Geologiske Undersøgelse Series D 6*, 7–23.
- Bahnsen, H., Knudsen, K. L. og Hansen, J. M. 1986: Bidrag til Læsøs geologi. *Danmarks Geologiske Undersøgelse Series D 6*, 72 pp.
- Bendixen, M., Clemmensen, L.B. & Kroon, A. 2014: Sandy berm and beach-ridge formation in relation to extreme sea levels: A Danish example from a micro-tidal environment. *Marine Geology* 344, 53–64.
- Berthelsen, A. 1978: The methodology of kineto-stratigraphy as applied to glacial geology. *Bulletin of the Geological Society of Denmark* 27 (special issue), 25–38.
- Bird, E. 2008: Coastal geomorphology. An introduction. *Wiley & Sons*, 411 pp.
- Bjørnsen, M., Clemmensen, L.B. & Murray, A. 2008: New evidence of the Littorina transgressions in the Kattegat: Optically Stimulated Luminescence dating of a beach-ridge system on Anholt, Denmark. *Boreas* 37, 157–168.
- Bradshaw, R., Hansen, J.M. & Møller, P.F. 1999: Om begrebet natur. Natur versus menneske i Kvartærtid. *Skoven 3/99*, 117–121.
- Bungum, H., Olesen, O., Pascal, C., Gibbons, S., Lindholm, C. & Vestøl, O. 2010: To what extent is the present seismicity of Norway driven by post-glacial rebound? *Journal of the Geological Society of London* 167, 373–384.
- Christensen, C. 1995: The Littorina transgressions in Denmark. In: Fischer, A. (ed.), *Man and Sea in the Mesolithic – Coastal Settlements Above and Below Present Sea Level*. *Oxbow Monograph*, Oxford, 15–22.
- Clemmensen, L.B. & Murray, A.S. 2010: Luminescence dating of Holocene spit deposits: an example from Skagen Odde, Denmark. *Boreas* 39, 154–162
- Clemmensen, L.B. & Nielsen, L. 2010: Internal architecture of a raised beach-ridge system (Anholt, Denmark) resolved by ground-penetrating radar investigations. *Sedimentary Geology* 223, 281–290.
- Clemmensen, L.B., Murray, A.S. & Nielsen, L. 2012a: Quantitative constraints on the sea level fall that terminated the Littorina Sea Stage, southern Scandinavia. *Quaternary Science Reviews* 40, 54–63.
- Clemmensen, L.B., Nielsen, L., Bendixen, M. & Murray, A. 2012b: Morphology and sedimentary architecture of a beach-ridge system (Anholt, the Kattegat sea): a record of punctuated coastal progradation and sea level change over the past ~1000 years. *Boreas* 41, 422–434.
- Cronin, T.M. 2012: Rapid sea level rise. *Quaternary Science Reviews* 56, 11–30.
- Edwards, R.J. 2006: Mid- to late-Holocene relative sea level change in southwest Britain and the influence of sediment compaction. *The Holocene* 16, 575–587.
- Engelhart, S.E., Horton, B.P., Douglas, B.C., Peltier, W.R. & Törnqvist, T.E. 2009: Spatial variability of late Holocene and 20<sup>th</sup> century sea level rise along the Atlantic coast of the United States. *Geology* 37, 1115–1118.
- Fredericia, J. 1985: Hydrogeologisk basisdatakort, Læsø. *Danmarks Geologiske Undersøgelse, Hydro-geological basis data map series*.
- Fredericia, J. & Grambo-Rasmussen, A. 1985: Kortlægning af kvartære gasfund i Vendsyssel. Fase 2. (2 volumes), 126 pp. Fase 3. rapport, 13 pp. *Danmarks Geologiske Undersøgelse, report series*.
- Gregersen, S. & Voss, P.H. 2014: Review of some significant claimed irregularities in Scandinavian postglacial uplift on timescales of tens to thousands of years – earthquakes in Denmark? *Solid Earth* 5, 109–118.
- Hansen, J.M. 1977: Sedimentary history of the island Læsø. *Bulletin of the Geological Society of Denmark* 26, 217–236.
- Hansen, J.M. 1980: Læsøs postglaciale udvikling i relation til den Fennoskandiske Randzone. *Dansk Geologisk Forening, Årsskrift for 1979*, 23–30.
- Hansen, J.M. 1986: Læsø: Et resultat af forkastningsbevægelser, jordskælv og niveauforandringer? *Danmarks Geologiske Undersøgelse Series D 6*, 47–72.
- Hansen, J.M. 1994: Læsøs tilblivelse og landskaber – om øen der rokker og hopper. *Danmarks Geologiske Undersøgelse & Geografforlaget*, 56 pp.
- Hansen, J.M. 1995: En ø's opståen, kystdannelse og vegetationsudvikling: Naturlige og menneskeskabte landskaber på Læsø. *Geologisk Tidsskrift* 2, 1–74, 2 folded maps.
- Hansen, J.M. 2009: On the origin of natural history: Steno's modern, but forgotten philosophy of science. *The Geological Society of America, Memoir* 203, p. 159–178.
- Hansen, J.M. 2010: The salt industry on the Danish Kattegat Island of Læsø (1150–1652): Hypersaline source, climatic dependence, and environmental impact. *Danish Journal of Geography* 110, 1–24.
- Hansen, J.M. 2011: Læsøs strandlinier – i lokalt/globalt og historisk/fremtidigt perspektiv. *Geologisk Nyt* 2011/6, 26–37.
- Hansen, J.M. 2015: Læsøs forhistorie og ældste stadier. *Museumsforeningen for Læsø, Årsskrift for 2014*, 12–25.
- Hansen, J.M., Aagaard, T. & Binderup, M. 2012: Absolute sea levels and isostatic changes of the eastern North Sea to central Baltic region during the last 900 years. *Boreas* 41, 180–208.
- Hede, M.U., Bendixen, M., Clemmensen, L.B., Kroon, A. & Nielsen, L. 2013: Joint interpretation of beach-ridge architecture and coastal topography show the validity of sea level

- markers observed in ground-penetrating radar data. *The Holocene* 23, 1238–1246.
- Hede, M.U., Sander, L., Clemmensen, L.B., Kroon, A., Pejrup, M. & Nielsen, L. 2015: Changes in Holocene relative sea-level and coastal morphology: A study of a raised beach ridge system on Samsø, southwest Scandinavia. *The Holocene* 25, 1402–1414. DOI: 10.1177/0959683615585834.
- Hill, E.M., Davis, J.L., Tamisiea, M.E. & Lidberg, M. 2010: Combination of geodetic observations and models for glacial isostatic adjustment fields in Fennoscandia. *Journal of Geophysical Research* 115, B07403, doi:10.1029/2009JB006967.
- Horton, B.P. & Shennan, I. 2002: Compaction of Holocene strata and the implications for relative sea level change on the east coast of England. *Geology* 37, 1083–1086.
- Houmark-Nielsen, M. 2003: Signature and timing of the Kattegat Ice Stream: onset of the LGM-sequence in the southwestern part of the Scandinavian Ice Sheet. *Boreas* 32, 227–241.
- Houmark-Nielsen, M. 2004: The Pleistocene of Denmark: a review of stratigraphy and glaciation history. In: Ehlers, J. & Gibbard (eds): *Quaternary glaciations – Extent and Chronology*. Elsevier, Amsterdam.
- Houmark-Nielsen, M. & Kjær, K.H. 2003: Southwest Scandinavia 40–15 ka BP: Palaeogeography and environmental change. *Journal of Quaternary Science* 18, 769–786.
- Iversen, J. 1967: Naturens udvikling siden sidste istid. In: Arne Nørvang & Torben J. Meyer (eds): *Landskabernes opståen*. Danmarks Natur 1, 345–445. Politikens Forlag.
- Japsen, P. & Britze, P. 1991: Det danske Bassin, Kalk Gruppen. Kort over den vertikale tykkelse (The Danish Basin, Chalk Group, Isochore map). *Danmarks Geologiske Undersøgelse Map Series* 29.
- Jensen, P., Aagaard, I., Burke Jr., R.A., Dando, P.R., Jørgensen, N.O., Kuijpers, A., Laier, T., O'Hara, S.C.M. & Schmaljohann, R. 1992: 'Bubbling reefs' in the Kattegat: submarine landscapes of carbonate-cemented rocks support a diverse ecosystem at methane seeps. *Marine Ecology Progress Series* 83, 103–112.
- Jessen, A. 1897: Beskrivelse til geologiske Kort over Danmark. Kortbladene Læsø og Anholt. *Danmarks Geologiske Undersøgelse*, 2. Række 4, 48 pp., 2 maps.
- Jessen, A. 1922: Stenalderhavets Udbredelse i det nordlige Jylland. *Danmarks Geologiske Undersøgelse*, 2. Række 25, 112 pp.
- Jessen, A. 1936: Vendsyssels Geologi. *Danmarks Geologiske Undersøgelse*, 5. Række 2, 195 pp.
- Jørgensen, N.O. 1980: Gypsum formation in recent submarine sediments from Kattegat, Denmark. *Chemical Geology* 28, 349–353.
- Jørgensen, N.O. 1992: Methane-derived carbonate cementation of marine sediments from the Kattegat, Denmark: Geochemical and geological evidence. *Marine Geology* 103, 1–13.
- Khan, S.A., Knudsen, P. & Tscherning, C.C. 2006: Crustal deformations at permanent GPS sites in Denmark. In: Sanso, E. (ed.): *A Window on the Future of Geodesy*, 556–560. Springer, Berlin.
- Krog, H. 1965: On the Post-Glacial development of the Great Belt. *Baltica* 2, 47–60.
- Krog, H. 1968: Late-Glacial and Postglacial Shoreline Displacements in Denmark. In: R.B. Morrison & H.E. Wright Jr. (eds): *Means of correlation of Quaternary successions* 8, 421–135.
- Laier, T. 1992: Shallow gas in northern Kattegat and southern Skagerrak. Meeting Proceedings, *Geologiska Foreningen i Stockholms Förhandlingar* 114, 235–251.
- Laier, T., Jørgensen, N.O., Buchardt, B., Cederberg, T. & Kuijpers, A. 1992: Accumulation and seepages of biogenic gas in northern Denmark. *Continental Shelf Research* 12, 1173–1186.
- Lambeck, K., Antonioli, F., Purcell, A. & Silenzi, S. 2004: Sea level change along the Italian coast for the past 10,000 years. *Quaternary Science Reviews* 23, 1567–1598.
- Larsen, G., Bauman, J. & Bjørn, O. 1986: Kvartærgeologiske forhold under havbunden i Læsø Rende. *Dansk Geologisk Forening, Årsskrift for 1985*, 39–46.
- Lykke-Andersen, A.-L. 1990: Foraminiferal stratigraphy of Quaternary deposits in boring no. 51.12 Anholt, Kattegat. *Danmarks Geologiske Undersøgelse, Series B* 15, 40 pp.
- Lykke-Andersen, H. 1992a: Massebevægelser i Vendsyssels og Kattegats kvartære aflejringer. *Dansk Geologisk Forening, Årsskrift for 1990–1991*, 93–97.
- Lykke-Andersen, H. 1992b: Nogle hovedtræk af Kattegats kvartære geologi. *Dansk Geologisk Forening, Årsskrift for 1990–1991*, 57–65.
- Lykke-Andersen, H. & Borre, K. 2000: Aktiv tektonik i Danmark – der er liv i Sorgenfrei-Tornquist Zonen. *Geologisk Nyt* 6/2000, 12–13. Copenhagen: Geological Survey of Denmark and Greenland.
- Lykke-Andersen, H., Knudsen, K.L. & Christiansen, C. 1993a: The Geokat project - a study of the Late Quaternary evolution of the Kattegat Sea. *Boreas* 22, 267–268.
- Lykke-Andersen, H., Knudsen, K.L. & Christiansen, C. 1993b: The Quaternary of the Kattegat area, Scandinavia: a review. *Boreas* 22, 269–281.
- Lysdahl, P. 1985: Minder fra Læsøs oldtid. *Museumsforeningen for Læsø, Årbog for 1984*, 8–12.
- Lysdahl, P. 1987: Et stenalderkar. *Museumsforeningen for Læsø, Årbog for 1986*, 35–36.
- Læsø Kommune, Nordjyllands Amt og Skov- og Naturstyrelsen 1989: Råstofkortlægning på Læsø, 96 pp. (Municipal decision paper).
- Mertz, E.-L. 1924: Oversigt over de sen- og postglaciale niveauforandringer. *Danmarks Geologiske Undersøgelse*, 2. Række 41, 50 pp.
- Michelsen, O. 1967: Foraminifera of the late-quaternary deposits of Læsø. *Meddelelser fra Dansk Geologisk Forening* 17, 205–264.
- Moucha, R., Forte, A.M., Mitrovica, J., Rowley, D.B., Quéré, S., Simmons, N.A. & Grand, S.P. 2008: Dynamic topography and long-term sea level variations: There is no such thing as a stable continental platform. *Earth and Planetary Science Letters* 271, 101–108.
- Mörner, N.-A. 1969: The late Quaternary history of the Kat-

- tegat Sea and the Swedish west coast. *Sveriges Geologiska Undersökning, Series C 640*, 487 pp.
- Mörner, N.-A. 1978: Faulting, fracturing and seismic activity as a function of glacial isostasy in Fennoscandia. *Geology* 6, 41–45.
- Mörner, N.-A. 1980: The northwest European “sea level laboratory” and regional Holocene eustacy. *Palaeogeography, Palaeoclimatology, Palaeoecology* 29, 281–300.
- Mörner, N.-A. 1995: Palaeoseismicity – The Swedish case. *Quaternary International* 25, 75–79.
- Mörner, N.-A. 2014: An  $M > 6$  Earthquake ~750 BC in Sweden. *Open Journal of Earthquake Research* 3, 66–81.
- Nielsen, A.H. 2008: On the evolution of beach-ridge plains – Luminescence dating, geomorphology and soil development at the Jerup beach-ridge plain, Denmark. Ph.D. thesis, Copenhagen University, 129 pp.
- Nielsen, A., Murray, A.S., Pejrup, M. & Elberling, B. 2006: Optically stimulated luminescence dating of a Holocene beach-ridge plain in northern Jutland, Denmark. *Quaternary Geochronology* 1, 305–312.
- Nielsen, L. & Clemmensen, L. 2009: Sea level markers identified in ground-penetrating radar data collected across a modern beach-ridge system in a microtidal regime. *Terra Nova* 21(6), 474–479.
- Nielsen, L.H. & Johannessen, P.N. 2009: Facies architecture and depositional processes of the Holocene–Recent accretionary forced regressive Skagen spit system, Denmark. *Sedimentology* 56, 935–968.
- Nielsen, L.H. & Johannessen, P.N. 2010: Accretionary, forced regressive shoreface sands of the Holocene–Recent Skagen Odde spit complex, Denmark – a possible outcrop analogue to fault-attached shoreface sandstone reservoirs. *Norwegian Petroleum Society, Special Publications* 10, 457–472.
- Noe-Nygaard, N., Knudsen, K.-L. & Houmark-Nielsen, M. 2006: Fra istid til og med Jægerstenalder. In: Larsen, G. (ed.): *Naturen i Danmark. Geologien*. Gyldendal, København, 303–332.
- Nordmann, V. 1903: En Klump sammenkittede Molluskskaller fra Havbunden ved Læsø. *Meddelelser fra Dansk Geologisk Forening* 9, 37–44.
- Olesen, M. (ed.) 2005: *Naturforholdene i havet omkring Læsø. Pilotprojekt Marin Nationalpark Læsø. Report for the working group on national parks*, 129 pp.
- Paradeisis-Stathis, S. 2015: *Evolution of a Barrier Island, Vegetation Cover and Climate Change – A Case Study of Stokken, Læsø*. Copenhagen University, Faculty of Science, 91 pp. (unpublished Master Thesis).
- Pedersen, S.A.S., Laier, T., Hansen, J.M. & Petersen, K.S. 1989: *Maringeologisk undersøgelse ved Læsø Rende. Dykkerundersøgelse af kalkcementering ved gasudstrømning i NV-Kattegat*. Danmarks Geologiske Undersøgelse Report series 35, 30 pp.
- Påsse, T. & Andersson, L. 2005: Shore-level displacement in Fennoscandia calculated from empirical data. *Geologiska Föreningen i Stockholms Förhandlingar* 127, 253–268.
- Sander, L., Hede, M.U., Fruergaard, M., Nielsen, L., Clemmensen, L.B., Kroon, A., Johannessen, P.N., Nielsen, L.H. & Pejrup, M. 2015: Coastal lagoons and beach ridges as complementary sedimentary archives for the reconstruction of Holocene relative sea-level changes. *Terra Nova (early view)*, DOI:10.1111/ter.12187.
- Sarmaja-Korjonen, K., Vasari, Y. & Hæggstrom, C.-A. 1991: *Taxus baccata* and influence from Iron Age man on the vegetation in Åland, SW Finland. *Annales Botanica Fennici* 28, 143–159.
- Scheck-Wenderoth, M. & Lamarche, J. 2004: Crustal memory and basin evolution in the Central European Basin System – new insights from a 3D structural model. *Tectonophysics* 397, 143–165.
- Schou, A. 1945: *Det marine Forland*. 236 pp. Copenhagen: Hagerups Forlag.
- Schou, A. 1969a: Danmark – et morænearkipel. In: Nørvang, A. & Meyer, T.J. (eds): *Kyst, Klit og Marsk*. Danmarks Natur 4, 9–17. Copenhagen: Politikens Forlag.
- Schou, A. 1969b: Kysten – kampzonen mellem hav og land. In: Nørvang, A. & Meyer, T.J. (eds): *Kyst, Klit og Marsk*. Danmarks Natur 4, 30–37. Copenhagen: Politikens Forlag.
- Schou, A. 1969c: Kystprofilen og dets udformning. In: Nørvang, A. & Meyer, T.J. (eds): *Kyst, Klit og Marsk*. Danmarks Natur 4, 52–58. Copenhagen: Politikens Forlag.
- Schou, A. 1969d: Det marine forland – de havskabte kystsletter. In: Nørvang, A. & Meyer, T.J. (eds): *Kyst, Klit og Marsk*. Danmarks Natur 4, 66–71. Copenhagen: Politikens Forlag.
- Schou, A. 1969e: Materialevandringen langs kysten. In: Nørvang, A. & Meyer, T.J. (eds): *Kyst, Klit og Marsk*. Danmarks Natur 4, 71–81. Copenhagen: Politikens Forlag.
- Schou, A. 1969f: Kystudligningen. In: Nørvang, A. & Meyer, T.J. (eds): *Kyst, Klit og Marsk*. Danmarks Natur 4, 81–85. Copenhagen: Politikens Forlag.
- Schou, A. 1969g: Hævede kystlinjer. In: Nørvang, A. & Meyer, T.J. (eds): *Kyst, Klit og Marsk*. Danmarks Natur 4, 187–190. Copenhagen: Politikens Forlag.
- Stoklund, B. 1973: *Tømmerskuderne fra Læsø. Et kapitel af skudehandelens historie*. Handels- og Søfartsmuseets Årbog for 1972.
- Stoklund, B. 1980: *Bosættelse og bebyggelse på Læsø*. Vendsyssel Årbog 1980. Historisk Samfund for Vendsyssel, 7–56.
- Stoklund, B. 1986: *Hakkemøg, foldtørv og træk*. *Tidsskrift for Folkelivsgranskning* 29, 51–69.
- Stoklund, B. 1990: *Tørvegødning – en vigtig side af hedebondens driftsystem*. *Landbohistorisk Tidsskrift* 1990(1), 47–72.
- Stoklund, B. 1999: *Turf Manuring in the Danish Island of Læsø*. *Geografisk Tidsskrift, Special Issue* 1999(1), 209–214.
- Stoklund, B. 2007: *Fra salt til tømmers*. In: Nielsen, H.G. (ed.): *Fra Reformation til Enevælde. Renæssancen i Nordjylland 1536/1600*. Hals, Nordjyske Museers Østkystnetværk, 339–366.
- Tamura, T., Fumitoshi, M., Futoshi, N., Kazuaki, W. & Yoshiki, S. 2008: Ground-penetrating georadar profiles of Holocene raised beach-ridge deposits in the Kujukuri strand plain, Pacific coast of eastern Japan. *Marine Geology* 248, 11–27.

- Vangkilde-Pedersen, T., Lykke-Andersen, H. & Lind, G. 1993: Dislocated Quaternary deposits in southeastern Kattegat – a glacial or gravitational phenomenon? *Boreas* 22, 329–336.
- Vejbæk, O.V. & Britze, P. 1994: Top præ-Zechstein. Toppen af bjergarter ældre end Zechstein, Strukturelt tidskort (Top pre-Zechstein, Structural time map). Danmarks Geologiske Undersøgelse, Map Series 45.
- Vellev, J. 1991: Die Salzproduktion in Dänemark – besonders auf der Insel Læsø. In: Ingenhaeff, W. (ed.): *Das Salz in der Rechts- und Handelsgeschichte*, 413–438. Hocquet & Palme.
- Vellev, J. 1993: Saltproduktion på Læsø, i Danmark og i Europa. Hikuin, 108 pp.
- Vellev, J. 2001: Salt på Læsø. In: Poul Christensen (ed.): *Læsø Salt – i Røg og Damp*. Læsø Produktions-skole og Saltsyderi, 31–52.
- von Post, L. 1933: A Gothiglacial Transgression of the Sea in South Sweden. *Geografiska Annaler* 15, 225–254.
- Woodworth, P.L., White, N.J., Jevrejeva, S., Holgate, S.J., Church, J.A. & Gehrels, W.R. 2009: Evidence for accelerations of sea level on multi-decade and century timescales. *International Journal on Climatology* 29, 777–789.



# Distribution and significance of foraminiferal biofacies on an aphotic Danian bryozoan mound, Karlstrup, Denmark

EMILIE GRØNBÆK SPRINGER, JAN AUDUN RASMUSSEN & LARS STEMMERIK



Springer, E.G., Rasmussen, J.A. & Stemmerik, L. 2016. Distribution and significance of foraminiferal biofacies on an aphotic Danian bryozoan mound, Karlstrup, Denmark. © 2016 by Bulletin of the Geological Society of Denmark, Vol. 64, pp. 57-67. ISSN 2245-7070. ([www.2dgf.dk/publikationer/bulletin](http://www.2dgf.dk/publikationer/bulletin)).

In this study, the distribution of benthic foraminifers across a Danian bryozoan mound in Karlstrup quarry, Denmark, is analysed in 22 samples using multivariate analysis. Three foraminiferal biofacies are established, each representing a distinct part of the mound. The *Anomalinoidea-Cibicides-Osangularia* Biofacies is characteristic of the relatively pure carbonate sediments on the crest and flanks of the bryozoan mound. The *Patellina* Biofacies occurs at the mound flanks and is particularly common in marly sediments. The *Spirillina* Biofacies characterises the crest of the bryozoan mound, in both marly and pure carbonate sediments.

Variations in the plankton/benthos ratio indicate that the benthic foraminifers prefer the marly sediments to pure limestone and mound flanks relative to the mound top. It is likely that the benthic foraminifers avoided the more powerful currents at the mound crest. The common occurrence of spirillinids on the mound top may represent the remnant of a rich, siliceous sponge community.

**Keywords:** Palaeoecology, benthic foraminifers, biofacies, Danian, Karlstrup quarry, bryozoan mounds.

Emilie Grøn­bæk Springer [[emiliegspringer@gmail.com](mailto:emiliegspringer@gmail.com)], Gentofte Kommune, Natur og Miljø, Bernstorffsvej 161, DK-2920 Charlottenlund, Denmark. Jan Audun Rasmussen [[janr@snm.ku.dk](mailto:janr@snm.ku.dk)] and Lars Stemmerik [[lars.stemmerik@snm.ku.dk](mailto:lars.stemmerik@snm.ku.dk)], Natural History Museum of Denmark, University of Copenhagen, Øster Voldgade 5–7, DK-1350 Copenhagen K, Denmark. JAR from April 1st 2016: [[jan.rasmussen@museummors.dk](mailto:jan.rasmussen@museummors.dk)], Museum Mors/Fossil and Mo-clay Museum, Skarrehagevej 8, DK-7900 Nykøbing Mors, Denmark.

Corresponding author: Jan Audun Rasmussen

Received 24 September 2015  
Accepted in revised form  
27 January 2016  
Published online  
12 April 2016

Lower Danian cool-water bryozoan mounds are common in a NW–SE trending facies belt along the north-eastern margin of the Danish Basin from eastern Sjælland to northern Jylland, Denmark (Fig. 1; Thomsen 1995; Bjerager & Surlyk 2007). The mounds are believed to reflect deposition in relatively deep water, below the photic zone, and pass south- and westwards into deep water chalk deposits (Thomsen 1995). The Danian mounds are 50–110 m long with a relief of 5 to more than 10 m above the sea floor (Cheetham 1971; Thomsen 1976, 1983; Bjerager & Surlyk 2007). The benthic fauna is dominated by bryozoans in a carbonate mud matrix. Octocorals are locally common while echinoids, crinoids, serpulid worms, brachiopods, bivalves, calcareous sponges and benthic foraminifers are minor elements (Bjerager & Surlyk 2007). The mounds are poorly cemented and samples therefore easy to disintegrate, making them ideal for faunal studies.

Studies of fossil and recent epifaunal and infaunal benthic foraminifers have demonstrated that shell morphology usually reflects adaptations to life strategies in the different microhabitats (e.g. Bernhard 1986; Corliss & Chen 1988; Koutsoukos & Hart 1990; Kaiho 1991; Murray 1991, 2006). The usually high abundance of benthic foraminifers in seabed samples and their ability to react quickly to environmental changes make them well suited for ecological and palaeoecological studies. In the present study, we analyse the distribution of benthic foraminifers across a single Danian bryozoan mound exposed in an old quarry at Karlstrup some 25 km southwest of Copenhagen (Fig. 1, Fig. 2), with the aim to improve the understanding of its evolution over time and its dependency on the sea-floor conditions. We have established three palaeoecological biofacies based on multivariate analysis of the benthic foraminifer assemblage in 22 samples, each of them characterising certain parts of the bryo-

zoan mound. Five genera, *Anomalinoides*, *Cibicides*, *Osangularia*, *Patellina* and *Spirillina*, constitute 73% of the benthic foraminiferal assemblage. The relative variations in abundance between these genera have shown to be useful in the palaeoecological analysis.

The analysis of the benthic foraminifers in the Karlstrup mound supplements earlier analyses of the benthic macrofauna in Danian bryozoan mounds from Jylland and Stevns Klint (Fig. 1; Thomsen 1976; Bjerager & Surlyk 2007).

## Geological setting

The Danish Basin forms part of an extensive basin that covered north-western Europe during the late Cretaceous and earliest Danian (Surlyk 1997). The basin was bounded to the north by the inverted Sorgenfrei–Tornquist fault zone and to the south by the Ringkøbing–Fyn basement high (Fig. 1).

The study area of Karlstrup quarry is located in the south-eastern part of the basin. Quarrying in the area started in 1843 and ended in 1975; the quarry is now

a recreational area and the walls are either flooded or partly overgrown (Gravesen 1983, 1993). The studied bryozoan mound is located along the western wall of the quarry. It forms part of the Stevns Klint Formation, and the occurrence of the planktic foraminifers *Parasubbotina pseudobulloides* and *Subbotina trivialis* in all the studied samples, together with the lack of younger species such as *Subbotina triloculinoides* and *Globanomalina compressa*, show that the mound was deposited during the early Danian *P. pseudobulloides* Subzone (P1a) of Berggren & Miller (1988). Thus, it correlates biostratigraphically with the top of the Cerithium Limestone Member and the lower part of the overlying bryozoan mounds of the Korsnæb Member at Stevns Klint (Rasmussen *et al.* 2005). Additionally, the occurrence of the echinoid *Tylocidaris oedumi* in the mound shows that it correlates with the *T. oedumi* Zone of Rosenkrantz (1937). The bryozoan-rich limestones were included in the Korsnæb Member of the Stevns Klint Formation by Surlyk *et al.* (2006). They dominate the lower Danian in a facies belt across northern Sjælland and northern Jylland where they form important groundwater reservoirs. The thickness varies from 30–45 m in northern Jylland to 5–20 m on Sjælland (Thomsen 1995; Surlyk *et al.* 2006).

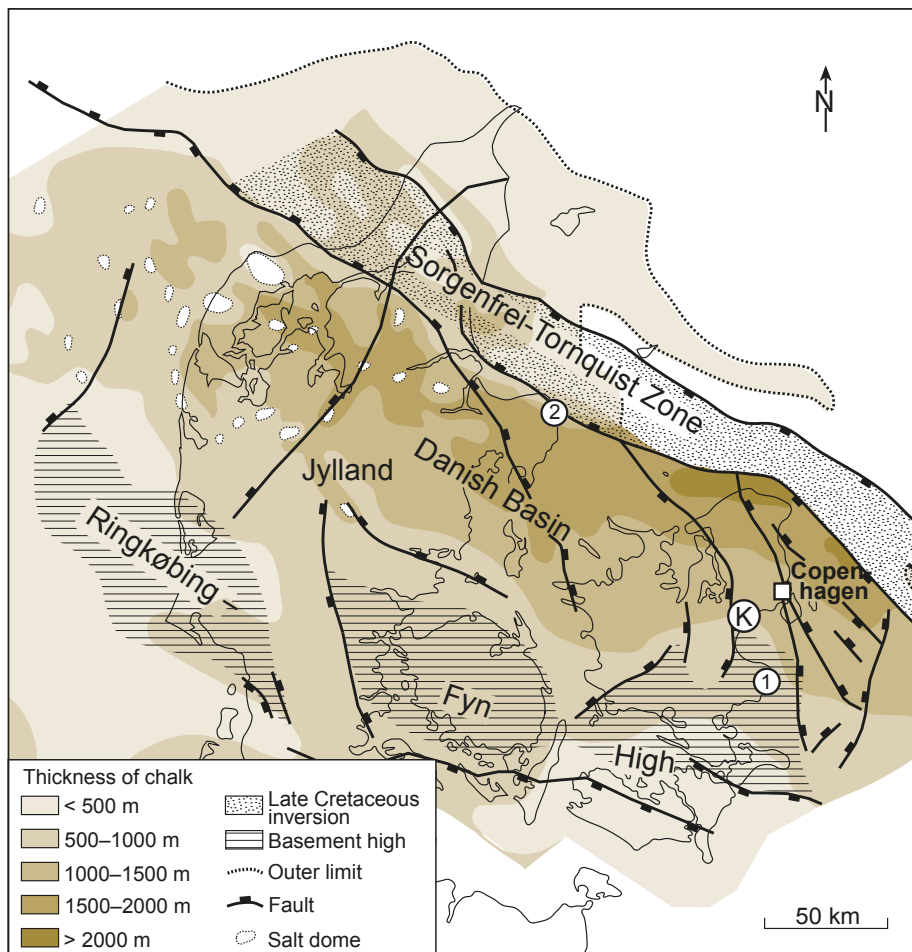


Fig. 1. Karlstrup quarry (K) is situated approximately 25 km south-west of Copenhagen, Denmark (map modified after Stemmerik *et al.* 2006). Additional localities mentioned in the text are Stevns Klint (1) and Karlby Klint (2).

The shape and growth of the bryozoan mounds are controlled by availability of food and bottom currents. The mounds are asymmetric and the highest density of bryozoans is found on the steep flanks facing the currents, where higher availability of food gave favourable conditions for colony growth (Thomsen 1976, 1983). The palaeocurrents were flowing towards WNW under the influence of the palaeotopography and the Coriolis force, and accordingly the bryozoan mounds migrated in a direction varying from SW to SE (Surlyk *et al.* 2006; Bjerager & Surlyk 2007). The bryozoan mounds in the Karlstrup quarry have the steepest flanks towards the SSW and S, which agrees with the orientation at Karlby Klint (Thomsen 1983) and Stevns Klint (Bjerager & Surlyk 2007).

## Material and methods

Twenty-two samples of approximately 200 g were collected for analysis from two bryozoan packstone beds with thin marly layers. The limestone beds, which are separated by flint horizons, can be traced across the selected mound. Samples were taken at eight vertical sections across the mound (Fig. 2). Where possible, three samples were taken at each section: one in the basal part of each of the two selected limestone beds and one in a marly layer in the upper bed. The lower limestone bed is referred to as bed A, the upper limestone is bed B, and the marly horizon is referred to as the M layer (Fig. 3).

Sixty grams of each sample were placed in a drying

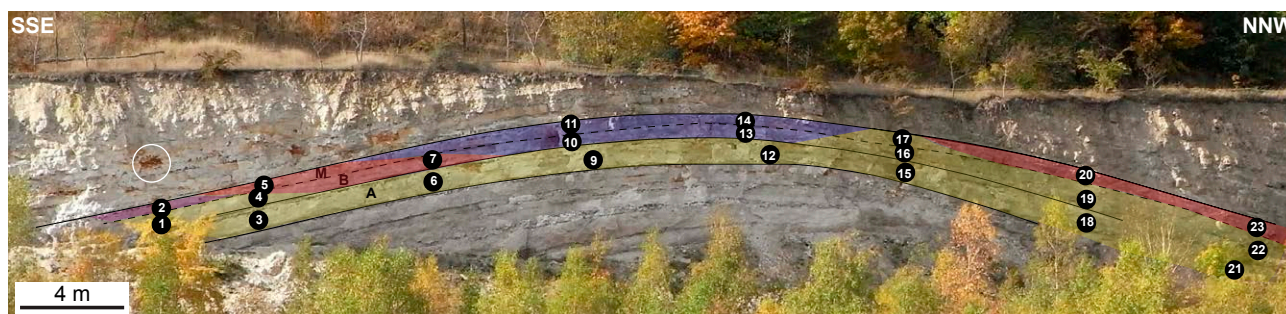


Fig. 2. The studied lower Danian bryozoan mound in the western wall of Karlstrup quarry. Twenty-two samples (numbers 1–7, 9–23, all with prefix P not shown here) were collected across the mound in two limestone beds (A and B) and one marly layer (M). Yellow shading marks the distribution of the *Anomalinoidea-Cibicides-Osangularia* Biofacies, red shading corresponds to the *Patellina* Biofacies, and blue shading marks the *Spirillina* Biofacies. Layer M at sample 2 is shaded purple, as sample 2 shares characteristics of both the *Spirillina* and the *Patellina* biofacies. The white circle is a characteristic area also visible in Fig. 3.



Fig. 3. Close-up of the southern flank of the bryozoan mound. Limestone beds A and B are separated by continuous flint bands. Samples were collected from the basal part of beds A and B and in the distinct marly layer (M) towards the top of bed B. The white circle is a characteristic area also visible in Fig. 2. Persons for scale.

cabinet for 24 hours, then reduced to 50 g and put in a dish soap solution for at least a week. The solution was stirred approximately every other day. Thereafter the material was wet-sieved through 1 mm and 63  $\mu\text{m}$  sieves. The 1 mm to 63  $\mu\text{m}$  fractions were dried, weighed, and split into suitable volumes. Splits from each sample were examined through a binocular microscope.

The ratio between planktic and benthic foraminifers is named the P/B ratio. It is expressed as  $100 \times P / (P+B)$ , which is the percentage of planktic foraminifera in the total foraminiferal assemblage. Approximately 200 foraminifers were picked from each sample to establish the P/B ratio, resulting in 2741 benthic and 5555 planktic foraminifers. Subsequently, additional splits were picked for palaeoecological analysis, resulting in 100–200 benthic specimens per sample and 4194 benthic specimens in total. The benthic foraminifers and selected planktic foraminifers were assigned to order, family, genus, or species level. Selected benthic species from the present data set have been taxonomically described and photographed using a Scanning Electron Microscope (Springer 2013).

The distribution of benthic foraminifers, especially the so-called reduced benthic assemblage (see below), was analysed statistically with two different multivariate statistical methods – correspondence analysis and cluster analysis – using the PAST software package (Hammer *et al.* 2001, Hammer 2012).

Ordination and clustering are the two main categories of multivariate methods employed in palaeoecological analyses. The principal method used in this study is Correspondence Analysis, which is a nonparametric ordination method that maximizes the correspondence between genus scores and sample scores. It is based on relative rather than absolute numbers from the data set. In this case it means that the relative number of the selected genera in each sample is more important than the absolute abundance. The advantage of the Correspondence Analysis is that genera and samples are ordinated simultaneously and scaled similarly. Thus, it is possible to plot the genus scores (R-mode) and the sample scores (Q-mode) in the same scatter diagram to show the relationship between them. Genera which plot close to each other in the CA plot show a related distribution and are typically relatively common in the same samples. Similarly, closely spaced localities are characterised by the occurrence of similar foraminiferal assemblages.

## Data set reduction

A total of 4194 benthic foraminifers were counted and identified using the methods described above. The total number of benthic foraminifers collected

from each sample varies between 82 and 506, and all samples except P12 and P19 contained more than 100 benthic foraminifers (Table 1). All observed benthic foraminifers are calcareous with a hyaline test. Approximately 85% of the benthic foraminifers were identified to the order level and 80% to genus level.

Based on a study of benthic foraminifers, Fatela & Taborada (2002) analysed the importance of both the total and relative abundance of taxa in palaeoecological studies. They showed that approximately 300 specimens of a population give a reliable statistical result, but concluded also that in studies primarily focusing on dominant taxa that each comprise >5% of the total fauna a collection of 100 specimens gives a sufficient degree of statistical reliability. These recommendations are followed here, and our statistical analyses were carried out on a reduced genus group, where genera comprising less than 5% were discarded. Consequently, the five dominating genera – *Cibicides*, *Anomalinoidea*, *Osangularia*, *Patellina* and *Spirillina* – which each constitute more than 5% of the total benthic foraminiferal assemblage were treated statistically. In total, this reduced benthic assemblage includes 3070 specimens constituting 73% of the total benthic assemblage. The four most abundant species are *Cibicides succedens*, *Osangularia lens*, *Anomalinoidea midwayensis* and *Anomalinoidea* sp. A.

## Results

### P/B – the ratio between planktic and benthic foraminifers

Gibson (1989) investigated the P/B ratio in a variety of settings and showed that the relative portion of planktic foraminifers generally correlates with distance from shore and/or water depth, and thus they are relatively more abundant with increasing depths in shelf and slope settings. In this work, the P/B ratio varies from 40.9% to 91.8% and is generally lower in the marly M layer (average 50.6%) than in the more pure limestone beds A and B (average 71.3%). Furthermore, in all three layers the P/B ratios are slightly higher near the mound crest (average 70%) than at the mound flanks (average 61%).

### Multivariate statistical analyses

The Morisita similarity index was selected for the unweighted pair-group average (UPGMA) cluster analysis. This index is widely used in ecological studies and is favoured by its independence of sample size and diversity (Wolda 1981).

Table 1. Number of identified benthic foraminiferal specimens in each sample

Sample	P1	P2	P3	P4	P5	P6	P7	P9	P10	P11	P12	P13	P14	P15	P16	P17	P18	P19	P20	P21	P22	P23	Total
<i>Anomalinoideis midwayensis</i> ?	12	2	10	6	0	13	5	6	7	4	0	12	14	5	8	4	6	6	7	3	6	7	143
<i>Anomalinoideis</i> sp. A	11	6	26	4	9	24	8	18	9	3	10	40	37	18	32	21	20	7	16	64	13	15	411
<i>Anomalinoideis</i> spp.	7	1	1	2	0	0	0	2	2	4	1	5	4	4	3	1	0	3	1	5	0	0	46
<i>Buliminida</i> morfotype A	0	0	0	0	0	0	0	2	0	0	0	0	0	0	1	0	0	0	0	0	0	0	3
<i>Charltonina</i> spp.	0	0	0	0	0	0	0	0	0	0	0	0	0	0	0	0	0	0	0	2	0	0	2
<i>Charltonina</i> ? sp.	1	0	0	0	0	0	0	0	0	0	0	0	0	0	0	0	0	0	0	0	0	0	1
<i>Cibicides</i> spp.	21	4	18	7	8	6	10	13	3	4	6	3	30	3	15	25	17	9	13	33	9	12	269
<i>Cibicides succedens</i>	19	9	16	20	9	14	4	17	7	5	4	9	18	5	11	17	27	8	10	41	8	15	293
<i>Cibicidoides</i> spp.	0	0	0	0	0	1	0	0	0	0	0	0	0	0	7	1	0	0	0	0	0	0	9
Discorbidae morfotype A	2	0	0	0	0	0	0	0	0	0	1	0	0	0	0	0	0	0	0	0	2	0	5
<i>Eponides</i> spp.	0	0	0	0	0	0	0	0	0	0	0	0	0	0	0	0	0	0	0	0	0	2	2
<i>Gavelinopsis</i> spp.	0	0	1	0	0	0	0	0	0	0	0	0	0	0	0	0	1	0	0	0	0	0	2
<i>Globulina</i> ?	1	0	0	0	0	0	0	0	0	0	0	0	0	0	0	0	0	0	0	0	0	0	1
<i>Guttulina</i> sp.	1	0	0	0	0	0	0	0	0	0	0	0	0	0	0	0	0	0	0	0	0	0	1
<i>Gyroidinoideis</i> spp.	0	0	0	0	0	2	0	0	0	0	0	1	1	0	1	0	0	0	0	2	1	0	8
<i>Lagena</i> sp. A	0	0	0	0	0	0	0	0	0	0	0	0	0	0	0	0	2	0	0	0	0	0	2
Lagenida morfotype A	0	0	0	0	0	0	1	1	0	0	0	0	0	0	0	0	0	0	0	0	0	0	2
Lagenidae morfotype A	0	0	0	0	0	0	0	0	0	0	0	0	0	0	0	0	0	0	1	0	0	0	1
<i>Lenticulina</i> spp.	0	0	1	1	0	1	0	2	0	0	0	0	0	1	1	0	1	1	0	1	1	1	12
<i>Nodosaria</i> cf. <i>spinescens</i>	0	0	0	0	0	0	0	0	0	0	0	0	0	0	0	0	0	0	0	1	0	0	1
Nodosariidae morfotype A	1	0	0	0	0	0	0	0	0	0	0	0	0	0	0	0	0	0	0	0	0	0	1
<i>Nonionella</i> ?	0	0	0	0	0	0	0	0	0	0	0	0	0	0	0	0	0	0	0	1	0	0	1
cf. <i>Nonionella</i> sp.	1	0	0	0	0	0	0	0	0	0	0	0	0	0	0	0	0	0	0	0	0	0	1
<i>Osangularia lens</i>	36	11	21	21	5	25	30	9	19	18	14	18	47	17	67	35	25	12	17	30	25	21	523
<i>Patellina</i> spp.	4	40	28	2	73	38	50	7	44	20	9	7	61	20	0	32	13	2	58	24	3	60	595
<i>Planulina</i> ? spp.	1	0	0	0	0	1	0	1	0	2	1	0	1	0	0	0	0	0	0	2	0	0	9
Polymorphinidae morfotype A	0	0	0	0	0	0	0	0	0	0	0	0	0	1	1	1	0	0	0	0	0	0	3
aff. <i>Pyrulina</i> sp.	1	0	0	0	0	0	0	0	0	0	0	0	0	0	0	0	0	0	0	0	0	0	1
cf. <i>Pyrulinoides</i> sp.	0	0	0	0	0	0	0	0	0	0	0	0	0	0	1	0	0	0	0	0	0	0	1
<i>Pullenia</i> spp.	0	0	0	2	2	1	0	0	0	0	0	0	0	1	0	0	1	2	0	1	0	2	12
<i>Pullenia</i> ?	2	0	0	0	0	0	0	0	0	0	0	0	0	0	0	0	0	0	0	0	0	0	2
<i>Pyrulina</i> sp. A	0	0	0	0	0	0	0	0	0	0	0	0	0	0	1	0	0	0	0	0	0	0	1
<i>Rosalina</i> aff. <i>globularis</i>	0	1	4	0	1	11	2	0	0	2	0	3	11	0	1	5	5	4	0	5	3	2	60
<i>Rosalina</i> sp. A	0	0	0	0	0	0	0	0	0	1	0	0	0	0	1	1	0	0	0	0	0	0	3
<i>Rosalina</i> sp. C	0	0	0	0	0	0	0	2	6	0	0	1	0	1	1	3	0	0	1	0	0	0	15
<i>Rosalina</i> sp. D	0	0	0	0	1	0	0	0	0	0	0	0	0	0	0	0	0	0	0	0	1	0	2
<i>Rosalina</i> sp. E	0	0	0	0	0	0	0	0	0	0	0	0	1	0	0	0	0	0	0	0	0	1	2
<i>Rosalina</i> sp. F	0	0	0	0	0	0	0	0	1	1	0	0	0	0	0	2	0	0	0	0	0	3	7
<i>Rosalina</i> sp. AA	0	0	0	0	0	0	0	0	0	0	0	0	0	0	0	1	0	0	0	0	0	0	1
<i>Rosalina</i> spp.	0	0	0	0	0	0	0	0	6	0	0	13	8	0	0	0	0	0	0	0	0	0	27
cf. <i>Rosalina</i>	1	0	0	0	0	0	0	0	0	0	0	0	0	1	0	0	0	0	0	0	0	0	2
<i>Rosalina</i> sp. B	0	0	0	0	0	0	0	0	0	0	0	14	0	0	1	0	0	0	0	0	0	0	15
Rotaliida A.	1	1	0	2	1	2	2	0	16	10	0	28	41	3	5	0	3	0	1	3	3	0	122
Rotaliida B.	0	0	0	1	0	0	0	0	0	7	0	0	20	0	0	0	1	0	0	0	0	0	29
Rotaliida C.	0	0	0	0	0	0	0	0	3	7	0	11	11	2	0	0	1	0	0	0	0	1	36
<i>Spirillina</i> spp.	5	44	55	2	42	34	22	10	76	57	8	71	159	11	23	27	11	8	34	67	7	17	790
<i>Stilostomella</i> spp.	1	0	5	1	1	2	0	1	0	0	0	3	7	3	3	2	2	0	3	4	0	0	38
<i>Tappanina selmensis</i>	1	0	0	0	0	2	7	0	8	5	0	8	23	1	3	1	0	0	0	2	0	4	65
Genus et species indet. A	2	0	0	0	0	0	1	1	0	0	0	0	0	0	1	0	0	0	0	0	0	0	5
Genus et species indet. B	0	0	0	0	0	0	0	7	0	0	0	0	0	0	0	0	1	0	0	0	0	0	8
Genus et species indet. C	18	5	14	21	12	28	9	11	0	0	17	0	0	28	37	17	12	10	22	18	33	30	342
Genus et species indet. D	9	0	3	5	0	3	8	0	0	0	5	0	0	7	17	8	11	10	2	4	13	3	108
Genus et species indet. E	0	0	0	3	0	0	1	0	0	0	0	0	0	2	6	0	2	0	1	0	0	2	17
Genus et species indet. F	1	1	1	5	0	3	15	0	0	4	10	19	12	1	22	4	2	0	9	11	6	10	136
Total	160	125	204	105	164	211	175	110	207	154	86	266	506	135	270	208	164	82	196	324	134	208	4194

In the correspondence analysis, *Cibicides* and *Osangularia* plot closely together near *Anomalinoidea* in the left-hand side of the diagram (Fig. 4), whereas *Patellina* and *Spirillina* plot near the two corners in the right-hand side.

The R-mode dendrogram for the cluster analysis based on the Morisita similarity index differs from the correspondence analysis plot in showing a closer relation between *Cibicides* and *Anomalinoidea* than between *Cibicides* and *Osangularia*. Otherwise, the resulting R-mode dendrogram (Fig. 5A) is in agreement with the correspondence analysis plot. Both methods show that the genera divide into two main groups consisting of *Cibicides*, *Anomalinoidea* and *Osangularia* in one group, and *Patellina* and *Spirillina* in the other. Furthermore, the distribution of *Anomalinoidea*, *Cibicides* and *Osangularia* show a higher degree of similarity than that of *Patellina* and *Spirillina*. The Q-mode dendrogram (Fig. 5B) corresponds well with the correspondence analysis results, and the three main sample clusters form a basis for the distribution of foraminiferal biofacies described below.

## Foraminiferal biofacies

Based on the correspondence analysis, the cluster analysis, and the quantitative distribution of the five analysed genera, three biofacies are recognised: *Anomalinoidea*-*Cibicides*-*Osangularia* Biofacies, *Patellina* Biofacies and *Spirillina* Biofacies (Fig. 4, Fig. 5A, B).

### *Anomalinoidea*-*Cibicides*-*Osangularia* Biofacies

Definition. Together, *Anomalinoidea*, *Cibicides* and *Osangularia* constitute more than 50% of the reduced genus group (see above).

Characteristics. Dominated by the nominate genera, this biofacies also includes relatively common specimens of *Spirillina* (14%) and *Patellina* (8%). Specimens of *Rosalina* (2.2%), *Stilostomella* (1.1%), *Lenticulina* and *Cibicoides* occur sporadically.

Distribution. The biofacies characterises the relatively pure carbonate sediments on both the crest and flanks of the bryozoan mound.

Occurrence. P1, P3, P4, P6, P9, P12, P15, P16, P17, P18, P19, P21 and P22.

### *Patellina* Biofacies

Definition. *Patellina* constitutes more than 33% of the reduced genus group (see above).

Characteristics. *Patellina* dominates the biofacies, but *Spirillina* (18%), *Cibicides* (10.8%), *Osangularia* (10%) and *Anomalinoidea* (9%) are also common. Additional, scattered genera include *Tappanina* (1.3%), *Rosalina* (1.3%), *Stilostomella*, *Pullenia* and *Eponides*.

Distribution. The biofacies characterises the bryozoan mound flanks and is particularly common in the marly sediments.

Occurrence. P5, P7, P20 and P23. P2 shares characteristics of both the *Spirillina* Biofacies and the *Patellina* Biofacies.

### *Spirillina* Biofacies

Definition. *Spirillina* constitutes more than 33% of the reduced genus group.

Characteristics. Dominated by *Spirillina*, this biofacies also includes *Patellina* (13.7%), *Anomalinoidea* (12.0%), *Osangularia* (9%) and *Cibicides* (7%). Less common benthic genera include *Rosalina* (4.5%), *Tappanina* (3.5%) and *Stilostomella*.

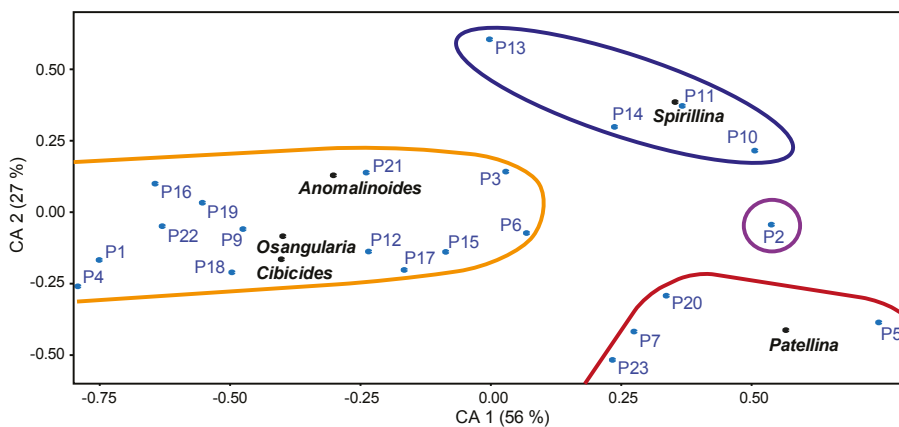


**Fig. 4.** Correspondence analysis plot based on a reduced benthic foraminiferal assemblage including all genera that comprise more than 5% of the total assemblage. Samples P1, P3, P4, P6, P9, P12, P15–19, P21 and P22 belong to the *Anomalinoidea*-*Cibicides*-*Osangularia* Biofacies (enclosed by an orange curve). Sample P2 shares characteristics of both the *Spirillina* and *Patellina* Biofacies (enclosed in a purple ring). Samples P5, P7, P20 and P23 represent the *Patellina* Biofacies (enclosed by a red curve). Samples P10, P11, P13 and P14 belong to the *Spirillina* Biofacies (enclosed by a blue curve). Note that 56% of the overall variation is seen along the CA 1 axis and only 27% along the CA 2 axis.

**Distribution.** The biofacies characterises the crest of the bryozoan mound where it occurs in both marls and pure carbonate facies.

**Occurrence.** P10, P11, P13 and P14. P2 shares characteristics with both the *Spirillina* Biofacies and the *Patellina* Biofacies.

Following the definitions of Corliss & Chen (1988), epifaunal foraminifers are recognised as those that live on or within the uppermost centimetre of the substrate, while infaunal foraminifers live below the uppermost centimetre of the substrate. Typically, epifaunal species are characterised by trochospirally coiled, plano-convex or biconvex tests, while infaunal species commonly have unornamented, elongate, biserially or triserially coiled torpedo-shaped or flattened tests or are planispiral with a rounded periphery (Corliss & Chen 1988, Kaiho 1991). In addition, anaerobic specimens are generally smaller than aerobic (Bernhard 1986). Epifaunal specimens represent 98% of the total benthic assemblage from the bryozoan mounds of Karlstrup. The content of infaunal benthic specimens is insignificant and averages 2% (Table 2). The scattered infaunal specimens are represented by *Tappanina selmensis*, *Stilostomella* spp. and a species of Buliminida morphotype A which are confined to the area near the crest of the mound. Infaunal specimens are typically most common in assemblages of the *Spirillina* Biofacies.

## Palaeoenvironmental significance

Overall, the foraminiferal assemblage contains 65% planktic specimens. According to the empirical equation of Van der Zwaan *et al.* (1990), this indicates a depositional depth of about 350 m. However, as discussed recently by Rasmussen & Sheldon (2015), this value is probably biased towards a deeper setting because the equation was based on depositional settings other than those of the very fine-grained chalk sea sediments. The common occurrence of azooxanthellate octocorals within the Danian deposits (Bernecker & Weidlich 2006) strongly indicates a palaeo-depth below the photic zone, but probably not deeper than 200–300 m as indicated by the common occurrence of the typical inner shelf foraminifer genera *Spirillina* and *Patellina* documented in the present paper. Hennig (1899) suggested a comparable depth for the middle Danian bryozoan mounds of the Faxe quarry. A recent study on cold-water, stylasterine corals from the middle Danian Faxe Formation (Lauridsen & Bjerager 2014) indicate a similar depositional depth of 200–400 m by comparison with modern stylasterine corals.

It is assumed that the relatively small variations in the P/B ratios on the bryozoan mound are not related to changes in water depth but instead to other environmental changes. If it is further assumed that the deposition of planktic foraminifers was uniform across the

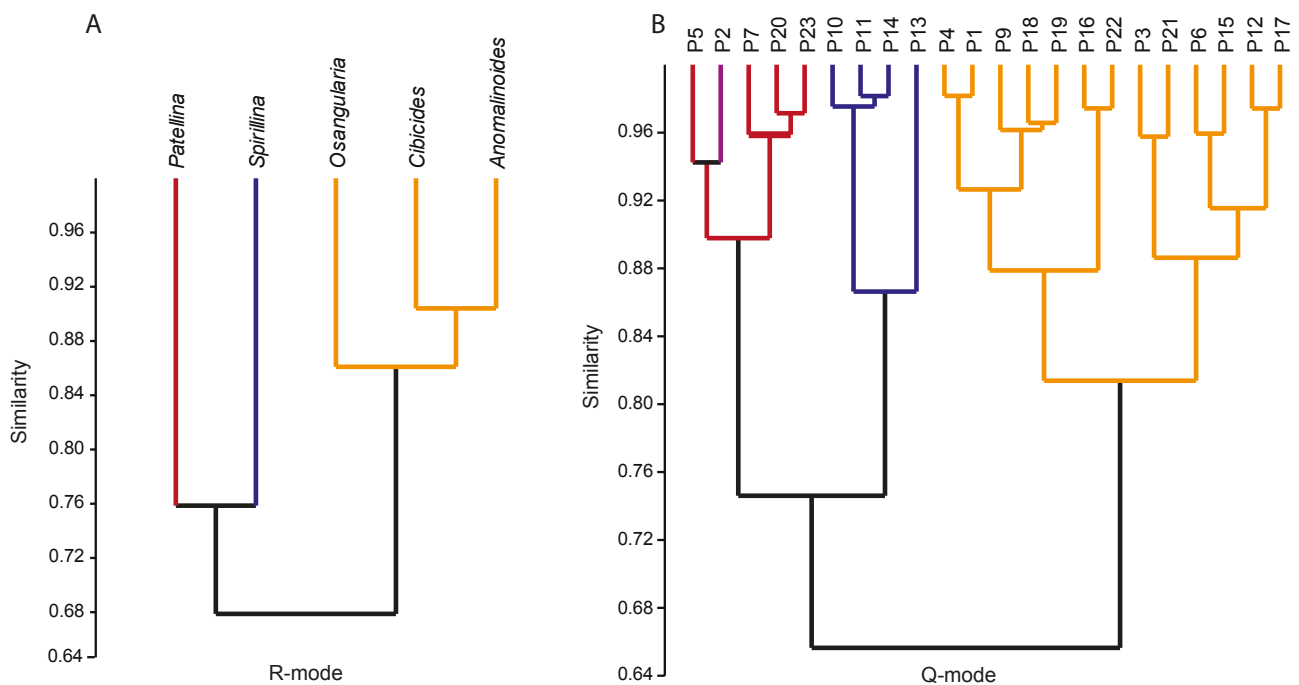


Fig. 5. Cluster analysis using the Morisita similarity index on a reduced benthic foraminiferal assemblage including all genera that comprise more than 5% of the total assemblage. **A:** R-mode dendrogram showing the level of similarity between the five dominating genera: *Anomalinoidea*, *Cibicides*, *Osangularia*, *Patellina* and *Spirillina*. **B:** Q-mode dendrogram showing the level of similarity between the content of the five dominating genera in each sample. See Fig. 4 for explanation of colours.

mound with minimal secondary transportation, the variation in the P/B ratio is best explained by relative changes in the abundance of benthic foraminifers. Following that assumption, the P/B ratio reflects a tendency towards a higher concentration of benthic foraminifers in the marl layer (M layer) compared to the two pure limestone layers (A and B beds), and on the flanks relative to the mound top. Thus, the benthic foraminifers seem to follow the same pattern as the bryozoans described by Thomsen (1983), avoiding the most powerful currents near the crest of the mound.

Several studies have indicated that the epifaunal/infaunal foraminiferal ratio reflects the organic carbon flux to the sea floor and/or the oxygen content near the sea floor and the uppermost centimetres of the underlying sediment (e.g. Bernard 1986; Corliss & Chen 1988; Corliss 1991; Kaiho 1991, 1994), but also other factors such as competition for food and space is important (Van der Zwaan *et al.* 1999). As a rule, an increase in the organic matter content triggers a decrease in the oxygen content of the pore water caused by microbial metabolism (Reolid & Martinez-Ruiz 2012). The Danian mounds contain a rich and diverse fauna of benthic organisms indicating excellent ecological conditions including well-oxygenated bottom water and a high food supply. It seems likely that the sparse infaunal fauna is related to the relatively coarse-grained structure of the bottom sediments (average 57 wt% > 63 µm), especially at the crest (70 wt% > 63 µm), and the relatively strong bottom currents that swept the mounds. Several modern studies have shown that these factors are inhibiting for infaunal foraminifers, but enhancing for epifaunal foraminifers (e.g. Schönfeld 2002; Schönfeld *et al.* 2011).

### Lithological influence on the distribution of biofacies

The lower of the two relatively pure limestone layers, bed A (Fig. 2, Fig. 3), is strongly dominated by the *Anomalinoïdes-Cibicides-Osangularia* Biofacies which contains 65.8% of the analysed benthic foraminifers. Of these, the two first-mentioned genera are most common and make up 25.6% and 23.2% of the analysed genera, respectively, while *Ossangularia* accounts for 17% of the specimens. Similarly, the *Anomalinoïdes-Cibicides-Osangularia* Biofacies dominates the overlying limestone layer, bed B, but here the abundance of *Ossangularia* increases from 17% to 26.1%, while *Anomalinoïdes* and *Cibicides* decrease to 22.9% and 21.5%, respectively. *Spirillina* and *Patellina* constitute less than 20% on average in both limestone beds.

The marl layer (M) deposited in the upper part of bed B is characterised by a foraminiferal fauna that is strikingly different from the fauna in the two

studied limestone beds. The relative abundance of the *Anomalinoïdes-Cibicides-Osangularia* Biofacies drops significantly to 39.3%, while the *Spirillina* and *Patellina* Biofacies increase to 29.8% and 30.8%, respectively; these genera seem to be able to take advantage of the higher content of siliciclastic mud and silt in this layer. The reason for this change is not clear. The three nominate genera of the *Anomalinoïdes-Cibicides-Osangularia* Biofacies are recognised as epifaunal taxa. *Anomalinoïdes* had its convex, umbilical side buried in the substrate, and it has been interpreted as having various feeding strategies. More precisely, it has been considered an active herbivorous, detritivorous, or omnivorous deposit feeder with a broad test that probably was well-suited for muddy substrates (Koutsoukos & Hart 1990). This is comparable to *Ossangularia*, which Koutsoukos & Hart (1990) interpreted as an active herbivorous, detritivorous, or omnivorous deposit feeder. A different mode of life is seen in *Cibicides*, which may have been passive, attached and herbivorous (Koutsoukos & Hart 1990) or possibly an attached passive suspension feeder (Murray 1991). Many Palaeogene species of *Cibicides* preferred the inner and middle

Table 2. Samples on bryozoan mound. Karlstrup quarry

Samples	Position on mound	Layer/Bed (Fig. 2)	Biofacies	P/B ratio 100*(P/P+B) (%)	Infaunal specimens (%)
P1	SSE flank	B	ACO	77.1	1.3
P2	SSE flank	M	P/S	45.6	0.0
P3	SSE flank	A	ACO	44.7	2.5
P4	SSE flank	B	ACO	75.4	1.0
P5	SSE flank	M	P	42.9	0.6
P6	SSE flank	A	ACO	75.7	1.9
P7	SSE flank	B	P	69.0	4.0
P9	Crest	A	ACO	79.7	2.7
P10	Crest	B	S	55.0	3.9
P11	Crest	M	S	53.2	3.2
P12	Crest	A	ACO	91.8	0.0
P13	Crest	B	S	67.1	4.1
P14	Crest	M	S	54.9	5.9
P15	Crest	A	ACO	79.1	3.0
P16	Crest	B	ACO	85.5	2.6
P17	Crest	M	ACO	66.7	1.4
P18	NNW flank	A	ACO	64.7	1.2
P19	NNW flank	B	ACO	76.2	0.0
P20	NNW flank	M	P	40.9	1.5
P21	NNW flank	A	ACO	67.5	1.9
P22	NNW flank	B	ACO	61.0	0.0
P23	NNW flank	M	P	50.3	1.9

ACO: *Anomalinoïdes-Cibicides-Osangularia* Biofacies; P: *Patellina* Biofacies; S: *Spirillina* Biofacies

P/B: The percentage of planktic foraminifers (P) of the total foraminiferal assemblage (planktic+benthic (P+B))

shelf environments (Murray *et al.* 1989), but they also occur in deeper, marine settings (Murray 1991).

The distinctive increase in the abundance of *Spirillina* within the marl layer may be related to its mode of life as attached or semi-attached to hard substrates favouring epifaunal suspension feeding (Langer 1993) or grazing (Reolid *et al.* 2008), commonly occurring on the inner shelf at depths less than 100 m (Murray 1991). An alternative view was presented by Koutsoukos & Hart (1990) who suggested that *Spirillina* was an epifaunal, active herbivorous, detritivorous, or omnivorous deposit feeder on muddy substrates where the broad test may have functioned as a snow-shoe. Murray (1991) interpreted *Patellina* as an attached, epifaunal suspension feeder, but it was also suggested that the genus may have been capable of an active life mode, with the umbilical side buried in the sediment, as an herbivorous or detritivorous deposit feeder (Koutsoukos & Hart 1990).

### Distribution of foraminiferal biofacies across the bryozoan mound

Seven samples from the SSE flank (samples P1–P7), nine from the mound crest (samples P9–P17), and six from the NNW flank (samples P18–P23) were analysed. Although genera of the *Anomalinoidea*-*Cibicides*-*Osangularia* Biofacies are most common at both the flanks and at the mound top, a more complex pattern appears when the mean abundances of the five main genera are analysed. Overall, *Patellina* (24.3%) characterises the SSE flank, while *Spirillina* (28.1%) typifies the crest of the mound. Similarly, when both the A, B and M (marl) beds are considered, *Cibicides* (25.4%) dominates the NNW flank, but also *Anomalinoidea* (22.5%) and *Osangularia* (19.1%) are common here. If only the marl layer is considered, *Patellina* characterises the two flanks and *Spirillina* the mound top. The most common infaunal species observed, *Tappanina selmensis*, constitutes 2% of the total benthic assemblage in the B and M beds at the mound crest. It is absent from the A bed. It inhabited primarily the outer neritic environments (Van Morkhoven *et al.* 1986). Although *T. selmensis* is rare, its presence indicates that at least sporadic areas with soft seabottom sediments existed at the mound top allowing an infaunal mode of life.

A survey of seven sample splits from three samples from the SSE flank, one sample from the mound crest and three samples from the NNW flank revealed that bryozoans are, by far, the most dominating supplementary fossil group, followed by serpulid worms and echinoids. Moreover, the concentration of bryozoan fragments are 2.1 times more common in the flank samples than in the top sample in the 1–2 mm

fraction, measured as bryozoan fragments per gram of sediment. Very small bryozoan fragments (63–250  $\mu\text{m}$ ) are distinctly more common at the NNW flank (lee side) than at the SSE flank, while large bryozoan and serpulid fragments (> 2 mm) are more common at the SSE flank. Thomsen (1976, 1983) observed this difference in the size of the bryozoan fragments between the two flanks from bryozoan mounds of the lower Danian Karlby Klint. The difference is caused by a reinforcement of the bryozoans due to the stronger influence of currents on the steep flank.

A number of physical, chemical and biological factors that affected the bryozoan mound controlled the distribution of foraminiferal biofacies. Significant limiting factors include food availability (organic matter) and oxygenation (Van der Zwaan *et al.* 1999), but also light, temperature, salinity, depth, substrate, water flow velocity and competition from other organisms are important.

Reolid *et al.* (2008) found that in the Jurassic the abundance of *Spirillina* was linked to the food supply, and the genus was usually common during high mesotrophic conditions characterised by a moderate amount of dissolved nutrients. *Spirillina* was considered an epifaunal grazer that indicate the presence of significant bacterial populations related to organic carbon particles (Reolid *et al.* 2008; Reolid & Martinez-Ruiz 2012). Moreover, Reolid & Martinez-Ruiz (2012) concluded that the abundance of *Spirillina* decreased during intervals with oxygen depletion.

Interestingly, Reuter *et al.* (2013) observed that spirillinid foraminifers (*Spirillina* and/or *Patellina*) appeared in high abundances in both Miocene and Late Jurassic sponge reefs but the group was less common in the surrounding sediments; they concluded that the spirillinids populated the water channels within the internal parts of sponges, which provided both food and protection. Accordingly, it may be speculated that the mound crest at Karlstrup was originally populated by siliceous sponges which served as habitats for the spirillinids. This is supported by a comprehensive study on the Danian bryozoan mounds of Stevns Klint by Bjerager & Surlyk (2007), who showed that siliceous sponge spicules were dissolved during burial but are preserved as voids in hardgrounds. They estimated that siliceous sponges might have constituted possibly 10–30% of the mound fauna, given that they were the main source of the silica forming the very common thick flint bands and nodules in the mounds. Accordingly, the common occurrence of spirillinids in the mound crest sediments of the Karlstrup quarry may be the remains of a former, rich, siliceous sponge community which was inhabited by grazing and/or filter feeding *Spirillina* and *Patellina*.

## Conclusions

Three foraminiferal biofacies have been established by multivariate analysis of the benthic foraminifer assemblage. The distribution of biofacies across the bryozoan mound shows an obvious preference in both mound area and environmental setting between the pure limestone and marly layers. The *Anomalinoidea-Cibicides-Osangularia* Biofacies is characteristic of the relatively pure carbonate sediments on the crest and flanks of the mound. The *Patellina* biofacies occurs on the bryozoan mound flanks and is particularly common in the marly sediments, whereas the *Spirillina* Biofacies characterizes the crest of the bryozoan mound in both marly and pure carbonate sediments.

*Spirillina* and *Patellina* may be associated with siliceous sponges (Reuter *et al.* 2013) and the common occurrence of spirillinids on the mound crest may reflect that a rich community of siliceous sponges originally inhabited this part of the mound. The sponges later became the main source of silica for the flint bands and nodules of the bryozoan mound (Bjerager & Surlyk 2007).

The ratio between planktic and benthic foraminifers (P/B) and the common occurrence of the typical inner shelf genera *Spirillina* and *Patellina* indicate a depositional depth below the photic zone but probably not deeper than 200–300 m. This is comparable with previously suggested depositional depth estimates for the middle Danian bryozoan mounds of the Faxe quarry, eastern Denmark (Hennig 1899; Lauridsen & Bjerager 2014).

It is proposed that the P/B ratio further reflects a tendency of the benthic foraminifers to prefer the marly sediments (M layer) compared to the pure limestone (beds A and B), and the mound flanks relative to the mound top. This pattern is similar to that of the bryozoans avoiding the powerful currents near the mound crest (Thomsen 1983).

The very low number of infaunal species within the assemblage strongly indicates well-oxygenated conditions during the time of mound formation, which is further supported by the presence of very common *Spirillina*.

## Acknowledgements

We are indebted to Karen Louise Knudsen and Erik Thomsen for careful and highly constructive reviews. Sten Lennart Jakobsen is thanked warmly for advice and fruitful help with sample preparation.

## References

- Berggren, W.A. & Miller, K.G. 1988: Paleogene tropical planktonic foraminiferal biostratigraphy and magnetobiochronology. *Micropaleontology* 34, 362–380.
- Bernecker, M. & Weidlich, O. 2006: Paleocene bryozoans and coral mounds of Fakse, Denmark: Habitat preferences of isidid octocorals. *Courier Forschungsinstitut Senckenberg* 257, 7–20.
- Bernhard, J.M. 1986: Characteristic assemblages and morphologies of benthic foraminifera from anoxic, organic-rich deposits: Jurassic through Holocene. *Journal of Foraminiferal Research* 16, 207–209.
- Bjerager, M. & Surlyk, F. 2007: Benthic palaeoecology of Danian deep-shelf bryozoans mounds in the Danish Basin. *Palaeogeography, Palaeoclimatology, Palaeoecology* 250, 184–215.
- Cheetham, A.H. 1971: Functional morphology and biofacies distribution of Cheilostome Bryozoa in the Danian Stage (Paleocene) of southern Scandinavia. *Smithsonian Contributions to Paleobiology* 6, 87 pp.
- Corliss, B.H. 1991: Morphology and microhabitat preferences of benthic foraminifera from the northwest Atlantic Ocean. *Marine Micropaleontology* 17, 195–236.
- Corliss, B.H. & Chen, C. 1988: Morphotype patterns of Norwegian Sea deep-sea benthic foraminifera and ecological implications. *Geology* 16, 716–719.
- Fatela, F. & Taborda, R. 2002: Confidence limits of species proportions in microfossil assemblages. *Marine Micropaleontology* 45, 169–174.
- Gibson, T.G. 1989: Planktonic benthonic foraminiferal ratios: Modern patterns and Tertiary applicability. *Marine Micropaleontology* 15, 29–52.
- Gravesen, P. 1983: Maastrichtien/Danien-grænsen i Karlstrup Kalkgrav (Østsjælland). *Dansk Geologisk Forening, Årsskrift for 1982*, 47–58.
- Gravesen, P. 1993: Early Danian species of the echinoid genus *Tylocidaris* (Cidaridae, Psychocidarinae) from eastern Denmark. *Contributions to Tertiary and Quaternary Geology* 30, 41–73.
- Hammer, Ø. 2012: PAST: Reference manual version 2.17. <http://folk.uio.no/ohammer/past/>.
- Hammer, Ø., Harper, D.A.T. & Ryan, P.D. 2001: PAST: Paleontological Statistics Software Package for Education and Data Analysis. *Palaeontologia Electronica* 4, 1, 9 pp. [http://palaeo-electronica.org/2001\\_1/past/issue1\\_01.htm](http://palaeo-electronica.org/2001_1/past/issue1_01.htm).
- Hennig, A. 1899: Studier öfver den baltiska Yngre kritans bildningshistoria. *Geologiska Föreningens i Stockholm Förhandlingar* 21, 19–82 (Häft 1) and 133–188 (Häft 2).
- Kaiho, K. 1991: Global changes of Paleogene aerobic/anaerobic benthic foraminifera and deep-sea circulation. *Palaeogeography, Palaeoclimatology, Palaeoecology* 83, 65–85.
- Kaiho, K. 1994: Benthic foraminiferal dissolved oxygen index and dissolved oxygen levels in the modern ocean. *Geology* 22, 719–722.

- Koutsoukos, E.A.M. & Hart, M.B. 1990: Cretaceous foraminiferal morphogroup distribution patterns, palaeocommunities and trophic structures: A case study from the Sergipe Basin, Brazil. *Transactions of the Royal Society of Edinburgh, Earth Sciences* 81, 221–246.
- Langer, M. 1993: Epiphytic foraminifera. *Marine Micropaleontology* 20, 235–265.
- Lauridsen, B.W. & Bjerager, M. 2014: Danian cold-water corals from the Baunekule facies, Faxe Formation, Denmark: a rare taphonomic window of a coral mound flank habitat. *Lethaia* 47, 437–455.
- Murray, J.W. 1991: Ecology and palaeoecology of benthic foraminifera. Longman Scientific and Technical, New York, 397 pp.
- Murray, J.W. 2006: Ecology and Applications of Benthic Foraminifera. Cambridge University Press, Cambridge. 426 pp.
- Murray, J.W., Curry, D., Haynes, J.R. & King, C. 1989: Palaeogene. In: Jenkins, D. G. & Murray, J. W. (eds): Stratigraphical atlas of fossil foraminifera, 490–536. Ellis Horwood Limited, Chichester.
- Rasmussen, J.A. & Sheldon, E. 2015: Late Maastrichtian foraminiferal response to sea-level change and organic flux, Central Graben area, Danish North Sea. In: Kear, B.P., Lindgren, J., Hurum, J.H., Milàn, J. & Vajda, V. (eds): Mesozoic Biotas of Scandinavia and its Arctic Territories. Geological Society, London, Special Publications 434, 25 pp. Online first, doi:10.1144/SP434.13.
- Rasmussen, J.A., Heinberg, C. & Håkansson, E. 2005: Planktonic foraminifers, biostratigraphy and the diachronous nature of the lowermost Danian Cerithium limestone at Stevns Klint, Denmark. *Bulletin of the Geological Society of Denmark* 52, 113–131.
- Reolid, M. & Martínez-Ruiz, F. 2012: Comparison of benthic foraminifera and geochemical proxies in shelf deposits from the Upper Jurassic of the Prebetic (southern Spain). *Journal of Iberian Geology* 38, 449–465.
- Reolid, M., Rodríguez-Tovar, F.J., Nagy, J. & Olóriz, F. 2008: Benthic foraminiferal morphogroups of mid to outer shelf environments of the Late Jurassic (Prebetic Zone, southern Spain). Characterization of biofacies and environmental significance. *Palaeogeography, Palaeoclimatology, Palaeoecology* 261, 280–299. doi:10.1016/j.palaeo2008.01.021.
- Reuter, M., Piller, W.E. & Brandano, M. 2013: Fossil psammobiontic sponges and their foraminiferal residents, central Apennines, Italy. *Palaios* 28, 614–622.
- Rosenkrantz, A. 1937: Bemærkninger om det østjællandske Daniens Stratigrafi og Tektonik. *Meddelelser fra Dansk Geologisk Forening* 9, 199–212.
- Springer, E.G. 2013: En palæoøkologisk analyse af den benthiske foraminiferfauna i en nedre Danien bryozobanke fra Karlstrup Kalkgrav. Unpublished MSc dissertation, Natural History Museum of Denmark, University of Copenhagen, 103 pp.
- Schönfeld, J. 2002: Recent benthic foraminiferal assemblages in deep high-energy environments from the Gulf of Cadiz (Spain). *Marine Micropaleontology* 44, 141–162.
- Schönfeld, J., Dullo, W.-C., Pfannkuche, O., Freiwald, A., Rüggeberg, A., Schmidt, S. & Weston, J. 2011: Recent benthic foraminiferal assemblages from cold-water coral mounds in the Porcupine Seabight. *Facies* 57, 187–213.
- Stemmerik, L., Surlyk, F., Klitten, K., Rasmussen, S.L. & Schovsbo, N. 2006: Shallow core drilling of the Upper Cretaceous Chalk at Stevns Klint, Denmark. *Geological Survey of Denmark and Greenland Bulletin* 10, 13–16.
- Surlyk, F. 1997: A cool-water carbonate ramp with bryozoan mounds; Late Cretaceous–Danian of the Danish Basin. In: James, N.P. & Clarke, J.A.D. (eds): Cool-water Carbonates. Special publication, SEPM 56, 293–307, Tulsa, OK, USA.
- Surlyk, F., Damholt, T. & Bjerager, M. 2006: Stevns Klint, Denmark: Uppermost Maastrichtian chalk, Cretaceous–Tertiary boundary, and Lower Danian bryozoan mound complex. *Bulletin of the Geological Society of Denmark* 54, 1–48.
- Thomsen, E. 1976: Depositional environment and development of Danian bryozoan biomicrite mounds (Karlby Klint, Denmark). *Sedimentology* 23, 485–509.
- Thomsen, E. 1983: Relation between currents and the growth of Palaeocene reef-mounds. *Lethaia* 16, 165–184.
- Thomsen, E. 1995: Kalk og kridt i den danske undergrund. In: Nielsen, O.B. (ed.): Danmarks Geologi fra Kridt til i dag 1, 32–67. Geologisk Institut, Aarhus Universitet.
- Van Morkhoven, F.P.C.M., Berggren, W.A. & Edwards, A.S. 1986: Cenozoic cosmopolitan deep-water benthic foraminifera. *Bulletin des Centres de Recherches Exploration, Production Elf-Aquitaine, Memoire* 11, 421 pp.
- Van der Zwaan, G.J., Jorissen, F.J. & de Stigter, H.C. 1990: The depth dependency of planktonic/benthic foraminiferal ratios; constraints and applications. *Marine Geology* 95, 1–16.
- Van der Zwaan, G.J., Duijnste, I.A.P., Den Dulk, M., Ernst, S.R., Jannink N.T. & Kouwenhoven, T.J. 1999: Benthic foraminifers: proxies or problems? A review of paleoecological concepts. *Earth-Science Reviews* 46, 213–236.
- Wolda, H. 1981: Similarity Indices, Sample Size and Diversity. *Oecologia* 50, 296–302.



# First record of tetrapod footprints from the Carboniferous Mesters Vig Formation in East Greenland

JESPER MILÀN, HENDRIK KLEIN, SEBASTIAN VOIGT & LARS STEMMERIK



Milàn, J., Klein, H., Voigt, S., & Stemmerik, L., 2016. First record of tetrapod footprints from the Carboniferous Mesters Vig Formation in East Greenland. ©2016 by Bulletin of the Geological Society of Denmark, Vol. 64, pp. 69–76. ISSN 2245-7070. ([www.2dgf/publikationer/bulletin](http://www.2dgf/publikationer/bulletin)).

A single slab with Late Palaeozoic tetrapod footprints from East Greenland has been housed at the Natural History Museum of Denmark for decades without scientific notice. The specimen comes from the Mesters Vig Formation of northern Scoresby Land in East Greenland and contains a monospecific assemblage of tetrapod footprints that we assign to *Limmopus* Marsh 1894. As there is no significant morphological difference from other records of this ichnogenus from North America, Europe and North Africa, the described tetrapod footprints can be referred to eryopoid temnospondyl trackmakers. *Limmopus* is well-known from Upper Carboniferous and Lower Permian continental deposits of palaeoequatorial Pangea. Identification of *Limmopus* tracks is in agreement with the supposed Late Carboniferous age of the Mesters Vig Formation and thereby also the first evidence of Carboniferous tetrapods from Greenland.

**Keywords:** Carboniferous, vertebrate tracks, *Limmopus*, Temnospondyli, Traill Ø Group, Mesters Vig Formation.

Jesper Milàn [[jesperm@oesm.dk](mailto:jesperm@oesm.dk)], Geomuseum Faxe, Østsjælland Museum, Østervej 2, DK-4640 Faxe, Denmark; also Natural History Museum of Denmark, Øster Voldgade 5–7, DK-1350 Copenhagen K., Denmark. Hendrik Klein [[hendrik.klein@combyphone.eu](mailto:hendrik.klein@combyphone.eu)], Saurierwelt Paläontologisches Museum, Alte Richt 7, D-92318 Neumarkt, Germany. Sebastian Voigt [[s.voigt@pfalzmuseum.bv-pfalz.de](mailto:s.voigt@pfalzmuseum.bv-pfalz.de)], Urweltmuseum GEOSKOP, Burg Lichtenberg (Pfalz), Burgstraße 19, D-66871 Thallichtenberg, Germany. Lars Stemmerik [[lars.stemmerik@snm.ku.dk](mailto:lars.stemmerik@snm.ku.dk)], Natural History Museum of Denmark, Øster Voldgade 5–7, DK-1350 Copenhagen K., Denmark.

Corresponding author: Jesper Milàn

Received 29 February 2016  
Accepted in revised form  
28 June 2016  
Published online  
11 August 2016

A small sandstone slab was recently noted in the Greenland exhibition hall of the Natural History Museum of Denmark in Copenhagen, where it was on display labelled as “Permian reptile tracks” without further information. According to the original label, the specimen comes from Upper Carboniferous strata of East Greenland and was collected by E. Witzig during field work in 1950. Though the provenance and story of their discovery are supported by a firsthand account (Gilberg 1992), the fossil footprints have never been addressed in any scientific report. Thus, we present the first detailed description and ichnotaxonomic evaluation of the fossil vertebrate tracks and briefly discuss the biostratigraphy and depositional environment of the track-bearing strata. Other aspects discussed are palaeobiogeography and palaeoecology because this is the first evidence of Carboniferous tetrapods from Greenland.

## Material and methods

This work is based on fossil tetrapod footprints preserved in convex hyporelief on the lower surface of a slab of dark-brown, fine- to medium-grained sandstone from Upper Carboniferous strata of East Greenland. The specimen consists of two well-fitting pieces that measure about 50 cm in total length, 23.5 cm in total width and 1.5 cm in average thickness. It is stored at the Natural History Museum of Denmark in Copenhagen and catalogued as MGUH 31556. In order to study the fossil tetrapod tracks, the track-bearing slab was photographed under obliquely incident artificial light. Outline sketches of all imprints were drawn on transparency film and digitised with vector-based drawing software. A digital photogrammetric model was generated from 134 close-range photographs using Agisoft Photoscan. Measurements of fossil

tetrapod tracks were taken using standard methods (Haubold 1971; Leonardi 1987; Voigt 2005).

Institutional abbreviations used are: MGUH, Natural History Museum of Denmark; YPM, Yale Peabody Museum, New Haven, Connecticut, USA; NMMNH, New Mexico Museum of Natural History and Science, Albuquerque, New Mexico, USA.

## Geological Setting

MGUH 31556 was found about 400 m above sea level on the slopes of the Langelinie mountain (72°09' N, 24°07' W) in the vicinity of the former lead mine at Mesters Vig, northern Scoresby Land, East Greenland (Fig. 1). In this part of East Greenland, the Carboniferous succession is up to 2000 m thick and composed of continental sediments that were deposited in a N–S trending, at least 350 km long rift basin extending

from Jameson Land in the south to Clavering Ø in the north (Fig. 1; Witzig 1954; Kempter 1961; Vigran *et al.* 1999).

The Carboniferous deposits of northern Scoresby Land are referred to the Mesters Vig Formation of the Traill Ø Group. The Mesters Vig Formation is subdivided into five members (Fig. 2; Witzig 1954; Kempter 1961; Perch-Nielsen *et al.* 1972). The base of the formation is not exposed in northern Scoresby Land, but elsewhere the continental Carboniferous sediments are seen to rest unconformably on Devonian and older rocks (Vigran *et al.* 1999). The formation is unconformably overlain by marine deposits of the Upper Permian Foldvik Creek Group.

MGUH 31556 was found loose and its exact stratigraphic position is unknown, although it most likely belongs to either the Blyklippen or Profilbjerget Member of the Mesters Vig Formation. All sediments of the Mesters Vig Formation contain a palynoflora dominated by *Potonieisporites* and have been correlated to

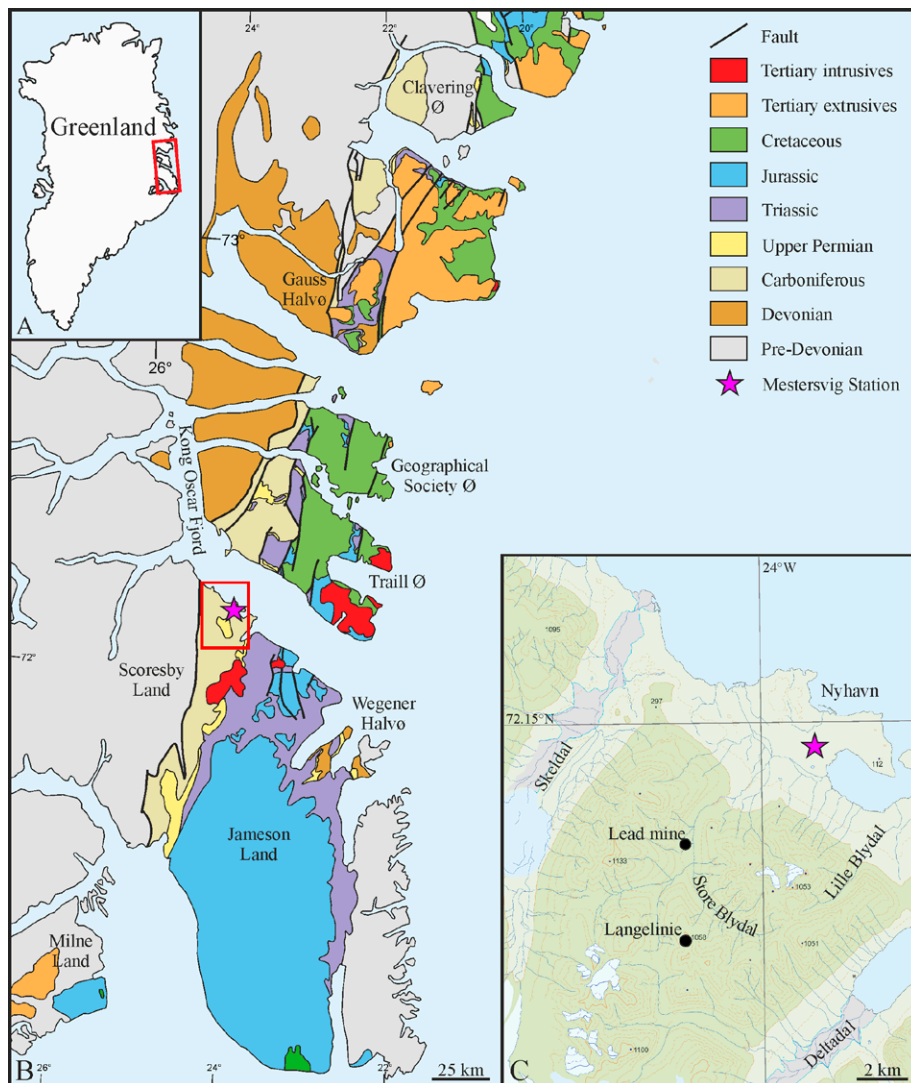


**Fig. 1.** Maps showing the locality on the east coast of Greenland where the track-bearing slab was found. **A:** Index map. **B:** Simplified geological map of the area between Jameson Land and Clavering Ø showing the distribution of Carboniferous non-marine sediments in central East Greenland. **C:** Detailed map showing the location of Langelinie in northern Scoresby Land where the track-bearing slab was found by E. Witzig in 1950. Maps modified from Stemmerik *et al.* (1997) and Higgins (2010).

the lower Cisuralian ('Autunian') of Europe (Piasecki 1984). Based on correlation to other Arctic microfloras, Vigran *et al.* (1999) concluded that this palynoflora is of Late Carboniferous rather than Early Permian age and correlated it with the Westphalian A RA Miospore Zone sensu Clayton *et al.* (1977), which corresponds to the upper Bashkirian to lower Moscovian stages (Fig. 2).

## Systematic ichnology

### *Ichnogenus Limmopus* Marsh 1894

*Type ichnospecies. Limmopus vagus* Marsh 1894.

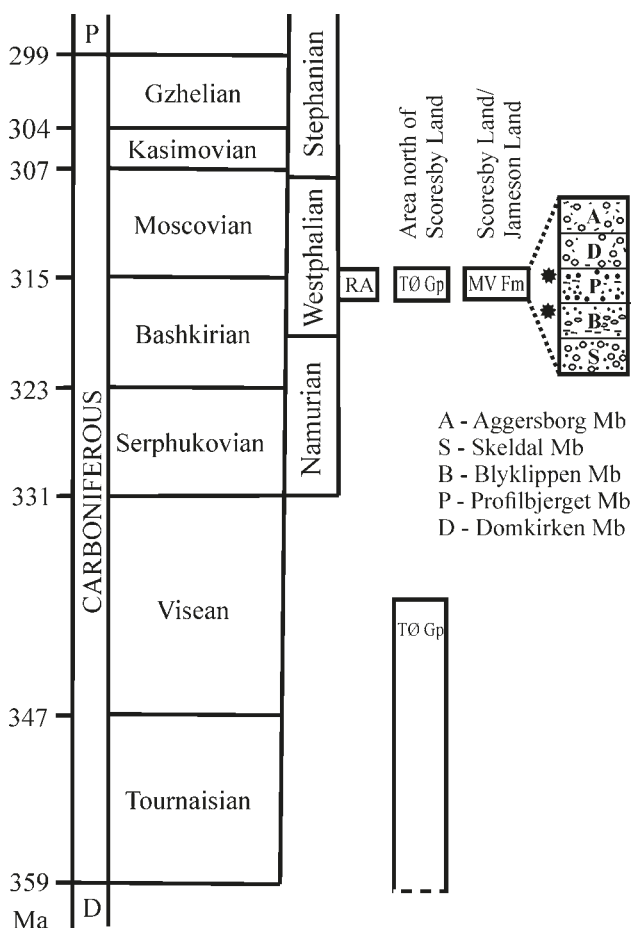


**Fig. 2.** Stratigraphy of the Carboniferous non-marine succession in East Greenland showing the age of the Traill Ø Group (TØ Gp) and the Mesters Vig Formation (MV Fm). Modified from Vigran *et al.* (1999). Ages in Ma from Gradstein *et al.* (2012). RA: *Radizonates aligerens* Miospore Zone of Clayton *et al.* (1977). Subdivision of the Mesters Vig Formation according to Perch-Nielsen *et al.* (1972). Asterisk marks the most likely stratigraphic position of the investigated material.

*Diagnosis* (after Haubold 1971, 1996; Voigt 2005). Trackways of a quadrupedal tetrapod with plantigrade to semiplantigrade imprints, pace angulation 80°–96°, stride : pes length = 3–5.5 : 1; pes impressed closely behind manus, pentadactyl, digits increasing in length from I–IV, digit IV longest, digit V as long as digit II and occasionally missing, short and broad oval sole, in deeply impressed imprints with proximolateral 'heel', robust basal pad of digit I, distal ends of digits rounded; manus tetradactyl with short broad, distally rounded digits, digits increasing in length from I–III, digit III longest, digit IV slightly shorter (80–90% of digit III), mostly longer than digit II, digit I with deeply impressed proximal pad similar to that in the pes.

*Description.* MGUH 31556 shows at least 12 tetrapod tracks that range in preservation from a very shallow impression of some digit tips to a very deep imprint lacking any anatomically controlled feature. The majority of traces are moderate to deep, more or less distinctly preserved imprints with stout and distally rounded digits (Figs 3–4). This kind of imprint measures 50–55 mm in length and 55–70 mm in width. The number of preserved digits varies between two and four to maybe five. Palm and sole impressions are poorly defined and show an approximately straight, slightly convex or slightly concave proximal margin. The digits increase in length from I to III. Digit IV, if present at all, is either longer or shorter than III. Most of the imprints show a well developed pad proximal to digit I, imitating an additional digit. Close to the centre and the edge of the slab, there is the only impression that preserves five digits. The digits of this imprint increase in length from I to IV and digit V is about as long as digit II (Fig. 4A, C–D, 5A).

The differences in the relative length of digit IV are interpreted to refer to manual and pedal tracks, respectively. A short fourth digit may characterize tetradactyl manual tracks, whereas a long fourth digit may belong to (originally pentadactyl, but in most cases preservationally tetradactyl) pedal tracks. Following this interpretation, MGUH 31556 shows three or four pedal and at least five manual tracks. Three manus–pes couples can be differentiated that all point to an inwardly rotated manual track (Fig. 3C).

## Discussion

The described tracks from MGUH 31556 are most similar to *Limmopus* Marsh 1894. This assignment is mainly based on the tetradactyl manus imprint and the relatively short, broad and clawless digits. Another characteristic feature of *Limmopus* is the presence of a

well developed basal pad proximal to digit I of both manus and pes imprints (Baird 1952; Voigt 2005).

The ichnogenus *Limnopus* was introduced for Pennsylvanian tetrapod footprints from Kansas (Marsh 1894). Since then, numerous other records have been mentioned from Upper Carboniferous and Lower Permian strata of Europe, North America and North Africa (Baird 1952, 1965; Haubold 1973; Martino 1991; Haubold *et al.* 1995; Voigt 2005; Voigt *et al.* 2011a, b; Marchetti *et al.* 2013, 2015; Lagnaoui *et al.* 2014; Lucas *et al.* 2015; Voigt and Haubold 2015; Voigt and Lucas 2015a, b). *Limnopus* tracks are remarkably similar to the ichnogenus *Batrachichnus* first described from Pennsylvanian strata of Pennsylvania (Woodworth 1900).

The discrimination of *Batrachichnus* and *Limnopus* tracks has been extensively discussed but is still an unresolved issue (Baird 1952; Haubold 1970, 1971, 1996; Tucker & Smith 2004; Voigt 2005). According

to Haubold (1996), tracks of both ichnogenera differ in the imprint proportions, relative length of digits, the trackway width as well as the imprint size (e.g., *Batrachichnus* pedal tracks are shorter than 30 mm). Voigt (2005) proposed the following distinguishing features: (1) relative length of manual digit IV, which is considered to reach 80–90 % of digit III in *Limnopus*, but only 60–70 % in *Batrachichnus*, giving manual tracks of *Batrachichnus* a more bilaterally symmetrical shape; (2) plantar surface of *Limnopus* with broad-oval pad and occasional proximolateral extension, whereas the sole of *Batrachichnus* pedal tracks is structureless; (3) *Limnopus* manual tracks are strongly inwardly rotated with respect to the midline and the pedal tracks, whereas the inward rotation of the manual track is less significant in *Batrachichnus*; (4) *Batrachichnus* pedal tracks range in size from less than 10 mm up to almost 40 mm, *Limnopus* pedal tracks may well

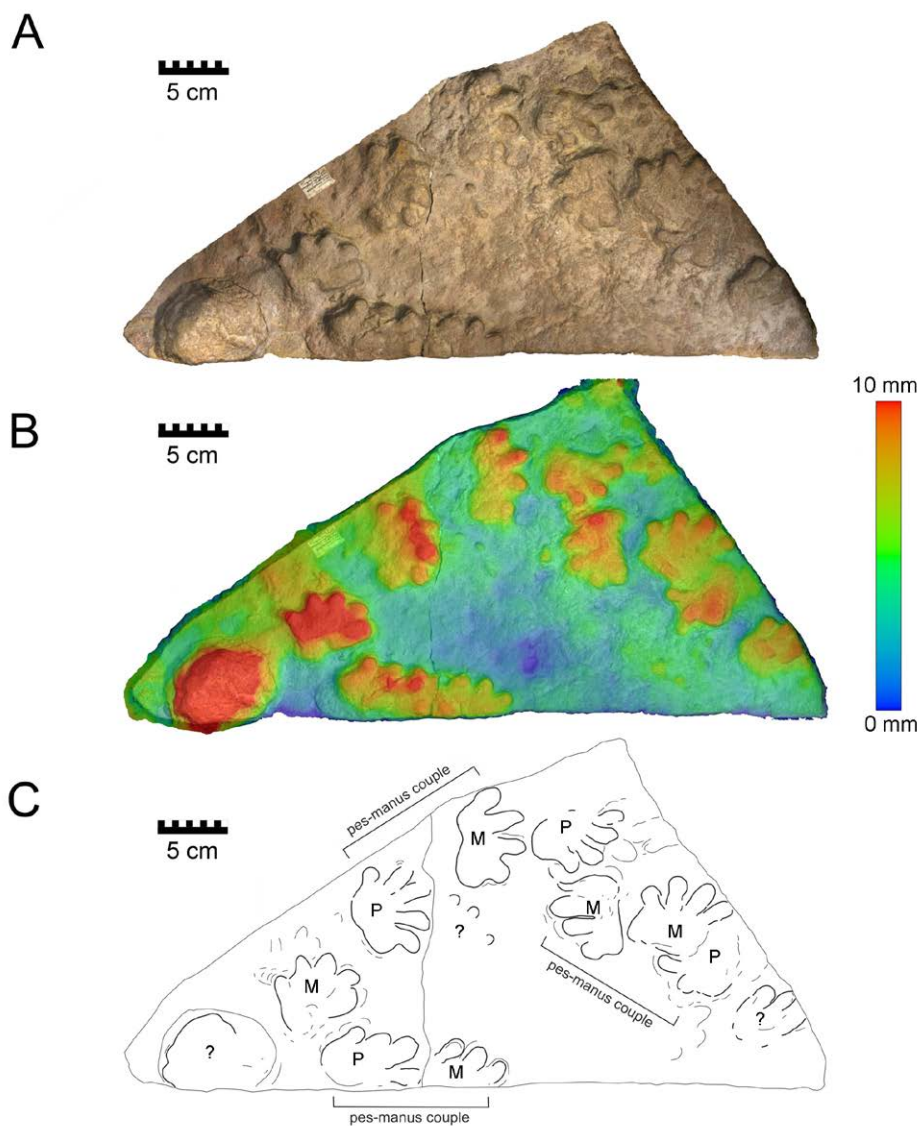


**Fig. 3.** Overview of slab MGUH 31556 from the Upper Carboniferous Mesters Vig Formation of East Greenland, with footprints preserved as convex hyporelief on the lower surface and assigned here to *Limnopus* isp. **A–B:** Photogrammetric models with B as coloured depth map. **C:** Interpretative drawing with demarcated pes (P) and manus (M). 3D models by Peter Falkingham.

exceed 60 mm in length. According to the imprint size, the relative length of the fourth digit of the manus, and the strongly inwardly rotated manus, the tracks of MGUH 31556 are much more similar to *Limnopus* than to *Batrachichnus*.

Numerous ichnospecies have been introduced for *Limnopus* or combined with this ichnogenus during the last century (Baird 1952, 1965; Haubold 1971, 1996, 2000; Voigt 2005; Lucas & Dalman 2013). With respect to anatomically controlled features of the imprint morphology and trackway pattern, hitherto discriminated *Limnopus* ichnospecies are not justified (Voigt 2005). *Limnopus heterodactylus* (King 1845) is the first named ichnospecies of *Limnopus* but is based on an isolated manus–pes imprint that, moreover, is ambiguous with respect to the relative length of pedal digit V (lectotype; Lucas & Dalman 2013). The second named *Limnopus* ichnospecies is *Limnopus vagus* Marsh 1894 that was designated the type ichnospecies. As it is known from full digit proportions and complete trackways, *L. vagus* is considered to be a valid ichnospecies. The most complete pedal track of MGUH 31556 shows a fifth digit that is about the same length as all other known *Limnopus* pedal tracks (Baird 1952; Haubold 1971; Voigt 2005; Fig. 5). As there is some degree of uncertainty regarding the quality of tracks and especially the lack of true trackways, we prefer to keep the described *Limnopus* tracks from Greenland in open nomenclature at the ichnospecies level.

## Track makers

*Limnopus* is most commonly considered to be the track

of eryopoid temnospondyls (Baird 1965; Haubold 1971, 1996, 2000; Voigt 2005). Although a four-digit manus is characteristic of both temnospondyls and microsaur, the latter can be ruled out because of their smaller size compared with the tracks of MGUH 31556. *Limnopus* may refer to amphibians that were able to spend a considerable part of their life outside the water in subadult to adult ontogenetic stages (Haubold 1996; Voigt 2005).

## Biostratigraphy, palaeobiogeography and palaeoecology

Available biostratigraphic data suggest that the tetrapod footprints of MGUH 31556 were produced during the Late Carboniferous at a time when central East Greenland was located some 10–15° north of the palaeoequator. The sedimentary record indicates overall warm and humid conditions with floodplains dominating the central axis of active rift basins and better drained sediments along the margins (Vigran *et al.* 1999). Associated flora (e.g. *Lepidodendron* and *Calamites*; Witzig 1951) and fauna (e.g. ‘palaeoniscid’ fishes; Moy-Thomas 1942) support palaeoenvironmental conditions with sufficient rainfall and a relatively high groundwater table.

*Limnopus* tracks are hitherto exclusively known from palaeoequatorial regions of Pangea in North America (Marsh 1894; Baird 1952, 1965; Voigt & Lucas 2015a, b), Europe (Haubold 1971; Gand 1988; Voigt 2005; Marchetti *et al.* 2013, 2015), and North Africa

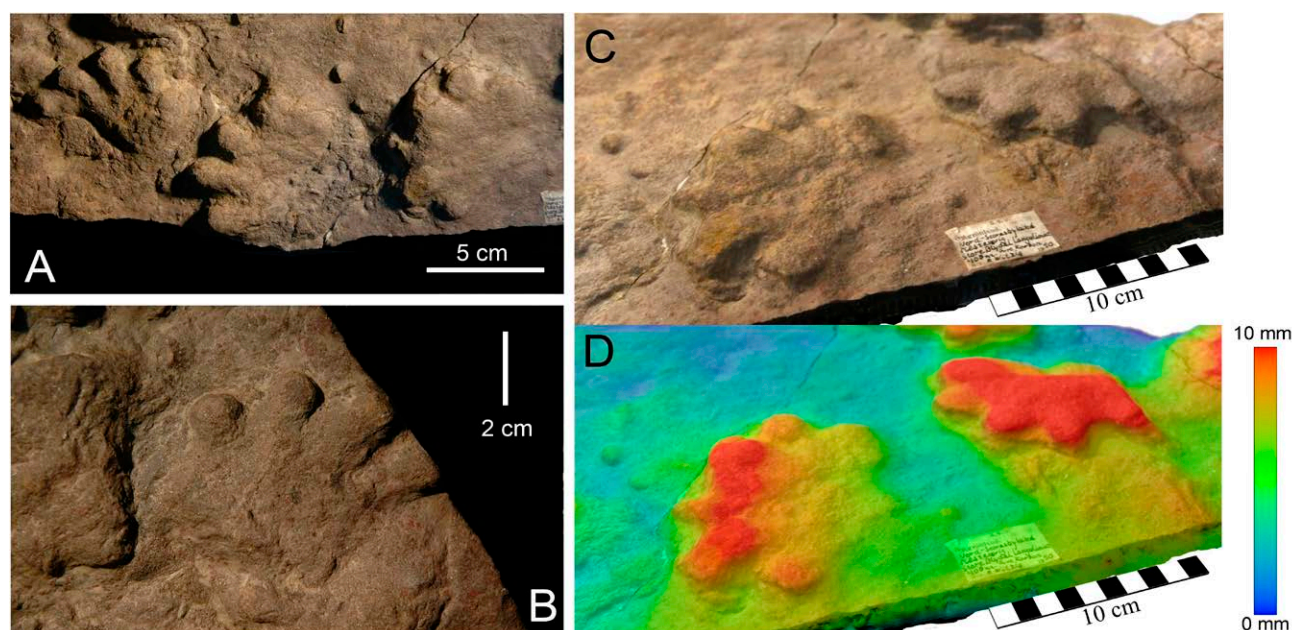


**Fig. 4.** Close-ups of selected tracks from slab MGUH 31556 from the Upper Carboniferous Mesters Vig Formation of East Greenland. **A:** Pes–manus couple corresponding to specimen in Fig. 5A and an isolated pes (left). **B:** Isolated manus. **C–D.** Photogrammetric models, with D as coloured depth map, of relatively well-preserved manus and pes imprints. 3D models by Peter Falkingham.

(Voigt *et al.* 2011a, b). All records are restricted to Upper Carboniferous and Lower Permian strata (Haubold 1971; Gand 1988; Gand & Durand 2006; Voigt 2005; Voigt & Lucas 2015a, b, in press).

The oldest occurrence of *Limnopus* is from the Salop Formation of Great Britain currently correlated with the Kasimovian stage of the Upper Carboniferous (Haubold & Sarjeant 1973; Tucker & Smith 2004), whereas the last occurrence is from upper Lower Permian (Artinskian) strata of the Italian Southern Alps (Marchetti *et al.* 2013, 2015). Possibly, older (Lower Carboniferous) records are hidden behind similar footprints that have been assigned to the ichnogenus *Palaeosauropus*, and the latter could be a junior synonym of *Limnopus* (Hay 1902; Lucas *et al.* 2010). However, *Palaeosauropus* is not well enough known to be readily compared to *Limnopus* (Lucas *et al.* 2010; Fillmore *et al.* 2012). If the Bashkirian-Moscovian age of the Mesters Vig Formation is correct, MGUH 31556 from East Greenland would predate the first occur-

rence of *Limnopus* by *c.* 8–10 Ma. Irrespective of the exact chronostratigraphic position of the footprint-bearing beds, the identification of *Limnopus* is at least in agreement with a supposed Late Carboniferous age of the Mesters Vig Formation. The rift basins of East Greenland are composed of thick successions of Palaeozoic and Mesozoic terrestrial to marine sediments that locally contain significant vertebrate remains (Bendix-Almgreen 1976; Henriksen & Higgins 1976). The Devonian succession on Ymer Ø is the famous locality for the early tetrapods, *Ichthyostega* and *Acanthostega*, as well as numerous fishes (e.g. Jarvik 1952; Bendix-Almgreen 1976; Blom *et al.* 2005, 2007; Clack *et al.* 2012). The overlying Carboniferous deposits of this area have yielded a diverse palaeoflora (Witzig 1951, 1954; Halle 1953; Pedersen 1976) and fossil fishes (e.g. Nielsen 1932; Moy-Thomas 1942; Bendix-Almgreen 1975), but no tetrapod remains as yet. Therefore, the footprints of MGUH 31556 are also the first evidence of Carboniferous tetrapods from Greenland.

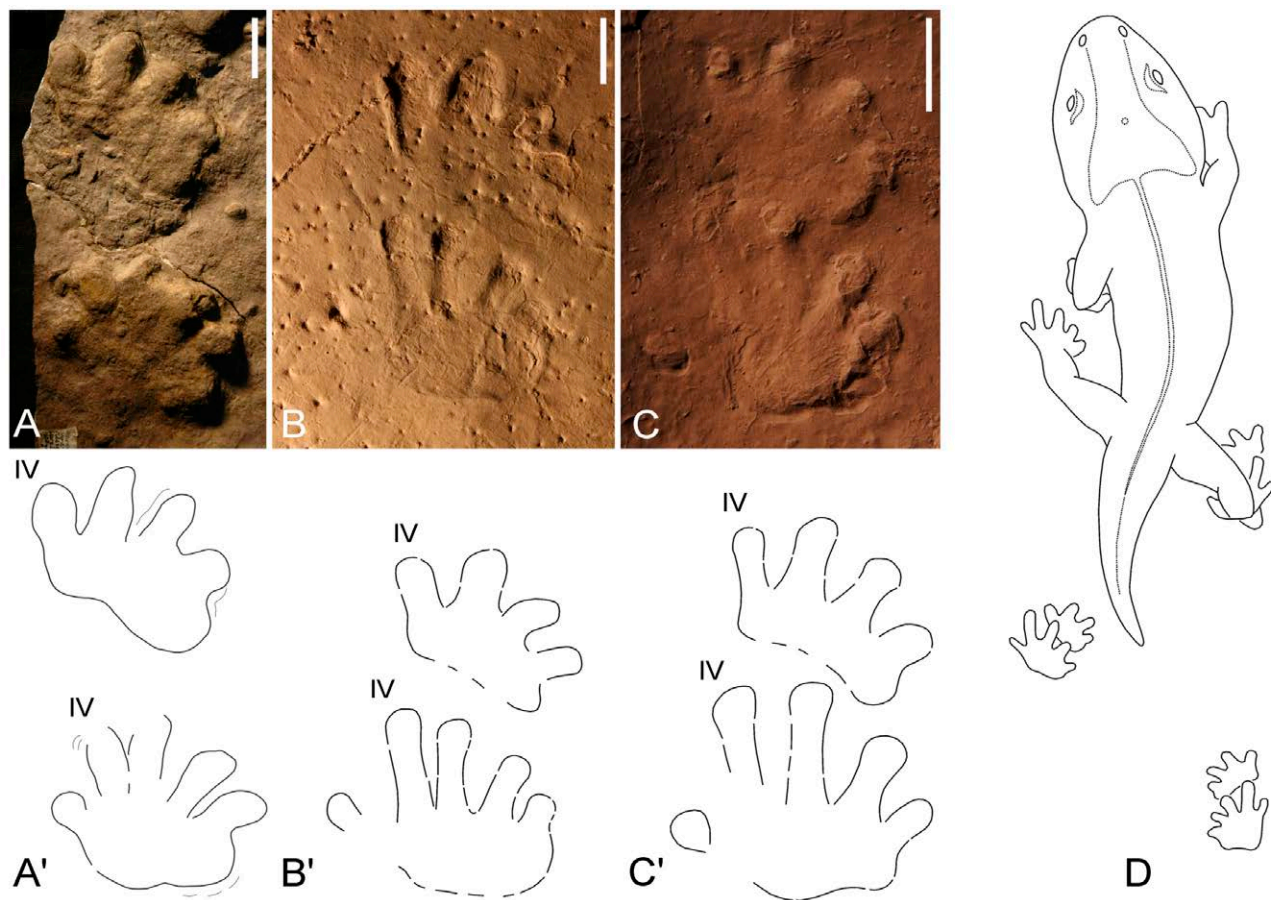


**Fig. 5.** Comparison of *Limnopus* tracks from various localities. **A, A'**: tracks from the Upper Carboniferous Mesters Vig Formation of East Greenland. **B, B'**: tracks from the Upper Carboniferous/Pennsylvanian of Kansas. **C, C'**: tracks from the Lower Permian of New Mexico. The pictures show a generally uniform morphology of pes and manus tracks. Material: (A, A') MGUH 31556; (B, B') YPM 405, Yale Peabody Museum New Haven, Connecticut; (C, C') NMMNH P-24603, New Mexico Museum of Natural History Albuquerque, New Mexico. Scale bars equal 1 cm. **D**: Hypothetical reconstruction of the *Limnopus* track maker and its gait, modified from Baird (1952).

## Conclusions

The terrestrial Mesters Vig Formation of northern Scoresby Land, East Greenland, yields fossil tetrapod footprints, opening the potential for future investigations in the area.

A single slab and the only known specimen with fossil tetrapod footprints from the Mesters Vig Formation was collected in 1950 and is housed at the Natural History Museum of Denmark in Copenhagen.

Assignable tetrapod tracks on this specimen all correspond to medium-sized tracks of the ichnogenus *Limnopus*, considered to be made by eryopoid temnospondyls.

The biostratigraphic age of *Limnopus* is in agreement with a supposed Late Carboniferous age of the Mesters Vig Formation.

The find of *Limnopus* tracks in the Mesters Vig Formation is the first evidence of Carboniferous tetrapods from Greenland and an important biogeographical marker.

## Acknowledgements

Peter Falkingham from Liverpool John Moors University kindly provided 3D photogrammetric models of the tracks. Sten Lennart Jakobsen, Natural History Museum of Denmark, is thanked for practical help during the study of the specimen. Furthermore we thank Jennifer A. Clack and Spencer G. Lucas for their comments and constructive reviews.

## References

- Baird, D. 1952: Revision of the Pennsylvanian and Permian footprints *Limnopus*, *Allopus* and *Baropus*. *Journal of Paleontology* 26, 832–840.
- Baird, D. 1965: Footprints from the Cutler Formation. U.S. Geological Survey Professional Paper 503, 47–50.
- Bendix-Almgreen, S.E. 1975: Fossil fishes from the marine late Palaeozoic of Holm Land – Amdrup Land, North-East Greenland. *Meddelelser om Grønland* 195(9), 1–38.
- Bendix-Almgreen, S.E. 1976: Palaeovertebrate faunas of Greenland. In: Escher, A. & Watt, W.S. (eds), *Geology of Greenland*, 538 – 573. Geological Survey of Greenland, Copenhagen.
- Blom, H., Clack, J.A. & Ahlberg, P.E. 2005: Localities, distribution and stratigraphical context of the Late Devonian tetrapods of East Greenland. *Meddelelser om Grønland, Geoscience* 43, 1–50.
- Blom, H., Clack, J.A., Ahlberg P.E. & Friedman, M. 2007: Devonian vertebrates from East Greenland: a review of faunal composition and distribution. *Geodiversitas* 29, 119–141.
- Clack, J.A., Ahlberg, P.E., Blom, H. & Finney, S.M. 2012: A new genus of Devonian tetrapod from East Greenland with new information on the lower jaw of *Ichthyostega*. *Palaeontology* 55, 73–86.
- Clayton, G., Coquel, R., Doubinger, J., Gueinn, K., Loboziak, S., Owens, B. & Streeb, M. 1977: Carboniferous miospores of western Europe: Illustrations and zonation. *Mededelingen Rijks Geologische Dienst* 29, 1–71.
- Fillmore, D.L., Lucas, S.G. & Simpson, E.L. 2012: Ichnology of the Mississippian Mauch Chunk Formation, eastern Pennsylvania. *New Mexico Museum of Natural History and Science Bulletin* 54, 1–139.
- Gand, G. 1988: Les traces de vertébrés tétrapodes du Permien français. Thèse de Doctorat d'Etat ès Sciences Naturelles, Université de Bourgogne, Edition Centre des Sciences de la Terre, Dijon; 341 pp.
- Gand, G. & Durand, M. 2006: Tetrapod footprint ichno-associations from French Permian basins. Comparisons with other Euramerican ichnofaunas. *Geological Society, London, Special Publication* 265, 157–177.
- Gilberg, A. 1992: Blyminen ved Mestersvig i Østgrønland. *Tidsskriftet Grønland* 1992, 289–311.
- Gradstein, F.M., Ogg, J.G., Schmitz, M.D. & Ogg, G.M. 2012. *The geologic time scale 2012*. Elsevier, 1176 pp.
- Halle, T.G. 1953: The Carboniferous flora of East Greenland. *Proceedings of the 7<sup>th</sup> International Botanical Congress, Stockholm 1950*, 594–596.
- Haubold, H. 1970: Versuch der Revision der Amphibien-Fährten des Karbon und Perm. *Freiberger Forschungshefte C* 260, 83–117.
- Haubold, H. 1971: Ichnia Amphibiorum et Reptiliorum fossilium. *Encyclopedia of Paleoherpertology* 18, 1–124.
- Haubold, H. 1973: Die Tetrapodenfährten aus dem Perm Europas. *Freiberger Forschungshefte C* 285, 5–55.
- Haubold, H. 1996: Ichnotaxonomie und Klassifikation von Tetrapodenfährten aus dem Perm. *Hallesches Jahrbuch für Geowissenschaften B* 18, 23–88.
- Haubold, H. 2000: Tetrapodenfährten aus dem Perm – Kenntnisstand und Progress 2000. *Hallesches Jahrbuch für Geowissenschaften* 22, 1–16.
- Haubold, H. & Sarjeant, W.A.S. 1973: Tetrapodenfährten aus den Keele und Enville Groups (Permokarbon: Stefan und Autun) von Shropshire und South Staffordshire, Großbritannien. *Zeitschrift für Geologische Wissenschaften* 1, 895–933.
- Haubold, H., Hunt, A.P., Lucas, S.G. & Lockley, M.G. 1995: Wolfcampian (Early Permian) vertebrate tracks from Arizona and New Mexico. *New Mexico Museum of Natural History and Science Bulletin* 6, 135–165.
- Hay, O.P. 1902: Bibliography and catalogue of the fossil Vertebrata of North America. *U.S. Geological Survey Bulletin* 179, 868 pp.
- Henriksen, N. & Higgins, A.K. 1976: East Greenland Caledonian fold belt. In: Escher, A. & Watt, W.S. (eds), *Geology of Greenland*, 183 – 246. Geological Survey of Greenland, Copenhagen.

- Higgins, A.K. 2010: Exploration history and place names of northern East Greenland. Geological Survey of Denmark and Greenland Bulletin 21, 368 pp.
- Jarvik, E. 1952: On the fish-like tail in the ichthyostegid stegocephalians with a description of a new crossopterygian from the Upper Devonian of East Greenland. Meddelelser om Grønland 114, 1–90.
- Kempter, E. 1961: Die Jungpaläozoischen Sedimente von Süd Scoresby Land. Meddelelser om Grønland 164(1), 123 pp.
- King, A.T. 1845. Description of fossil footmarks, found in the Carboniferous series in Westmoreland County, Pennsylvania. American Journal of Science 48(2), 343–352.
- Lagnaoui, A., Voigt, S., Saber, H. & Schneider, J. 2014: First occurrence of tetrapod footprints from Westphalian strata of the Sidi Kassem Basin, central Morocco. Ichnos 21, 223–233.
- Leonardi, G. 1987: Glossary and Manual of Tetrapod Footprint Palaeoichnology, Ministerio Minas Energie, Departamento Nacional da Produção Mineral, Brasilia, 117 pp.
- Lucas, S.G. & Dalman, S.G. 2013: Alfred King's Pennsylvanian tetrapod footprints from western Pennsylvania. New Mexico Museum of Natural History and Science Bulletin, 60, 233–239.
- Lucas, S.G., Fillmore, D.L. & Simpson, E.L. 2010: The Mississippian tetrapod footprint ichnogenus *Palaeosauropus*: Extramorphological variation and ichnotaxonomy. Ichnos 17(3), 177–186.
- Lucas, S.G., Krainer, K., Dimichele, W.A., Voigt, S., Berman, D.S., Henrici, A.C., Tanner, L.H., Chaney, D.S., Elrick, S.D., Nelson, W.J. & Rinehart, L.F. 2015: Lithostratigraphy, Biostratigraphy and sedimentology of the Upper Paleozoic Sangre de Cristo Formation, southwestern San Miguel county, New Mexico. In: Lindline, J., Petronis, M. & Zebrowski, J. (eds), New Mexico Geological Society 66th Annual Fall Field Conference Guidebook, 211–228.
- Marchetti, L., Avanzini, M. & Conti, M.A. 2013: *Hyloidichnus bifurcatus*, 1927 and *Limnopus heterodactylus* (King, 1845) from the Early Permian of Southern Alps (N Italy): A new equilibrium in the ichnofauna. Ichnos 20, 202–217.
- Marchetti, L., Ronchi, A., Santi, G., Schirolli, P. & Conti, M.A. 2015: Revision of a classic site for Permian tetrapod ichnology (Collio Formation, Trompia and Caffaro valleys, N Italy), new evidences for the radiation of captorhinomorph footprints. Palaeogeography, Palaeoclimatology, Palaeoecology 433, 140–155.
- Marsh, O.C. 1894: Footprints of vertebrates in the Coal Measures of Kansas. American Journal of Science 48, 81–84.
- Martino, R.L. 1991: *Limnopus* trackways from the Conemaugh Group (Late Pennsylvanian), southern West Virginia. Journal of Paleontology 65, 957–972.
- Moy-Thomas, J. A. 1942: Carboniferous Palaeoniscids from East Greenland. The Annals and the Magazine of Natural History 9, 11th series, 737–759.
- Nielsen, E. 1932: Permo-Carboniferous fishes from East Greenland. Meddelelser om Grønland 86(3), 1–63.
- Pedersen, K.R. 1976: Fossil Floras of Greenland. In: Escher, A. & Watt, W.S. (eds), Geology of Greenland, 536–573. Geological Survey of Greenland, Copenhagen.
- Perch-Nielsen, K., Bromley, R.G., Birkenmajer, K. & Aellen, M. 1972: Field observations in Palaeozoic and Mesozoic sediments of Scoresby Land and northern Jameson Land. Rapport Grønlands Geologiske Undersøgelse 48, 39–59.
- Piasecki, S. 1984: Preliminary palynostratigraphy of the Permian – Lower Triassic sediments in Jameson Land and Scoresby Land, East Greenland. Bulletin of the Geological Society of Denmark 32, 138–144.
- Stemmerik, L., Clausen, O.R., Korstgård, J., Larsen, M., Piasecki, S., Seidler, L., Surlyk, F. & Therkelsen, J. 1997: Petroleum geological investigations in East Greenland: project “Resources of the sedimentary basins of North and East Greenland”. Geology of Greenland Survey Bulletin 176, 29–38.
- Tucker, L. & Smith, M.P. 2004: A multivariate taxonomic analysis of the Late Carboniferous vertebrate ichnofauna of Alveley, southern Shropshire, England. Palaeontology 47, 679–710.
- Vigran, J.O., Stemmerik, L. & Piasecki, S. 1999: Stratigraphy and depositional evolution of the uppermost Devonian – Carboniferous (Tournaisian-Westphalian) non-marine deposits in north-east Greenland. Palynology 23, 115–152.
- Voigt, S. 2005: Die Tetrapodenichnofauna des kontinentalen Oberkarbon und Perm im Thüringer Wald – Ichnotaxonomie, Paläoökologie und Biostratigraphie. Göttingen, Cuvillier, 179 pp.
- Voigt, S. & Haubold, H. 2015: Permian tetrapod footprints from the Spanish Pyrenees. Palaeogeography, Palaeoclimatology, Palaeoecology 417, 112–120.
- Voigt, S. & Lucas, S.G. 2015a: Permian tetrapod ichnodiversity of the Prehistoric Trackways National Monument (south-central New Mexico, U.S.A.). New Mexico Museum of Natural History and Science Bulletin 65, 153–167.
- Voigt, S. & Lucas, S.G. 2015b: On a diverse tetrapod ichnofauna from Early Permian red beds in San Miguel County, north-central New Mexico. In: Lindline, J., Petronis, M. & Zebrowski, J. (eds), New Mexico Geological Society 66th Annual Fall Field Conference Guidebook, 241–252.
- Voigt, S. & Lucas, S.G. in press: Outline of a Permian tetrapod footprint ichnostratigraphy. Geological Society, London, Special Publications.
- Voigt, S., Lagnaoui, A., Hminna, A., Saber, H. & Schneider, J.W. 2011a: Revisional notes on the Permian tetrapod ichnofauna from the Tiddas Basin, central Morocco. Palaeogeography, Palaeoclimatology, Palaeoecology 302, 474–483.
- Voigt, S., Saber, H., Schneider, J.W., Hmich, D. & Hminna, A. 2011b: Late Carboniferous–Early Permian tetrapod ichnofauna from the Khenifra Basin, central Morocco. Geobios 44, 399–407.
- Witzig, E. 1951: Einige Jung-Paläozoische Pflanzen aus Ostgrønland. Meddelelser om Grønland 114 (11), 1–35.
- Witzig, E. 1954: Stratigraphische und tektonische Beobachtungen in der Mesters Vig-Region (Scoresbyland, Nordostgrønland). Meddelelser om Grønland 72(5), 1–26.
- Woodworth, J.B. 1900: Vertebrate footprints on Carboniferous shales of Plainville, Massachusetts. Bulletin of the Geological Society of America 11, 449–454.

# Correlation of the Palaeogene successions on the North-East Greenland and Barents Sea margins

THOMAS GULDBORG PETERSEN, NIELS ERIK HAMANN & LARS STEMMERIK



Petersen, T.G., Hamann, N.E. & Stemmerik, L. 2016. Correlation of the Palaeogene successions on the North-East Greenland and Barents Sea margins. ©2016 by Bulletin of the Geological Society of Denmark, Vol. 64, pp. 77–96. ISSN 2245-7070. ([www.2dgf/publikationer/bulletin](http://www.2dgf/publikationer/bulletin)).

In this study we use seismic stratigraphy to link the Palaeogene succession of the North-East Greenland shelf with that of the more accurately dated Cenozoic succession on the partly conjugate Norwegian margin in the West Barents Sea. The margins show a comparable stacking of seismic facies and we propose that this symmetry reflects a genetic relationship between the conjugate plates. On both margins, the earliest deposition is constricted by highs inherited from Mesozoic rifting. On the North-East Greenland shelf, the Danmarkshavn Ridge forms a barrier, whereas the footwall uplift along the west margin of Veslemøy High constrains the deposition in the West Barents Sea area. Pronounced progradational events shifted the depocentres of both margins towards the central axis of breakup during the more tectonically active breakup phase. Deposition during the early drift stage is dominated by a relatively homogenous distribution of sediments across both margins and further basinward migration of the depocentres. Based on correlation of the seismic stratigraphic units, the Palaeogene succession of the North-East Greenland shelf is subdivided into pre-breakup deposits of early Paleocene age, syn-breakup deposits of latest Paleocene to early Eocene age and (early) drift deposits of late Eocene to Oligocene age.

Thomas Guldborg Petersen [[thomas.guldborg.petersen@hotmail.com](mailto:thomas.guldborg.petersen@hotmail.com)], Department of Geosciences and Natural Resources Management, University of Copenhagen, Øster Voldgade 10, DK-1350 Copenhagen K, Denmark. Niels Erik Hamann, DONG Energy, Nesa Allé 1, 2820 Gentofte, Denmark. Lars Stemmerik [[lars.stemmerik@snm.ku.dk](mailto:lars.stemmerik@snm.ku.dk)], Natural History Museum, University of Copenhagen, Øster Voldgade 5–7, DK-1350 Copenhagen K, Denmark, and University Centre in Svalbard, P.O. Box 156, N-9171, Longyearbyen, Norway.

Dating of seismic sequences represents a major challenge in stratigraphic and paleogeographic analyses, hydrocarbon exploration and resource assessment of sedimentary basins without well control (Gautier *et al.* 2009). The North-East Greenland shelf is one such ‘white spot’ where dating of the depositional basins and their infill is tentative and based on comparison to nearby outcrops and information from the better investigated Norwegian margin (Hamann *et al.* 2005). In North-East Greenland, only the youngest of the pre-Quaternary sediments have been drilled by ODP well 913 that reaches down into the Eocene, and seismic correlation to this borehole provides firm dating of the youngest seismic units on the oceanic crust (Berger & Jokat 2008). The location of the seismic and well data is presented in Fig. 1.

In this paper we discuss and test the potential of using age data from the conjugate Norwegian margin to improve dating of the Palaeogene succession on the North-East Greenland shelf since outcrop data from East and North Greenland are sparse (Hamann *et al.*

2005). The Palaeogene succession offshore North-East Greenland was recently described and linked to the breakup of the northern North Atlantic by dividing it into seismic units dated as pre- and syn-breakup and early drift in age (Petersen *et al.* 2015). The succession records the opening of the northern North Atlantic, so a more precise dating of the seismic units could help to better understand the evolution of the North-East Greenland shelf compared to the Norwegian margin.

The comparison between the Greenland and Norwegian margins is somewhat challenged by the complexity of the opening between North-East Greenland and the Barents Shelf and the timing of the shift from strike-slip motion to seafloor spreading in the De Geer Mega Shear zone (Figs 2, 3) (Voss & Jokat 2009). The conjugate margin to the southern Danmarkshavn and Thetis basins is the Lofoten-Vesterålen-Senja segment of the Norwegian margin, whereas the western Barents Sea margin including the Sørvestsnaget Basin and Veslemøy High is conjugate to the northern part of the North-East Greenland shelf, including the northern

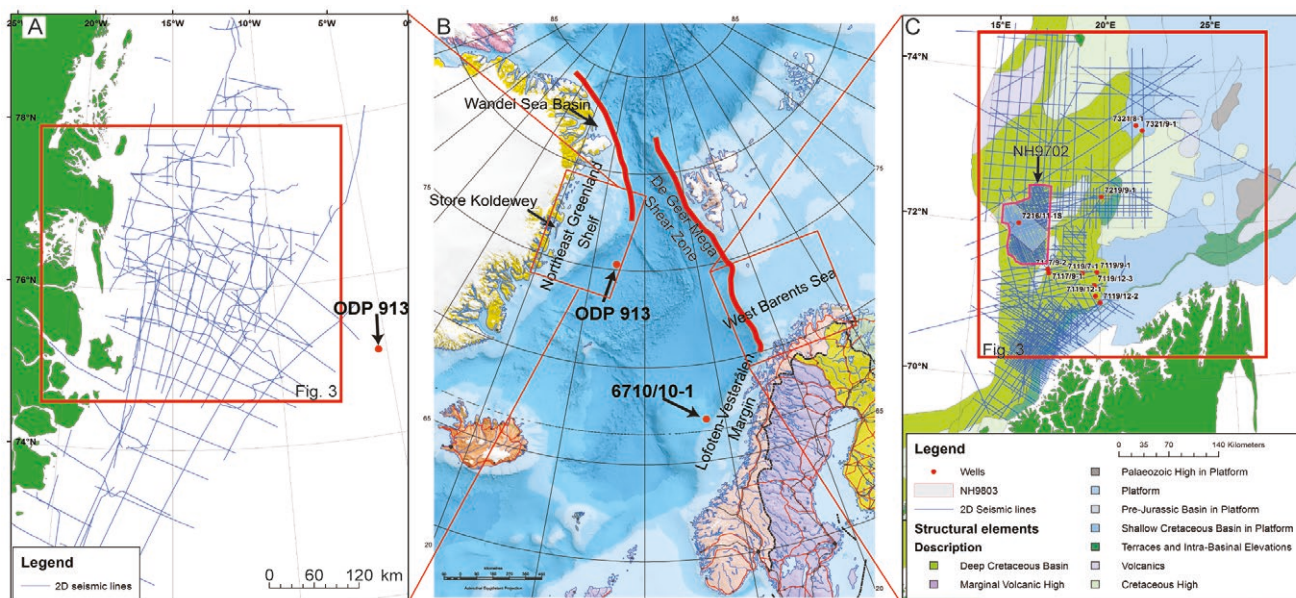


Fig. 1. A: Seismic data available for this study of the North-East Greenland margin. B: Overview of the North Atlantic region. The two black frames show the locations of maps A and C; the thick red lines are the De Geer Mega Shear Zone. North-East Greenland Map modified from <http://atlas.gc.ca/>. C: Seismic data and wells on the Barents Shelf (Modified from [www.npd.no](http://www.npd.no)).

Danmarkshavn and Wandel Sea basins (Fig. 2) (e.g. Tsikalas *et al.* 2001).

The temporal and spatial resolution of the spreading history of the northern North Atlantic is well documented by magnetic anomalies in the oceanic crust (Talwani & Eldholm 1977; Tsikalas *et al.* 2008; Gaina *et al.* 2009; Ogg 2012). Spreading in the Norwegian-Greenland Sea started at *c.* 55 Ma (Chron C25) (Fig. 2a) (Ziegler & Cloetingh 2004). Several changes of spreading direction and speed occurred during the early opening history, most prominently during the Eurekan Orogeny between 49 and 47 Ma (Chron C22n–C21n, based on the magnetostratigraphy of Ogg 2012) when the spreading rates between Eurasia and Laurentia slowed down significantly as a result of compression in the Canadian Arctic Islands (Fig. 2C). The onset of opposite absolute plate motion started at *c.* 33 Ma (Chron C12r), and at 25 Ma (Chron C7r) full separation was achieved along most of the newly formed continental margins (Gaina *et al.* 2009; Døssing *et al.* 2010) (Fig. 2C). The orientation of the De Geer Mega Shear zone relative to plate motion directions caused differences in the tectonic regimes along the Norwegian Sea, West Barents Sea and North-East Greenland conjugate margins (Breivik *et al.* 1998; Olesen *et al.* 2007). Extension dominated along the North-East Greenland and Norwegian Sea margins; the northern Wandel Sea segment of the North-East Greenland margin was dominated by complex strike-slip tectonics (Døssing *et al.* 2010), and compression prevailed in Spitsbergen (Dore 1991; Bergh & Grogan

2003; Bruhn & Steel 2003; Ryseth *et al.* 2003; Gernigon *et al.* 2009).

The Palaeogene succession on the North-East Greenland shelf is characterized by unique depositional geometries shifting from low angle clinoformal packages in basinal lows to progradational packages of steep clinoforms and finally successions with sub-horizontal geometries (Petersen *et al.* 2015). The shift in depositional geometries has been interpreted in a rift to drift margin context to reflect the ongoing opening of the northern North Atlantic (Petersen *et al.* 2015).

## Setting

The North-East Greenland shelf covers the area from *c.* 70°N to 82°N along the East Greenland coast and is up to 500 km wide (Fig. 1). The shelf is dominated by N–S to NNE–SSW oriented structural highs and basins formed during prolonged late Palaeozoic and Mesozoic rifting (Hamann *et al.* 2005). The most prominent structural elements are the Koldewey Platform, the Danmarkshavn Basin, the Danmarkshavn Ridge, and the Thetis Basin at the outer edge of the shelf (Fig. 3) (Hamann *et al.*, 2005). The Palaeogene succession is up to *c.* 850 milliseconds (ms) (in the order of 800–1000 m) thick and unconformably overlies the N–S trending Mesozoic and Palaeozoic structural elements. Evidence of Cenozoic volcanism is mostly absent on the northern part of the shelf, whereas both intrusives

and extrusives are common both onshore and offshore south of *c.* 75°N (Brooks 2011; Petersen *et al.* 2015).

The only well penetrating Palaeogene deposits offshore North-East Greenland is ODP Site 913 on the oceanic crust at 75°29'N, 06°96'W (Fig. 1B). It was used by Berger and Jokat (2008) to subdivide the Cenozoic succession into a pre-mid-Miocene GB-1 and a post-mid-Miocene GB-2 unit. However, the locality of this well is not ideal for seismic correlation with the succession in the Danmarkshavn Basin. Scattered Tertiary

outcrops in North and North-East Greenland have all been attributed to the Paleocene–Lower Eocene (Lyck & Stemmerik 2000; Nøhr-Hansen *et al.* 2011).

The North-East Greenland shelf is the conjugate margin to the West Barents Sea margin in the north and northeast and the Lofoten-Vesterålen margin to the east and southeast. Although part of the same conjugate margin system, the Lofoten-Vesterålen margin is tectonically very different from the West Barents Sea margin, since it was dominated by extensional deformation during the continental breakup, whereas the Barents Sea margin was dominated by transtensional deformation (Tsikalas *et al.* 2001; Gaina *et al.* 2009). Potential field data have been used to identify transverse lineaments segmenting the Lofoten-Vesterålen margin and correlation to North-East Greenland has been suggested (Tsikalas *et al.* 2005), although the lineaments have been disputed and seen as artefacts caused by poor data quality (Olesen *et al.* 2007). In the current study, no evidence of hard linked transforms has been identified in the seismic data on the North-East Greenland shelf. Faereth (2012) has described an E–W accommodation zone at 68°30'N offshore Norway, acting as a right-lateral, soft-linked transfer zone across which the dips and strikes of the faults change orientation. On the North-East Greenland shelf, right-lateral offset of the two segments of the Danmarkshavn Ridge is seen in map view (Fig. 3). There is no evidence of transform faulting separating the two segments of the ridge, consistent with a soft-linked transform. The transfer zone on the North-East Greenland shelf aligns with the accommodation zone of Faereth (2012) when reconstructing the plates to a pre/syn-breakup position.

On the Barents Sea shelf, Palaeogene sediments are limited to the western margin which covers the area from Spitsbergen in the north to the Norwegian Finnmark coast in the south and extends from 15°E to 25°E (Fig. 1). The continental to oceanic transition zone is named from south to north: The Senja Fracture Zone which consists of a sheared margin, the Vestbakken Volcanic Province associated with pull-apart tectonics, and the Hornsund Fault Zone (Fig. 3) (Faleide *et al.* 1996). From east to west, the most prominent structural elements in the West Barents Sea area are the Hammerfest and Bjørnøya Basins which are separated by the Loppa High in the east, and the Harstad, Tromsø and Sørvestsnaget Basins at the continental margin west of 20°E. The Senja Ridge and its elongation into the Veslemøy High subdivide the Sørvestsnaget Basin from the Tromsø Basin in the east (Fig. 3) (Knutsen & Vorren 1991). The Loppa High forms the eastern boundary of the Palaeogene deposits due to deepening of the erosional incision towards the east (Gernigon & Brønner 2012). Evidence of significant volcanism

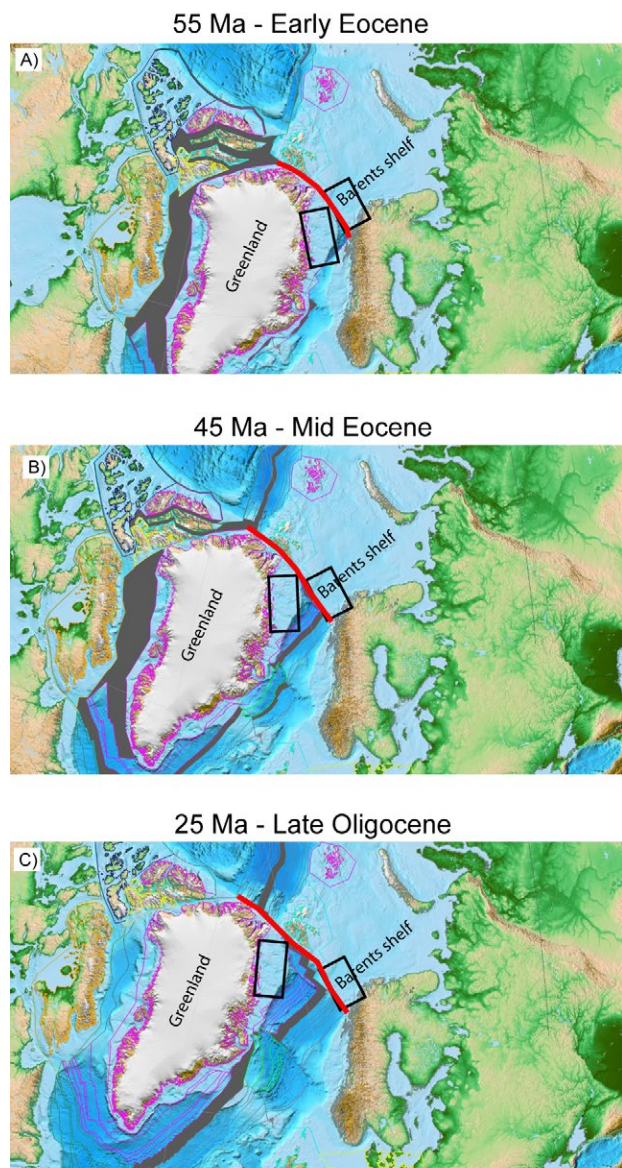


Fig. 2. Plate tectonic reconstruction of Greenland and Eurasia. **A:** Initial geometry prior to the opening. **B:** Eurekan orogeny where compression in the Canadian Arctic Islands can be seen, as well as compression at the west coast of Svalbard. **C:** Complete breakup along most of the margins, except for the Wandel Sea area (Reconstruction based on Gplates: [www.gplates.org](http://www.gplates.org)). Thick red lines are the De Geer Mega Shear Zone.

is seen in the Vestbakken Volcanic Province, a deep pull-apart basin created due to transtensional tectonics along the de Geer zone during the breakup at c. 51 Ma (Chron C23) (Tsikalas *et al.* 2002).

Several seismic stratigraphic schemes have been proposed for the Palaeogene deposits in the western Barents Sea (Table 1). Vorren (1991) was the first to establish a seismic stratigraphic framework based on mapping of three units in the Hammerfest Basin and five units in an area roughly corresponding to the Sørvestsnaget Basin and the southern Vestbakken Volcanic Province. Later, Faleide *et al.* (1993) refined the stratigraphy based on new seismic data, and further refinements of the seismic stratigraphy and better correlation between the basins were presented by Fiedler & Faleide (1996) and Ryseth *et al.* (2003) (Table 1), including correlation to well 7216/11-1s

in the Sørvestsnaget Basin (Ryseth *et al.* 2003). The relatively complete succession of Palaeogene strata exposed in the Central Basin onshore Spitsbergen (Svalbard) forms a transgressive-regressive succession of fluvio-deltaic and marine sandstones and offshore shales deposited in a foreland basin which developed during the evolution of the West Spitsbergen Fold Belt (Bruhn & Steel 2003)

The foreland basin was initially, during the Paleocene, sourced from the east but later the drainage pattern changed and during the Eocene the source area was the evolving West Spitsbergen Fold Belt to the west (e.g. Bruhn and Steel, 2003; Petersen *et al.* 2016). The evolution of the Central Basin thus differs from the strike-slip dominated Sørvagnet Basin and Vestbakken Volcanic Province, adding to the complexity of the breakup history along the Barents Sea margin.

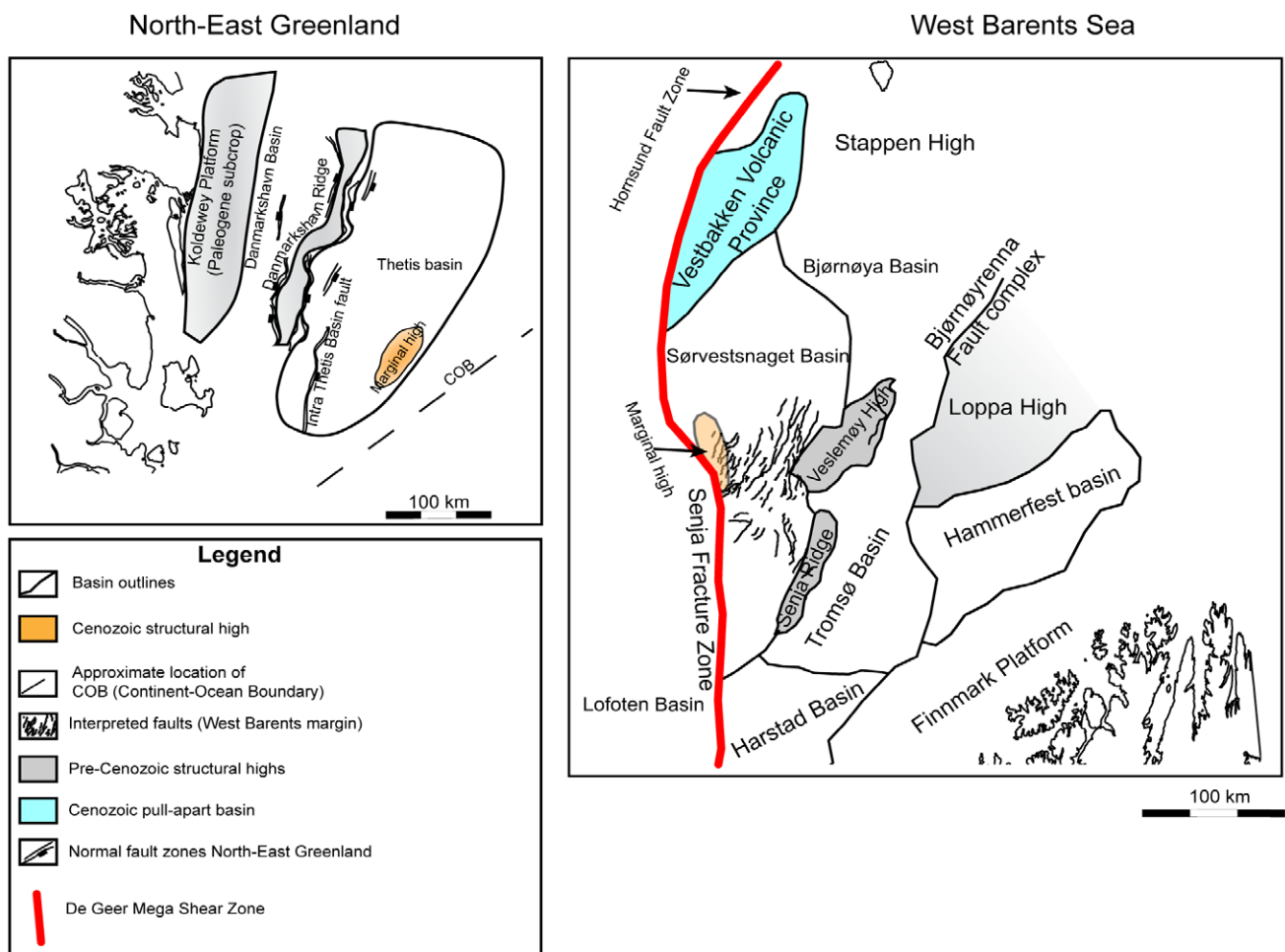


Fig. 3. Maps showing the main structural elements of the North-East Greenland shelf and the West Barents Sea. For location see Fig. 1. The North-East Greenland margin is dominated by NNE–SSW trending highs and lows, from west to east named Koldewey Platform, Danmarkshavn Basin, Danmarkshavn Ridge and Thetis Basin. The West Barents Sea margin includes the Lofoten Basin, Vestbakken Volcanic Province, Sørvestsnaget Basin, Veslemøy High and Senja Ridge lineament and the Tromsø Basin. The Palaeogene succession is absent due to erosion further east across the Loppa High. The De Geer Mega Shear Zone includes several fault zones.

Table 1.1. Overview of the seismic stratigraphic sub-divisions of the Paleocene to Miocene succession in the West Barents Sea shelf area.

Vorren 1991		Faleide <i>et al.</i> 1993		Fiedler & Faleide 1996		Ryseth <i>et al.</i> 2003		This study	
Sub-division	Comments	Subdivision	Comments	Sub-division	Comments	Subdivision	Comments	Subdivision	Comments
	Intra Miocene (15.5 Ma)			Te1-Te4			Central Sør-vestsnaget Basin		Unit top ages
ThB/TeB						Base Miocene		Oligocene(?)	
								Near top Eocene	
						Intra Middle Eocene		Mid Eocene seismic horizon	
	Intra Eocene (50 Ma)		Base Eocene		Base at 55 Ma				
ThA/TeA								Lower Eocene seismic horizon	
		BE						Paleocene seismic horizon 2	
								Paleocene seismic horizon 1	
		BT	Base Cenozoic						
						Near top Cretaceous		Base Cenozoic	

## North-East Greenland margin

The continental breakup in the North Atlantic was associated with volcanism onshore East Greenland, and seismic observations reveal that the sedimentary succession on the East Greenland shelf south of *c.* 75°N is heavily intruded by volcanic rocks (Brooks 2011; Larsen *et al.* 2014). The East Greenland volcanics form part of the North Atlantic Large Igneous Province (NALIP) that covers substantial areas of the North Atlantic margin from the Rockall Plateau to the Vøring Margin on the Eurasian side, and the entire East Greenland margin south of *c.* 75° N (Brooks 2011; Larsen *et al.* 2014). The NALIP formed as a response to the opening of the North Atlantic and was emplaced between 64 Ma to 25 Ma with a distinct peak in the earliest Eocene, corresponding to the time of continental breakup (Brooks 2011; Larsen *et al.* 2014). The heating associated with the volcanism may have caused the observed uplift of the East Greenland margin, and from the seismic data it is evident that the North-East Greenland margin was most heavily eroded in the south where the intrusions are the most frequent (Petersen *et al.* 2015). This is also consistent with observations further south in East Greenland where the C5 event of Japsen *et al.* (2014) records early Eocene thermal uplift.

The stratal geometry of six seismic units in the Palaeogene succession along the inner, western part of the North-East Greenland shelf and three units in the

eastern part of the shelf is believed to reflect the volcanic uplift history, and has facilitated a division into the pre-, syn- and post-volcanic successions described in details by Petersen *et al.* (2015) and summarized below and in Fig. 4. The data set used for these studies is part of in the NEG08 and KANUMAS surveys of the North-East Greenland shelf.

### Pre-breakup succession

On the North-East Greenland shelf the Palaeogene succession rests unconformably on deeply eroded Mesozoic deposits (Hamann *et al.* 2005; Petersen *et al.* 2015). Initially, deposition was constrained to the Danmarkshavn Basin by the Danmarkshavn Ridge, which apparently acted as a positive element prior to and during the breakup. Low angle, eastward prograding clinoforms and a stacked mound complex infill the structural lows of the Danmarkshavn Basin (marked in yellow in Fig. 4A), and are overlain by sediments with plane parallel, low amplitude bedding (Petersen *et al.* 2015). The pre-breakup succession (yellow interval in Fig. 4) represents initial progradation into the basin, and isochrone maps show that the succession is constrained to the Danmarkshavn Basin by the Danmarkshavn Ridge (Fig. 5). The observed low-angle clinoforms and the mounded structures are consistent with deposition in a tectonically relatively quiet period with low source-to-sink relief of the depositional system. It is therefore interpreted as pre-dating the main

volcanic event and the thermal uplift that may have occurred during continental breakup (Brooks 2011; Larsen *et al.* 2014). The main volcanic event occurred in the earliest Eocene, meaning that the pre-breakup unit is Paleocene in age (Larsen *et al.* 2014).

There is evidence of channel incision along the western edge of the Danmarkshavn Basin implying lowering of the base level during or after deposition. The cause of this incision is not well understood, but a possible explanation could be a sea level drop at the Cretaceous/Palaeogene interface (Miller *et al.* 2005).

### Syn-breakup succession

In the Danmarkshavn Basin, the overlying succession (blue interval in Fig. 4) is dominated by clinoform packages prograding across the basin from the southwest to the northeast. The proximal part of the

succession consists of relatively high angle clinoforms, and based on their steepness it is suggested that they contain the coarsest facies of the Palaeogene succession and represent a pronounced regression. The upper boundary of the syn-breakup interval is erosive towards the west which is believed to reflect the depositional response to regional uplift associated with the volcanism (Petersen *et al.* 2015). During this time interval, the main axis of sediment transport as defined by the location of depocentres and presence of clinoforms was shifted southwards from a position directly east of Store Koldewey to a position *c.* 100 km farther to the south (Fig. 5).

During the breakup phase, volcanism onshore and offshore most likely caused an increasing amount of uplift and erosion towards the south in the Danmarkshavn Basin, observed as truncation of reflectors at the upper boundary of the syn-breakup unit (see top of

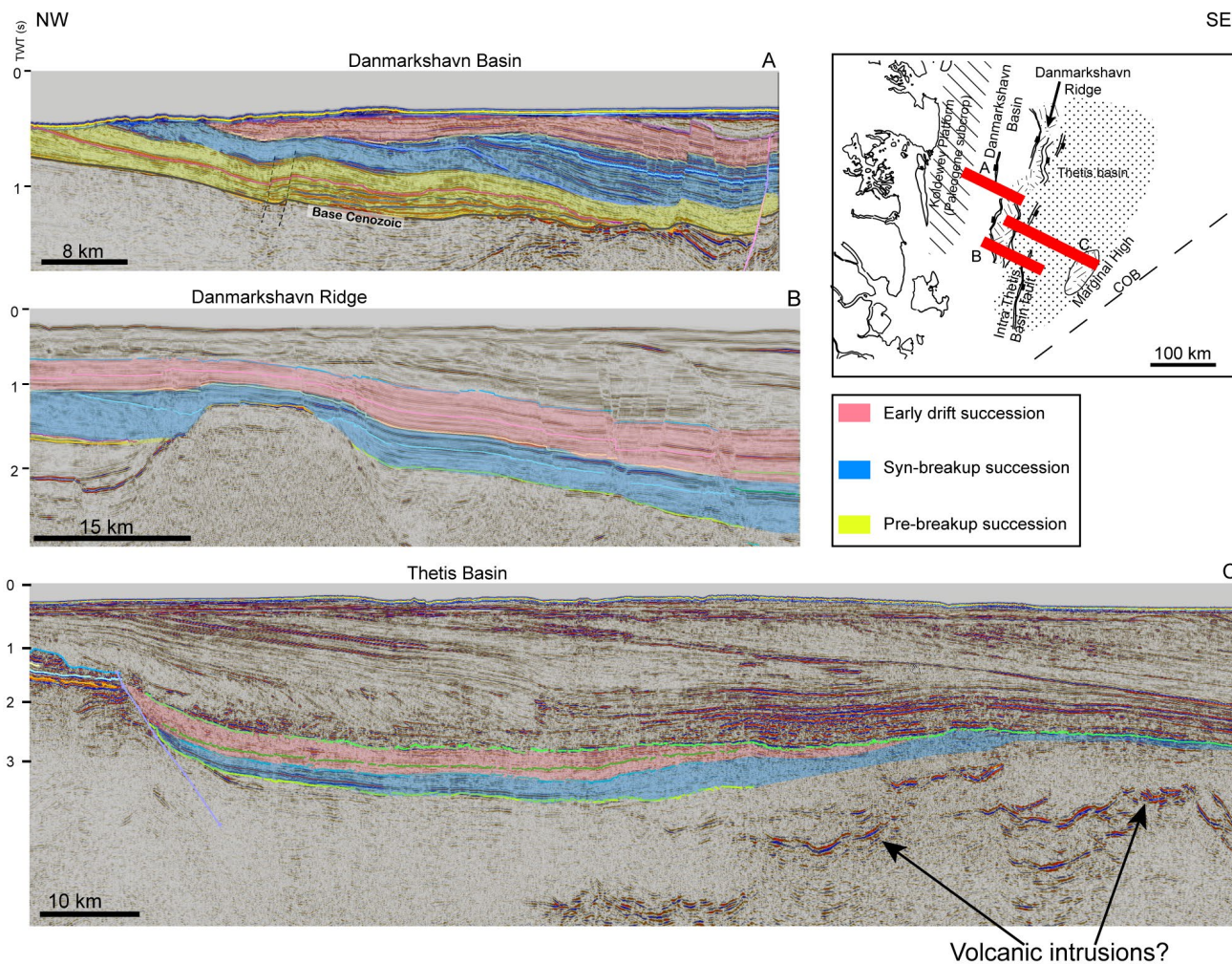


Fig. 4. Three seismic sections showing the geometry of the pre-breakup, syn-breakup and early drift Palaeogene succession, **A**: in the Danmarkshavn basin, **B**: across the Danmarkshavn Ridge, and **C**: in the Thetis Basin. Note that the sections are not presented in a N-S order, but they represent a proximal to distal order.

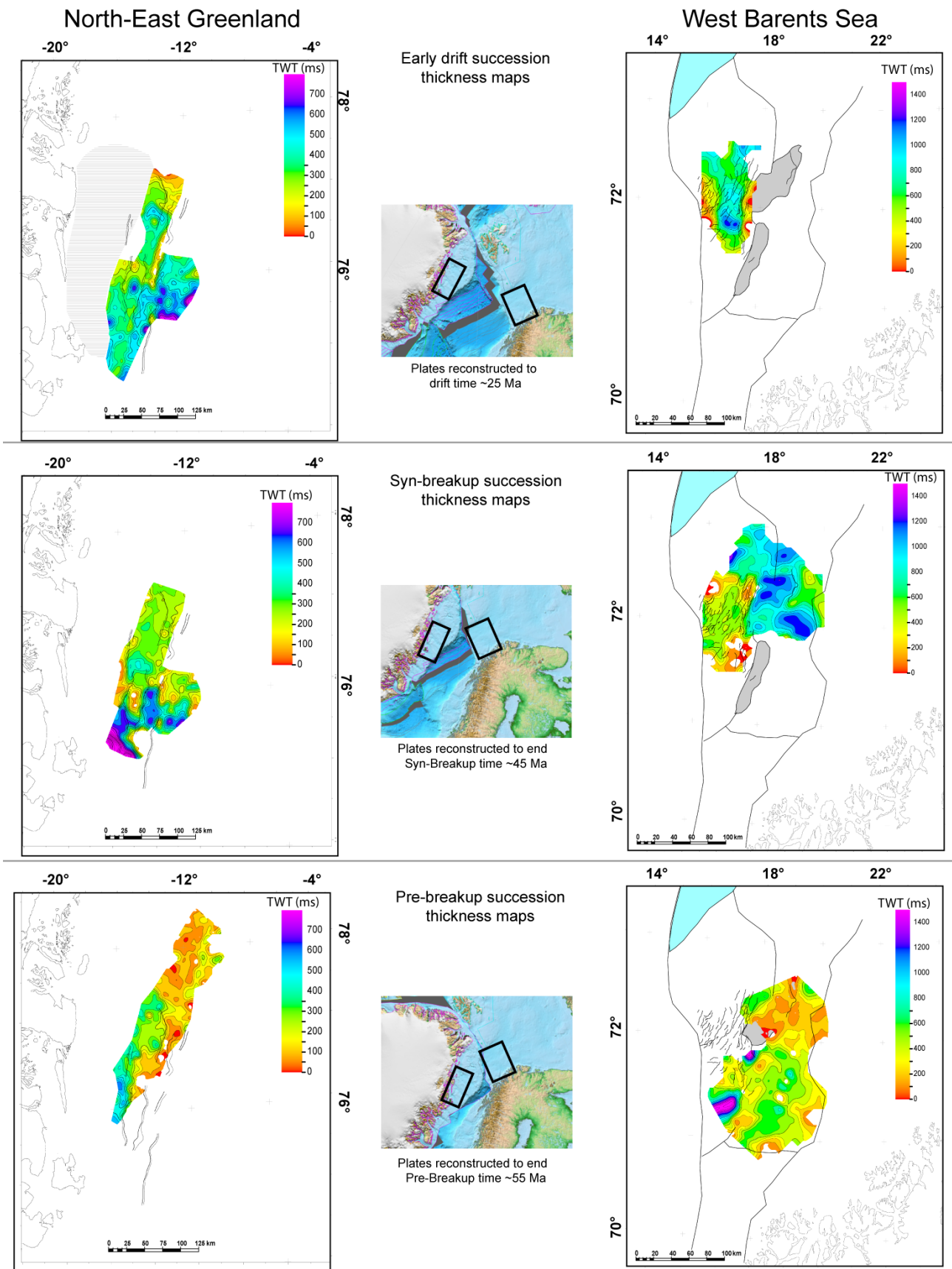


Fig. 5. Thickness maps as TWT maps showing locations of the main depocentres of pre-breakup, syn-breakup and early drift sediments with associated plate reconstructions representative for the plate geometries at the time of the deposition (plates reconstructed using Gplates: [www.Gplates.org](http://www.Gplates.org)). A pronounced shift of depocentre towards the breakup axis is observed along both margins, which is a key observation for the correlation.

blue interval in Fig. 4A–B). This uplift caused a tilting of the margin towards the east to northeast, with associated erosion of mostly Paleocene deposits to the west and southwest, and increasing accommodation space in the more distally located Thetis Basin. There, the succession is characterised by plane parallel, low amplitude reflections, indicative of relatively homogeneous sediments, potentially deposited in a sublittoral setting. Correlation between the Danmarkshavn Basin and the Thetis Basin is somewhat hampered by the Danmarkshavn Ridge, especially in the lower part of the succession (Petersen *et al.* 2015).

### Early drift succession

The upper part of the Palaeogene succession (pink interval in Fig. 4) was deposited during a time interval dominated by large-scale subsidence across the North-East Greenland shelf which yielded a relatively constant thickness of the deposited succession across the shelf (Fig. 5; Petersen *et al.* 2015). Some increase in subsidence centrally in the Thetis basin is however recorded in the isochrone map of the early drift package (Fig. 4). The seismic data suggests that this increase in accommodation space is due to compaction of the thick Mesozoic succession of the Thetis Basin, since any faulting post-dates the deposition of the early drift succession (Fig. 5). Apparently, the Danmarkshavn Ridge no longer acted as a positive bathymetric element and deposition occurred in a low energy environment, most likely beneath wave base, based on the dominance of seismic facies characterised by sub-parallel internal reflections. Little or no evidence of tectonics are observed during this stage of the basin evolution, and the succession is attributed to a drift setting post-dating continental breakup.

## West Barents Sea Margin

The geological evolution of the Western Barents Sea is relatively well documented (Knutzen & Larsen 1997; Ryseth *et al.* 2003; Geissler & Jokat 2004; Tsikalas *et al.* 2008). Palaeogene deposits are only preserved in a narrow zone along the margin of Eurasia consisting of the Vestbakken Volcanic Province, the Sørvestsnaget Basin, the Veslemøy High, the Senja Ridge, the Tromsø Basin and the Harstad Basin (Fig. 3) as they are eroded away further to the east as the result of Neogene incision. The succession is included in the Torsk Formation, Sotbakken Group, and is interpreted as dominated by marine, sublittoral to outer shelf claystones with rare deep-marine sandprone turbidites in the Sørvestsnaget Basin (Dalland *et al.* 1988; Ryseth *et*

*al.* 2003). The sediments infilling the Western Barents Sea margin were derived from the eastern Barents Sea, where uplift and erosion of the underlying Palaeozoic–Mesozoic succession are widespread (Smelror & Basov 2009).

In this study, we focus on stratal geometries and their relation to the evolution of the margin during the Palaeogene breakup. The database consists of 2D seismic lines supplemented with 3D seismic and well data, and most seismic interpretations are based on the NH9702 2D and the NH9803 3D seismic surveys (Fig. 1C), (with support from additional vintage data sets). We have used public domain stratigraphic data from the Norwegian Petroleum Directorate ([www.npd.no](http://www.npd.no)) to date the seismically defined units, and we have focussed on a number of key stratigraphic horizons, including the Base Paleocene, Top Paleocene, Early Eocene, Middle Eocene, and Base Neogene. Since our focus is on seismic units to be used for large-scale comparison with the North-East Greenland shelf, more detailed dating of the wells is not part of the current study.

The integration of seismic and well data allows us to distinguish six seismic units and thereby constrain shifts in deposition temporally. Correlation of the Palaeogene succession on the Loppa High, Senja Ridge and Sørvestsnaget Basin (Fig. 6) is based on information from the completion logs of wells 7117/9-1 and 7219/9-1, and data in Ryseth *et al.* (2003) for well 7216/11-1S.

### Lower Paleocene seismic unit

The lower boundary is the Base Cenozoic seismic horizon and the top is Paleocene seismic horizon 1 (Fig. 7). The unit is restricted to fault-controlled lows along the western margin of the Loppa High and on the Veslemøy High (Fig. 7). It is not identified in the Sørvestsnaget Basin and is therefore only dated on the highs to the east. The Lower Paleocene seismic unit has been tied to well 7219/9-1, providing a base Paleocene age for the lower part and an early(?) Paleocene age for the upper part of the unit (Fig. 6).

The onset of Cenozoic sedimentation on the West Barents Sea Margin is recorded by low angle, sub-parallel seismic facies characteristic for the Lower Paleocene seismic unit. The Lower Paleocene deposits display an onlapping, lenticular internal architecture on the Veslemøy High. Footwall uplift along the western margin and of the high itself may have caused the Veslemøy High to be a positive structural element during the earliest Paleocene and it may have acted as a barrier for sediment input from the east. This assumption is based on the absence of the Lower Paleocene seismic unit in the Sørvestsnaget

Basin. Alternatively, lowermost Paleocene deposits are present in the Sørvestsnaget Basin, but are simply not recognised due to poor correlation across the fault zone separating the Sørvestsnaget Basin from the Veslemøy High.

The seismic facies suggests that the Lower Paleocene sediments were deposited in the distal part of a prograding system sourced from the east. This is in line with the pattern recognised in Spitsbergen and consistent with regional models (e.g. Smelror & Basov 2009; Petersen *et al.* 2016). The stratal geometries indicate deposition in a tectonically quiet period, and this is supported by the well log motifs which indicate a dominance of shaly sediments across the region throughout the Paleocene with a noticeable exception in the interval from c. 3500 to 3700 m MD (Measured Depth) in well 7216/11-1S where abundant tuffaceous fragments indicate vicinity to active volcanism (Fig.

6; Ryseth *et al.* 2003). Based on the stratal geometries and the dating of the succession, the Lower Paleocene seismic unit reflects deposition prior to breakup.

### Paleocene seismic unit 2

The top of Paleocene seismic unit 2 is defined by Paleocene seismic horizon 2 (Fig. 7). Paleocene seismic unit 2 has a wider distribution than the underlying unit and reflects deposition sourced from the east and transgression of the highs east of the Sørvestsnaget Basin (Ryseth *et al.* 2003). It is tied to well 7219/9-1 with a suggested early (?) to end Paleocene age.

During this stage deposition became more widespread on the Veslemøy High, Loppa High and Tromsø Basin and was no longer constrained by fault blocks. The lower-to-upper Paleocene succession overlaps the rotated fault blocks on the Veslemøy High,

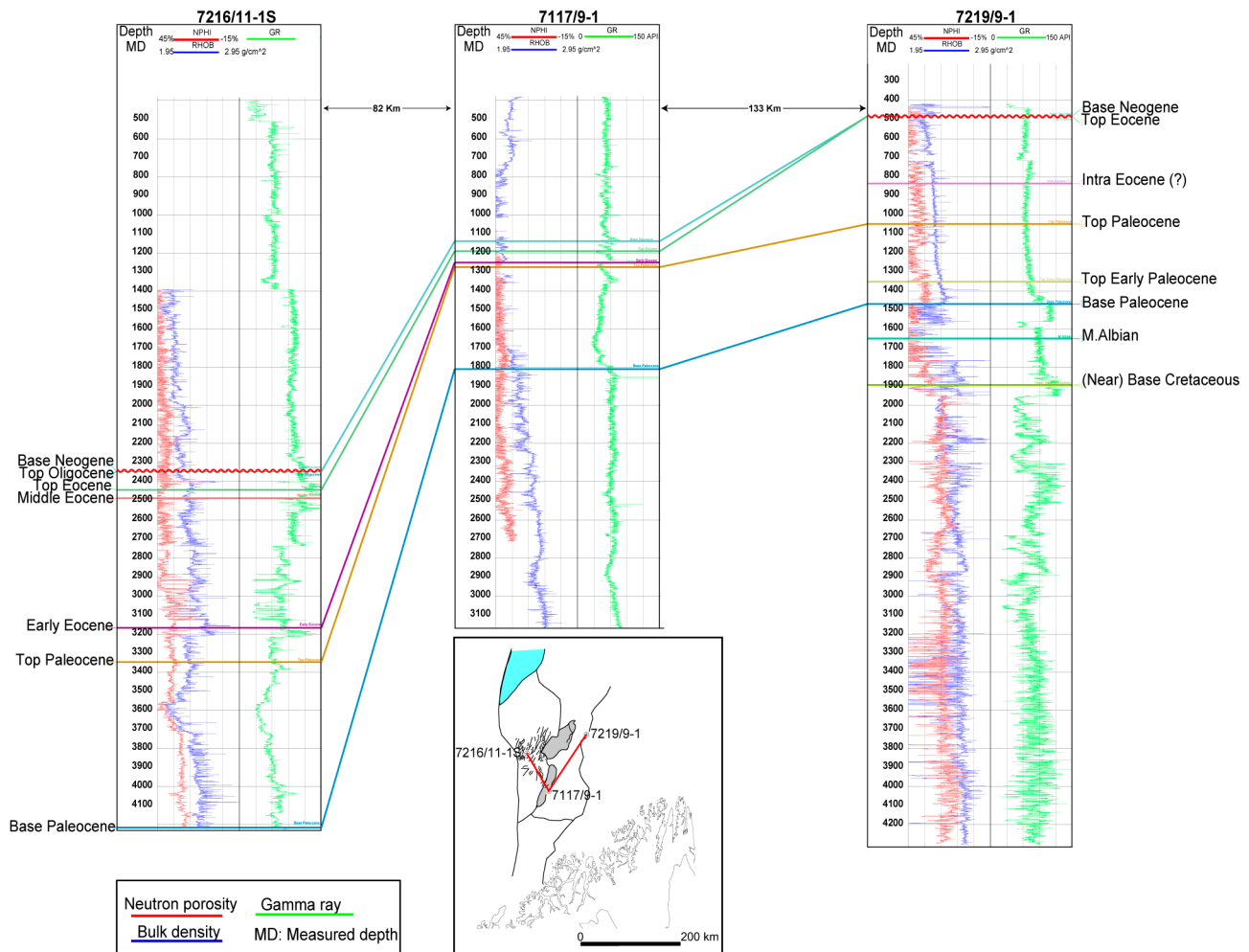


Fig. 6. Log correlation panel of wells 7219/9-1, 7117/9-1 and 7216/11-1S across the Loppa High, the Senja Ridge and the Sørvestsnaget Basin showing the Paleocene pre-breakup succession, the Eocene breakup package and the Oligocene early drift deposits. MD: Measured Depth in metres.

and maximum thickness is observed in the Tromsø Basin. Although the Paleocene seismic horizon 2 cannot be defined near the transition to the Sørvestsnaget Basin, it is clear that the seismic reflectors immediately above the Paleocene seismic horizon 1 display divergence from east to west toward the fault zone that separates the Veslemøy High from the Sørvestsnaget Basin in the west (Fig. 8), the Tertiary Hinge Line of Faleide (1988). This indicates that the West Barents Sea Margin underwent large wavelength subsidence prior to onset of the opening of the Norwegian-Greenland Sea in the earliest Eocene (Gaina *et al.* 2009; Gernigon *et al.* 2009).

The Paleocene seismic unit 2 is generally characterised by sub-parallel internal seismic facies indicating an aggradational rather than progradational stacking pattern, consistent with sedimentation in a sublittoral setting (Fig. 8) (Posamentier & Kolla 2003). Progradational stacking patterns are recognized in the Bjørnøyrenna area (Faleide *et al.* 1993), where well data indicate the presence of relatively sandprone facies. The amount of progradation increases during this period, but there is still no evidence of significant deepening of the basin, consistent with a pre-breakup age of the unit.

### Lower Eocene seismic unit

The top of the Lower Eocene seismic unit is the lower Eocene seismic horizon (Figs 7, 8). The unit transgresses the Veslemøy High into the Sørvestsnaget Basin, with a large-scale reflection pattern that may suggest deposition in the distal part of a westwards prograd-

ing system. The thickness increases westwards into a depocentre localised over the fault zone that separates the Sørvestsnaget Basin and the Veslemøy High, making correlation between the two areas uncertain (Fig. 8). This indicates that significant accumulation of sediments occurred prior to the tectonic event that created the Sørvestsnaget Basin, as also indicated by the underlying lower-to-upper Paleocene succession. The Lower Eocene unit is tied to wells 7216/11-1S and 7219/9-1, suggesting a latest Paleocene to mid Eocene age for the succession (Ryseth *et al.* 2003).

Due to poor correlation across the fault zone, the actual timing of the subsidence east of the Tertiary Hinge Line on the Veslemøy High is not well constrained, but thickness variations across the rotated fault blocks in the Sørvestsnaget Basin indicate syn-tectonic deposition. The succession is erosionally truncated on the crest of the footwall block (Fig. 8) east of the fault zone separating the Sørvestsnaget and Vestbakken Volcanic Province Basins from the Veslemøy High and Stappen High areas (the Tertiary Hinge Line). The syn-depositional faulting and noticeable increase of progradation into the Sørvestsnaget Basin both point towards deposition during a time period with increased tectonic activity and uplift of the hinterland, and the Lower Eocene seismic unit is believed to reflect deposition during early breakup.

### Middle Eocene seismic unit

The top of the middle Eocene seismic unit is the mid Eocene seismic horizon (Fig. 9). The unit is tied to well 7216/11-1 S according to Ryseth *et al.* (2003) (Fig. 6). The

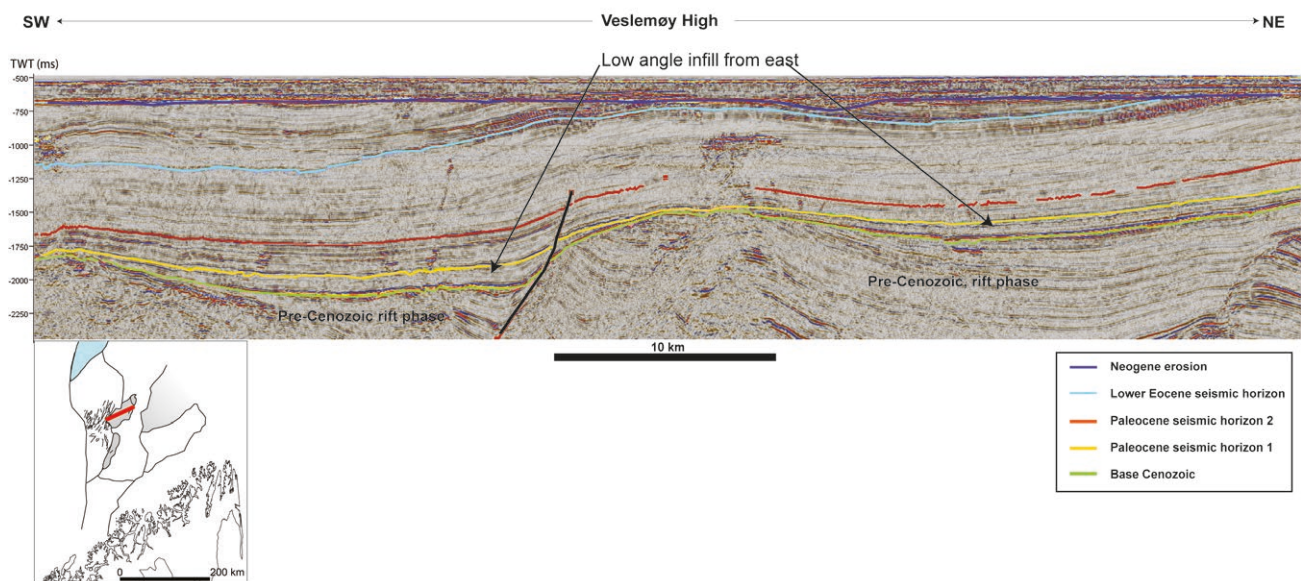


Fig. 7. Seismic section across the Veslemøy High (NH9702-234). Low angle infill dominates in the lows between the uplifted footwalls. For location of inset map see Fig. 1.

tie is robust, with reliable ages in the well and good quality 3D seismic data. The unit is only described in the Sørvestsnaget Basin due to erosion of the eastern margin of the basin or non-deposition.

The eastern extent of the middle Eocene succession onto the Veslemøy High is relatively poorly constrained by well data. A seismic tie between well 7216/11-1 S and 7219/9-1 is not possible due to erosion of the crest of the fault separating the Sørvestsnaget basin from the Veslemøy High (Eocene erosion seismic horizon in Fig. 9). The middle Eocene succession records a substantial westwards shift of the depocentre from the Veslemøy and Loppa Highs into the Sørvestsnaget Basin.

The Middle Eocene seismic unit is dominated by a chaotic to transparent seismic facies in the basalinal lows of the Sørvestsnaget Basin. The unit onlaps the Veslemøy High–Senja Ridge structural lineament in the east. It may also be present on the Marginal High that delineates the Sørvestsnaget Basin towards the west.

The incision at the fault crest of the Eocene erosion seismic horizon (Figs 8, 9) sourced the steep, local-

ised fans or wedges observed on the down-faulted, hanging wall block of the Sørvestsnaget Basin (Fig. 8). The age of these fans is poorly constrained since they have not been drilled. But since the fans downlap onto the lower Eocene seismic horizon and the mid Eocene seismic horizon, the Eocene erosional event is approximately mid Eocene in age.

A series of en échelon normal faults are observed throughout the Sørvestsnaget Basin (Figs 3, 9) offsetting the lower Palaeogene succession. The fault offset terminates synchronously at the mid Eocene seismic horizon, which provides an upper temporal constraint of the fault movements. This is consistent with early rift phase faulting, where minor faults are evenly distributed across the rift basin (Gawthorpe & Leeder 2000; Fig. 9). This is in contrast with the interpreted time equivalent seismic units in North-East Greenland, where only limited faulting is observed, but it can be attributed to the transtensional nature of the West Barents Sea margin. The unit thins significantly across the Marginal High where it displays local uplift-related erosion.

The faults in the Sørvestsnaget Basin are oriented

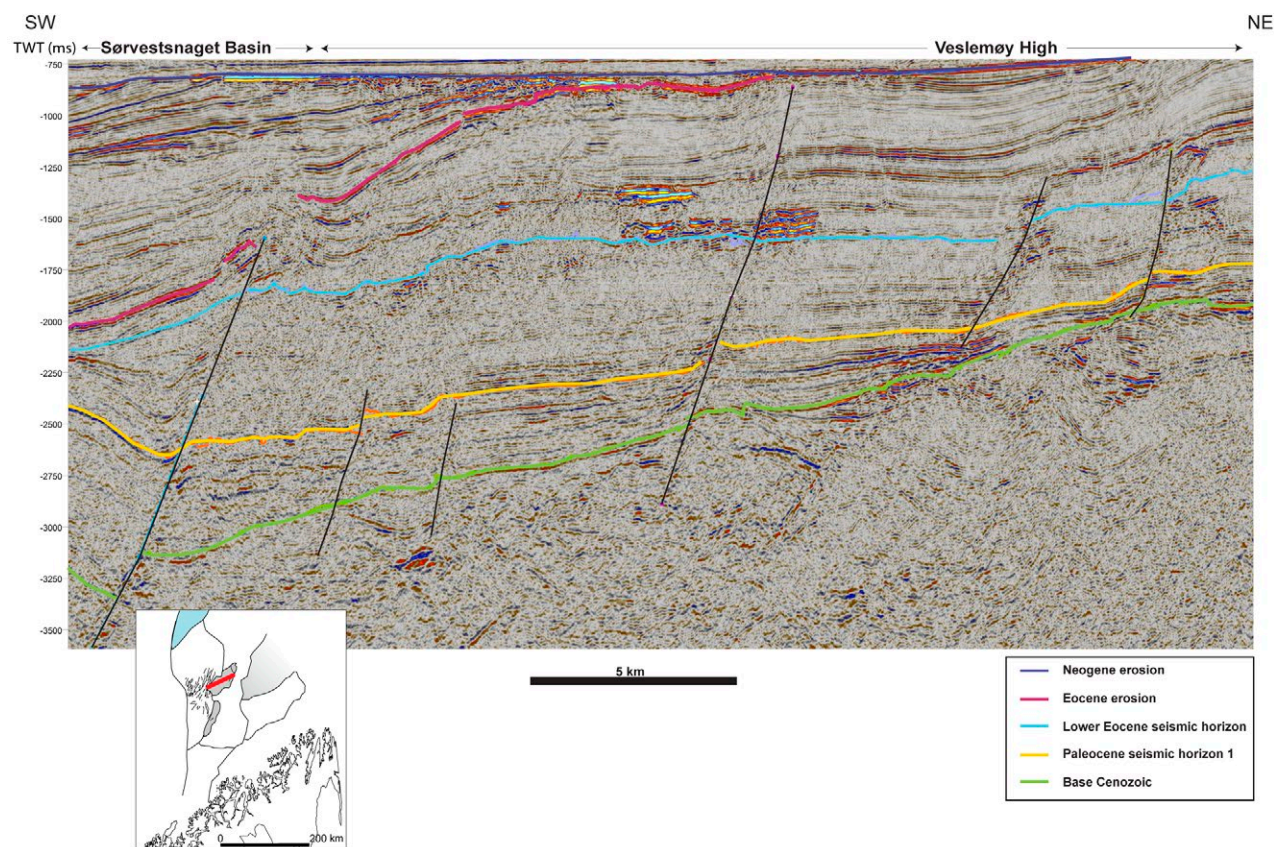


Fig. 8. Seismic example (NH9702-234) of the transition zone between the Veslemøy High and the Sørvestsnaget Basin. Note the Eocene erosion below the magenta horizon relating to footwall uplift along the western margin of the Veslemøy High. Localized wedge shaped deposits are observed west of the black fault separating the Veslemøy High to the east and the Sørvestsnaget Basin in the west. For location of inset map see Fig. 1.

N-S in the southern part of the basin and show a clockwise rotation to NNE-SSW further north (Fig. 3). The rotation roughly coincides with the transition from the Senja Ridge to the Veslemøy High (Fig. 3). The Sørvestsnaget Basin was created by dextral movement along a releasing bend in the plate margin (Ryseth *et al.* 2003; Gaina *et al.* 2009). Compared to analogue models for pull-apart basins (Wu *et al.* 2009), the fault configuration of the Sørvestsnaget Basin (Fig. 3) clearly resembles the expected fault geometries of a pull-apart basin in a transverse fault system. The middle Eocene succession was deposited during the breakup of the western Barents Sea and North-East Greenland. The subsequent deepening generated deep marine conditions in the Sørvestsnaget Basin (Ryseth *et al.* 2003).

### Upper Eocene seismic unit

The lower boundary is the Mid Eocene Seismic Horizon and the upper boundary is the Near Top Eocene reflection (Fig. 9). The interval is only tied to well 7216/11-1 S in the Sørvestsnaget Basin. The depocen-

tre of this seismic unit is located in the Sørvestsnaget Basin and coincides with that of the Middle Eocene Seismic Unit. The thickest well penetration of the Eocene succession is recorded in well 7216/11-1S in the Sørvestsnaget Basin where c. 1000 m of Eocene sediments are present (Fig. 6). The seismic observations also show a clear westward shift in depocentre during the Eocene (Fig. 5). Seismic data indicate even larger thicknesses centrally in the Sørvestsnaget Basin compared to well 7216/11-1S, implying significant subsidence of the Sørvestsnaget Basin during the Eocene and start of drifting following continental breakup.

The seismic facies of the upper Eocene deposits predominantly displays low amplitude to chaotic reflectivity (Fig. 9). Low angle progradational to aggradational geometries are present across the basin. Downlap terminations are observed on the mid Eocene horizon and on the Marginal High (far left in Fig. 9). This indicates that the Marginal High acted as a positive bathymetric element during deposition of the upper Eocene succession. Truncation below the Near Top Eocene Seismic Horizon is observed centrally in

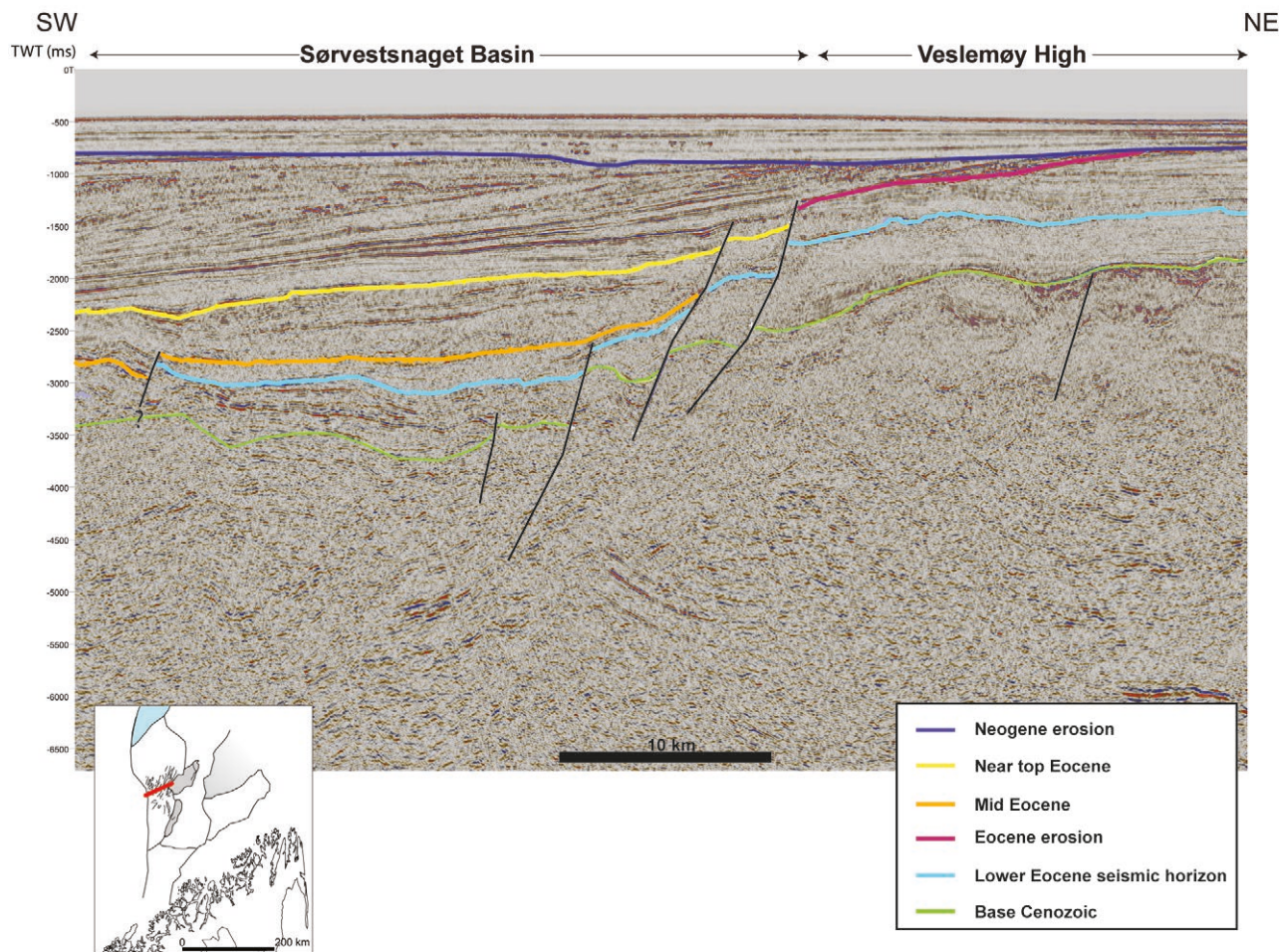


Fig. 9. Seismic transect across the Veslemøy High–Sørvestsnaget Basin transition (NH9702-234). Substantial subsidence of the basin during the Eocene is seen towards SW.

the Sørvestsnaget Basin. The incision deepens towards the Marginal High, indicating that the erosion was related to uplift of the Marginal High in Late Eocene to Early Oligocene times. The tectonic activity during the late part of the Eocene seems low compared to the preceding period, since very few faults intersect the upper Eocene interval (Fig. 9). Furthermore, the faults are located closer to the Marginal High.

The upper Eocene interval records significant changes in both thickness and lithology across the area (Fig. 6). In well 7219/9-1, it is relatively thick (c. 500 m) and intersected by westwards deepening, post-Palaeogene erosional incision (observed in the seismic data). This indicates that original thickness most likely exceeded 500 m. The Eocene succession in well 7117/9-1 on the Senja Ridge is less than 100 m thick, which implies that it was uplifted and acted as a positive bathymetric element during the Eocene. The uplift of the Senja Ridge coincides with uplift of the Veslemøy High immediately to the north, as observed in seismic cross sections (Fig. 8).

The petrophysical well logs indicate shale dominance in the Eocene except in the interval from c. 2900 to 3150 m MD in 7216/11-1S where several sand beds are recorded in log data and cores (Ryseth *et al.*, (2003). Intraformational faulting is observed towards the centre of the basin and is often associated with environments dominated by fine-grained material and relatively high sedimentation rates (Cartwright & Lonergan 1996). This is consistent with the seismic facies and lithology recorded in wells, that the depositional environment was predominantly sublittoral.

## Oligocene deposits

The Oligocene succession is c. 100 m thick in well 7216/11-1S (Fig. 6) (Ryseth *et al.* 2003). Due to the condensation of the seismic reflections and a lack of a firm well tie, a top Oligocene horizon is not included in the study.

Oligocene deposits are only observed in the Sørvestsnaget Basin (Ryseth *et al.* 2003). The Senja Ridge, Veslemøy High and the Marginal High formed positive bathymetric elements during this period, since reflections immediately above the Near Top Eocene Seismic Horizon show onlap onto the highs in the Sørvestsnaget basin (Fig. 9). Oligocene sediments are only present in the two westernmost wells, 7216/11-1S and 7117/9-1 (Fig. 6), indicating that no Oligocene sediments were deposited east of the Sørvestsnaget Basin.

The seismic geometries indicate deposition during a tectonically quiet period during early drift. The limited tectonic activity observed during the late Eocene continued during the Oligocene. Deposition coincides with the onset of diverging absolute plate

motions between Eurasia and North-East Greenland, thus marking the full evolution into passive margins along the breakup margins (Gaina *et al.* 2009).

## Lofoten-Vesterålen Margin

At the Lofoten-Vesterålen margin, the conjugate to the southern North-East Greenland margin (Tsikalas *et al.* 2001), Palaeogene deposits are only preserved in the deeper parts of the basins due to post-Eocene erosion (Faereth 2012). The erosion deepens away from the breakup axis (Bergh *et al.* 2007), as also observed on the North-East Greenland shelf (Petersen *et al.* 2015) and in the West Barents Sea area.

The Paleocene succession on the Lofoten-Vesterålen Margin is described to have prograding wedge geometries downlapping on Cretaceous sediments (Tasrianto & Escalona 2015). They are included in the Danian to upper Paleocene Tang and Tare formations which in well 6710/10-1 are composed of shales with interbedded tuffs, interpreted to be deposited in a deep marine environment formed as the result of thermal subsidence following extensive Cretaceous (and earlier) rifting events (Tsikalas *et al.* 2001; Bergh *et al.* 2007). This part of the succession resembles the pre-breakup succession on the North-East Greenland margin.

Well 6706/6-1 in the northern Vøring Basin, just south of the Lofoten-Vesterålen Margin, is reported to contain Palaeogene sandstones derived from Greenland (Norwegian Petroleum Directorate 2010). When reconstructing the plates back to a syn-breakup setting, the well site is located proximal to the area affected by uplift in North-East Greenland (Petersen *et al.* 2015), and the two margins appear to have shared sedimentary source area prior to the breakup. Continental breakup was initiated in the early Eocene (Faereth 2012), synchronous with the other margins surrounding the Norwegian-Greenland Sea (Olesen *et al.* 2007; Gaina *et al.* 2009).

## Evolution of the West Barents Sea

By integrating the information presented in the previous sections, we here present a model for the evolution of the West Barents Sea during the Palaeogene (Fig. 10). This model encompasses previous studies (e.g. Faleide *et al.* 1993; Richardsen *et al.* 1991; Ryseth *et al.* 2003), supplemented with interpretations of features important for the correlation to North-East Greenland. The described seismic units are associated with the

three main phases of the breakup history: Pre-breakup units (Lower Paleocene, Lower–upper Paleocene), breakup units (Lower Eocene, Middle Eocene) and (early) drift units (Upper Eocene, Oligocene). Fig. 10 displays the large-scale geometries of the sediments deposited during these three phases.

The geometry of the lower Paleocene succession suggests deposition during a tectonically relatively quiet period following a period of non-deposition along the western Barents Sea margin (Dalland *et al.* 1988; Knutsen & Vorren 1991; Gaina *et al.* 2009). The Loppa High was a positive topographic element during the Paleocene and possibly acted as a local source area since prograding clinoforms of this age are observed on and west of the high (Figs 7, 10). However, progradation was somewhat limited and the larger parts of the adjacent Tromsø Basin are characterized by sub-horizontal reflections suggesting sublittoral deposition. Tsikalas *et al.* (2005) report some Late Cretaceous–Early Paleocene deformation along the margin, but the effects on deposition were limited. Evidence of fault movements that predate the onset

of continental breakup includes footwall uplift of the Senja Ridge and the Veslemøy High, recorded by the onlap of the Paleocene reflectors (Fig. 10A).

Palaeogene normal faulting is observed both east and west of the Sørvestsnaget Basin. The seismic data suggest that faulting started along the eastern margin of the basin and then migrated westward towards the margin of the shelf, causing westward migration of the depocentre (Fig. 5). The westward translation of faulting culminates in the De Geer Mega Shear Zone that separates the Sørvestsnaget Basin from the Lofoten Basin (Fig. 3). The Marginal High was uplifted during this fault culmination, indicated by onlap onto the high and erosion of its top. The distribution and orientation of the faults in the Sørvestsnaget Basin are consistent with models of transtensional pull-apart basins where en échelon soft linked faults outline the basin (Wu *et al.* 2009).

The seismic data show evidence of prograding clinoforms building out from the east into structural lows and across highs along the West Barents Sea margin during the Palaeogene (Fig. 10). The thickness

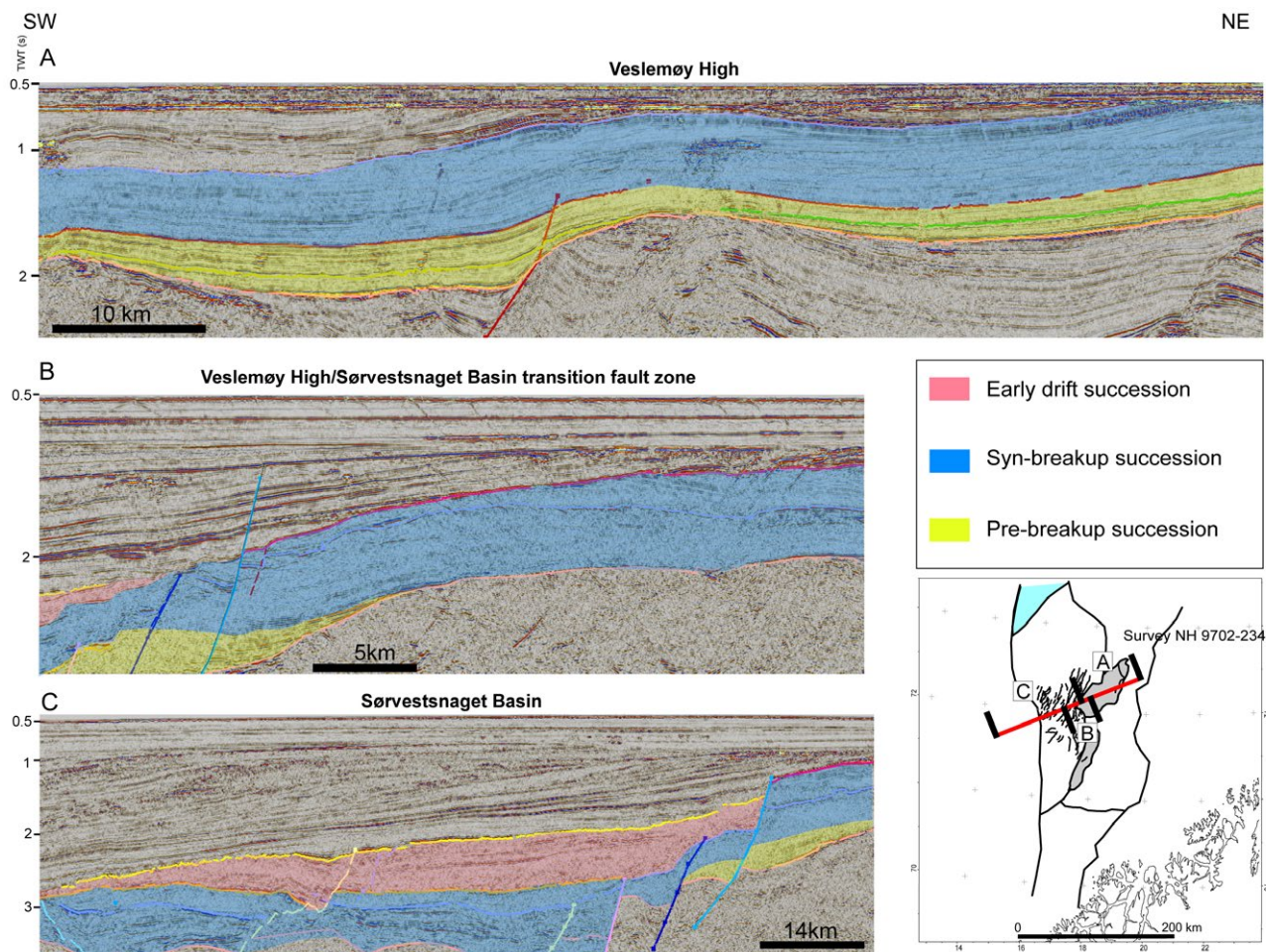


Fig. 10. Three seismic examples from the West Barents Sea, showing the subdivision of the Palaeogene succession. See text for detailed description. For location of inset map see Fig. 1.

variations observed between the Loppa High, Senja Ridge and Sørvestsnaget Basin further illustrate the evolution before, during and after breakup (Fig. 5). The pre-breakup succession, represented by the Paleocene interval, shows relatively homogenous thicknesses across the margin, whereas the Eocene breakup succession displays significant thickness changes as

this interval is condensed across the Senja Ridge. The thicknesses of the early drift sequence, as represented by the upper Eocene to Oligocene succession, are significantly smaller than those of the underlying intervals. This indicates condensation of the early drift succession on the continental margin and a westward shift of the depocentre into the Lofoten Basin.

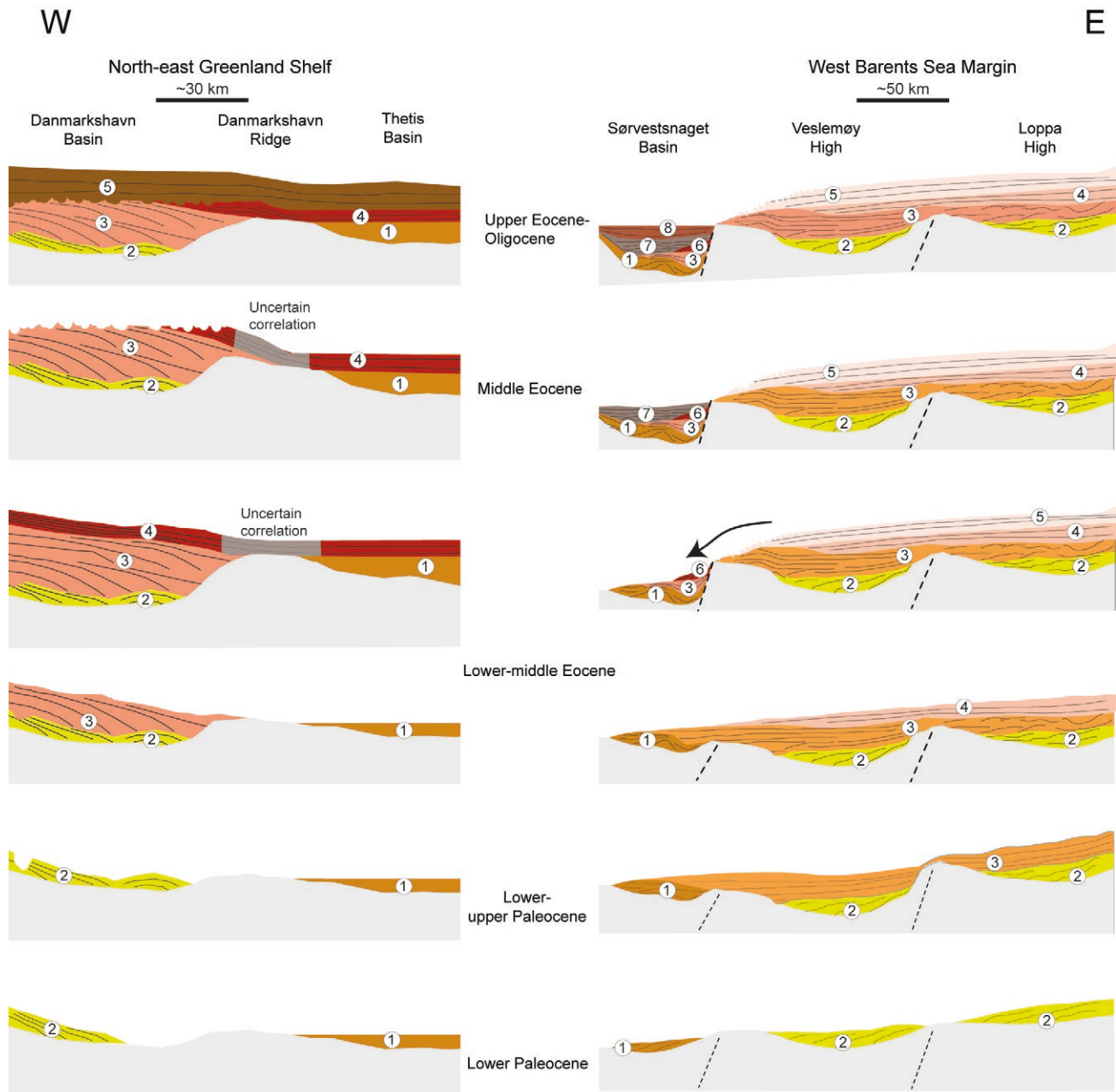


Fig. 11. Simplified correlation across the conjugate margins based on similarities in depositional geometries. The pre-breakup deposits (Lower–Upper Paleocene) are characterised by low angle clinoforms filling out basinal lows. The syn-breakup succession (Eocene) displays steeper clinoforms than below and a more pronounced progradation across structural highs on both sides. The early drift interval (Middle Eocene–Oligocene) of the conjugate margins is dominated by sub-horizontal stratal geometries, with a large extent in the North-East Greenland area, whereas the deposition is centred in the Sørvestsnaget Basin and in the Lofoten Basin further west (not displayed) on the West Barents Sea margin. Colours are solely used to distinguish individual seismic units and hold no other significance. Numbering refers to the chronostratigraphic chart presented in Fig. 12.

## Conjugate margin seismic correlation

By combining the information from the seismic stratal geometries with the temporal constraints derived from wells drilled in the West Barents Sea, as well as the timing of volcanism in North-East Greenland, we suggest the correlation scheme shown in Fig. 11. The chronostratigraphic correlation of the seismic units of the North-East Greenland and the Western Barents Sea margins is based on the described similarities of stratal stacking patterns at the two margins. The common thermal and plate tectonic history during continental breakup forms the framework for the correlation. All available stratigraphic information is utilised to date the seismic sections. (Faleide *et al.* 1993; Faleide *et al.* 1996; Ryseth *et al.* 2003). Significant structural differences exist between the two margins, as the northwest Eurasian margin is dominated by complex compressional, strike-slip and extensional tectonics (Saettem *et al.* 1994; Tsikalas *et al.* 2002), whereas the North-East Greenland margin is mostly dominated by extensional tectonics during the Palaeogene breakup (Petersen *et al.* 2015). This is primarily observed as a higher frequency of faulting during the pre-breakup and syn-breakup phases on the West Barents Sea margin. This is most likely caused by the transverse motions along the De Geer Mega Shear zone, where true passive margin development occurred later compared to North-East Greenland.

The lower Palaeogene seismic stratal geometries are dominated by infill between structural highs that formed positive bathymetrical elements on both margins (Figs 4A, 10A–C). In the West Barents Sea area, the rotated fault blocks of the Veslemøy High and Senja Ridge are positive structural elements (Fig. 5). On the North-East Greenland margin the Danmarkshavn Ridge separates depositional areas from the incipient breakup zone. The Danmarkshavn Ridge has a position similar to that of the rotated fault blocks on the West Barents Sea Margin (Figs 4A,B, 5, 11). Both margins show evidence of low angle prograding to sub-parallel infill to be focused in the lows, which is consistent with deposition on flooded end-Mesozoic inherited topography. Relatively low gradients in both the basin and hinterland are expected in this setting (Hamann *et al.* 2005; Worsley 2008; Petersen *et al.* 2015). Deposition is interpreted to take place in the tectonically relatively quiet period following the prolonged Late Palaeozoic–Mesozoic rifting that occurred in the region prior to the opening of the North Atlantic (Doré 1991). Therefore, the succession is interpreted to predate continental breakup, and a Paleocene age for the pre-breakup package on the North-East Greenland shelf is suggested by correlation with the West Barents

Sea margin (Fig. 4A, marked in yellow, and Figs 11, 12).

A distinct increase in the angle and amplitude of prograding clinoforms mark the onset of the continental breakup, most likely caused by thermal heating in relation to the break-up volcanism (recorded in the lower Eocene deposits on the conjugate margins) (Figs 4B, 10B, 11). Uplift of the proximal areas of the margins and subsidence towards the central zone of breakup caused an overall increase in depositional gradient and sediment influx onto the shelf areas, thus marking a significant change which can be dated to near the Paleocene–Eocene transition in the Barents Sea (Fig. 9). A similar age for the onset of large scale progradation is suggested for North-East Greenland. The progradational succession has an erosive upper boundary which we interpret as the effect of volcanic induced thermal doming (Petersen *et al.* 2015), deepening towards the south and west (Fig. 4A, B). We suggest an earliest Eocene age for the onset of the deposition of the syn-breakup package in North-East Greenland (Fig. 4A) (Petersen *et al.* 2015).

Plane-parallel seismic facies tops the Palaeogene succession on both margins, suggesting deposition in a relatively quiet, deep marine setting (Figs 4C, 10C, 11), as confirmed in well bores penetrating this level on the Barents Sea margin. The well data indicate a Late Eocene to Oligocene age for the plane-parallel packages (Fig. 6) (Ryseth *et al.* 2003). Similar ages are suggested for the seismic units included in the early drift succession on the North-East Greenland shelf. The age of the upper boundary of the succession is associated with some uncertainty.

## Chronostratigraphic implications

A pronounced symmetry of the seismic geometries is observed across the North-East Greenland and West Barents Sea margins, and we propose that this symmetry reflects a genetic, temporal relationship of the conjugate margin set (Fig. 12). The two margins show a comparable stacking of seismic facies. The locus of the sedimentation shifted synchronously towards the breakup axis on both the West Barents Sea and North-East Greenland margins, most pronounced on the West Barents Sea margin (Fig. 12). Figure 5 shows that pre-breakup deposition is constricted by basinal highs on both margins. On the Greenland side, the Danmarkshavn Ridge forms the barrier, whereas the footwall uplift along the west margin of the Veslemøy High forms the barrier in the West Barents Sea area (Fig. 1, pre-breakup interval on Fig. 12).

During the volcanically active breakup phase, pronounced progradational events shifted the depo-

centres of both margins further towards the central axis of breakup (Figs 11, 12). This is also observed in the thickness distribution of the sediments deposited during breakup (Fig. 5). Basinal highs are overstepped and sediments accumulate in the basins near the breakup zone. The breakup phase was dominated by an increase in both accommodation space and sediment supply as basins were formed near the breakup axis and the hinterland produced more sediment due to an increased gradient of the depositional system (Fig. 12). In the Sørvestsnaget Basin on the Barents Sea margin, extensive normal faulting occurred during this period (Fig. 9) as a result of pull-apart tectonism, whereas the southern North-East Greenland Margin was less tectonically deformed (Fig. 4). Tectonism that influenced the depositional fairways are however observed in the Eureka region, most likely including the Wandel Sea (Petersen *et al.* 2016).

Following breakup, early drift deposition is dominated by a relatively homogenous distribution of sediments across both margins and further basinward migration of the depocentres. Post-breakup erosion intersects the Palaeogene succession on both margins, hampering any palaeogeographic interpretation away from the central axis of breakup (Fig. 5). In the West Barents Sea, the Veslemøy High–Senja

Ridge area is apparently uplifted during this phase (Figs 11, 12), and hence deposition is restricted to the Sørvestsnaget Basin, but other studies have shown that deposition during early drifting also occurred further to the west in the Lofoten Basin (Ryseth *et al.* 2003). The distribution and limited lateral thickness variations are consistent with this succession representing deposition during a relatively quiet period of thermally related, large scale subsidence following the heating of the margins during the breakup volcanism. The transition to early drift deposition is observed on both margins as aggradational geometries with onlaps on the structural highs (Fig. 12). Evidence of a common tectonic history is also found in the form of a soft-linked, right-lateral transfer zone that correlates between Lofoten-Vesterålen and North-East Greenland (Faerseth 2012; Petersen *et al.* 2015).

## Conclusions

The seismic units identified on the North-East Greenland shelf and in the West Barents Sea have been correlated on the basis of their stratal geometries and their relation to plate tectonic and volcanic events, thus

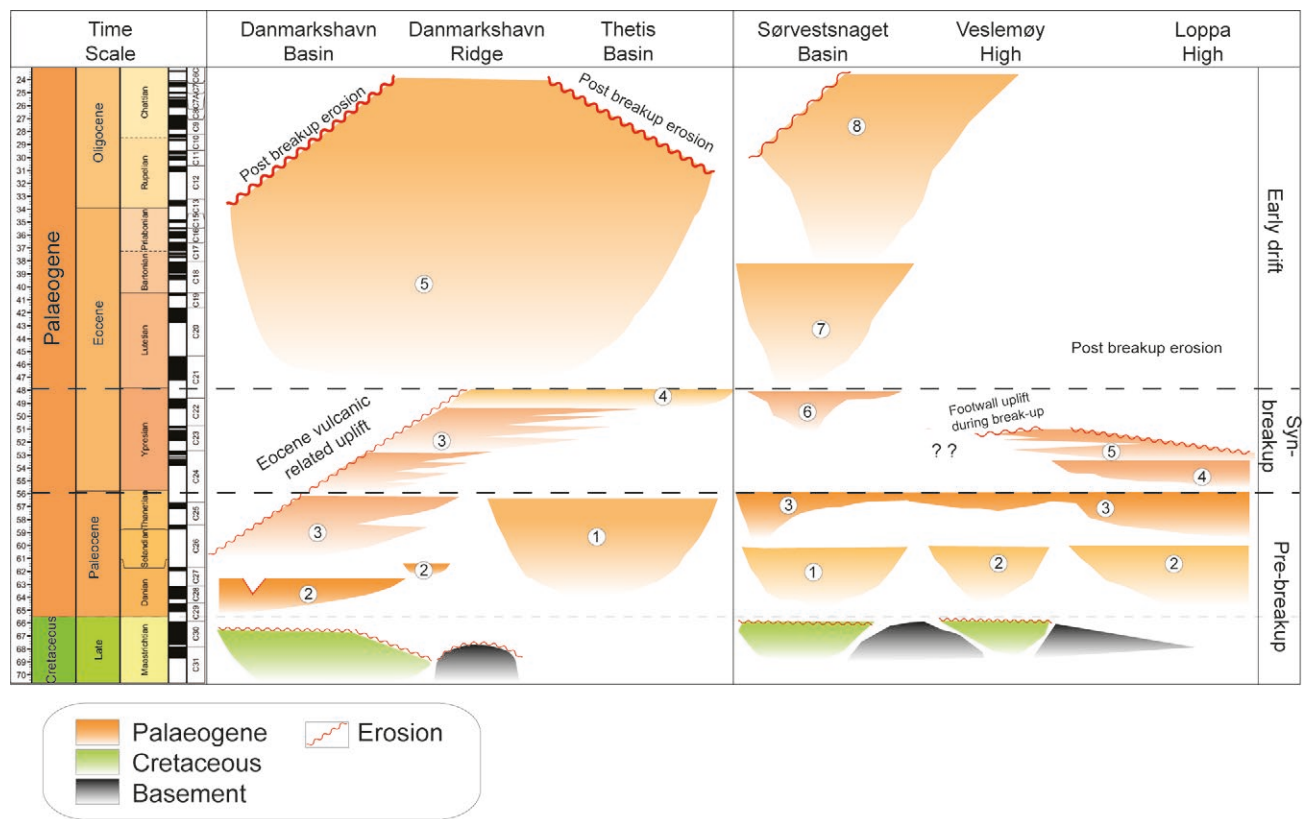


Fig. 12. Simplified chronostratigraphic chart correlating the individual depositional units identified at both conjugate margins. The absolute ages are associated with some uncertainty. Numbers refer to the seismic units shown in Fig. 11.

facilitating a more robust dating of the Palaeogene succession on the North-East Greenland shelf.

A comparison with the Lofoten-Vesterålen Margin revealed depositional geometries of the Tang and Tare Formations that correlate well with the pre-breakup succession in North-East Greenland. Paleocene sandstones in Norwegian well 6706/6-1 derived from North-East Greenland suggest a linkage between the two areas prior to and potentially during the time of volcanic uplift (Norwegian Petroleum Directorate 2010; Petersen *et al.* 2015).

A simplified correlation scheme of the Palaeogene interval between the North-East Greenland shelf and the West Barents Sea margin is proposed (Fig. 12). The scheme is based on the subdivision of the Palaeogene into three main packages. The pre-breakup, syn-breakup and early drift successions are well described and dated in the West Barents Sea. In contrast, the Palaeogene succession on the North-East Greenland margin has previously only been assigned to seismic megasequences (Hamann *et al.* 2005; Tsikalas *et al.* 2005). Correlating individual units across the continental breakup zone and relating them to the large-scale plate tectonics lowers the uncertainty of the dating of Palaeogene seismic units offshore North-East Greenland.

The pre-breakup succession of the North-East Greenland shelf consists of low-angle clinoforms and basin floor fans and is dated as Paleocene, and therefore predates the continental breakup (Figs 11, 12). The North-East Greenland shelf was relatively tectonically quiet during this period, where deposition was mostly restricted to the Danmarkshavn Basin. In contrast, the West Barents Sea margin underwent significant transtensional tectonism during this period.

The Eocene breakup interval displays pronounced progradation across both the North-East Greenland and West Barents Sea margins in response to an increased gradient of the depositional system, thus increasing sediment input into the basins. Structurally, the breakup phase of the North-East Greenland succession is relatively quiet. The Danmarkshavn Ridge is overstepped by prograding clinoforms, and seismic reflections are correlated into the Thetis basin. A similar pattern is observed in the West Barents Sea area, where structural highs are overstepped, and the depositional system display progradation and lateral shift of depocentre towards the breakup axis (Figs 11, 12). However, in contrast to the North-East Greenland margin, the Barents Sea margin is associated with a significant amount of normal faulting in the Sørvestsnaget Basin due to its transtensional nature. The Late Eocene–Oligocene early drift phase was dominated by deposition below wave base, with hemipelagic sedimentation over a flooded continental

margin. Tectonism was limited during this period, with only minor evidence of fault activity at the margins. Thermal cooling was the main process creating the accommodation space and generated seismic units of relatively homogenous thicknesses.

## Acknowledgements

The authors wish to thank DONG Energy and the KANUMAS partners (BP, Chevron, Exxon, JOGMEG, Shell and Statoil) for providing the data and significant financial support for this study. Several people at conferences have commented on the current work, which helped to improve this manuscript. Furthermore, the manuscript benefitted greatly from the input of the reviewers.

## References

- Berger, D. & Jokat, W. 2008: A seismic study along the East Greenland margin from 72 degrees N to 77 degrees N. *Geophysical Journal International* 174(2), 733–748.
- Bergh, S.G., Eig, K., Klovjan, O.S., Henningsen, T., Olesen, O. & Hansen, J.A. 2007: The Lofoten-Vesterålen continental margin: a multiphase Mesozoic-Palaeogene rifted shelf as shown by offshore-onshore brittle fault-fracture analysis. *Norwegian Journal of Geology* 87(1–2), 29–58.
- Bergh, S.G. & Grogan, P. 2003: Tertiary structure of the Sorkapp-Hornsund Region, South Spitsbergen, and implications for the offshore southern extension of the fold-thrust Belt. *Norwegian Journal of Geology* 83(1), 43–60.
- Breivik, A.J., Faleide, J.I. & Gudlaugsson, S.T. 1998: Southwestern Barents Sea margin: late Mesozoic sedimentary basins and crustal extension. *Tectonophysics* 293(1–2), 21–44.
- Brooks, C.K. 2011: The East Greenland rifted volcanic margin. *Geological Survey of Denmark and Greenland Bulletin* 24, 96 pp.
- Bruhn, R. & Steel, R. 2003: High-resolution sequence stratigraphy of a clastic foredeep succession (Paleocene, Spitsbergen): An example of peripheral-bulge-controlled depositional architecture. *Journal of Sedimentary Research* 73(5), 745–755.
- Cartwright, J.A. & Lonergan, L. 1996: Volumetric contraction during the compaction of mudrocks: a mechanism for the development of regional-scale polygonal fault systems. *Basin Research* 8(2), 183–193.
- Dalland, A., Worsley, D. & Ofstad, K. 1988: A lithostratigraphic scheme for the Mesozoic and Cenozoic succession offshore mid- and northern Norway. *NPD-Bulletin* 4, 1–65.
- Doré, A.G. 1991: The Structural Foundation and Evolution of Mesozoic Seaways between Europe and the Arctic. *Palaeogeography Palaeoclimatology Palaeoecology* 87(1–4), 441–492.

- Døssing, A., Stemmerik, L., Dahl-Jensen, T. & Schlindwein, V. 2010: Segmentation of the eastern North Greenland oblique-shear margin - Regional plate tectonic implications. *Earth and Planetary Science Letters* 292(3-4), 239-253.
- Faereth, R.B. 2012: Structural development of the continental shelf offshore Lofoten-Vesterålen, northern Norway. *Norwegian Journal of Geology* 92(1), 19-40.
- Faleide, J.I., Myhre, A.M. & Eldholm, O. 1988: Early Tertiary volcanism at the western Barents Sea margin. Geological Society, London, Special Publication 39, 135-146.
- Faleide, J.I., Solheim, A., Fiedler, A., Hjelstuen, B.O., Andersen, E.S. & Vanneste, K. 1996: Late Cenozoic evolution of the western Barents Sea-Svalbard continental margin. *Global and Planetary Change* 12(1-4), 53-74.
- Faleide, J.I., Vagnes, E. & Gudlaugsson, S.T. 1993: Late Mesozoic-Cenozoic Evolution of the South-Western Barents Sea in a Regional Rift Shear Tectonic Setting. *Marine and Petroleum Geology* 10(3), 186-214.
- Fiedler, A. & Faleide, J.I. 1996: Cenozoic sedimentation along the southwestern Barents Sea margin in relation to uplift and erosion of the shelf. *Global and Planetary Change* 12(1-4), 75-93.
- Gaina, C., Gernigon, L. & Ball, P. 2009: Palaeocene-Recent plate boundaries in the NE Atlantic and the formation of the Jan Mayen microcontinent. *Journal of the Geological Society* 166, 601-616.
- Gautier, D.L., Bird, K.J., Charpentier, R.R., Grantz, A., Houseknecht, D.W., Klett, T.R., Moore, T.E., Pitman, J.K., Schenk, C.J., Schuenemeyer, J.H., Sørensen, K., Tennyson, M.E., Valin, Z.C. & Wandrey, C.J. 2009: Assessment of Undiscovered Oil and Gas in the Arctic. *Science* 324(5931), 1175-1179.
- Gawthorpe, R.L. & Leeder, M.R. 2000: Tectono-sedimentary evolution of active extensional basins. *Basin Research* 12(3/4), 195-218.
- Geissler, W.H. & Jokat, W. 2004: A geophysical study of the northern Svalbard continental margin. *Geophysical Journal International* 158(1), 50-66.
- Gernigon, L. & Brönnner, M. 2012: Late Palaeozoic architecture and evolution of the southwestern Barents Sea: insights from a new generation of aeromagnetic data. *Journal of the Geological Society* 169(4), 449-459.
- Gernigon, L., Olesen, O., Ebbing, J., Wienecke, S., Gaina, C., Mogaard, J.O., Sand, M. & Myklebust, R. 2009: Geophysical insights and early spreading history in the vicinity of the Jan Mayen Fracture Zone, Norwegian-Greenland Sea. *Tectonophysics* 468(1-4), 185-205.
- Hamann, N.E., Whittaker, R.C. & Stemmerik, L. 2005: Geological development of the Northeast Greenland Shelf. Geological Society, London, Petroleum Geology Conference series 6, 887-902.
- Japsen, P., Green, P.F., Bonow, J.M., Nielsen, T.F.D. & Chalmers, J.A. 2014: From volcanic plains to glaciated peaks: Burial, uplift and exhumation history of southern East Greenland after opening of the NE Atlantic. *Global and Planetary Change* 116, 91-114.
- Knutsen, S.M. & Larsen, K.I. 1997: The late Mesozoic and Cenozoic evolution of the Sorvestsnaget Basin: A tectonostratigraphic mirror for regional events along the Southwestern Barents Sea Margin? *Marine and Petroleum Geology* 14(1), 27-54.
- Knutsen, S.M. & Vorren, T.O. 1991: Early Cenozoic Sedimentation in the Hammerfest Basin. *Marine Geology* 101(1-4), 31-48.
- Larsen, L.M., Pedersen, A.K., Tegner, C. & Duncan, R.A. 2014: Eocene to Miocene igneous activity in NE Greenland: northward younging of magmatism along the East Greenland margin. *Journal of the Geological Society* 171(4), 539-553.
- Lyck, J.M. & Stemmerik, L. 2000: Palynology and depositional history of the Paleocene? Thyra Ø Formation, Wandel Sea Basin, eastern North Greenland. In: Stemmerik, L. (ed), Palynology and deposition in the Wandel Sea Basin, eastern North Greenland. *Geology of Greenland Survey Bulletin* 187, 21-49.
- Miller, K.G., Kominz, M.A., Browning, J.V., Wright, J.D., Mountain, G.S., Katz, M.E., Sugarman, P.J., Cramer, B.S., Christe-Blick, N. & Pekar, S.F. 2005: The Phanerozoic record of global sea-level change. *Science* 310(5752), 1293-1298.
- Nøhr-Hansen, H., Nielsen, L.H., Sheldon, E., Hovikoski, J. & Alsen, P. 2011: Palaeogene deposits in North-East Greenland. *Geological Survey of Denmark and Greenland Bulletin* 23, 61-64.
- Norwegian Petroleum Directorate 2010: Geofaglig vurdering av petroleumressursene i havområdene utenfor Lofoten, Vesterålen og Senja. Oljedirektoratet (Norwegian Petroleum Directorate). <http://www.npd.no/publikasjoner/rapporter/petroleumressurser-i-havomradene-utenfor-lofoten-vesteralen-og-senja---geofaglig-vurdering/>.
- Ogg, J.G. 2012. The Geomagnetic Polarity Time Scale. In: Gradstein, F.M., Schmitz, J.G.O.D. & Ogg, G.M. (eds), *The Geologic Time Scale*, 85-113. Elsevier, Boston.
- Olesen, O., Ebbing, J., Lundin, E., Mauring, E., Skilbrei, J.R., Torsvik, T.H., Hansen, E.K., Henningsen, T., Midboe, P. & Sand, M. 2007: An improved tectonic model for the Eocene opening of the Norwegian-Greenland Sea: Use of modern magnetic data. *Marine and Petroleum Geology* 24(1), 53-66.
- Petersen, T.G., Hamann, N.E. & Stemmerik, L. 2015: Tectono-sedimentary evolution of the Paleogene succession offshore Northeast Greenland. *Marine and Petroleum Geology* 67, 481-497.
- Petersen, T.G., Thomsen, T.B., Olaussen, S. & Stemmerik, L. 2016: Provenance shifts in an evolving Eureka foreland basin; the Tertiary Central Basin, Spitsbergen. *Journal of the Geological Society* 173(4), 634-648.
- Posamentier, H.W. & Kolla, V. 2003: Seismic Geomorphology and Stratigraphy of Depositional Elements in Deep-Water Settings. *Journal of Sedimentary Research* 73(3), 367-388.
- Richardson, G., Henriksen, E. & Vorren, T.O. 1991: Evolution of the Cenozoic Sedimentary Wedge during Rifting and Sea-Floor Spreading West of the Stappen High, Western Barents Sea. *Marine Geology* 101(1-4), 11-30.

- Ryseth, A., Augustson, J.H., Charnock, M., Haugerud, O., Knutsen, S.M., Midbøe, P.S., Opsal, J.G. & Sundsbo, G. 2003: Cenozoic stratigraphy and evolution of the Sorvestsnaget Basin, southwestern Barents Sea. *Norwegian Journal of Geology* 83(2), 107–130.
- Saettem, J., Bugge, T., Fanavoll, S., Goll, R.M., Mørk, A., Mørk, M.B.E., Smelror, M. & Verdenius, J.G. 1994: Cenozoic Margin Development and Erosion of the Barents Sea - Core Evidence from Southwest of Bjornoya. *Marine Geology* 118(3–4), 257–281.
- Smelror, M. & Basov, V.A. 2009. Geological history of the Barents Sea. Geological Survey of Norway, Atlas. Trondheim: Geological Survey of Norway.
- Talwani, M. & Eldholm, O. 1977: Evolution of the Norwegian-Greenland Sea. *Geological Society of America Bulletin* 88(7), 969–999.
- Tasrianto, R. & Escalona, A. 2015: Rift architecture of the Lofoten-Vesterålen margin, offshore Norway. *Marine and Petroleum Geology* 64, 1–16.
- Tsikalas, F., Eldholm, O. & Faleide, J.I. 2002: Early Eocene sea floor spreading and continent-ocean boundary between Jan Mayen and Senja fracture zones in the Norwegian-Greenland Sea. *Marine Geophysical Researches* 23(3), 247–270.
- Tsikalas, F., Faleide, J.I., Eldholm, O. & Wilson, J. 2005: Late Mesozoic–Cenozoic structural and stratigraphic correlations between the conjugate mid-Norway and NE Greenland continental margins. *Geological Society, London, Petroleum Geology Conference series* 6, 785–801.
- Tsikalas, F., Faleide, J.I. & Kuszniir, N.J. 2008: Along-strike variations in rifted margin crustal architecture and lithosphere thinning between northern Vøring and Lofoten margin segments off mid-Norway. *Tectonophysics* 458(1-4), 68–81.
- Tsikalas, F., Inge Faleide, J. & Eldholm, O. 2001: Lateral variations in tectono-magmatic style along the Lofoten–Vesterålen volcanic margin off Norway. *Marine and Petroleum Geology* 18(7), 807–832.
- Vorren, T.O., Richardsen, G., Knutsen, S.M. & Henriksen, E. 1991: Cenozoic Erosion and Sedimentation in the Western Barents Sea. *Marine and Petroleum Geology* 8(3), 317–340.
- Worsley, D. 2008: The post-Caledonian development of Svalbard and the western Barents Sea. *Polar Research* 27(3), 298–317.
- Wu, J.E., McClay, K., Whitehouse, P. & Dooley, T. 2009: 4D analogue modelling of transtensional pull-apart basins. *Marine and Petroleum Geology* 26(8), 1608–1623.
- Ziegler, P.A. & Cloetingh, S. 2004: Dynamic processes controlling evolution of rifted basins. *Earth-Science Reviews* 64(1–2), 1–50.

# *Obliquorhynchia* (gen. nov.): An asymmetric brachiopod from the middle Danian Faxø Formation, Denmark

ANE ELISE SCHRØDER, BODIL W. LAURIDSEN & FINN SURLYK



Schrøder, A.E., Lauridsen, B.W. & Surlyk, F. 2016. *Obliquorhynchia* (gen. nov.): An asymmetric brachiopod from the middle Danian Faxø Formation, Denmark. © 2016 by Bulletin of the Geological Society of Denmark, Vol. 64, pp. 97–109. ISSN 2245-7070 ([www.2dgf.dk/publikationer/bulletin](http://www.2dgf.dk/publikationer/bulletin)).

The diverse brachiopod fauna from the middle Danian cool-water coral mounds of the Faxø Formation, Denmark, includes the new genus *Obliquorhynchia* that exhibits an asymmetric folding of the frontal commissure, a rare feature in brachiopods. Two of the most abundant brachiopod species found in the Faxø Formation, '*Rhynchonella*' *flustracea* and '*Rhynchonella*' *faxensis*, are considered conspecific and are both referred to *Obliquorhynchia*. In the literature, the species name *flustracea* has been ascribed to von Schlotheim. However, the original species name proposed by von Schlotheim in his catalogue (1832, 65, no 62) was *lustraceus*. This remained a *nomen nudum* until von Buch (1834) published a description based on the material of von Schlotheim and changed the name to *flustracea*. The species is thus ascribed to von Buch. A lectotype for *Obliquorhynchia flustracea* (von Buch 1834) is designated and illustrated here.

Keywords: *Obliquorhynchia* (gen. nov.), '*Rhynchonella*' *flustracea*, '*Rhynchonella*' *faxensis*, asymmetric brachiopods, middle Danian, Faxø Formation, Denmark.

Ane Elise Schrøder [[a.schroder.e@gmail.com](mailto:a.schroder.e@gmail.com)], Geological Survey of Denmark and Greenland, Øster Voldgade 10, DK-1350 Copenhagen K, Denmark (also Østsjælland Museum, Højerup Bygade 38, DK-4660, Højerup, Denmark). Bodil W. Lauridsen [[bwl@geus.dk](mailto:bwl@geus.dk)], Geological Survey of Denmark and Greenland, Øster Voldgade 10, DK-1350 Copenhagen K, Denmark. Finn Surlyk [[finns@ign.ku.dk](mailto:finns@ign.ku.dk)], University of Copenhagen, Department of Geosciences and Natural Resource Management, Øster Voldgade 10, DK-1350 Copenhagen K, Denmark.

Received 15 June 2016  
Accepted in revised form  
24 October 2016  
Published online  
23 November 2016

Brachiopods are very common in most of the coral and bryozoan mound facies of the middle Danian Faxø Formation in eastern Denmark. The most common brachiopod species '*Rhynchonella*' *flustracea* and '*Rhynchonella*' *faxensis* are present in all the coral mound facies, with the exception of mudstone and floatstone facies. They are here considered as conspecific and are referred to as *Obliquorhynchia flustracea* (as revised herein). The specimens exhibit commissural asymmetry, which is a relatively rare feature in articulated brachiopods (Fürsich & Palmer 1984). The success of this species was probably due to an adaptation to a life between the branches of the scleractinian coral *Dendrophyllia candelabrum* (Asgaard 1968). The species is very commonly found sitting in this position.

Modern asymmetric brachiopods are known from tropical reef systems and cool-water coral mounds at relatively deep, cool settings, notably from the Atlantic Ocean (Elliott 1948, 1958; Atkins 1959, 1960, 1961; Freiwald *et al.* 2002; Freiwald *et al.* 2004; Henry & Roberts 2007). In the fossil record asymmetric brachiopods are commonly found in association with tropical coral

reef and cool-water coral mound facies (Rózycki 1948; Ager 1965, 1967; Asgaard 1968). Asymmetry in Mesozoic brachiopods from tropical reefs is particularly prevalent in the order Rhynchonellida (Afanasjeva 2014). The form of asymmetry in this order is mainly confined to the frontal commissure and is described as commissural asymmetry. The asymmetry is most conspicuous at the commissure, but will in general affect the overall shape of the brachiopod.

The two former species *Terebratula flustracea* von Buch 1834 and *Rhynchonella faxensis* Posselt 1894 from the Faxø Formation, exposed in the Faxø limestone quarry in eastern Denmark, both exhibit commissural asymmetries to varying degrees. Starting with the work of Asgaard (1968) *Terebratula flustracea* von Buch and *Rhynchonella faxensis* Posselt have been referred to with the genus name *Rhynchonella* in inverted commas. For the sake of simplicity, this form is used throughout in the present paper when referring to older works.

'*R.*' *flustracea* was described by von Buch (1834, 1835) based on the material collected by von Schlotheim in

coral limestone in the Faxø quarry. *R. faxensis* was described by Posselt (1894) as a new species based on 20 specimens collected in the quarry. He noted that the specimens of *R. faxensis* were rather similar to *R. flustracea* and relatively rare, but erected the new species on the basis of minor details in external morphology such as number of ribs and occasional uniplication of the commissure. In the original material collected by von Schlotheim, which comprised nine syntypes (now one lectotype and eight paralectotypes, as revised herein) of *R. flustracea* (Museum Für Naturkunde Leibniz-Institut Berlin, number MB.B.9116.1–9), one paralectotype actually possesses the characteristics that Posselt (1894) used in his description of *R. faxensis* as a new species, such as fewer ribs and a uniplicate commissure.

The aim of this study is to erect a new rhynchonellid brachiopod genus, *Obliquorhynchia* gen. nov. based on material from the middle Danian Faxø Formation, and to describe the variation within the two types of asymmetric brachiopods here classified as one species, *Obliquorhynchia flustracea*.

## Geological setting

The Faxø Formation represents a middle Danian cool-water complex of interfingering coral and bryozoan mounds (Lauridsen *et al.* 2012). The coral mounds were established by the azooxanthellate scleractinian coral species *Dendrophyllia candelabrum* (Hennig 1899), *Oculina becki* (Nielsen 1922) and *Faksephyllia faxøensis* (Lyell 1837), shortly after the mass extinction at the Cretaceous–Palaeogene (K/Pg) boundary. Two million years after the K/Pg boundary the coral mounds started to grow on top of bryozoan mounds in relatively deep water below the photic zone over the easternmost part of the Ringkøbing–Fyn High, limiting the Danish Basin to the south (Floris 1980; Bernecker & Weidlich 1990, 2005; Lauridsen *et al.* 2012; Lauridsen & Bjerager 2014). The formation consists of a number of different bryozoan and coral limestone facies (Lauridsen *et al.* 2012). The formation is exposed in the Faxø limestone quarry, Denmark, in the Limhamn quarry, Malmö, Southern Sweden, and has been encountered in several boreholes south of Faxø. The Baunekule facies

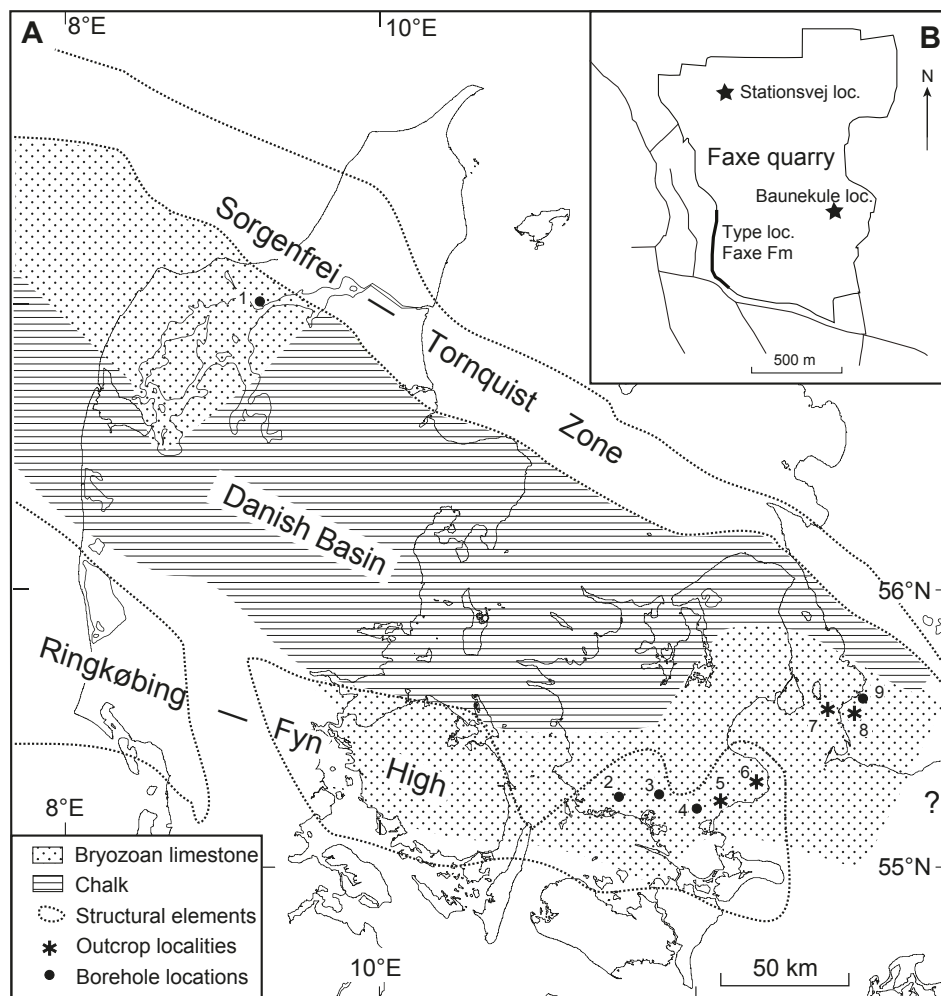


**Fig. 1.** A: Map of the Danish Basin with the main structural elements and distribution of middle Danian bryozoan limestone, including isolated coral mound complexes and chalk (coccolith Zone 5 of Thomsen 1995). Locations of selected outcrops and boreholes where middle Danian coral limestone have been encountered: 1, Aggersborggaard; 2, Spjellerup; 3, Herlufsholm; 4, Everdrup; 5, Faxø quarry; 6, Stevns Klint; 7, Flinterenden-Trindelenden, Øresund (both submarine outcrop and borings); 8, Limhamn quarry; 9, Malmö. B: Map of Faxø limestone quarry with the Baunekule facies localities and type section of the Faxø Formation indicated. Modified from Lauridsen & Bjerager (2014).

of Lauridsen *et al.* (2012) occurs in the upper part of the formation. It consists of non-consolidated coral rudstone to floatstone forming isolated, lensoidal bodies in the coral mound flanks. The facies contains a well-preserved high-diversity fauna of calcitic and originally aragonitic-shelled invertebrates. More than 300 species have been described from the facies, comprising more than 80% of the species from the Faxe Formation (Lauridsen & Bjerager 2014; Lauridsen & Schnetler 2014). The Baunekule facies is known from the east-central and north-western parts of the quarry (Fig. 1). Ravn (1903) described the facies for the first time; however, the section with this occurrence located in the centre of the quarry has been removed by quarrying. In the 1970s the facies was recorded from a locality in the east-central part below the road Stationsvej by Sten Lennart Jakobsen and Søren Bo Andersen, but this has now also been quarried away. In the 1990s a new occurrence of the Baunekule facies was exposed nearby (Lauridsen *et al.* 2012). Currently, the facies is not exposed in the quarry.

## Material and methods

The material studied in the present paper was collected by the late Alice Rasmussen in the beginning of the 1990s at the Stationsvej locality in the Faxe limestone

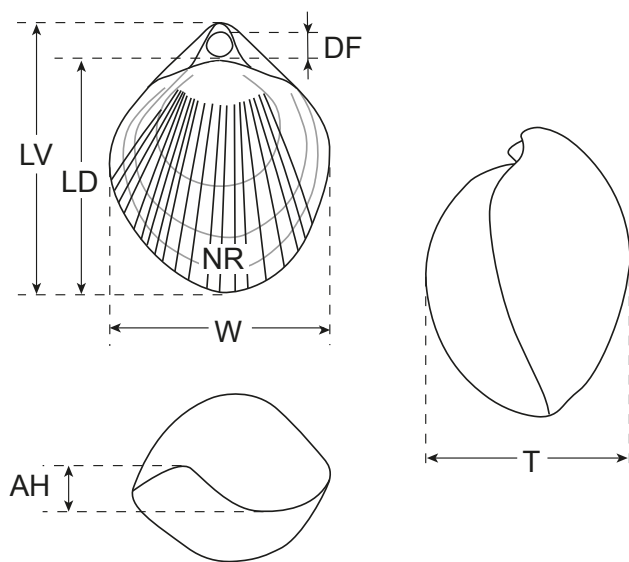


**Fig. 2.** Measured dimensions referred to in the text. LV: length of the ventral valve. LD: length of the dorsal valve. W: width. DF: diameter of the foramen. NR: number of ribs. T: thickness. AH: height of asymmetry. It is measured from the lowest to the highest point on the frontal commissure line on the anterior part of the specimen. AH is here shown on a sinistroasymmetric specimen.

quarry. More material was collected by the authors in the type section of the Faxe Formation in the western part of the quarry (Lauridsen *et al.* 2012). The samples are housed at Østsjællands Museum, Denmark. The material from the Baunekule facies comprises 2986 specimens with both dorsal and ventral valves intact, 12 ventral valves and 9 dorsal valves. The material from the type section alone comprises 940 specimens.

Bivariate regressions, Hotelling's  $T^2$  test and a principal component analysis (PCA) were undertaken in order to investigate if '*R.* *flustracea*' and '*R.* *faxensis*' represent two species or if they are conspecific. The statistical tests and PCA analysis are based on standard measurements commonly used in the descriptions of new brachiopod species (e.g. Steinich 1965; Surlyk 1970; Johansen 1987; see Fig. 2). Both inner and external morphologies have been assessed.

A total of 10 specimens from the Baunekule facies were attached by the ventral valve to a glass slide with UV hardening glue and opened manually using dissection needles to expose the inner morphology. The dimensions of the morphological features here are however, difficult to quantify due to poor preservation of the crura and overgrowth of calcite crystals, and no statistical tests were carried out on the inner morphology.

All individuals from the Baunekule facies were examined in terms of external symmetry/asymmetry expressed by the frontal commissure. Asymmetry on the commissure is either 'left-handed' or 'right-handed' and is expressed as a bend on the frontal commissure in anterior view, and is comparable to the period of a sine wave where one side is sloping upwards with respect to the other side. If the left side of the commissure, in anterior view with the ventral valve oriented downwards, slopes upwards with respect to the right side, it is referred to as 'sinistroasymmetry' (Fig. 2), and if the right side slopes upwards with respect to the left side, it is referred to as 'dextroasymmetry'.

A total of 48 complete specimens from the Baunekule facies were selected in order to quantify and compare the morphological variation. The morphological dimensions measured are defined in Fig. 2. AH is a morphological dimension that measures the degree of asymmetry. It is measured from the lowest to the highest point on the frontal commissure line on the anterior part of the specimen. Symmetrical individuals have an AH value of 0 mm. An asymmetrical individual has an AH value higher than 0 mm. A higher AH value thus equals a higher degree of asymmetry expressed by the frontal commissure.

Principal component analysis (PCA), Hotelling's  $T^2$  test and regressions were conducted using the PAST software package (Hammer *et al.* 2001; Hammer & Harper 2006; Hammer 2012).

Photographed specimens, with the exception of the designated lectotype, have been coated with ammonium chloride.

Abbreviations used: OESM – Østsjællands Museum; MB – Museum Für Naturkunde Leibniz-Institut Berlin.

## Results

Six of the opened specimens have their crura covered in calcitic crystals and it was not possible to determine the type of crura or hinge. However, four specimens have intact and well-preserved hinges and crura,

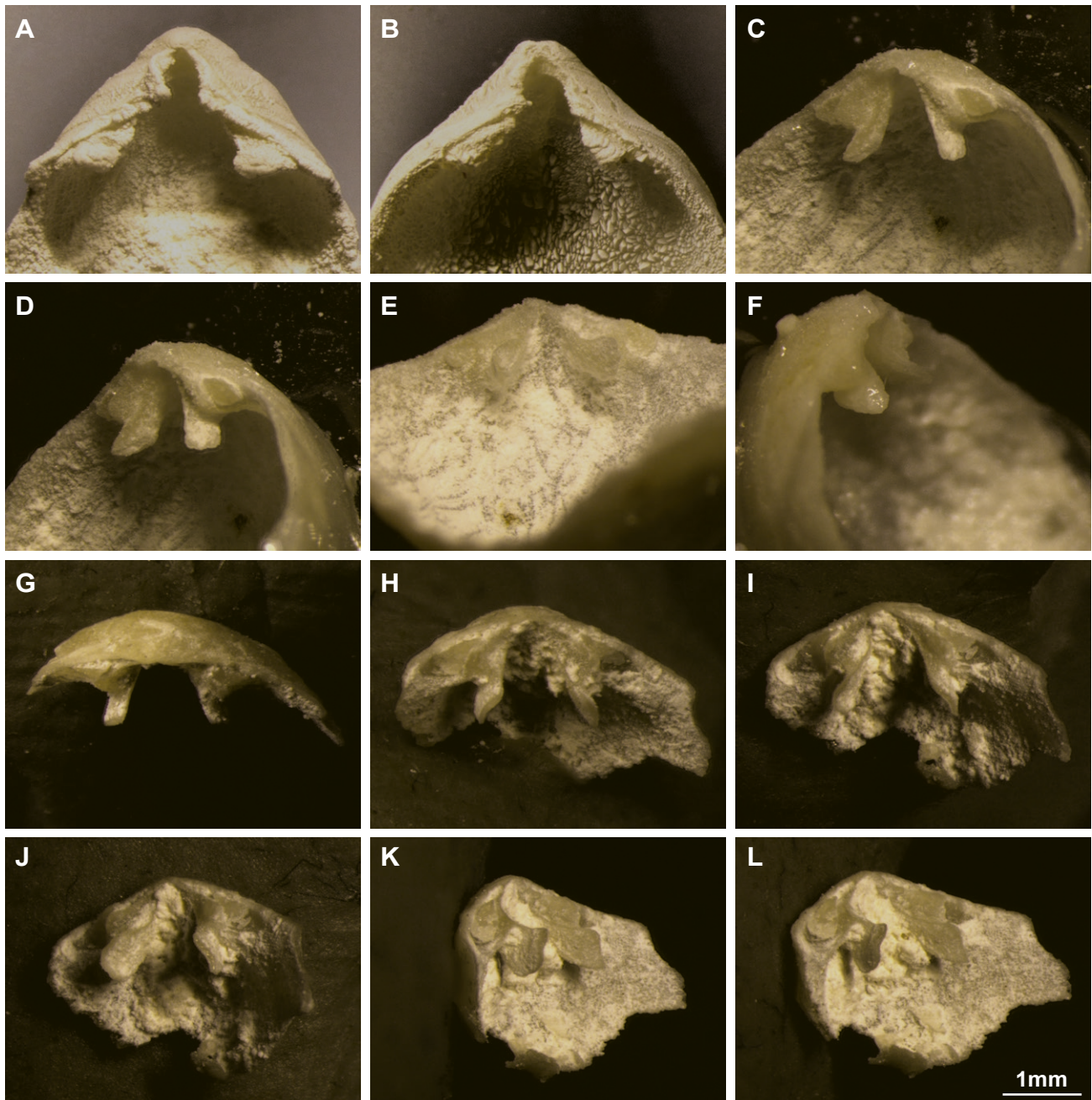


**Fig. 3.** Internal structures of *Obliquorhynchia flustracea* (von Buch 1834). The new genus *Obliquorhynchia* is erected in this paper. **A:** Hingeline with thick, robust, triangular hinge teeth, OESM-10064-0116. **B:** Hingeline with thick, robust, triangular hinge teeth, OESM-10064-0117. **C–F:** Ventral, dorso-ventral, posterior and lateral view of crura, OESM-10064-0118. **G–L:** Ventral, posterior-ventral, tilted posterior-ventral, ventro-lateral and tilted ventral and ventro-lateral view, OESM-10064-0119. The external morphology of specimens reflects the characteristics formerly used to describe and distinguish '*R.*' *flustracea* (von Buch 1834) (A and C–F) and '*R.*' *faxensis* (Posselt 1894) (B and G–L). Scale bar = 1 mm for all pictures.

allowing them to be referred to subfamily level. The specimens reflect the morphology used as characteristic of *'R.' flustracea* and *'R.' faxensis* respectively. The type of hinge and crura is the same in both types (Fig. 3).

The morphological variations between *'R.' flustracea* and *'R.' faxensis* were quantified and compared based on 48 specimens. Of these specimens, 38 were picked at random among both adults and juveniles in the different symmetry groupings: adults were subdivided into sinistroasymmetric, dextroasymmetric, uniplicate, rectimarginate and 'peculiar' asymmetric, whereas juvenile specimens were subdivided into sinistroasymmetric, dextroasymmetric and rectimarginate. The remaining 10 specimens were picked at random from 89 specimens. These specimens exhibit traits characteristic of *'R.' faxensis* and are all asymmetric.

The frontal commissure is rectimarginate, uniplicate, sinistroasymmetric or dextroasymmetric. There is a higher frequency of commissural asymmetry in adult individuals (58.7%) compared to juveniles (8.8%) and there is a lower frequency of adults exhibiting a

rectimarginate commissure (8.5%) compared to juveniles (16.5%) (Fig. 4A). Only 4.5% of the specimens exhibit uniplication of the frontal commissure. A few of the adult specimens (2%) display a different form of asymmetry which cannot be ascribed to any of the aforementioned forms. Asymmetry is still present, but in contrast to sinistro- and dextroasymmetry, this asymmetry is most conspicuous in brachial and ventral views, with only little asymmetry expressed by the frontal commissure. This form is regarded as 'peculiar' asymmetry, only observed in adult specimens (Fig. 4A, Fig. 5A–C).

Bivariate linear regressions, RMA algorithm, on LV/LD, LV/W and LV/AH were applied in order to test whether there is a correlation between the morphological measurements of *'R.' flustracea* and *'R.' faxensis*. The fitted line in the scatter plot of LV/LD is  $y = 0.8679x - 0.0249$  ( $Tn-2 = 76.00$ ,  $t = 2.00$ ,  $P < 0.05$ ) (Fig. 4B). The fitted line in the scatter plot of LV/W is  $y = 0.9253x - 0.4434$  ( $Tn-2 = 28.87$ ,  $t = 2.00$ ,  $P < 0.05$ ) (Fig. 4C). In the scatter plot of LV/AH the data are fitted to an exponential function by log transformation:  $y = 0.0222e^{0.4712x}$  ( $Tn-2 = 14.71$ ,  $t = 2.045$ ,  $P < 0.05$ ) (Fig.

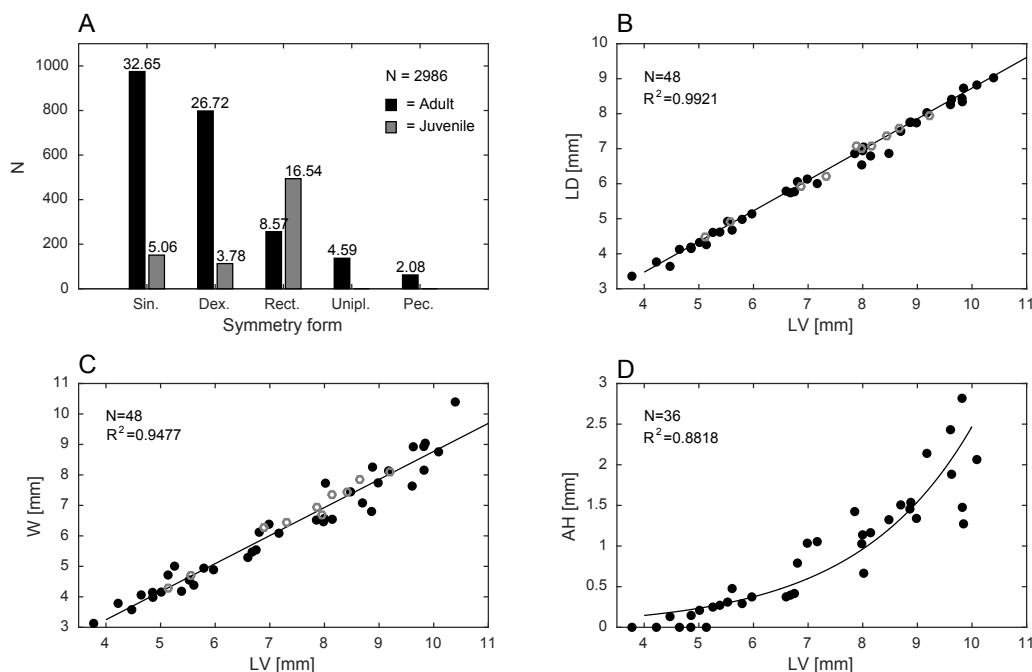


**Fig. 4. A:** Histogram showing the distribution of specimens according to symmetry/asymmetry expressed by the frontal commissure. Adult: black, juvenile: grey, N: number of specimens, Sin.: sinistroasymmetry, Dex.: dextroasymmetry, Rect.: rectimarginate, Unipl.: uniplicate, Pec.: peculiar. Values above each column show the distribution of specimens in percentage of the total sample size of 2986 specimens. **B–D:** Scatter diagrams plotting with regression lines, showing intraspecific variability of *Obliquorhynchia flustracea* (von Buch 1834), r: correlation coefficient, N: number of specimens, black filled dots are specimens exhibiting traits of both *'R.' flustracea* (von Buch 1834) and *'R.' faxensis* (Posselt 1894), grey open circles exhibit traits with closer resemblance to *'R.' faxensis* (Posselt 1894). Both types of specimen are used in calculation of regression lines and level of significance. **B:** LV/LD: length of ventral valve plotted against length of dorsal valve. **C:** LV/W: length of ventral valve plotted against width. **D:** LV/AH: length of ventral valve plotted against height of asymmetry. The onset of asymmetry is established when the specimen has reached a length (LV) between 4 and 6 mm.

4D). Only the data where AH > 0 mm are included in the exponential model (N = 31). All three plots show significant correlation between the morphological dimensions, indicating that '*R.* *flustracea*' and '*R.* *faxensis*' belong to the same species.

Juvenile shells appear smooth, but ribs are visible when the specimens are coated in ammonium chloride, normally in the form of weakly developed striate or finely capillate costae. Some adults and juvenile specimens with apparently smooth shell surfaces are recognised even when coated. This is due to diagenetic dissolution of the outer layer of the calcitic shell, thus causing the shell surface to appear smooth (Fig. 5B). The number of ribs (NR) varies from 7 to 49 measured on the ventral valve. NR has not been included in the statistical analyses due to this variability and differences in preservation of the external layer of the calcitic shell. The measurements of thickness (T) are not normally distributed and are excluded from the analyses.

Principal component analysis (PCA) and Hotelling's  $T^2$  test were conducted on 10 specimens exhibiting traits characteristic of '*R.* *flustracea*' (5 sinistro- and 5 dextroasymmetric), and 10 specimens exhibiting traits characteristic of '*R.* *faxensis*' (5 sinistro- and 5 dextroasymmetric) (Fig. 6). The characteristics are very subtle and only confined to the external shell morphology. In most instances, it is impossible to distinguish specimens based on the description of Posselt (1894), since there is a gradual transition between '*R.* *faxensis*' and '*R.* *flustracea*' (Fig. 5D). The specimens used are those showing the largest differences in external morphology. The PCA analysis (multivariate normality  $E_p = 10.48$  and  $p = 0.39 > 0.05$ ) of '*R.* *flustracea*', illustrates that all of the *faxensis* population falls within the 95% confidence ellipse describing the '*R.* *flustracea*' population, indicating they belong to the same species. The PC1 component or axis is interpreted as a size axis: All five variables, AH, DF, LV, LD, W tilt more or less towards the right, illustrating that they increase in value

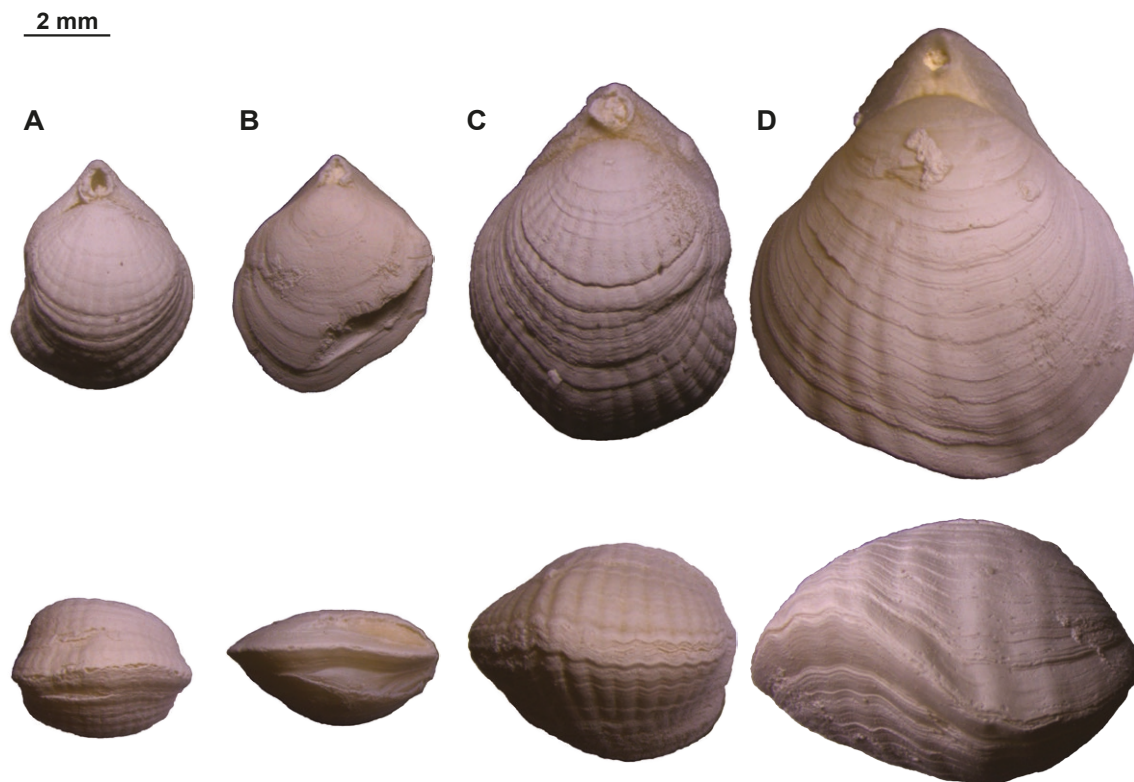


**Fig. 5.** *Obliquorhynchia flustracea* (von Buch 1834). All specimens are from the Baunekule facies, Faxe Formation. Each specimen is shown in dorsal and frontal view. **A–C** are examples of peculiar asymmetry. **A:** An asymmetric specimen where the asymmetry affects especially the left side of both valves, OESM-10064-0112. **B:** A specimen with no visible ribs, caused by diagenetic dissolution of the outer layer of the calcitic shell, with asymmetry affecting the right and anterior part of both valves, OESM-10064-0113. **C:** A specimen with asymmetry affecting the right side of both valves and the frontal commissure, OESM-10064-0114. **D:** A strongly sinistroasymmetric specimen, but with few and flattened costae and an extremely small foramen with no significant pedicle collar development compared to the size of specimen, transitional between '*R.* *faxensis*' and '*R.* *flustracea*' OESM-10064-0115. Scale bar = 2 mm.

with higher scores on PC1. PC2 is interpreted as an asymmetry/width difference axis as indicated by the upward-directed AH vector (Fig. 6). Thus, specimens with high scores on this axis are more asymmetric, longer and narrower, whereas specimens with lower scores are wider, shorter and less asymmetric. PC1 represents 95.7 % of the total variance and PC2 3.1 %. Variance-covariance matrix was used for the PCA plot. The Hotelling's  $T^2$  test, which is a multivariate analogue to the  $t$  test, calculates the probability  $p = 0.12$  (Box'  $M = 27.9$  and  $p = 0.18$   $p > 0.05$ ), indicating that the two species show no significant difference based on the five selected variables.

## Systematic palaeontology

Phylum Brachiopoda Duméril 1806

Subphylum Rhynchonelliformea Williams, Carlson, Brunton, Holmer & Popov 1996

Class Rhynchonellata Williams, Carlson, Brunton, Holmer & Popov 1996

Order Rhynchonellida Kuhn 1949

Superfamily Pugnacoidea Rzhonsnitskaia 1956

Family Basiliolidae Cooper 1959

Subfamily Basiliolinae Cooper 1959

*Obliquorhynchia* gen. nov.

*Lectotype.* *Terebratula flustracea* MB.B.9116.1, original from the collection of von Schlotheim (1832, cat. 65 no 62), described by von Buch (1834, p. 63); here designated as lectotype and illustrated in Fig. 7A–D.

*Derivation of name.* From latin 'obliquus' meaning 'sloping' and 'rhynchia' as the genus belongs to the order Rhynchonellida.

*Diagnosis.* Small subtriangular to rounded-subpentagonal in outline; greatest width about mid valve; globose subequibiconvex to dorsibiconvex; shell surface finely capillate to costellate; frontal commissure varies from rectimarginate, strongly asymmetric to occasionally broadly uniplicate; beak short, erect or suberect; foramen small, circular, submesothyrid; pedicle collar well-developed; deltidial plates small, conjunct, auriculate; ventral valve with thick, triangular hinge teeth; widely spaced crura, widening anteriorly with inner surface concave and outer surface strongly convex, hamiform; outer hinge plate narrow, no inner hinge plate; dorsal valve without median septum or median ridge.

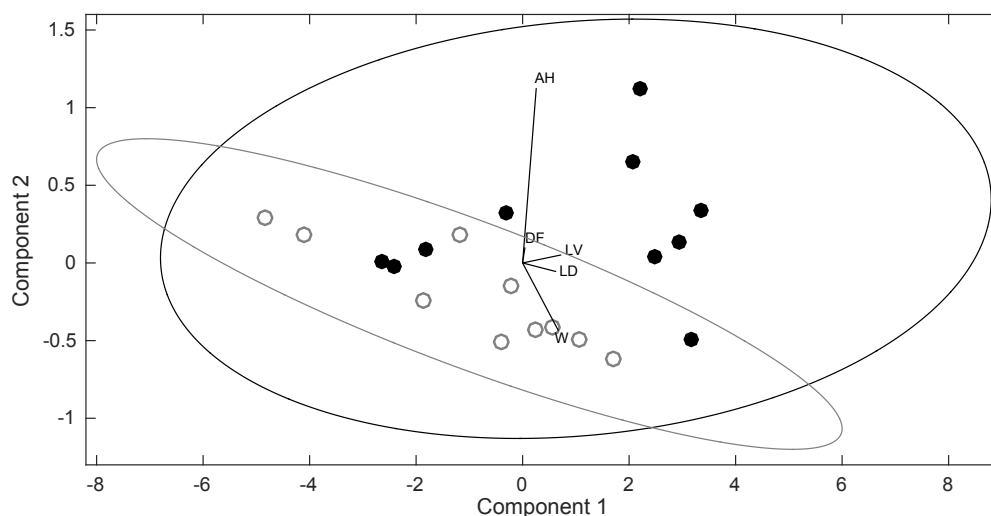


**Fig. 6.** Principal component analysis (PCA) of measured dimensions LV, LD, W, DF and AH of *Obliquorhynchia flustracea* (von Buch 1834). Ten specimens exhibiting traits characteristic of '*R.* *flustracea*' (von Buch 1834) (5 sinistro- and 5 dextroasymmetric), and 10 specimens exhibiting traits characteristic of '*R.* *faxensis*' (Posselt 1894) (5 sinistro- and 5 dextroasymmetric). A plot of scores and loadings on PC1 and PC2 of the species is shown together with the 95% confidence ellipses. Black filled dots: '*R.* *flustracea*' (von Buch 1834). Grey open dots: '*R.* *faxensis*' (Posselt 1894). Axis PC1 is interpreted as being controlled mainly by size, while PC2 is affected primarily by asymmetry (AH) and width (W).

*Remarks on the diagnosis.* The type of crura is one of the most important characters when defining the affinity to superfamilies in the revised classification of the order Rhynchonellida used in the Treatise on Invertebrate Paleontology, part H, volume 4 (Savage *et al.* 2002a). The type of crura of this taxon was previously misidentified as raduliform (Asgaard 1968) which would group it as a genus under the superfamily Rhynchonelloidea (Owen & Manceñido 2002). The crura are in fact hamiform and not raduliform. The absence of a median septum and a cardinal process places the taxon in the superfamily Pugnacoidea, family Basiliolidae (Savage *et al.* 2002b). These features and the occurrence of asymmetry place the taxon in the subfamily Basiliolinae. The material differs from the existing basiliolid genera in this subfamily in having hamiform crura together with a larger number of and finer ribs and predominantly strong asymmetry, justifying the erection of the new genus *Obliquorhynchia*.

***Obliquorhynchia flustracea* (von Buch 1834)**

Fig. 3, Fig. 5, Fig. 7, Fig. 8

1832 *Terebratula lustraceus*, von Schlotheim, catalogue 65, no 62 (*nomen nudum*)

1834 *Terebratula flustracea*, von Buch, p. 63

1834 *Terebratula flustracea*, Leonhard & Bronn, p. 619, 623

1835 *Terebratula flustracea*, von Buch, p. 83

1848 *Rhynchonella danica*, d'Orbigny, p. 295

1866 *Terebratula flustracea*, Fischer-Benzon, p. 17

1885 *Rhynchonella flustracea*, Lundgren, p. 39, pl. 1 fig. 35–37

1894 *Rhynchonella flustracea*, Posselt, p. 31–32 pl. 2 fig. 1–3

1894 *Rhynchonella faxensis*, Posselt, p. 30–31 pl. 2 fig. 4–9

1909 *Rhynchonella flustracea*, Nielsen, p. 158

1968 '*Rhynchonella*' *flustracea*, Asgaard, p. 110 fig. 4

1968 '*Rhynchonella*' *faxensis*, Asgaard, p. 112 fig. 5

1970 '*Rhynchonella*' *flustracea*, Asgaard, p. 363

1987 '*Rhynchonella*' *faxensis*, Meyer, pl. 8 fig. 6–10

2008 '*Rhynchonella*' *flustracea*, Dulai *et al.*, p. 199–200

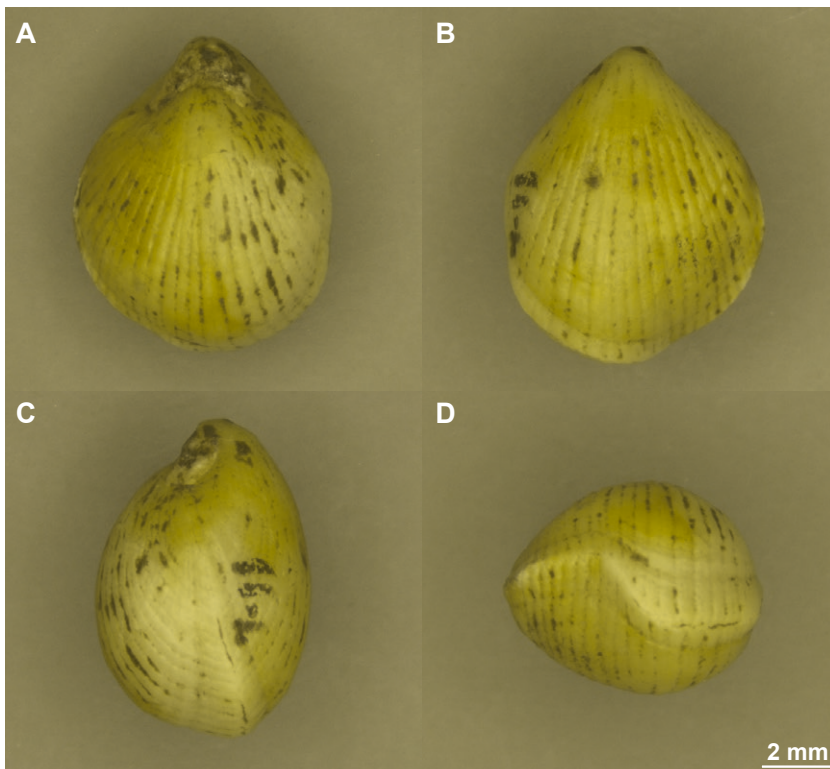


**Fig. 7. A–D:** Dorsal, ventral, lateral and anterior view of the lectotype of *Obliquorhynchia flustracea* (von Buch 1834), MB.B.9116.1. Scale bar = 2 mm.

2008 '*Rhynchonella faxensis*, Dulai *et al.*, p. 200

2010 '*Rhynchonella flustracea*, Motchurova-Dekova & Harper, p. 109–117, fig. 3–4

2012 '*Rhynchonella flustracea*, Lauridsen *et al.*, fig. 10A

2012 '*Rhynchonella faxensis*, Lauridsen *et al.*, fig. 10J

*Lectotype.* *Terebratula flustracea* MB.B.9116.1, original from the collection of von Schlotheim (1832, cat. 65 no 62) described by von Buch (1834, p. 63); here designated as lectotype and illustrated in Fig. 7A–D.

*Material.* The material was collected by Alice Rasmussen at the Stationsvej locality where the Baunekule facies was exposed in the 1990s. It is housed at Østsjællands Museum, Denmark. The material of von Schlotheim was collected from coral limestones in the Faxe limestone quarry. The samples are housed at the Museum Für Naturkunde, Berlin, Germany.

*Stratigraphical age.* Middle Danian.

*Occurrence.* *Obliquorhynchia flustracea* (von Buch 1834) is known from the middle Danian Faxe Formation, Faxe limestone quarry in Denmark (von Buch 1834, 1835; Posselt 1894; Nielsen 1909; Asgaard 1968, 1970; Lauridsen *et al.* 2012), Annetorp in south-west Sweden (Lundgren 1885), and the Vigny Formation, France (Meyer 1987). It is only found in association with the scleractinian coral *Dendrophyllia candelabrum*.

*Diagnosis.* As for the genus.

*Description, external characters.* Shell relatively small, the adult shell reaches a length of 5–11 mm, measured at the ventral valve. Subpentagonal in outline and rounded anteriorly. Shell varies from globose sub-equibiconvex to dorsibiconvex. Juvenile specimens mainly symmetrical subtriangular to subpentagonal in outline in both dorsal and ventral view. Most adults exhibit strong commissural asymmetry which affects the overall shape of the individual in dorsal, ventral and frontal views. Frontal commissure either rectimarginate, strongly sinistral or dextroasymmetric, occasionally broadly uniplicate. In some specimens that exhibit uniplication the sulcus is shifted towards either right or left in frontal view. Such specimens are considered dextro- or sinistral asymmetric or transitional between uniplicate and asymmetric. Maximum width anterior to the midline of the shell. Presence and form of ribs varies greatly between both individuals and growth stages. In juveniles, ribs are striate or finely capillate. In adults, ribs are normally

present in the form of stronger costae. Uniplicate specimens generally have fewer ribs, taking the form as broader and rounded costae, in some cases only recognisable in the sulcus. Number of ribs varies from 7 to 49 measured on the ventral valve. Ribs begin in the umbonal region but are more pronounced at the anterior margin. The number of ribs is greatest along the margin, due to intercalation. Faint growth lines are present in older growth stages. Specimens exhibiting sinistral- or dextroasymmetry show positive, exponential correlation between size of individuals (LV) and degree of asymmetry (AH) (Fig. 4D, Fig. 8). Beak suberect to erect in adults. Deltidial plates small and separated, auriculate in juveniles and conjunct in adults. During ontogenesis the foramen changes from triangular hypothyrid to circular submesothyrid with a well-developed pedicle collar.

*Description, internal characters.* Ventral valve has thick, robust, triangular hinge teeth. Outer hinge plates narrow and without inner hinge plates. Dorsal valve has widely spaced hamiform crura, with inner surface concave and outer surface strongly convex, widening to anteriorly almost spatulate in dorsoventral view (Fig. 3). Dorsal valve has no median septum or median ridge.

*Remarks.* The name of the species was proposed by von Schlotheim in *Systematisches Verzeichniss der Petrefacten-Sammlung des verstorbenen wirklichen Geheimen Raths* under the species name *lustraceus* (1832, catalogue 65, no 62). This is a catalogue of von Schlotheim's manuscript names and collections. It includes no illustrations or species descriptions. The species name and a description were published by von Buch (1834, 1835), but the species name was changed to *flustracea*, with reference to the nine specimens in the collection of von Schlotheim. Von Buch did not include an illustration of the species in this or any later works (1834, 1835, 1840). Neither von Schlotheim nor von Buch designated a holotype and there are no illustrations found in any of the earlier works of von Schlotheim, such as *Die Petrefactenkunde auf ihrem jetzigen Standpunkte durch die Beschreibung seiner Sammlung versteinertes und fossiler Überreste des Thier- und Pflanzenreichs* (1820) or *Beiträge zur Naturgeschichte der Versteinerungen in geognostischer Hinsicht* (1813, 1822). Von Schlotheim has been cited as author of the species name *flustracea*, even though it is von Buch (1834, 1835) who actually published the description under the name *flustracea* and not *lustraceus* which was the manuscript name originally proposed by von Schlotheim. The species name *lustraceus* is thus considered a *nomen nudum*. The lack of illustration in von Buch's (1834) description could pose a problem of the validity of the name. However, he cited the col-

lection of von Schlotheim of nine syntype specimens instead. This collection (MB.B.9116.1–9) still exists and is accessible at the Museum für Naturkunde in Berlin. The species is thus ascribed to von Buch (1834) (see Art. 50 and 51 of ICZN 1999). After the designation of a lectotype herein, the collection no longer consists of nine syntypes, but of one lectotype and eight paralectotypes. Of the now eight paralectotypes of

*Obliquorhynchia flustracea* (MB.B.9116.2–9) one specimen actually possesses the characteristics e.g. fewer number of ribs and uniplication that Posselt (1894) used in his description of '*R.* *faxensis*'. He included an illustration but did not designate a holotype and never referred to a specific collection or a set of syntypes. '*R.* *faxensis*' is thus considered a junior synonym of *Obliquorhynchia flustracea* (see. Art 11 of ICZN 1999).

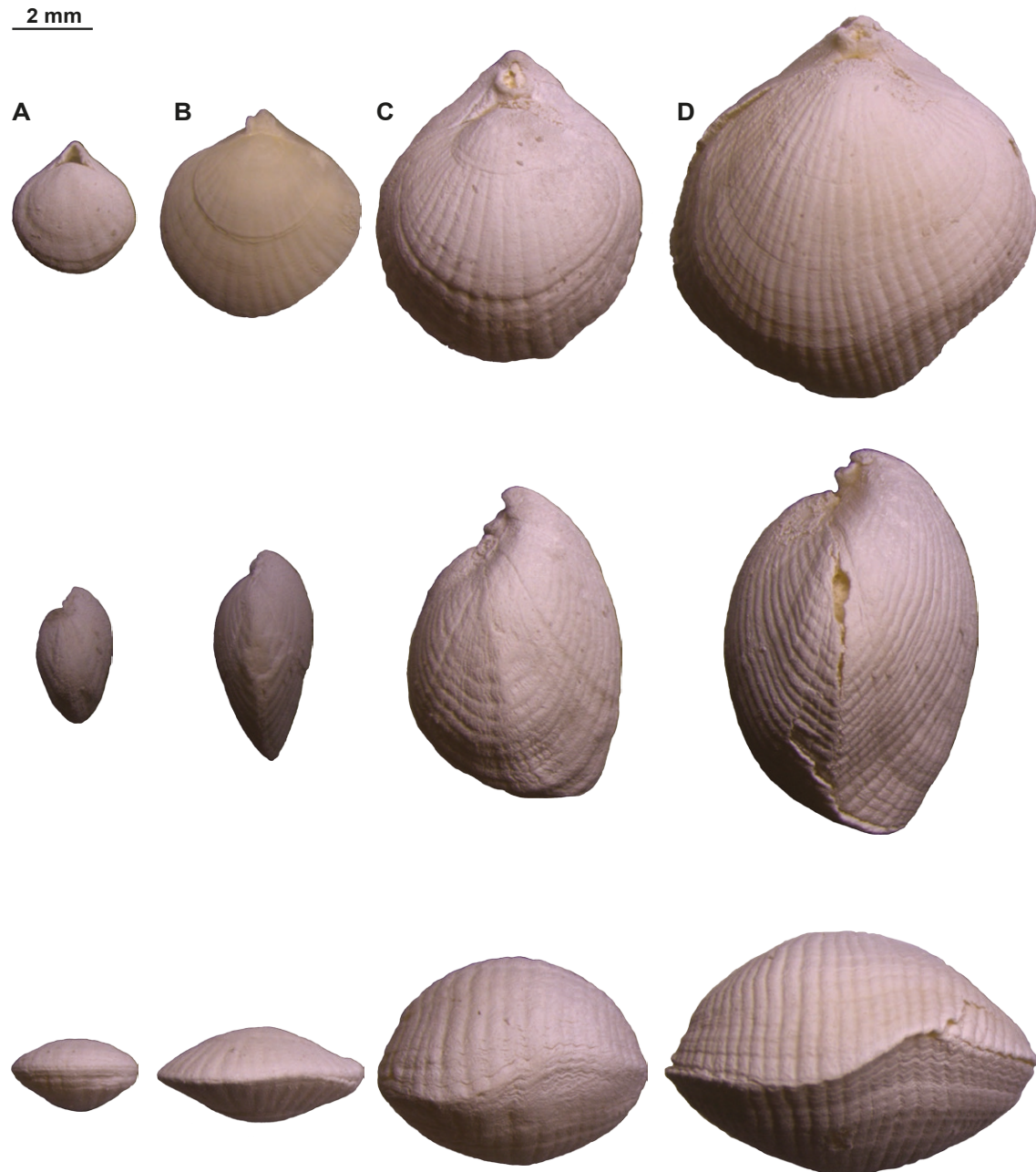


**Fig. 8.** *Obliquorhynchia flustracea* (von Buch 1834). All specimens are from the Baunekule facies, Faxse Formation, Faxse limestone quarry. Each specimen is shown in dorsal, lateral and frontal view. **A:** Symmetrical specimen with a rectimarginate commissure line and with few and capillate ribs, OESM-10064-0111. **B:** Specimen with incipient dextrosymmetry noticeable in brachial and frontal view, OESM-10064-0078. **C:** Specimen with developed dextrosymmetry that is evident in all views, OESM-10064-0073. **D:** Strongly dextrosymmetric specimen, OESM-10064-0110. Scale bar = 2 mm.

## Conclusions

The external morphology of *Obliquorhynchia flustracea* (von Buch 1834) is extremely variable. The original characteristics used to distinguish 'R.' *flustracea* (von Buch 1834) and 'R.' *faxensis* (Posselt 1894) are exclusively confined to minor details in the external morphology. In the literature, there has been a tendency to refer to 'R.' *flustracea* as the 'asymmetric' species and 'R.' *faxensis* as the 'symmetric, uniplicate' species. However, both von Buch (1834, 1835) and Posselt (1894) stated that 'R.' *flustracea* had an extremely variable morphology and may commonly be asymmetric, but also symmetric specimens have been encountered.

Frequency distributions of specimens from the Baunekule facies show a prevalence of commissural asymmetry in adults. Together with the correlation between LV and AH and the onset of asymmetry there seems to be a correlation between ontogenetic development and degree of asymmetry.

The bivariate regressions show that there is a significant positive correlation between the morphometric dimensions when both types are included. The principal component analysis (PCA) and Hotelling's  $T^2$  test show that there might be differences between specimens, but these are not significant, indicating, together with the regressions, that 'R.' *flustracea* and 'R.' *faxensis* are conspecific. The descriptions and illustrations of Posselt (1894) and Asgaard (1968) rather seem to reflect end members and differences in ontogenetic development of *Obliquorhynchia flustracea* (von Buch 1834) than two separate species.

## Acknowledgements

The studied material from the Baunekule facies was carefully collected and kindly placed at our disposal by the late Alice Rasmussen (Faxe). We wish to thank Arne Thorshøj Nielsen (Department of Geosciences and Natural Resource Management, University of Copenhagen) and Jan Audun Rasmussen (Museum Mors, Denmark) for fruitful discussions on taxonomic issues and statistics. Martin Aberhan and Carsten Lüter are thanked for their great help concerning the collection of von Schlotheim and use of microscope in Berlin, Museum für Naturkunde, Leibniz Institute for Evolution and Biodiversity Science. Jesper Milàn (Østsjællands Museum) is thanked for help regarding the registration of the material of Alice Rasmussen when it was donated to Østsjællands Museum. AES wishes to thank Østsjællands Museum for financial support, which made possible a short stay in Berlin,

Museum für Naturkunde, Leibniz Institute for Evolution and Biodiversity Science. We are grateful to Jan Audun Rasmussen (Museum Mors, Denmark) and Attila Vörös (Hungarian Natural History Museum) for useful reviews.

## References

- Afanasjeva, G.A. 2014: Asymmetry in brachiopods. *Paleontological Journal* 48, 11, 1207–1214.
- Ager, D.V. 1965: The adaptation of Mesozoic brachiopods to different environments. *Palaeogeography, Palaeoclimatology, Palaeoecology* 1, 143–172.
- Ager, D.V. 1967: Brachiopod palaeoecology. *Earth-Science Reviews* 3, 157–179.
- Asgaard, U. 1968: Brachiopod palaeoecology in the Middle Danian Limestones at Fakse, Denmark. *Lethaia* 1, 103–121.
- Asgaard, U. 1970: The syntypes of *Carneithyris incisa*. *Bulletin of the Geological Society of Denmark* 19, 361–367.
- Atkins, D. 1959: The growth stages of the lophophore of the brachiopods *Platidia davidsoni* (Eudes Deslongchamps) and *P. anomioides* (Philippi) with notes of the feeding mechanism. *Journal of the Marine Biological Association of the UK* 38, 103–133.
- Atkins, D. 1960: A new species and genus of Brachiopoda from Western Approaches, and the growth stages of the lophophore. *Journal of the Marine Biological Association of the UK* 39, 71–89.
- Atkins, D. 1961: The growth stages and adult structure of the lophophore of the brachiopods *Megerlia truncata* (Linnaeus) and *M. echinata* (Fischer and Oehlert). *Journal of the Marine Biological Association of the UK* 41, 95–111.
- Bernecker, M. & Weidlich, O. 1990: The Danian (Paleocene) coral limestone of Fakse, Denmark: a model of ancient aphotic, axooxanthellate coral mounds. *Facies* 22, 103–138.
- Bernecker, M. & Weidlich, O. 2005: Azooxanthellate corals in the Late Maastrichtian – Early Paleocene of the Danish basin: bryozoan and coral mounds in a boreal shelf setting. In Freiwald, A. & Roberts, J. M. (eds.): *Cold-water corals and ecosystems*, 3–25. Springer-Verlag, Berlin and Heidelberg.
- d'Orbigny, A.D. 1848: *Prodrome de Paléontologie stratigraphique universelle des animaux mollusques & rayonnés, faisant suite au Cours élémentaire de paléontologie et de géologie stratigraphiques*. 2. Victor Masson (eds.), Paris, p. 295.
- Dulai, A., Bitner, M.A. & Müller, P. 2008: A monospecific assemblage of a new rhynchonellide brachiopod from the Paleocene of Austria. *Fossils and Strata* 54, 193–201.
- Elliott, G.F. 1948: The evolutionary significance of brachial development in terebratelloid brachiopods. *The Annals and Magazine of Natural History* 5, 297–317.
- Elliott, G.F. 1958: An abnormal lophophore in *Macandrevia* (Brachiopoda). *Publications from the Biological Station, Esppegrend*, 21, *Årbok for Universitetet i Bergen, Naturvitenskapelig rekke* 2, 3–6.

- Fischer-Benzon, R.V. 1866: Ueber das relative Alter des Faxoe-Kalkes und über die in demselben vorkommenden Anomuren und Brachyuren. Schwers'sche Buchhandlung, 1–30.
- Floris, S. 1980: The coral banks of the Danian of Denmark. *Acta Palaeontologica Polonica* 25, 531–540.
- Freiwald, A., Hühnerbach, V., Lindberg, B., Wilson, J.B. & Campbell, J. 2002: The Sula Reef complex, Norwegian Shelf. *Facies* 47, 179–200.
- Freiwald, A., Fossa, J.H., Grehan, A., Koslow, T. & Roberts, J.M. 2004: Cold-water coral reefs. Out of sight – no longer out of mind. United Nations Environment Programme–World Conservation Monitoring Centre Biodiversity Series 22. UNEP-WCMC. Cambridge, UK. 86 pp.
- Fürsich F.T. & Palmer, T. 1984: Commissural asymmetry in brachiopods. *Lethaia* 4, 17, 251–265.
- Hammer, Ø. 2012: PAST: Reference manual version 2.17. <http://folk.uio.no/ohammer/past/>.
- Hammer, Ø. & Harper, D. 2006: *Paleontological Data Analysis*, 351 pp. Blackwell Publishing, Oxford.
- Hammer, Ø., Harper, D.A.T. & Ryan, P.D. 2001: PAST: Paleontological statistics software package for education and data analysis. *Palaeontologia Electronica* 4, 1, 9 pp. [http://palaeo-electronica.org/2001\\_1/past/issue1\\_01.htm](http://palaeo-electronica.org/2001_1/past/issue1_01.htm)
- Hennig, A. 1899: Studier öfver den baltiska Yngre kritans bildningshistoria. *Geologiska Föreningens i Stockholm Förhandlingar* 21, 19–82 and 133–188.
- Henry, L.A. & Roberts, J.M. 2007: Biodiversity and ecological composition of macrobenthos on cold-water coral mounds and adjacent off-mound habitat in the bathyal Porcupine Seabight, NE Atlantic. *Deep-Sea Research* 1, 54, 654–672.
- ICZN, 1999: *International Code of Zoological Nomenclature*. Fourth edition, 306 pp. The International Trust for Zoological Nomenclature, London.
- Johansen, M.B. 1987: Brachiopods from the Maastrichtian–Danian boundary sequence at Nye Kløv, Jylland, Denmark. *Fossils and Strata* 20, 1–99.
- Lauridsen, B.W., Bjerager, M. & Surlyk, F. 2012: The middle Danian Faxø Formation – a new lithostratigraphic unit and a rare taphonomic window into the Danian of Denmark. *Bulletin of the Geological Society of Denmark* 60, 47–60.
- Lauridsen, B.W. & Bjerager, M. 2014: Danian cold-water corals from the Baunekule facies, Faxø Formation, Denmark: a rare taphonomic window of coral mound flank habitat. *Lethaia* 47, 4, 437–455.
- Lauridsen, B.W. & Schnetler, K.I. 2015: A catalogue of Danian gastropods from the Baunekule facies, Faxø Formation, Denmark. *Geological Survey of Denmark and Greenland Bulletin* 32, 117 pp.
- Leonhard, K.C. & Bronn, H.G. 1834: *Neues Jahrbuch für Mineralogie, Geognosie, Geologie und Petrefaktenkunde*, 735 pp. Stuttgart, E. Schweizerbart's Verlagshandlung.
- Lundgren, B. 1885: Undersökningar öfver Brachiopoderna i Sverges Kritsystem, 1–72. Fr. Berlings Boktryckeri och Stilgjuteri.
- Lyell, C. 1837: On the Cretaceous and Tertiary Strata of the Danish Islands of Seeland and Moen. *Transactions of the Geological Society of London* 6, 243–257.
- Motchurova-Dekova, N. & Harper, D.A.T. 2010: Synchrotron radiation X-ray tomographic microscopy (SRXTM) of brachiopod shell interiors for taxonomy: preliminary report. *Annales géologiques de la péninsule Balkanique* 71, 109–117.
- Meyer J.C. 1987: Le récif danien de Vigny. *Saga informations* 26, 1–72.
- Nielsen, K.B. 1909: Brachiopoderne i Danmarks Kridtaflejringer. *Det Kongelige Danske Videnskabernes Selskabs Skrifter*, 7. Række, Naturvidenskabelig og Mathematisk Afdeling 4, 4, 127–178.
- Nielsen, K.B. 1922: Zoantharia from Senone and Paleocene Deposits in Denmark and Skaane. *Det Kongelige Danske Videnskabernes Selskabs Skrifter*, 8. Række, Naturvidenskabelig og Mathematisk Afdeling 5, 3, 199–233.
- Owen, E.F. & Manceñido, M. O. 2002: Rhynchonelloidea. In: R.L. Kaesler (ed.), *Treatise on Invertebrate Paleontology, Part H, Brachiopoda (revised)*, Volume 4, Geological Society of America and University of Kansas, Boulder, Colorado & Lawrence, Kansas, 1279–1308.
- Posselt, H.J. 1894: Brachiopoderne i den danske Kridtformation. *Danmarks Geologiske Undersøgelse II, Række 4*, 59 pp.
- Ravn, J.P.J. 1903: Molluskerne i Danmarks Kridtaflejringer. III Stratigrafiske Undersøgelser. *Det Kongelige Danske Videnskabernes Selskabs Skrifter* 6. Række, Naturvidenskabelig og Mathematisk Afdeling 11, 6, 335–446.
- Rózycki, S.Z. 1948: Remarks about Upper Jurassic Rhynchonellidae of the Cracow-Czestochowa Chain. *Bulletin du Service géologique de Pologne* 42, 16–40.
- Savage, N.M., Manceñido, M.O., Owen, E.F., Carlson, S.J., Grant, R.E., Dagys, A.S. & Dong-Li, S. 2002a: Rhynchonellida. In: R.L. Kaesler (ed.), *Treatise on Invertebrate Paleontology, Part H, Brachiopoda (revised)*, Volume 4, 1027–1376. Geological Society of America & University of Kansas Press, Boulder, Colorado & Lawrence, Kansas.
- Savage, N.M., Manceñido, M.O., Owen, E.F. & Dagys, A.S. 2002b: Pugnacoidea. In: Kaesler, R.L. (ed.): *Treatise on Invertebrate Paleontology, Part H, Brachiopoda (revised)*, Volume 4, 1165–1218. Geological Society of America & University of Kansas Press, Boulder, Colorado & Lawrence, Kansas.
- Steinich, G. 1965: Die artikulaten Brachiopoden aus der Rüggener Schreibkreide (Unter-Maastricht). *Paläontologische Abhandlungen* 2, 1, 1–220.
- Surlyk, F. 1970: Two new brachiopods from the Danish White Chalk (Maastrichtian). *Bulletin of the Geological Society of Denmark* 20, 152–161.
- von Buch, L. 1834: Ueber Terebrateln, mit einem Versuch, sie zu classificiren und zu beschreiben. Gedruckt in der Druckerei der Königlichen Akademie der Wissenschaften, 124 pp.
- von Buch, L. 1835: Ueber Terebrateln. *Abhandlungen der Königlichen Akademie der Wissenschaften zu Berlin, Physikalische Klasse (Jahrgang 1833)*, 21–144.
- von Buch, L. 1840: Beiträge zur Bestimmung der Gebirgsformationen in Rußland. Aus dem Funfzehnten Bande das

- Archivs für Mineralogie, Geognosie, Bergbau und Hüttenkunde besonders abgedruckt. Gedruckt und verlegt bei G. Reimer, 128 pp.
- von Schlotheim, E.F. 1813: Beiträge zur Naturgeschichte der Versteinerungen in geognostischer Hinsicht. Leonhard's Taschenbuch der Mineralogie 7, 1–134.
- von Schlotheim, E.F. 1820: Die Petrefactenkunde auf ihrem jetzigen standpunkte durch die Beschreibung seiner Sammlung versteinertes und fossiler Überreste des Thier- und Pflanzenreichs. Gotha, 432 pp.
- von Schlotheim, E.F. 1822: Beiträge zur Naturgeschichte der Versteinerungen in geognostischer Hinsicht. Denkschriften der Königlichen Academie, 13–36.
- von Schlotheim, E.F. 1832: Systematisches Verzeichniss der Petrefacten-Sammlung des verstorbenen wirklichen Geheimen Raths. Gotha, 100 pp.



# *Tomagnostus brantevikensis* n. sp. (Trilobita) from the middle Cambrian of Scania, Sweden

THOMAS WEIDNER & ARNE THORSHØJ NIELSEN



Weidner, T. & Nielsen, A.T. 2016. *Tomagnostus brantevikensis* n. sp. (Trilobita) from the middle Cambrian of Scania, Sweden. © 2016 by Bulletin of the Geological Society of Denmark, Vol. 64, pp. 111–116. ISSN 2245-7070 ([www.2dgf.dk/publikationer/bulletin](http://www.2dgf.dk/publikationer/bulletin)).

Sparse material of an agnostid trilobite, previously referred to as *Tomagnostus* cf. *corrugatus* (Illing 1916), is recognized as a new species, *T. brantevikensis* n. sp. It occurs in the middle Cambrian (= Cambrian provisional Series 3) *Triplagnostus gibbus* and *Acidusus atavus* zones (Almbackenian regional Stage) in Scania, southernmost Sweden, but is very rare. The new species resembles *T. corrugatus* (Illing 1916) and *T. perrugatus* (Grönwall 1902), but the cephalon is characterized by a tapering glabella, creating an elongate subtriangular outline, and a deltoid depression. The pygidium has an evenly rounded border, is non-spinose, and has a long axis with a non-elongate node. Both shields have a moderately wide border.

Keywords: Trilobites, agnostids, *Tomagnostus*, middle Cambrian, Scandinavia.

Thomas Weidner [[to.we@paradis.dk](mailto:to.we@paradis.dk)], Ravnholtvej 23, Rårup, 7130 Juelsminde, Denmark. Arne Thorshøj Nielsen [[arnet@ign.ku.dk](mailto:arnet@ign.ku.dk)], Department of Geosciences and Natural Resource Management, University of Copenhagen, Øster Voldgade 10, 1350 Kbh K, Denmark.

Corresponding author: Arne Thorshøj Nielsen

Received 25 August 2016  
Accepted in revised form  
11 November 2016  
Published online  
14 December 2016

Four species of the agnostid trilobite genus *Tomagnostus* Howell 1935 are known from Scandinavia (see Grönwall 1902; Westergård 1946; Weidner & Nielsen 2009, 2014, 2015). They occur in the *Triplagnostus gibbus* and *Acidusus atavus* zones of the middle Cambrian *Paradoxides paradoxissimus* Superzone (Fig. 1), and comprise *Tomagnostus fissus* (Lundgren in Linnarsson 1879), *T. perrugatus* (Grönwall 1902), *T. sibiricus* Pokrovskaya & Egorova in Savitsky *et al.* 1972, and *T. bothrus?* Robison 1994. Overall, representatives of *Tomagnostus* are common only in Scania and Bornholm, but sporadic occurrences are known also from the middle Cambrian of Öland, Närke and the Oslo area (Westergård 1946; Høyberget & Bruton 2008; Weidner & Nielsen 2009), as well as Västergötland (TW unpublished).

The coeval species *T. gracilis* (Illing 1916) and *T. corrugatus* (Illing 1916) have not been recorded from Scandinavia. For detailed descriptions of the *Tomagnostus* species including a summary of their geographical distribution and stratigraphical ranges, see Rushton (1979), Weidner & Nielsen (2014, 2015) and, in particular, Robison (1994) who presented a comprehensive review of species assigned to *Tomagnostus*.

*Tomagnostus* cf. *corrugatus*, illustrated by Westergård

(1946) from the *Triplagnostus gibbus* Zone of Brantevik, Scania (Fig. 2), was assigned to *T. corrugatus* by Pokrovskaya (1958), whereas Rushton (1979) considered the specimens possibly representing *T. deformis* Pokrovskaya 1958. Robison (1994) did not discuss the status of *T. cf. corrugatus* but reassigned all specimens identified with *T. deformis* to either *T. corrugatus* or *T. perrugatus* and we concur with this interpretation. However, *T. cf. corrugatus* sensu Westergård (1946) represents a new species of *Tomagnostus*, here described as *Tomagnostus brantevikensis* n. sp. Its cephalon resembles that of *T. corrugatus* whereas the pygidium is similar to that of *T. perrugatus*.

## Systematic palaeontology

The figured specimens of *T. brantevikensis* n. sp. are deposited in the Swedish Geological Survey (SGU), Uppsala, those of *T. perrugatus* are kept in the Museum of Evolution (PMU), Uppsala University, and the *T. corrugatus* material is in the collection of the Sedgwick Museum (SMA), University of Cambridge, UK.

Chronostratigraphy				Trilobite Biostratigraphy			Ranges of Scandinavian <i>Tomagnostus</i> species	
System	Series	Global Stage	Local Stage	Superzones	Polymerid zonation	Agnostid zonation		
Cambrian	Cambrian Series 3	Guzhangian	(Not defined)	<i>Paradoxides forchhammeri</i>	<i>Simulolenus alpha</i>	<i>Agnostus pisiformis</i>		
					(Not defined)	<i>Lejopyge laevigata</i>		
					<i>Solenopleura? brachymetopa</i>			
		Drumian	Almbackenian	<i>Paradoxides paradoxissimus</i>	(Not defined)	<i>Paradoxides davidis</i>		<i>Goniagnostus nathorsti</i>
						<i>Bailliella ornata</i>		<i>Ptychagnostus punctuosus</i>
								<i>Acidusus atavus</i>
						<i>Ctenocephalus exsulans</i>		<i>Triplagnostus gibbus</i>
		Stage 5	Bödan	<i>Acado-paradoxides oelandicus</i>	(Not defined)	<i>Acadoparadoxides pinus</i>		<i>Pentagnostus praecurrens</i>
						<i>Eccaparadoxides insularis</i>		(Not defined)

Fig. 1. Biozonation of the middle Cambrian (≈ Cambrian provisional Series 3) in Scandinavia. Ranges of Scandinavian species of *Tomagnostus* are also shown. Revised zonation and ranges according to Weidner & Nielsen (2015); local stages according to Nielsen & Schovsbo (2015).

## Family Ptychagnostidae Kobayashi 1939

### Genus *Tomagnostus* Howell 1935

*Type species* (by original definition). *Agnostus fissus* Lundgren in Linnarsson 1879, from the Exsulans Limestone Bed, *T. gibbus* Zone, near Brantevik, Scania, Sweden.

*Diagnosis*. See Robison (1994) and Shergold & Laurie (1997).

#### *Tomagnostus brantevikensis* n. sp.

Fig. 3A, B

1946 *Tomagnostus* cf. *corrugatus* (Illing 1916); Westergård, pp. 60, 61, pl. 8, figs 11, 12.

*Derivation of name*. The new name alludes to the small village of Brantevik on the east coast of Scania, well known for exposures of Cambrian strata along the shore.

*Holotype*. Complete specimen, SGU 4859, originally illustrated by Westergård (1946, pl. 8, fig. 12), here reillustrated in Fig. 3A. It derives from the *T. gibbus* Zone, Alum Shale Formation, Gislövshammar, Scania,

Sweden. Note that Westergård (1946, pl. 8, fig. 12) erroneously stated the magnification for his illustration as  $\times 4$ ; it is in fact  $\times 3$ .

*Material and occurrence*. Westergård (1946) reported this form from boulders of the *Triplagnostus gibbus* and *Acidusus atavus* zones found on the shore between Brantevik and Gislövshammar, eastern Scania. However, of his material only the two illustrated specimens (from the former zone) could be located in the SGU collection. Subsequent fossil collecting from this area has failed to locate additional new material of this apparently very rare form.

*Diagnosis*. A *Tomagnostus* species with moderately wide cephalic and pygidial borders. Glabella distinctly tapering, creating a subtriangular outline; deltoid depression developed. Pygidium with evenly rounded border, non-spinose; non-elongate node on M2.

*Description*. The thoracic segments are telescoped under the cephalon in the holotype (Fig. 3A), in which the cephalon is approximately  $\geq 6.0$  mm long and the pygidium measures 6.6 mm in length. Total reconstructed length was thus *c.* 15 mm (adding the length of the thorax). The other illustrated complete specimen (Fig. 3B) is 9.5 mm long, of which the cepha-

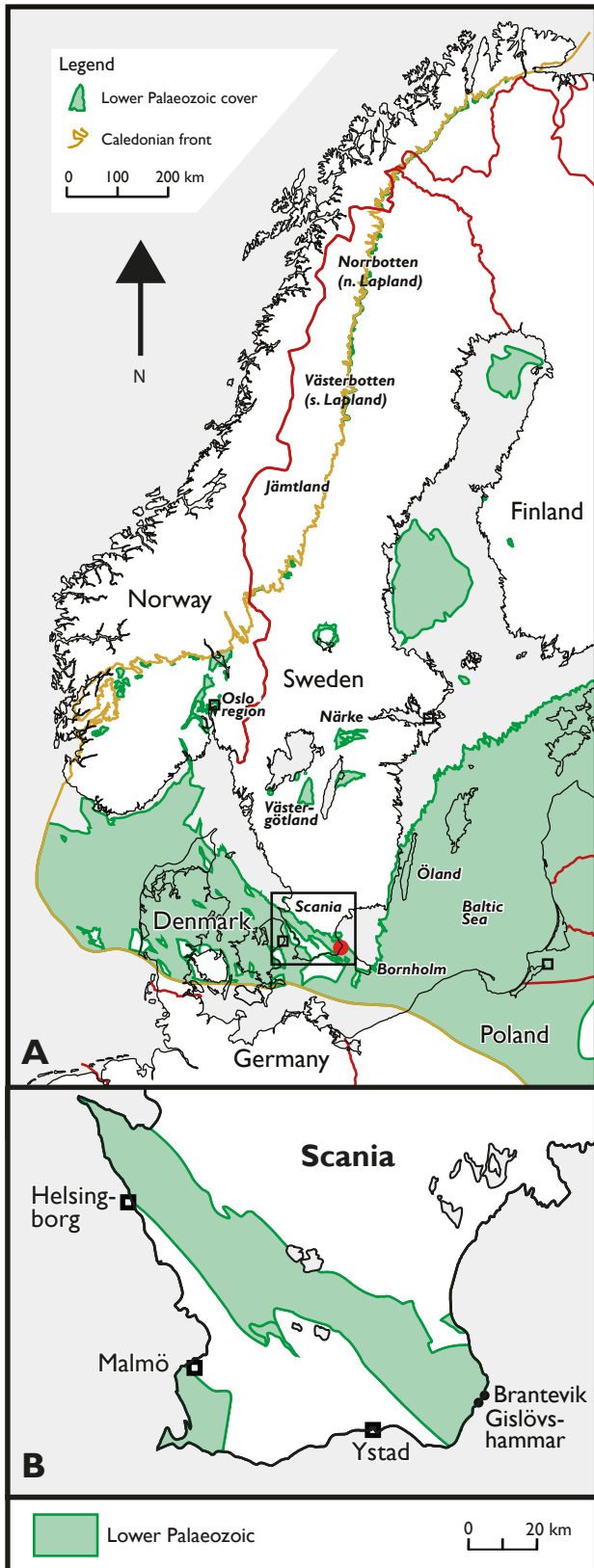


**Fig. 2. A:** Map of Scandinavia showing the distribution of Cambrian strata. Names of districts referred to in the text are also indicated. (Map modified from Nielsen & Schovsbo 2011). **B:** Map of Scania showing sites referred to in the text.

lon occupies 4.1 mm and the pygidium 4.2 mm. The larger specimen, although less perfectly preserved, is designated above as the holotype because it allows better comparison to large specimens of *T. corrugatus* and *T. perrugatus*.

The cephalon is rounded in outline and slightly wider than long, with a moderately wide border and a deltoid depression. The genae show long and deep radiating furrows and a distinct pair of anterior arcuate furrows adjacent to the anteroglabella. A vestigial posterior pair of arcuate furrows is indicated adjacent to the posteroglabella (Fig. 3A). Glabella is rather strongly tapering, giving it a subtriangular outline. Anteroglabella with a distinct frontal sulcus; posteroglabella with short and deep F1 and F2 furrows, M2 bears a narrow, elongate glabellar node (see also Westergård 1946, pl. 8, fig. 11). A shallow median depression separates the cheeks. The basal lobes are slightly elongate. The border, axial and transglabellar furrows are deep and narrow; the latter shallows medially. The thoracic segments are developed as in *T. perrugatus*, *T. corrugatus* and *T. sibiricus*; for description see Weidner & Nielsen (2015).

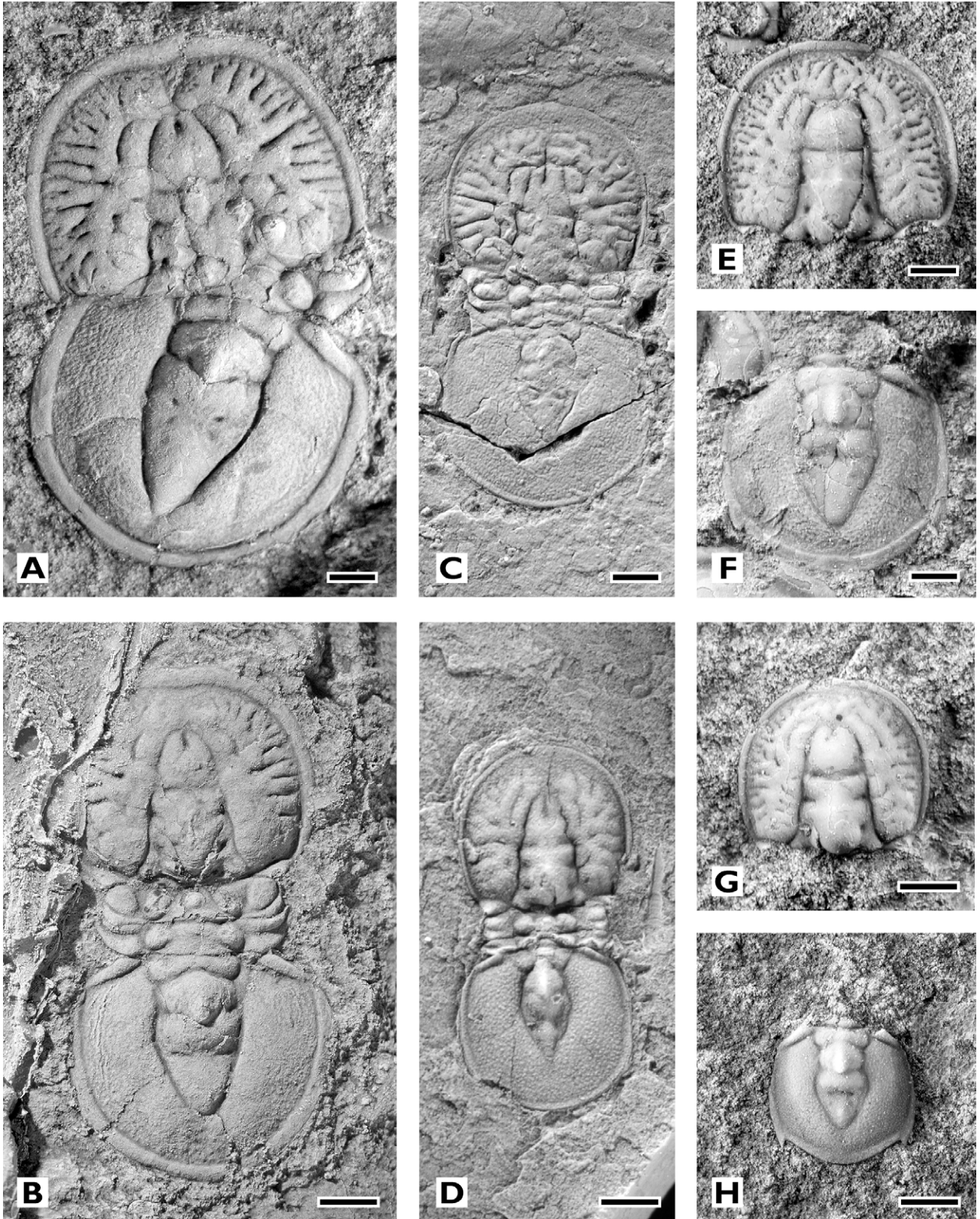
The pygidium is evenly rounded in outline and slightly wider than long. The border is moderately wide and flat, of even width throughout and without any trace of lateral pygidial swellings or incipient spines. The axis occupies about 70–80% of the pygidial length and accounts for c. 35% of the pygidial width. It tapers to a point and the posteroaxis has a transverse depression with a pair of distinct pits just anterior to the midlength with additional indistinct pairs of pits further back (Fig. 3A). The border furrow and the axial and F1 and F2 furrows are narrow. F1 bends forward, F2 is deflected backward by the M2 node which is less elongate than in *T. corrugatus*, *T. perrugatus* or *T. fissus*. Median postaxial furrow very faint.

*Remarks.* *Tomagnostus brantevikensis* n. sp. most closely resembles *T. corrugatus* and *T. perrugatus*. In larger cephalons of *T. corrugatus* from England (Rushton 1979, fig. 6A [here Fig. 3C], 7E), Greenland (Robison 1994, fig. 29: 5–6) and Siberia (Pokrovskaya 1958, pl. 2, fig. 2) the scrobiculation is more irregular than in *T. brantevikensis* n. sp. Therefore, the axial furrows are less distinct, but nevertheless the subtriangular shape of the glabella is still obvious and is a diagnostic feature for both *T. corrugatus* and *T. brantevikensis* n. sp. (see Rushton 1979, fig. 7E). The border of *T. corrugatus* is evenly rounded, distinctly narrower than in *T. brantevikensis* n. sp. and lacks the deltoid depression. The anterior part of the cheeks is finely granulated in *T. corrugatus*, a feature not developed in *T. brantevikensis* n. sp.

The differences between cephalons of *T. perrugatus* and *T. brantevikensis* n. sp. are more pronounced.

*Tomagnostus perrugatus* typically has a parallel-sided posteroglabella and a rounded or only slightly tapering anteroglabella *vs* a quite strongly tapering

glabella in *T. brantevikensis* n. sp.; besides, the border is evenly rounded, lacking a deltoid depression, and is narrower than in *T. brantevikensis* n. sp. (Fig. 3E, G;



Pokrovskaya 1958, pl. 2, figs 5–7, 9; Westergård 1946, pl. 8, figs 1, 3–4, 6–7; Savitsky *et al.* 1972, pl. 5, figs 7, 9; Egorova *et al.* 1982, pl. 5, fig. 5, pl. 54, fig. 9; Weidner & Nielsen 2014, fig. 20A–D; Weidner & Nielsen 2015, fig. 11K–O). Smaller cephalons of the three species are, however, quite alike (Figs 3B, D, G) and in order to assign smaller specimens unerringly to one of the species, an associated pygidium is required (Figs 3B, D, H).

Where the cephalon of *T. brantevikensis* n. sp. resembles that of *T. corrugatus*, the pygidium of *T. brantevikensis* n. sp. more closely resembles that of *T. perrugatus*. The latter is distinguished by having a more elongate axial node, extending for the entire length of M2, and posterolateral pygidial spines of variable length (see Westergård 1946, pl. 8, figs 2, 5, 8, 10; Robison 1994, fig. 31:2–3; Weidner & Nielsen 2015, fig. 11P–T). However, some illustrated pygidia have only tiny posterolateral swellings or a mere angulation of the pygidial border instead of spines (Pokrovskaya 1958, pl. 2, figs 5, 8–9; Rushton 1979, fig. 6C, E). The border is not as evenly rounded as in *T. brantevikensis* n. sp., and the lateral parts are generally almost straight until where the posterolateral spines protrude. There is an obtuse angle between the straight lateral parts and the posterior part of the border just inside the spine base (Fig. 3H; Pokrovskaya 1958, pl. 2, figs 5, 8–9; Weidner & Nielsen 2015, fig. 11P–S); the posterior part of the border may be broadly rounded or sharply curved (Pokrovskaya 1958, pl. 2, fig. 5, and Weidner & Nielsen 2015, fig. 11P–T, versus Pokrovskaya 1958, pl. 2, figs 6, 8–9; Rushton 1979, fig. 6C, E and Egorova *et al.* 1982, pl. 54, fig. 12). Furthermore, the border is narrowing anteriorly and often with a posterior collar (Fig. 3F; better seen in Westergård 1946, pl. 8, figs 2, 5; Egorova *et al.* 1982, pl. 54, fig. 12). Pokrovskaya (1958) realized the affinities between *T. deformis* and *T. perrugatus* and stated as key differential characters the narrowing anteroglabella and the “sharply triangular-rounded” posterior part of the pygidial border as well as the lack of posterolateral spines and collar in *T. deformis*. However, Pokrovskaya (1958) had only comparative

illustrations of *T. perrugatus* from Westergård (1946) at hand, and since then *T. perrugatus* has been treated and illustrated in numerous publications showing the *deformis* features as intraspecific variations of *perrugatus* (Savitsky *et al.* 1972; Rushton 1979; Egorova *et al.* 1982; Robison 1994; Weidner & Nielsen 2014, 2015). We therefore agree with the transfer of the material described as *deformis* to *T. perrugatus* as suggested by Robison (1994).

The pygidium of *T. corrugatus* is different from that of *T. brantevikensis* n. sp. in several features. The overall shape of the former is more quadrate than rounded and the axis is shorter and narrower and considerably more constricted at M2 than in *T. brantevikensis* n. sp. Furthermore, the border is distinctly narrower. Typical *T. corrugatus* pygidia have either vestigial spines or at least an angulation of the border (Fig. 3C; Pokrovskaya 1958; Rushton 1979; Robison 1994) whereas *T. brantevikensis* n. sp. has a smooth and evenly rounded border. Some specimens of *T. corrugatus* from Greenland (Robison 1994, fig. 29: 5–6) and Siberia (Pokrovskaya 1958, pl. 2, figs 1–3) have a longer axis than is typical for the species and are almost as long as those observed in *T. brantevikensis* n. sp. However, the more constricted axis and narrower border of *T. corrugatus* readily separates the two species.

## Conclusions

Four species of *Tomagnostus* have hitherto been reported from Scandinavia, viz. *T. bothrus?*, *T. fissus*, *T. perrugatus* and *T. sibiricus* (see Grönwall 1902, Westergård 1946, Weidner & Nielsen 2009, 2014, 2015). Material originally described as *T. cf. corrugatus* by Westergård (1946) is here recognized as a fifth species named *T. brantevikensis* n. sp. This form occurs sparsely in the *T. gibbus* and *A. atavus* zones of Scania, Sweden, according to Westergård (1946).

◀ **Fig. 3.** Comparison of *Tomagnostus brantevikensis* n. sp. with *T. corrugatus* and *T. perrugatus*. Black scale bars 1 mm. Upper row (A, C, E and F) shows larger specimens and lower row (B, D, G and H) shows smaller specimens. **A–B:** Complete specimens of *Tomagnostus brantevikensis* n. sp. from the *Triplagnostus gibbus* Zone, Alum Shale Formation, Gislövshammar, Scania, Sweden. Previously figured by Westergård (1946, pl. 8, figs 11, 12). **A:** Holotype, SGU 4859. **B:** Cast of SGU 4858; note that Westergård (1946, pl. 8 fig. 11) illustrated the inverted negative imprint. **C–D:** Complete specimens of *Tomagnostus corrugatus* (Illing 1916) from the *Tomagnostus fissus* Zone, Abbey Shales, England. Previously figured by Rushton (1979, fig. 6A, B). **C:** Lectotype, SMA 242. **D:** SMA 55446. **E–H:** *Tomagnostus perrugatus* (Grönwall 1902) from the Alum Shale Formation, Brantevik, Scania, Sweden. **E:** Cephalon, PMU 27361, *Triplagnostus gibbus* Zone. Previously figured by Weidner & Nielsen (2015, fig. 11K). **F:** Pygidium, PMU 27370, *Triplagnostus gibbus* Zone. Previously figured by Weidner & Nielsen (2015, fig. 11T). **G:** Smaller cephalon with atypical slightly triangular glabella, PMU 27365, *Triplagnostus gibbus* Zone. Previously figured by Weidner & Nielsen (2015, fig. 11O). **H:** Pygidium, PMU 25874, *Acidusus atavus* Zone. Previously figured by Weidner & Nielsen (2014, fig. 20F).

## Acknowledgements

We thank L. Wickström, SGU, Uppsala, for lending us the specimens of *T. brantevikensis* n. sp. previously illustrated by Westergård (1946). J.O.R. Ebbestad, Uppsala, and I. Korovnikov, Novosibirsk, helped us with Russian literature. Recommendations by referees John Laurie, Canberra, Australia, and Elena Naimark, Moscow, Russia, improved the final manuscript.

## References

- Egorova, L.I., Shabanov, Yu.Ya., Pegel, T.V., Savitsky, V.E., Suchov, S.S., Chernysheva, N.E. 1982: [Maya Stage of Type Locality (Middle Cambrian of Siberian platform)]. Academy of Sciences of the USSR, Ministry of Geology of the USSR, Transactions 8, 146 pp. [In Russian].
- Grönwall, K.A. 1902: Bornholms Paradoxideslag og deres Fauna. Danmarks Geologiske Undersøgelse, II Række 13, 1–230.
- Howell, B.F. 1935: Some New Brunswick Cambrian agnostians. Bulletin of the Wagner Free Institute of Science 10, 13–16.
- Høyberget, M. & Bruton, D. L. 2008: Middle Cambrian trilobites of the suborders Agnostina and Eodiscina from the Oslo Region, Norway. Palaeontographica. Abteilung A, Paläozoologie, Stratigraphie 286, 1–87.
- Illing, V.C. 1916: The Paradoxidian fauna of a part of the Stockingford Shale. Quarterly Journal of the Geological Society 71, 386–450.
- Kobayashi, T. 1939: On the Agnostids (part 1). Journal of the Faculty of Science, Imperial University of Tokyo, Section 2, (5) 5, 69–198.
- Linnarsson, G. 1879: Om Faunan i kalken med *Conocoryphe exsulans* ("Coronatuskalken"). Sveriges Geologiska Undersökning C 35, 1–31.
- Nielsen, A.T. & Schovsbo, N. 2011: The Lower Cambrian of Scandinavia: Depositional environment, sequence stratigraphy and palaeogeography. Earth-Science Reviews 107, 207–310.
- Nielsen, A.T. & Schovsbo, N. 2015: The regressive Early – Mid Cambrian 'Hawke Bay Event' in Baltoscandia: Epeirogenic uplift in concert with eustasy. Earth-Science Reviews 151, 288–350.
- Pokrovskaya, N.V. 1958: [Middle Cambrian agnostids of Yakutia, part I.] Akademii Nauk SSSR, Trudy Geologicheskogo Instituta 16, 1–96. [In Russian].
- Robison, R.A. 1994: Agnostoid trilobites from the Henson Gletscher and Kap Stanton formations (Middle Cambrian), North Greenland. Bulletin Grønlands Geologiske Undersøgelse 169, 25–77.
- Rushton, A.W.A. 1979: A review of the Middle Cambrian Agnostida from the Abbey Shales, England. Alcheringa 3, 43–61.
- Savitsky, V.E., Evtushenko, V.M., Egorova, L.I., Kontorovich, A.E. & Shabanov, Yu.Ya. 1972: [Cambrian of the Siberian platform (Judoma-Olenek type section, Kuonamsky Complex deposits).] Trudy Sibirskiy Nauchno-Issledovatel'skiy Institut Geologii, Geofiziki i Mineralnogo Syr'ya 130, 1–200. Nedra, Moscow. [In Russian].
- Shergold, J.H. & Laurie, J.R. 1997: Introduction to the Suborder Agnostina. In: R.L. Kaesler (ed.), Treatise on Invertebrate Paleontology. Part O. Arthropoda 1, Trilobita, revised. Volume 1, 331–383. The Geological Society of America, Inc. and the University of Kansas. Boulder, Colorado, and Lawrence, Kansas.
- Weidner, T. & Nielsen, A.T. 2009: The Middle Cambrian *Paradoxides paradoxissimus* Superzone on Öland, Sweden. GFF 131, 253–268.
- Weidner, T. & Nielsen, A.T. 2014: A highly diverse trilobite fauna with Avalonian affinities from the Middle Cambrian *Acidusus atavus* Zone (Drumian Stage) of Bornholm, Denmark. Journal of Systematic Palaeontology 12, 23–92.
- Weidner, T. & Nielsen, A.T. 2015: *Tomagnostus sibiricus* Pokrovskaya & Egorova, 1972 (Trilobita) from the Middle Cambrian Exsulans Limestone of Scania, Sweden. GFF 137, 9–19.
- Westergård, A.H. 1946: Agnostidea of the Middle Cambrian of Sweden. Sveriges Geologiska Undersökning C 477, 1–140.

# Instructions to authors

The Bulletin publishes articles normally not exceeding 30 printed pages, and short contributions not longer than 4 pages. Longer articles and monographs are also published, but in this case it is advisable to consult the chief editor before submitting long manuscripts. Short contributions may be comments on previously published articles, presentation of current scientific activities, short scientific notes, or book reviews.

Manuscripts with complete sets of illustrations, tables, captions, etc., should be submitted electronically to the chief editor (lml@geus.dk). The **main text** with references and figure captions should be either in Word or pdf format, **figures** should be in either pdf, jpeg, or tiff format, and **tables** should be in Word text format, i.e. written in lines with tab spacing between table columns, or in Excel format. "Word tables" are discouraged because they are not re-formatted easily. Consult the editor before submitting other formats.

Manuscripts will be reviewed by two referees; suggestions of referees are welcome. The final decision on whether or not a manuscript will be accepted for publication rests with the chief editor, acting on the advice of the scientific editors. Articles will be published in the order in which they are accepted and produced for publication.

## Manuscript

*Language* – Manuscripts should be in English. Authors who are not proficient in English should ask an English-speaking colleague for assistance before submission of the manuscript.

*Title* – Titles should be short and concise, with emphasis on words useful for indexing and information retrieval. An abbreviated title to be used as running title may also be submitted.

*Abstract* – An abstract in English must accompany all papers. It should be short (no longer than 250 words), factual, and stress new information and conclusions rather than describing the contents of the manuscript. Conclude the abstract with a list of key words.

*Main text* – Use 1.5 or double spacing throughout, and leave wide margins. Italics should be used only in generic and species names and in some Latin abbreviations (e.g. *c.*, *et al.*, *ibid.*, *op. cit.*).

*Spelling* – Geological units named after localities in Greenland, formal lithostratigraphical units and intrusions named after localities in Greenland remain unchanged even if the eponymous locality names have since been changed in accordance with modern Greenlandic orthography.

*References to figures, tables and papers* – References to figures and tables in the text should have the form: Fig. 1, Figs 1–3, Table 3 or as (Smith 1969, fig. 3) when the reference is to a figure in a cited paper.

References to papers are given in the form Smith (1969) or (Smith 1969). Combined citations by different authors are separated by a semicolon; two or more papers by same author(s) are separated by commas. Citations are mentioned chronologically and then alphabetically. Use '*et al.*' for three or more authors, e.g. Smith *et al.* (1985).

## Reference list

Use the following style:

Smith, A.A. 1989: Geology of the Bulbjerg Formation. Bulletin of the Geological Society of Denmark 38, 119–144. [Note that name of journal is given in full].

Smith, A.A., Jensen, B.B. & MacStiff, C.C. 1987: Sandstones of Denmark, 2nd edition, 533 pp. New York: Springer Verlag. [For more than 10 authors, use first author followed by *et al.*].

Smith, A.A., Jensen, B.B. & MacStiff, C.C. 1992: Characterization of Archean volcanic rocks. In: Hansen, D.D. *et al.* (eds): Geology of Greenland. Geological Survey of Denmark and Greenland Bulletin 40, 1397–1438. [More than three editors – therefore *et al.* form is used].

*Sorting* – Danish letters æ, ø and å (aa) are treated as ae, o and a (aa), respectively.

References are sorted by:

- 1: Alphabetically by the first author's surname
- 2: Papers by one author: two or more papers are arranged chronologically
- 3: Papers by two authors: alphabetically after second author's name. Two or more papers by the same two authors: chronologically.
- 4: Papers by three or more authors: chronologically. Papers from the same year are arranged alphabetically after second, third, etc. author's name.

Authors themselves are responsible for the accuracy and completeness of their references. The reference list must include all, and only, the references cited in the paper (including figures, tables etc).

## Illustrations

May be prepared in either black and white or colour. There is no colour charge. Horizontal illustrations are much to be preferred. Size of smallest letters in illustrations should not be less than 5.5 pt. Remember scale.

All figures (including photographs) should be submitted in electronic form ready for direct reproduction, i.e. having the dimensions of the final figure with a standard resolution of 300 dpi for photographs. Preferred formats are pdf, tiff and jpg.

*Size* – The width of figures must be 82 mm, 125 mm or 171 mm. Maximum height is 223 mm.

*Captions* – Captions to figures and plates must be delivered on separate pages, preferably at the end of the manuscript.

## Supplementary data files

Supplementary files are accepted. Such files may provide e.g. analytical data tables, detailed data documentation, illustrations with special effects, or videos.

## Proofs

Authors receive page proofs of the article after technical production. The cost of any alterations against the final manuscript will be charged to the author.

## Content, vol. 64

<i>Jens Morten Hansen, Troels Aagaard, Jens Stockmarr, Ingelise Møller, Lars Nielsen, Merete Binderup, Jan Hammer Larsen &amp; Birger Larsen:</i> Continuous record of Holocene sea-level changes and coastal development of the Kattegat island Læsø (4900 years BP to present).....	1
<i>Emilie Grønbæk Springer, Jan Audun Rasmussen &amp; Lars Stemmerik:</i> Distribution and significance of foraminiferal biofacies on an aphotic Danian bryozoan mound, Karlstrup, Denmark .....	57
<i>Jesper Milàn, Hendrik Klein, Sebastian Voigt &amp; Lars Stemmerik:</i> First record of tetrapod footprints from the Carboniferous Mesters Vig Formation in East Greenland.....	69
<i>Thomas Guldborg Petersen, Niels Erik Hamann &amp; Lars Stemmerik:</i> Correlation of the Palaeogene successions on the North-East Greenland and Barents Sea margins .....	77
<i>Ane Elise Schrøder, Bodil W. Lauridsen &amp; Finn Surlyk:</i> <i>Obliquorhynchia</i> (gen. nov.): An asymmetric brachiopod from the middle Danian Faxe Formation, Denmark.....	97
<i>Thomas Weidner &amp; Arne Thorshøj Nielsen:</i> <i>Tomagnostus brantevikensis</i> n. sp. (Trilobita) from the middle Cambrian of Scania, Sweden .....	111